Environment Canada
Environnement Canada

tario Agreement on Great Lakes Water Quality

Ministry of the Environment
Ontario

Assessment of Polyelectrolytes for Phosphorus Removal

Research Report No. 37

Research Program for the Abatement of Municipal Pollution under Provisions of the Canada-Ontario Agreement on Great Lakes Water Quality

Research Report No. 37 Assessment of Poly

CANADA-ONTARIO AGREEMENT

RESEARCH REPORTS

These RESEARCH REPORTS describe the results of investigations funded under the Research Program for the Abatement of Municipal pollution within the Provisions of the Canada-Ontario Agreement on Great Lakes Water Quality. They provide a central source of information on the studies carried out in this program through in-house projects by both Environment Canada and the Ontario Ministry of the Environment, and contracts with municipalities, research institutions and industrial organizations.

The Scientific Liaison Officer for this project was Mr. G. Rupke, Ontario Ministry of the Environment.

Enquiries pertaining to the Canada-Ontario Agreement RESEARCH PROGRAM should be directed to -

Wastewater Technology Centre,
Canada Centre for Inland Waters,
Environment Canada,
P.O. Box 5050,
Burlington, Ontario L7R 4A6

Ontario Ministry of the Environment,
Pollution Control Branch,
135 St. Clair Avenue West,
Toronto, Ontario M4V 1P5

ASSESSMENT OF POLYELECTROLYTES FOR PHOSPHORUS REMOVAL

by

A. Benedek, A.E. Hamielec, J.J. Bancsi
and T. Ishige
Wastewater Research Group
Department of Chemical Engineering
McMaster University

RESEARCH PROGRAM FOR THE ABATEMENT
OF MUNICIPAL POLLUTION UNDER THE
PROVISIONS OF THE CANADA-ONTARIO
AGREEMENT ON GREAT LAKES WATER QUALITY

Project No. 72-5-6

March, 1976

This document may be obtained from -

Training and Technology Transfer
Division (Water)
Environmental Protection Service
Environment Canada
Ottawa, Ontario
K1A 0H3

Ontario Ministry of the Environment
Pollution Control Branch
135 St. Clair Avenue West
Toronto, Ontario
M4V 1P5

REVIEW NOTICE

This report has been reviewed by the Technical Committee of the Canada-Ontario Agreement on Great Lakes Water Quality and approved for publication. Approval does not signify that the contents necessarily reflect the views and policies of either the Ontario Ministry of the Environment or Environment Canada, nor does mention of trade names or commercial products constitute endorsement or recommendation for use.

Commercial Letter & Litho Inc.

Ottawa, 1976

Cat. No.: En 43-11/37

ABSTRACT

A simple batch settling test has been developed to examine the process effectiveness of polyelectrolytes. The conditions for polyelectrolyte testing have been optimized and a theoretical data interpretation technique has been developed to permit the extrapolation of batch data to continuous clarifiers.

The shear and chemical degradation of solid polyelectrolyte during dissolution in water has been studied. Serious degradation and loss of effectiveness were noted under high shear, in the presence of ferrous ion, and with long term storage.

Polyelectrolyte application in phosphorus removal is expected to occur in conjunction with "coagulant-precipitants" such as alum, ferric chloride and lime. Thus, before assessing the effect of polyelectrolytes, the residual settled phosphorus concentration and the settling rate resulting from the addition of these three coagulant-precipitants were studied by themselves in model phosphate solutions as a function of phosphate type, pH and coagulant-precipitant dosage. The results indicated that substantial near colloidal, nonsettleable phosphorus precipitates can be formed with all three chemicals. The magnitude of this fraction was determined by pH. Condensed phosphates lowered the optimum precipitation pH in the aluminum and iron systems. The settling of the phosphorus bearing flocs was relatively poor and, in most cases, less than 90% removal would be expected at conventional clarifier overflow rates (600 $lgpd/ft^2$). In the aluminum and iron systems, condensed phosphates tended to lower floc settleability and a maximum allowable coagulant-precipitant dosage could be predicted as a function of initial alkalinity. The presence of magnesium increased the settling rate in the lime system substantially but only above a pH of 11.5.

The addition of polyelectrolytes slightly increased the removal of residual phosphorus and dramatically increased settling rates in the model solution systems. With polyelectrolytes, satisfactory performance is anticipated over a much wider pH range.

The results, in domestic wastewaters, with alum as the coagulant-precipitant, appeared similar to those of the model solutions. With alum alone, the maximum permissible overflow rate for 90% phosphorus removal was estimated at 400 lgpd/ft^2. With the addition of 0.3 mg/l polyelectrolyte, the permissible overflow rate typically increased to approximately 1500 lgpd/ft^2.

The results of a full scale study indicated agreement within 40% between laboratory predictions and full scale removals in the alum-domestic wastewater-polyelectrolyte system. The agreement was best between maximum permissible overflow rates (although alum only results were predicted conservatively in the laboratory) and worst in terms of predicting effluent concentrations. The plant operated very well with alum and polyelectrolyte addition prior to primary sedimentation over the one month period of the study, with secondary effluent phosphorus concentrations averaging approximately 0.4 mg/l as P.

A comparison of a large number of commercial polyelectrolytes indicated that the best polyelectrolyte for phosphorus removal is a 10-20% hydrolyzed polyacrylamide with a molecular weight above 8×10^6.

Studies on polyelectrolyte residuals, after sedimentation in model solution studies, indicated that a small concentration of polyelectrolyte can be expected to remain in solution and that this concentration is decreased as the ratio of polyelectrolyte mass to floc mass is reduced.

RESUME

Les auteurs ont mis au point un essai simple de décantation en discontinu afin d'examiner l'efficacité des polyélectrolytes. Ils ont optimalisé les conditions d'essai, et élaboré une méthode d'interprétation permettant l'extrapolation des données du traitement en discontinu aux clarificateurs à marche continue.

Le cisaillement et la dégradation chimique des polyélectrolytes solides au cours de leur dissolution dans l'eau ont été étudiés. On a observé une dégradation et une perte d'efficacité graves dans des conditions de cisaillement accentuées, en présence d'ions ferreux et lors d'un long entreposage.

L'application de polyélectrolytes pour l'élimination du phosphore devrait se faire en même temps que celle de "coagulants-précipitants" comme l'alun, le chlorure ferrique et la chaux. Par conséquent, avant de déterminer l'action des polyélectrolytes, on a étudié séparément, à l'aide de solutions modèles phosphatées, l'effet de l'addition de ces trois coagulants-précipitants sur la concentration résiduelle de phosphore et sur la vitesse de décantation, en fonction du type de phosphates, du pH et de la dose appliquée. Les résultats indiquent que ces trois substances peuvent produire une quantité importante de précipités phosphorés à l'état presque colloïdal et non décantables, mesurée à l'aide du pH. Les phosphates condensés abaissent le pH optimal de la précipitation en présence de chlorure ferrique et d'alun. La décantation des flocs phosphorés est relativement faible, et, dans la plupart des cas, on prévoit une élimination inférieure à 90% pour les clarificateurs ordinaires (600 gallons impériaux par jour et par pied carré). Les phosphates condensés ont tendance à dimineur la décantabilité des flocs, en présence d'alun et de chlorure ferrique, et une dose maximale permise de coagulant-précipitant pourrait être prédite à partir de l'alcalinité initiale. La présence de magnésium augmente considérablement la vitesse de décantation avec la chaux, mais seulement lorsque le pH est supérieur à 11.5.

L'addition de polyélectrolytes accroît légèrement l'efficacité d'élimination du phosphore résiduel et augmente fortement les vitesses de décantation dans les solutions modèles. On croit que les polyélectrolytes donneraient un rendement satisfaisant pour une gamme plus étendue de pH.

Lorsque l'alun est utilisé comme coagulant-précipitant dans les eaux usées domestiques, le rendement semble le même que pour les solutions modèles. Lorsque l'alun est employé seul, on estime à 400 gallons (UK) par jour et par pied carré le débit maximal permis du clarificateur pour l'obtention d'un taux d'élimination du phosphore de 90%. Si on ajoute 0.3 mg de polyélectrolytes par litre de débit passe normalement à environ 1 500 gal (UK)/j.pi^2.

Les résultats d'une étude à grande échelle du traitement d'eaux usées domestiques avec l'alun et des polyélectrolytes concordent à 40% près avec les prévisions fondées sur les essais de laboratoire. La concordance est meilleure pour les débits maximaux des clarificateurs permis (bien que les prédictions relatives à l'utilisation seule de l'alun aient été modestes) et moins bonne pour les concentrations dans l'effluent. L'addition d'alun et de polyélectrolytes s'est faite avant la décantation primaire, et le rendement de l'usine au cours de la période d'un mois qu'a duré l'expérience a été très bon (concentration moyenne de phosphore (P) de 0.4 mg/l dans l'effluent secondaire).

La comparaison d'un grand nombre de polyélectrolytes commerciaux indique que le meilleur est un polyacrylamide de 10 à 20% hydrolysé et de poids moléculaire supérieur à 8×10^6.

Des études des résidus de polyélectrolytes dans les solutions modèles après décantation indiquent qu'une petite quantité demeure en solution mais que sa concentration est proportionnelle au rapport de la masse de polyélectrolytes à la masse du floc.

TABLE OF CONTENTS

TABLE OF CONTENTS (CONT'D)

TABLE OF CONTENTS (CONT'D)

TABLE OF CONTENTS (CONT'D)

LIST OF FIGURES

LIST OF FIGURES (CONT'D)

LIST OF FIGURES (CONT'D)

LIST OF FIGURES (CONT'D)

LIST OF FIGURES (CONT'D)

LIST OF FIGURES (CONT'D)

LIST OF FIGURES (CONT'D)

LIST OF FIGURES (CONT'D)

LIST OF FIGURES (CONT'D)

LIST OF FIGURES (CONT'D)

LIST OF TABLES

1. INTRODUCTION

Recognition of the role of phosphorus in the eutrophication of surface waters during the late 1960's led to stringent regulations governing the concentration of phosphorus in effluents from domestic wastewater treatment plants located on the Lower Great Lakes watershed. To meet these requirements, most plants in southern Ontario chose to add one of three chemicals (alum, ferric chloride or lime) directly to the wastewater at a location upstream of either the primary or secondary clarifier. The inorganic phosphorus in domestic wastewater is expected to form metal phosphate precipitates and organic phosphorus may be trapped or adsorbed by the voluminous floc resulting from the precipitation process. Eventually, sedimentation is used to remove these phosphorus bearing flocs.

The addition of the above coagulant-precipitate chemicals may be unable to meet current effluent requirements (1 mg/l as P (total), 60% of time) in plants where:

(i) only primary clarification exists;
(ii) clarifiers are overloaded; or,
(iii) wastewater properties make precipitation or flocculation difficult.

In such cases, the addition of synthetic polyelectrolytes has been recommended as a possible solution. At the time this study was initiated, however, only a few other investigations had been reported in the literature. While these reports indicated that polyelectrolytes show great promise in phosphorus removal, they were all highly specific to wastewater and treatment plant characteristics. A prospective user of polyelectrolytes in Ontario was, therefore, faced with a very wide array of commercial polyelectrolytes without an adequate technique for laboratory assessment of potential usefulness. To help in the initial selection, and to avoid the need for wide ranging full scale evaluations, the Technical Committee of the Canada-Ontario Agreement on Great Lakes Water Quality decided to sponsor this investigation with the following broad objectives:

(i) to develop meaningful laboratory procedures for the

evaluation of benefits derived from polyelectrolyte addition;

(ii) to apply the developed procedures to a detailed assessment of polyelectrolyte application in a treatment plant designated; and,

(iii) to monitor the fate of polyelectrolytes during flocculation.

The rather extensive results have been grouped into eight sections and appendices to make reading and comprehension easier. Each section is self comprehensive.

Sections 2, 3, and 8 summarize results in response to objective (i); Sections 6 and 7 correspond to objective (ii); and, Section 9 summarizes work on objective (iii). Sections 4 and 5 were needed as background on floc settling, in order to select the most sensitive system for further study in Sections 6 and 7.

2. APPARATUS AND PROCEDURE FOR THE LABORATORY EVALUATION OF POLYMERIC FLOCCULANTS

2.1 Introduction

The laboratory evaluation of coagulants and flocculants has been traditionally based on the jar test (Black et al, 1957). In this test, different coagulant dosages are added to jars equipped with variable speed stirrers. Subsequent to periods of agitation required for the distribution of the added coagulant (rapid mix) and the flocculation of the resulting flocs (slow mix), the solids are allowed to settle (quiescent settling). After a period of quiescent settling, usually 30 minutes, a sample of the supernatant is withdrawn for analysis. Finally, the comparison of the analytical results from the various jars with different coagulant dosages leads to the choice of the optimum coagulant dosage.

Normally, nearly all of the flocs will settle in 30 minutes; therefore, the 30 minute sample is indicative of the "equilibrium" residual suspended solids (turbidity, phosphates, etc.) obtainable at a particular coagulant dosage. "Equilibrium" in this discussion refers to supernatant concentrations at infinite settling time. In continuous full scale clarifiers, short circuiting and excessive overflow rates often act to raise supernatant concentrations above the jar test "equilibrium" value.

Polymeric flocculants (or polyelectrolytes) are credited with two beneficial effects. First, they may or may not decrease the "equilibrium" solid concentration; second, they always increase floc settling rate. In phosphorus removal, as in many other applications, polyelectrolytes are added to improve the settling of an already formed metal coagulant-phosphate precipitate. For such applications, the conventional jar test is of little help.

Many methods can be used to extend the jar test to yield information on the nature of the flocs formed. These include visual or electronic floc size observations (Ontario Ministry of the Environment, 1972; Birkner and Margon, 1968), time to first floc (Peterson and Barlow, 1928), and slow stirring during "quiescent" settling (Rocheleau et al, 1970). These techniques provide at least an indirect, qualitative,

measure of floc settleability. The method of multiple sampling during quiescent settling (as first suggested by Cohen, 1957), however, is a direct measure of floc settleability. The importance of floc settling in flocculant applications suggested the adoption of this method for the present studies.

This section describes the modifications made to the jar test to accommodate multiple sampling, and a new data processing technique whereby jar test results can be used to qualitatively predict clarifier performance. Furthermore, tests on the reliability of the technique and the optimum conditions for flocculant additions are also described.

2.2 Theory

A typical set of results is shown in Figure 1, where residual concentration (in this case phosphorus) at the sampling port is plotted against time. Consider a sample taken at time t_1, in which the total phosphorus concentration is C_1. Then if the initial phosphorus concentration is C_o, the fraction of unsettled phosphorus at t_1 is C_1/C_o.

The fraction of C_1/C_o also corresponds to the fraction of particles with terminal velocity less than the velocity required for a particle to settle from the liquid surface to the level of the sampling port. Thus, if the liquid height above the sampling port at t_1 is h_1 and C_u is the residual phosphorus concentration at infinite time (or at a time when the slope of the settling curve is zero) a fraction, $(C_1-C_u)/(C_o-C_u)$ of the particles will have a velocity less than u, where

$$u = \frac{h_1}{t_1} \tag{1}$$

and

$$h_1 = h_o - \frac{V\,(N_1 - 1)}{A} \tag{2}$$

where A = horizontal cross sectional area of the jar;

h_o = initial liquid level above the sampling port;

N_1 = sample number; and,

V = volume of individual samples.

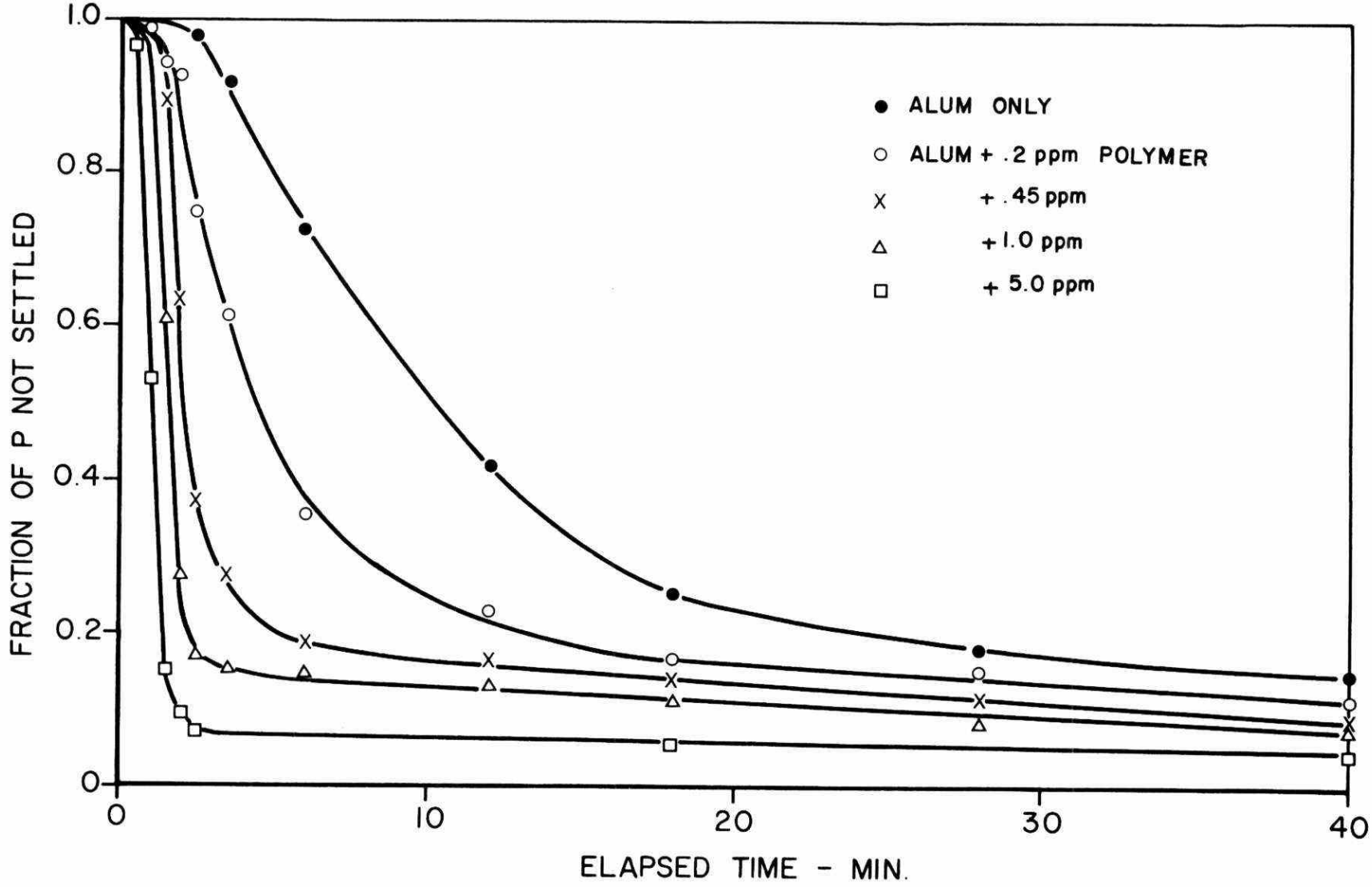

FIGURE 1. SETTLING OF ALUMINUM PHOSPHATE FLOCS IN DUNDAS RAW SEWAGE

Thus each curve in Figure 1 corresponds to a cumulative floc velocity distribution as shown in Figure 2.

The coordinates used in Figure 2 should be noted carefully. First, probability coordinates are used for the ordinate and logarithmic coordinates for the abscissa. Thus, a straight line should result for log-normal velocity distributions. Second, the abscissa is in terms of overflow rates rather than velocity, where overflow rates refer to the volumetric flow rate to a clarifier divided by its surface area. The dimensions of overflow rates can be reduced to those of velocity and once this is done, their magnitude is the same. On the basis of the Hazen-Camp (1946) ideal sedimentation tank theory, the overall removal in a clarifier is defined as

$$R = (1 - X_o) + \frac{1}{U_o} \int_o^{X_o} u\,dx \qquad (3)$$

where R = total fraction of settleable solids removed;

U_o = terminal velocity equal to the clarifier overflow rate; and,

X_o = fraction of settleable solids with terminal velocity less than U_o.

The integral term in Equation (3) is designed to correct for settling of particles entering the clarifier at elevations lower than the water surface. For clarifiers equipped with surface sluice gates, a relatively common arrangement, the integral term can be neglected, as it has been in this study. For other types of clarifiers, the predicted removals represent the minimum anticipated removal in the absence of short circuiting.

Thus, if terminal velocities are converted to overflow rates, by converting units of ft/min to gal/ft^2/day, the overflow rate distribution can be plotted as shown in Figure 2. Then, for any chosen solids removal requirement, $(1-X_o)$, the maximum allowable clarifier overflow rate can be estimated, e.g., in Figure 2, in the case of alum only, 90% of the flocs can be removed at a maximum overflow rate of 300 lgpd/ft^2 (360 gpd/ft^2, 15 m^3/day/m^2).

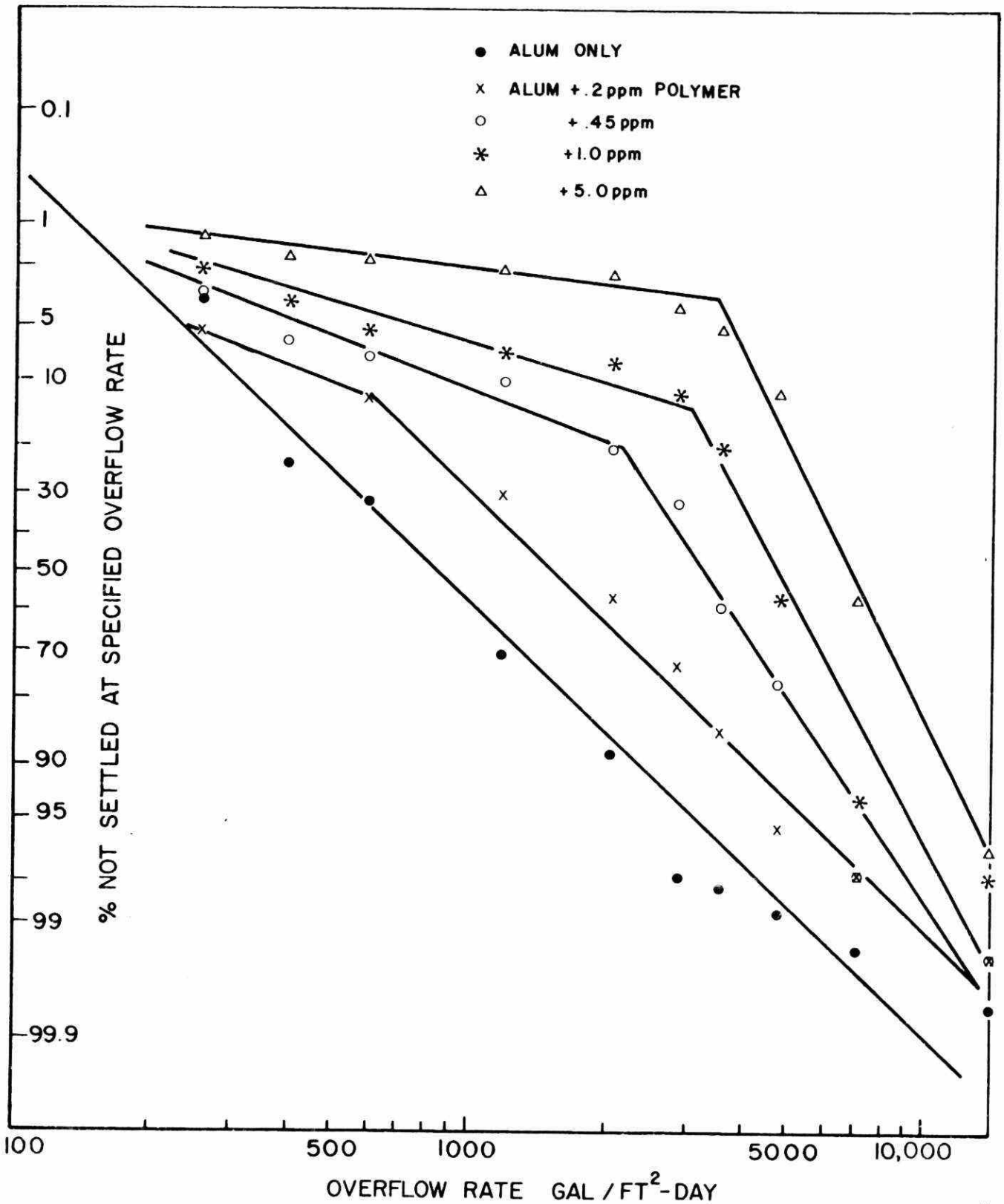

FIGURE 2. FLOC SETTLING VELOCITY DISTRIBUTION

Alternately, settling can be analyzed with the Cahn sedimentation apparatus. The Cahn apparatus measures the settled solids accumulated on the bottom of the settling vessel. Particle size distributions are easily obtained (Smith and Downing, 1970) with mathematical manipulation of the settling curve produced by the Cahn apparatus.

2.3 Experimental

2.3.1 Batch settling apparatus

Rectangular jars, with inside dimensions of 10 cm x 10 cm base and 35 cm height, were made from plexiglass. A horizontal sampling tube was inserted halfway across the jar at 7.62 cm from the bottom surface. The sampling probe had 3.2 mm (0.125 in) holes drilled 1 cm apart, perpendicular to the axis, with the hole at the inside end of the probe plugged as shown in Figure 3.

The Phipps and Bird six place stirrer was modified to accept the new jars by doubling the length of its legs and by adding a second identical impeller onto the lengthened shaft.

Discharge through the sampling port was controlled by solenoid valves which in turn were controlled by a sample sequencer. (See Figure 4 for the circuit diagram.) The sequencer was programmed to take a sample every 30 seconds for the first 2.5 minutes of the settling period. After the first 2.5 minutes, the sequencer increased the periods between samples such that a total of 12 samples were collected from each jar during a normal run.

The metallic coagulants were added with a system of pipettes. The pipettes were connected to both an air supply and a partial vacuum. The coagulant solution was drawn into the individual pipettes by the partial vacuum and simultaneous discharge, when desired, was possible by a slight pressure from the air supply.

Each batch settling apparatus test was begun by stirring the solution in the jar at 90 rpm with varying dosages of coagulant added at time zero. Stirring at 90 rpm (rapid mix) was continued for six minutes. When polymers were used, the polymer solution was added at the five minute mark with syringes. The stirrer speed was reduced to 30 rpm for a fourteen minute flocculation period.

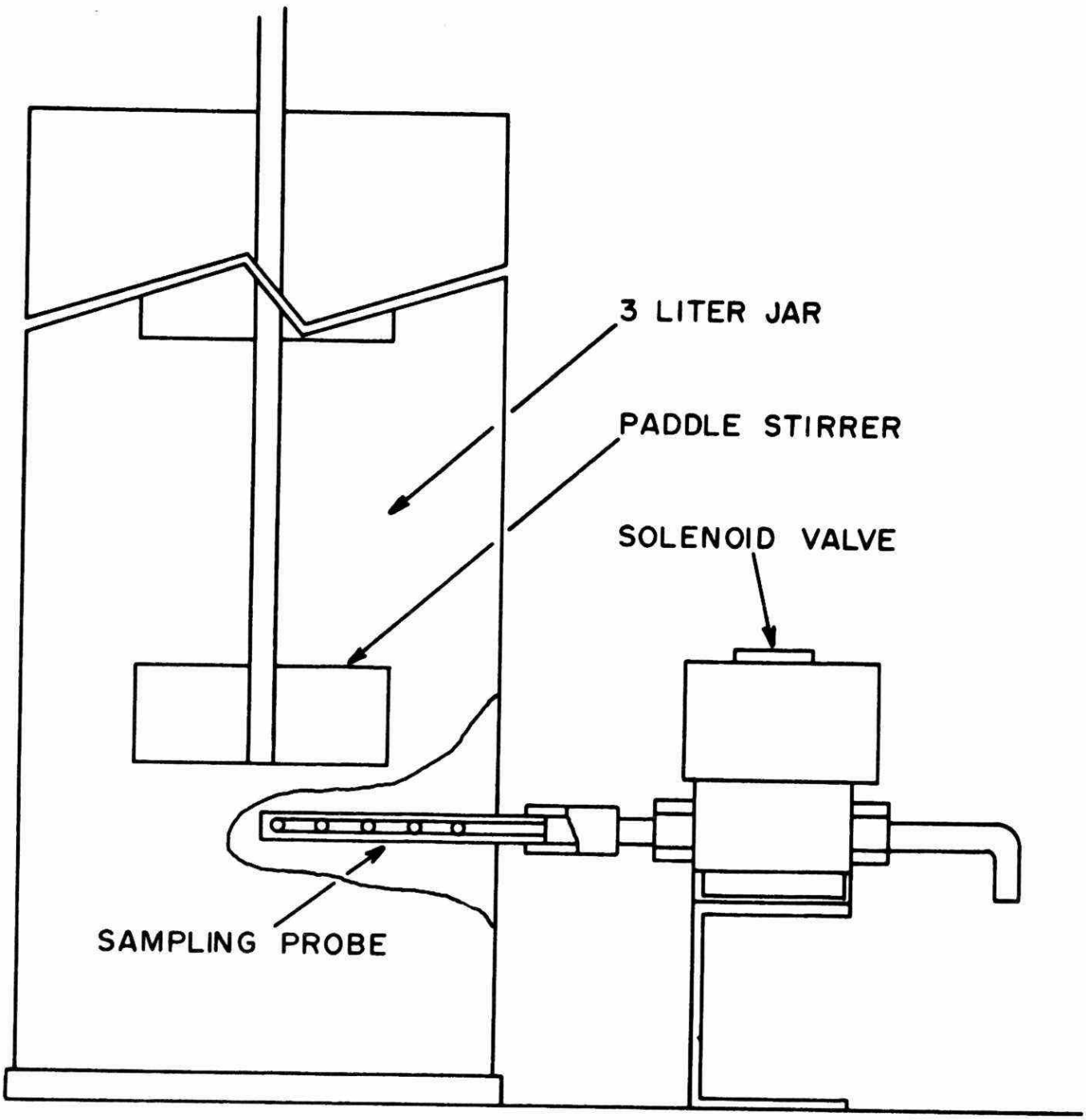

FIGURE 3. SCHEMATIC OF THE BATCH SETTLING APPARATUS

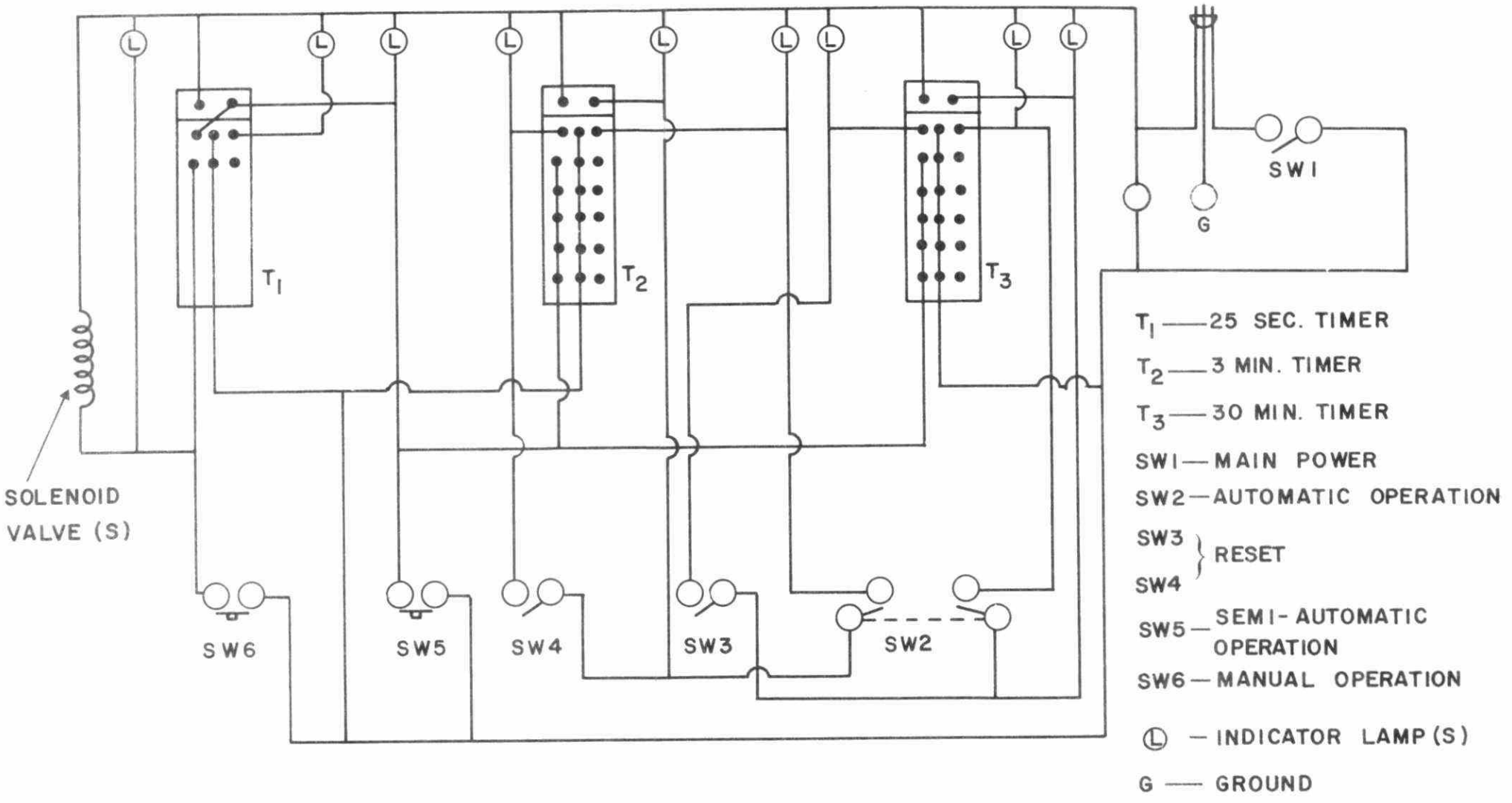

FIGURE 4. SAMPLE SEQUENCER FOR THE BATCH SETTLING APPARATUS

Just prior to the 20 minute mark, a sample was taken to establish or confirm the initial phosphorus concentration. At the 20 minute mark, the stirring was stopped and the automatic sample sequencer was started at the same time. The next 40 minutes constituted the quiescent settling period in which the sampling program was carried out.

2.3.2 Cahn electro balance

To determine the particle size and settling velocity distribution in the absence of sampling, the Cahn #7700 model RM-2 electro balance, in conjunction with the Cahn #2800 sedimentation accessory (Ventran Instrument Corp., 1971) and a Philips #8010 chart recorder, was used.

A run was begun with the solids slurry placed into the inner cylinder and dispersed with the supplied plunger. The settling vessel was then quickly placed under the electro balance. The system was left undisturbed until the slope of the trace on the recorder chart was zero.

2.3.3 Long tube settler

The tube was 8 ft long and 6 inches in diameter. Six sampling probes were placed 1 ft apart, the lowest one centred 0.25 inches from the bottom. For this particular experiment, the four middle probes were used to take samples. The lowest sampling probe was utilized for introducing air into the tube for initial mixing. Approximately seven gallons of raw sewage from the Dundas Pollution Control Centre was treated with 190 mg/l alum as $Al_2(SO_4)_3 \cdot 16H_2O$ and 0.3 ppm of Percol 730 providing an initial liquid level of 6 ft and 7 inches.

At time zero, the air line was shut off and 125 ml samples were collected, of which 100 ml was used for suspended solids determination and the balance for phosphorus analysis.

The period between samples was a minimum of one minute and was increased as the experiment progressed. The height of the liquid level was measured after each set of samples. Sampling was continued over a two and a half hour period.

2.3.4 Analysis

The samples that were destined for total phosphorus analysis were acidified with five drops of concentrated sulphuric acid. Sewage samples were then filtered through 0.45μ Sartorius membrane. All phosphorus analyses were carried out with the Technicon Auto-Analyzer according to Technicon's industrial methods 4-68 W and 3-68 W. The two methods are identical except for differences in sensitivity due to differences in colorimeter cell size.

The range of the 4-68 W is 0-25 ppm P, and that of the 3-68 W is 0-12 ppm P.

Suspended solids were determined with glass fibre filters. The procedure was in accordance with Standard Methods (APHA et al, 1971).

2.4 Results and Discussion

The effects of polymers are clearly shown by the above apparatus and procedure. As can be seen in Figure 2, permissible clarifier overflow rates were greatly increased by polymer addition. Looking at it another way, for a given clarifier and overflow rate, a very large increase in removals is possible with polymers, e.g., at 1000 lgpd/ft^2 (1200 gpd/ft^2, 49 m^3/day/m^2), 60% of flocs would not be removed with alum addition alone, while all but 1% of the flocs can be removed if polymers are added. Another interesting effect of polymer addition was the gradual development of two distinct groups of solids as polymer dosage was increased: an ever decreasing fraction of difficult to settle suspended matter; and, an ever increasing fraction of large and almost instantly settling flocs.

2.4.1 Experimental accuracy

There are some inherent errors in the batch settling apparatus test procedure described above:

i) the sedimentation pattern is interrupted by sampling; and,
ii) a changing sedimentation height, h, occurs as sampling proceeds.

In the design of the apparatus, careful consideration was given to minimizing the first error by distributed horizontal sampling ports, and a correction for the second error was introduced in the data analysis

(see Equation 2). Nonetheless, an experimental check on the magnitude of these errors is required for full assurance.

The Cahn sedimentation analysis system eliminates both of the above errors as it does not involve sampling. Therefore, the magnitude of the sampling error was checked by comparing the settling of identically prepared $CaCO_3$ dispersions in the batch settling apparatus and in the Cahn system. The results, in terms of velocity distribution, are plotted in Figure 5 and they show that the two systems yield very similar results, although at settling velocities of about 10 cm/min, slightly less particles settled in the batch settler apparatus test than in the electrobalance, and at settling velocities of about 1 cm/min, slightly more particles settled in the batch settling apparatus test.

2.4.2 Comparison to the long tube settling test

The design of clarifiers for dilute flocculant suspended solids is often based on the "Long Tube Settling Test" (Ford and Eckenfelder, 1970). In this test, the tube is "long" to simulate full scale clarifiers where flocculation can take place during the entire downward passage of a floc.

Figure 6 shows a typical settling curve obtained from one of the sampling ports of the long tube settler. Both phosphorus and suspended solids were monitored and, in this case, as for all other sampling, a simple line can be drawn to fit the data points if reduced (C/C_o) coordinates are used. Thus, the phosphorus precipitate appears to be fully enmeshed with the other suspended solids and the settling of chemical floc can be monitored equally well with either phosphorus or suspended solids. The floc settling velocity distributions at the four depths are shown in Figure 7. At each depth, the phosphorus data and the suspended solids data follow the same line. Floc growth was observed during settling, as indicated by the separation of lines in Figure 7. Examination of the average particle settling velocity, defined by the 50% mark on the probability axis, reveals a doubling of settling velocities as floc moves from the 32.6 cm to the 135.6 cm depth.

This indicates that the overflow rates obtained in the batch settling apparatus test were conservative, since the liquid level in the batch settling apparatus test above the sampling port was a maximum of 25 cm.

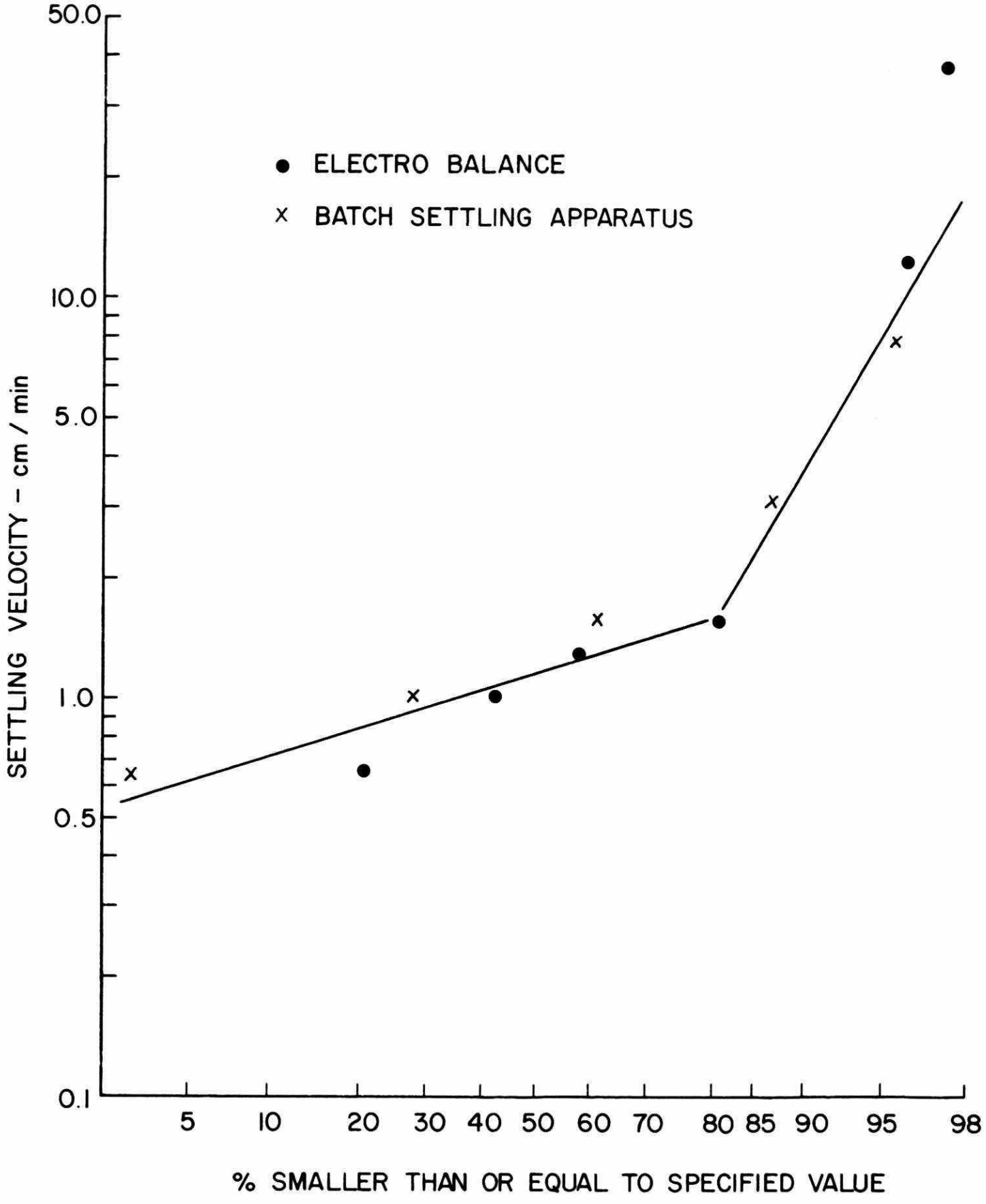

FIGURE 5. SETTLING VELOCITY DISTRIBUTION OF $CaCO_3$ SUSPENSION IN THE BATCH SETTLING APPARATUS AND THE CAHN SEDIMENTATION ANALYSIS SYSTEM

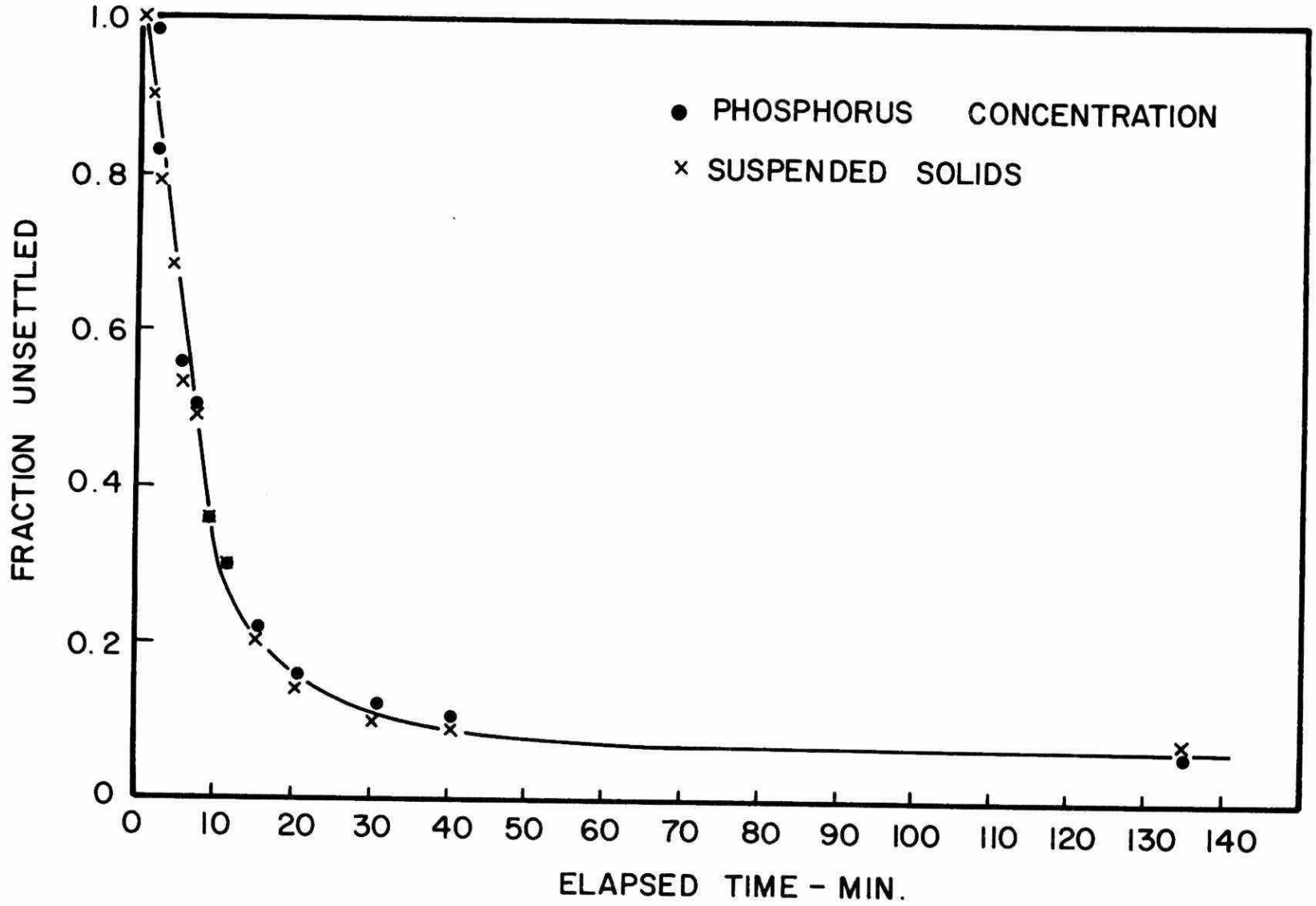

FIGURE 6. SETTLING CURVE OBTAINED WITH THE LONG TUBE SETTLER AS RESULT OF THE ADDITION OF 190 MG/1 AS $Al_2(SO_4)_3 \cdot 16\ H_2O$ ALUM AND 0.3 PPM PERCOL 730 TO DUNDAS RAW SEWAGE

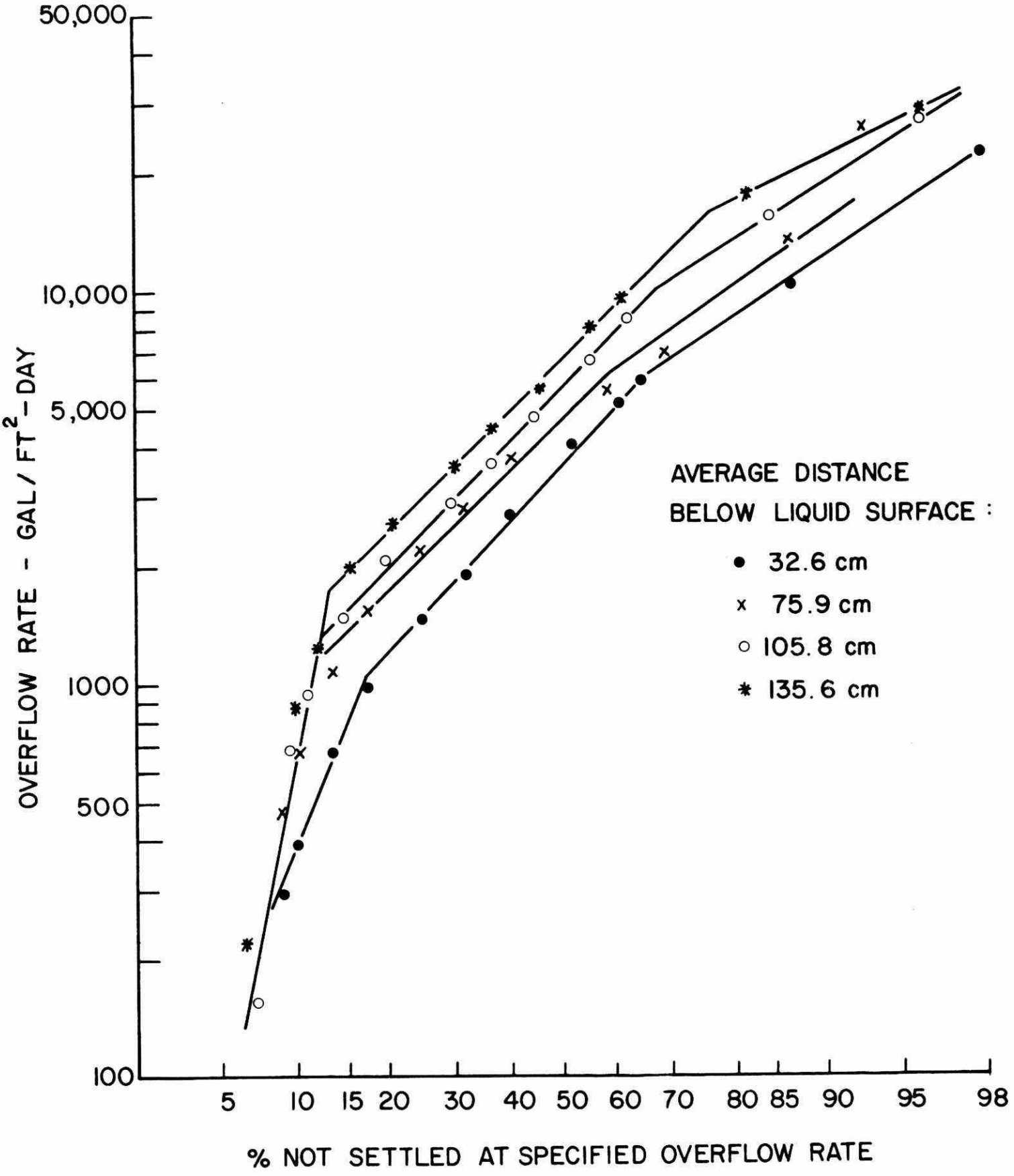

FIGURE 7. SETTLING VELOCITY DISTRIBUTION OBTAINED (FROM FIGURE 6) WITH THE LONG TUBE SETTLER

The velocity distribution at the 32.6 cm depth appears to be in good agreement with typical distributions obtained in the batch settling apparatus test.

2.4.3 Procedural parameters

The following procedural parameters must be chosen when conducting a batch settling apparatus test:

i) stirring rates during rapid and slow mix;
ii) stirring times during rapid and slow mix; and,
iii) elapsed time between the additions of metallic coagulant and polymeric flocculants.

Stirring rates were chosen on the basis of equipment constraints. Stirring rates during rapid mix should be very high (Jorden and Vrale, 1971). The maximum possible with the Phipps and Bird stirrer is 100 rpm. This speed, however, appeared difficult to maintain and, therefore, 90 rpm was chosen instead. The 30 rpm stirring speed during slow mix was chosen on the basis that this was the minimum speed sufficient to keep large flocs in suspension. Both stirring rates correspond closely to the usually recommended values (Ontario Ministry of the Environment, 1972). Procedural parameters (ii) and (iii) were chosen on the basis of the results of optimization tests shown in Figures 8 - 10. The effects of the duration of rapid mix following polymer addition on residual phosphorus concentration and overflow rates are shown in Figure 8. Residual phosphorus concentration appears to be independent of rapid mix time. Rapid mix time only marginally affects the overflow rates required to settle 90% of the flocs, with the effect becoming negligible after 30 seconds. Apparently, a minimum rapid mix time is required to form compact, well settling flocs.

Figure 9 shows that the period of flocculation or slow mix is surprisingly unimportant. Little meaningful difference can be detected in either the residual phosphorus concentration or in permissible overflow rates over the entire flocculation period tested, although a minor improvement may be noted up to about four minutes.

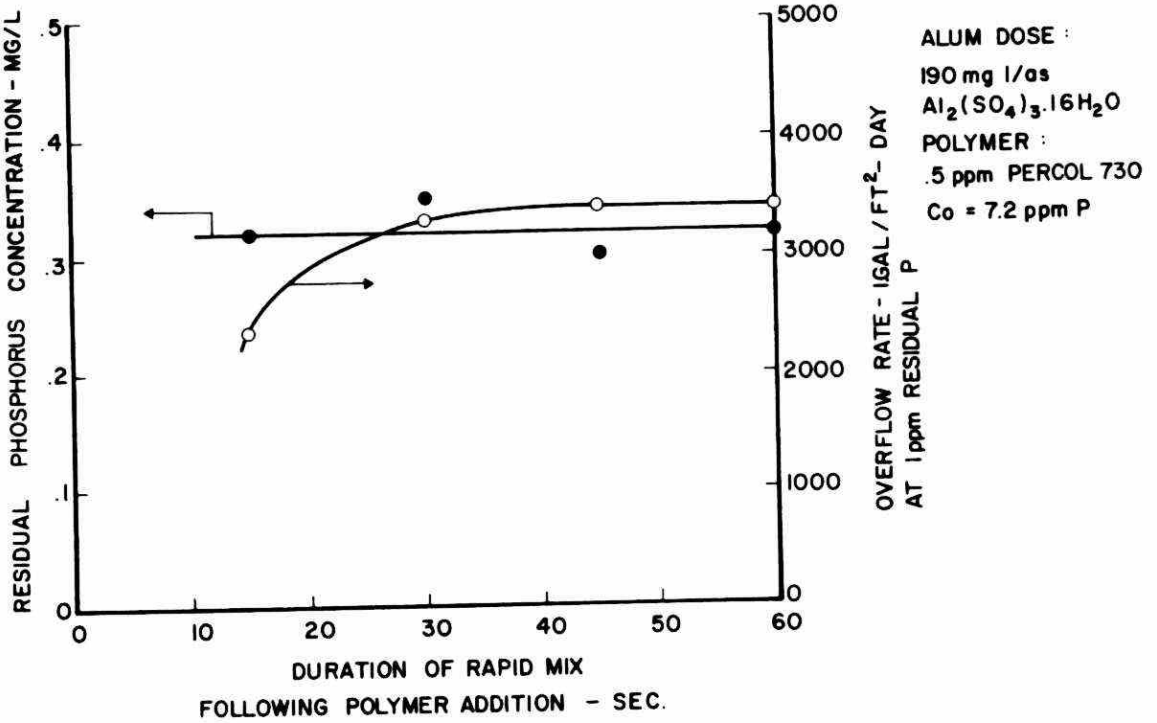

FIGURE 8. RAPID MIXING REQUIREMENTS FOLLOWING POLYELECTROLYTE ADDITION FOR DUNDAS RAW SEWAGE

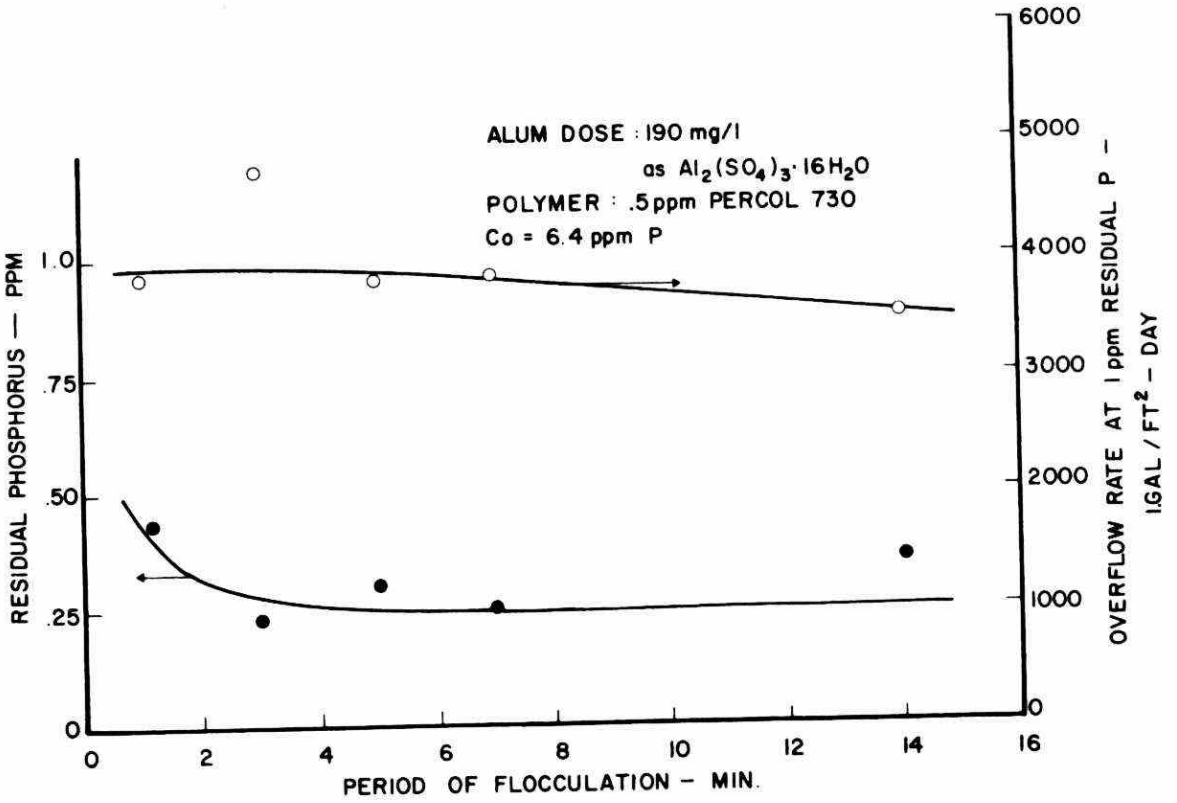

FIGURE 9. FLOCCULATION TIME REQUIREMENTS WITH POLYELECTROLYTE ADDITION FOR DUNDAS RAW SEWAGE

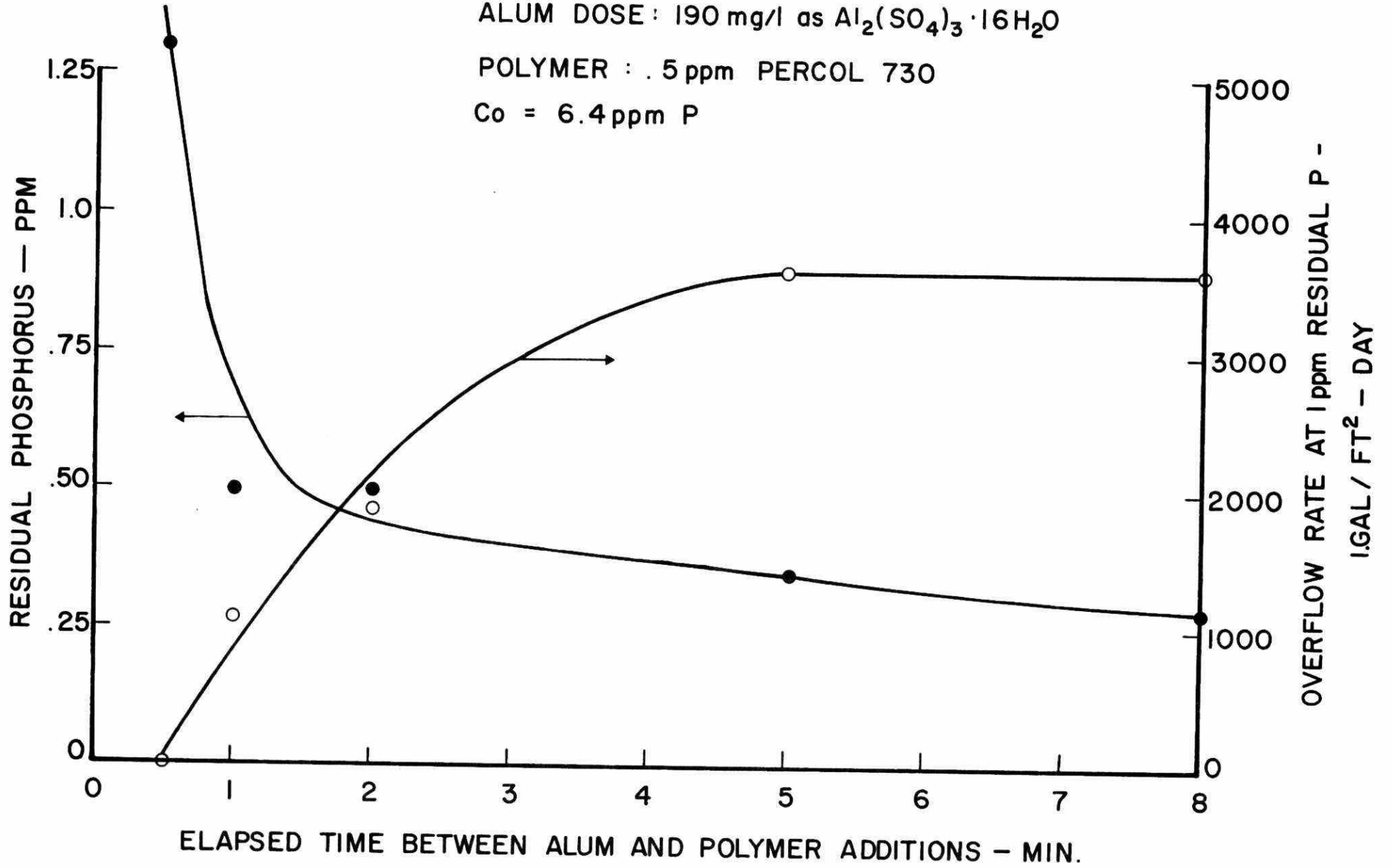

FIGURE 10. TIME DURATION BETWEEN ALUM AND POLYELECTROLYTE ADDITION FOR DUNDAS RAW SEWAGE

On the other hand, the elapsed rapid mix time between coagulant and flocculant addition had a pronounced effect on both residual phosphorus and overflow rates. On the basis of the data shown in Figure 10, a rapid mix time of five minutes appears to be required. The importance of this elapsed time has been noted by Beeghly (1969), who recommended a corresponding stirring time of four minutes. A probable explanation for the importance of this time is that up to the first five minutes, the alum floc is still forming. Thus, flocculant addition prior to this period results in ineffective flocculants buried within the developing flocs. Furthermore, the flocculation of the smaller incompletely formed flocs requires greater polyelectrolyte dosages because of the stoichiometry of flocculation by bridging (Stumm and O'Melia, 1968).

2.5 Conclusions

The following conclusions can be drawn:

1) It is possible to modify the traditional jar test to yield velocity size distributions which, in turn, can be used to estimate floc removal in clarifiers.

2) Settling in the batch settling apparatus has been shown to be unaffected by sampling errors.

3) In a chemical floc, phosphorus precipitate and other suspended solids enmesh. Phosphorus and suspended solids concentrations are equally effective in monitoring settling.

4) The settling rates calculated from the batch settling apparatus tests tend to be conservative due to lack of allowance for flocculation during settling.

5) The following minimum stirring times are recommended for chemical flocculation studies in the batch settling apparatus test:

i) five minutes of rapid mix between coagulant and polymer addition;

ii) one minute rapid mix after polymer addition; and,

iii) a minimum of four minutes of slow mix for flocculation.

3. CHEMICAL AND MECHANICAL SHEAR STABILITY OF POLYELECTROLYTES

3.1 Introduction

Synthetic high molecular weight polyelectrolytes appear to be most promising as flocculants for the rapid settling of colloidal particulate matter from wastewater. There are available a variety of commercial flocculants which are suitable for a range of particulate matter and waters. These are usually classified as anionic, nonionic and cationic. The majority of commercial polymer flocculants are available as solids. Prior to their use as flocculants, stock solutions ($\lesssim$ 0.5 wt%) are prepared and stored at ambient conditions. These very high molecular weight polymers have very small diffusion coefficients and dissolution is rather slow. Mechanical mixing is used to reduce dissolution times to reasonable levels. The longer polymer chains, which may reach molecular weights of 2×10^7 or greater, are more efficient as flocculants but unfortunately are susceptible to shear degradation (Abdel-Alim and Hamielec, 1973). Manufacturers recommend mixing at low shear rates; however, there appears to be no quantitative information published on the stability of a polymer of certain molecular weight at a given level of mechanical shear as might be experienced at the tip of a rotating impeller or at the edge of a baffle. In a recent investigation of the chemical stability of polyacrylamides (Haas and MacDonald, 1972) it was found that small concentrations of ferrous sulphate added to the aqueous polymer solution greatly accelerated polymer chain degradation in the absence of mechanical mixing. The degradation was followed qualitatively by measuring the solution viscosity at different times. No attempt was made to explain the rapid chain degradation in the presence of ferrous sulphate. This information created some concern as to whether some of the many chemical components in wastewaters might have similar effects on the stability of water-soluble polymers used for flocculation. A search of the commercial literature on polymer flocculants revealed no quantitative information on chemical stability.

Having revealed this serious lack of information in the literature, an experimental program was initiated to systematically investigate the chemical and mechanical shear stability of certain commercial poly-

electrolyte flocculants. This section reports on the chemical and mechanical shear stability of the commercial polyelectrolyte flocculants, Percol 730 (anionic polyelectrolyte supplied by Allied Colloids), Purifloc A23 (anionic polyelectrolyte supplied by Dow Chemical Co.) and Polyhall 402 (nonionic flocculant supplied by Stein-Hall Ltd.).

3.2 Experimental

3.2.1 Preparation of polymer stock solutions

The polymers investigated, and some of the properties supplied by manufacturers and measured in this investigation, are given in Table 1.

Figure 11 shows a schematic of the apparatus used to prepare stock solutions of the polymers. It consists of a cylindrical pyrex jar, 5.75 inches I.D. and 8 inches tall immersed in a water-bath, an agitator with a four-bladed turbine type impeller (blades 2.5 inches long and 0.5 inches wide), a homemade solids screw feeder, and a photocell to measure the impeller rpm. Stock solutions having 0.2 wt% polymer were prepared at room temperature. Two litres of distilled water (pH = 7) were charged into the jar and the impeller was rotated at 800-1000 rpm. Polymer was fed into the jar at a constant rate by rotating the screw in the feeder at 500 rpm. A total of 4 gm of polymer was added in this manner. The polymer particles fell onto the surface of the aqueous vortex and were swept singly into the bulk or the water, giving a homogeneous dispersion of water-swollen polymer particles. After complete addition of the polymer, the impeller speed was reduced to 400 rpm and agitation continued until all of the polymer particles had dissolved, based on visual inspection.

Five kinds of experiments were performed. These have been labelled A, B, C, D, and E and their purpose and description follow under separate headings.

3.2.2 Experiment A

This set of experiments was performed to investigate the stability of the polymers with respect to mechanical shear. Stock solutions of the polymers (0.2 wt%) were stirred in the jar with the impeller already described in Section 3.2.1. Impeller speeds in the range 400-1500 rpm were used. Degradation of the polymer chains was followed qualitatively by

TABLE 1. TECHNICAL DATA FOR POLYELECTROLYTE FLOCCULANTS SUPPLIED BY MANUFACTURERS

		Anionic Polymers		Nonionic
Trade Name		PERCOL 730	PURIFLOC A23	POLYHALL 402
Chemical Structure		Monomeric units of acrylamide (AM) and sodium acrylate or acrylic acid 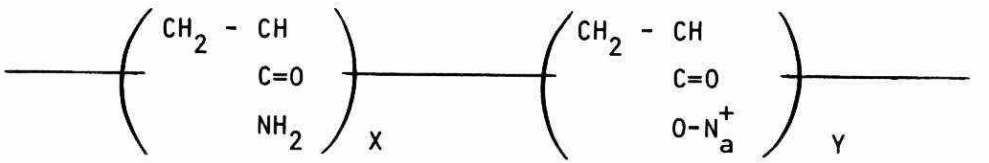		
% Hydrolysis		10	25 - 30	1
Mol. wt. $\bar{M}_w$		1.7×10^{7}*	$\sim 3\text{-}5 \times 10^{6}$	5.8×10^{6}*
0.2 wt% solution at 25°C*	pH	4.8-4.9	10.1	7.7
	Viscosity (cp)	250-270	1000-1100	1300
Manufacturer		Allied Colloids	Dow Chemical	Stein-Hall

* Data measured by present authors. The remaining information was supplied by the manufacturers.

PERCOL 730 is a copolymer of acrylic acid and acrylamide.
PURIFLOC A23 is a copolymer of sodium acrylate and acrylamide.

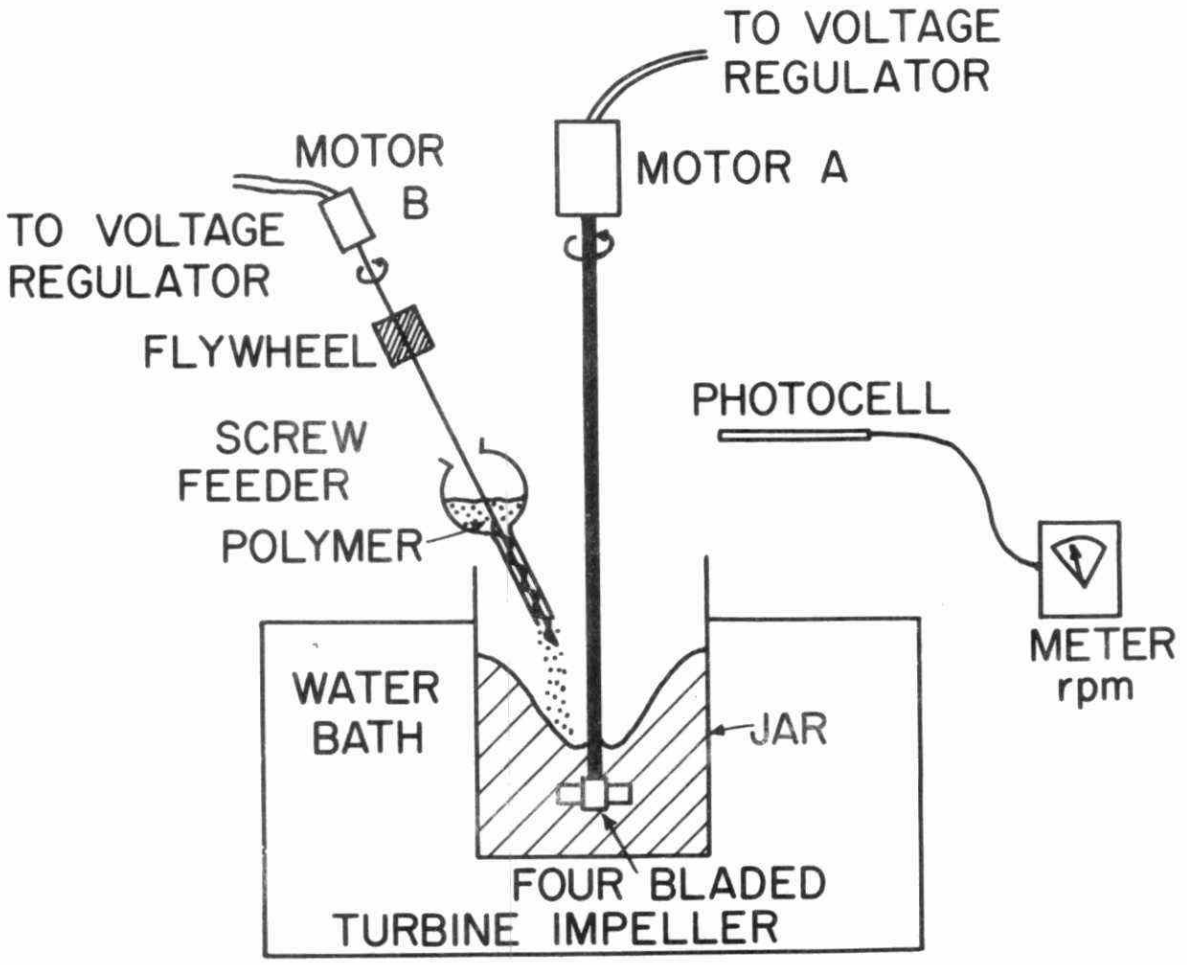

FIGURE 11. APPARATUS USED FOR PREPARATION OF AQUEOUS POLYMER SOLUTIONS

JAR: 4.75 INCH I.D. AND 8 INCH LONG
IMPELLER BLADE SIZE: 2.5 INCH LONG AND 0.5 INCH WIDE
BAFFLES: 0.575 INCH WIDE AND 8 INCH LONG

measuring solution viscosities using a Brookfield viscometer model LVF with a spindle rotation speed of 6 rpm. Some quantitative measurements of chain degradation were made using gel permeation chromatography and electron microscopy. Details of these measurements may be found elsewhere (Abdel-Alim and Hamielec, 1973 and 1974; Ishige and Hamielec, 1973).

3.2.3 Experiment B

This set of experiments was performed to investigate the chemical stability of the polymers in aqueous solution with the reagents $FeSO_4$, Fe_2SO_4 and $Al_2(SO_4)_3$.

Fresh stock solutions of the polymers, containing various amounts of these reagents, were stored in sealed glass bottles in a water bath at 25^oC. The viscosity and pH of these solutions were measured at intervals over a period of 30 days. One experiment was made with a solution free of dissolved oxygen.

3.2.4 Experiment C

This set of experiments was carried out to study the effect of pH on polymer chain conformation. A change in pH can cause a change in solution viscosity due to a reversible change in the effective coil size of a polymer chain (chain conformation). The chain conformation change occurs without breaking any chemical bonds and, therefore, can be reversed with an appropriate pH change.

Solutions of HCl and NaOH were added to fresh stock solutions of the polymers. The dilution effect on viscosity was small. Solution viscosity was measured immediately after the addition of acid or base. To some solutions, NaCl was added to observe its effect on chain conformation. Changes in polymer chain conformation were almost instantaneous upon addition of the reagents.

3.2.5 Experiment D

This set of experiments was carried out to estimate the maximum shear stress which occurs in a polymer solution agitated in a baffled tank with a turbine bladed impeller. A stock solution of Polyhall 402 (0.2 wt%) was agitated continuously at room temperature in the stirred tank shown in

Figure 11. Baffles were used to increase the shear stress and to reduce mixing time. The extent of chain degradation was followed by monitoring the solution viscosity.

Stirring at 1500 rpm was continued until constant viscosity was obtained. At this point, the degraded polyacrylamide was analyzed by gel permeation chromatography to obtain the critical molecular weight. The critical molecular weight is defined as the maximum molecular weight chain which is stable (does not degrade) at the maximum shear stress applied in the polymer solution. The maximum shear stress experienced by the polymer solution can be found using the following equation (Abdel-Alim and Hamielec, 1973).

$$M_c = \frac{3.59 \times 10^8}{\tau^{0.41}}$$

where M_c is the critical molecular weight, and

τ is the maximum applied shear stress in dynes/cm^2.

3.2.6 Experiment E

This set of experiments was performed to establish that higher molecular weight polymer chains are more effective as flocculants. A fresh stock solution of Percol 730 was diluted and evaluated as a flocculant for the removal of colloidal phosphorus compounds from wastewater. The jar test method used in this evaluation was described earlier. Percol 730 was then degraded with mechanical shear as outlined under Experiment A until an appreciable reduction in viscosity was noted (250 cp to 70 cp). This degraded Percol 730 was then evaluated as a flocculant in the same manner as with undegraded Percol 730. The molecular weight distributions of Percol 730, degraded and undegraded, were measured by electron microscopy. Additional proof of irreversible chain degradation was sought by stopping the impeller and observing whether any recovery in solution viscosity occurred over an extended period of several hours.

3.3 Results and Discussion

3.3.1 Preparation of stock solutions

The feed rate of solid polymer with a broad particle size distribution was found to be difficult to control. The gap width between the

screw and feeder tube was critical in obtaining well regulated solids flows. Too large a gap permitted rather large polymer particles to flow into the liquid. These took a long time to be swollen by water and then to dissolve. Too small a gap gave very slow feed rates. The optimum gap size gave a polymer feed time of 10 ± 5 min.

Fresh stock solutions of polymer (0.2 wt%) had viscosities in the range 250-1300 cp.

3.3.2 Experiment A

Figure 12 gives a summary of mechanical degradation obtained with Percol 730. Mixing with an impeller speed of 400 rpm caused no significant change in solution viscosity. At the high impeller speeds of 1000 and 1500 rpm, viscosity reductions were appreciable and irreversible. As would be expected for mechanical shear degradation of macromolecules, the rate and extent of degradation increased with increasing shear rate or rpm and approached limiting values (Abdel-Alim and Hamielec, 1973). The long agitation times required to reach a limiting viscosity are a direct result of the small translational diffusion coefficients of the high molecular weight polymer chains and their need to diffuse to high shear rate zones in the agitated fluid. Degradation of the higher molecular weight chains continues until all of them experience the maximum shear stress. Degradation of polymer chains by mechanical shear may be considered instantaneous (Abdel-Alim and Hamielec, 1973). The molecular weight distributions of degraded and undegraded Percol 730 measured by electron microscopy are shown in Figure 13. The degraded sample was obtained with an impeller speed of 1500 rpm for 15 hr. The viscosity reduction was 250-70 cp. It is clear that polymer chains of higher molecular weight were less stable in a shear field and that chains below a certain molecular weight (in the case of Percol 730, this molecular weight is $\sim 2.5 \times 10^7$) were stable for the applied shear stress.

The results for Purifloc A23 are shown in Figure 14. The viscosity of the fresh stock solution of Purifloc A23 is much larger than that of Percol 730 even though its average molecular weight is considerably smaller. This is undoubtedly due to the greater coil extension experienced by the polyacrylamide with the higher degree of hydrolysis. It is interesting to note that the extended coil conformation is more stable to

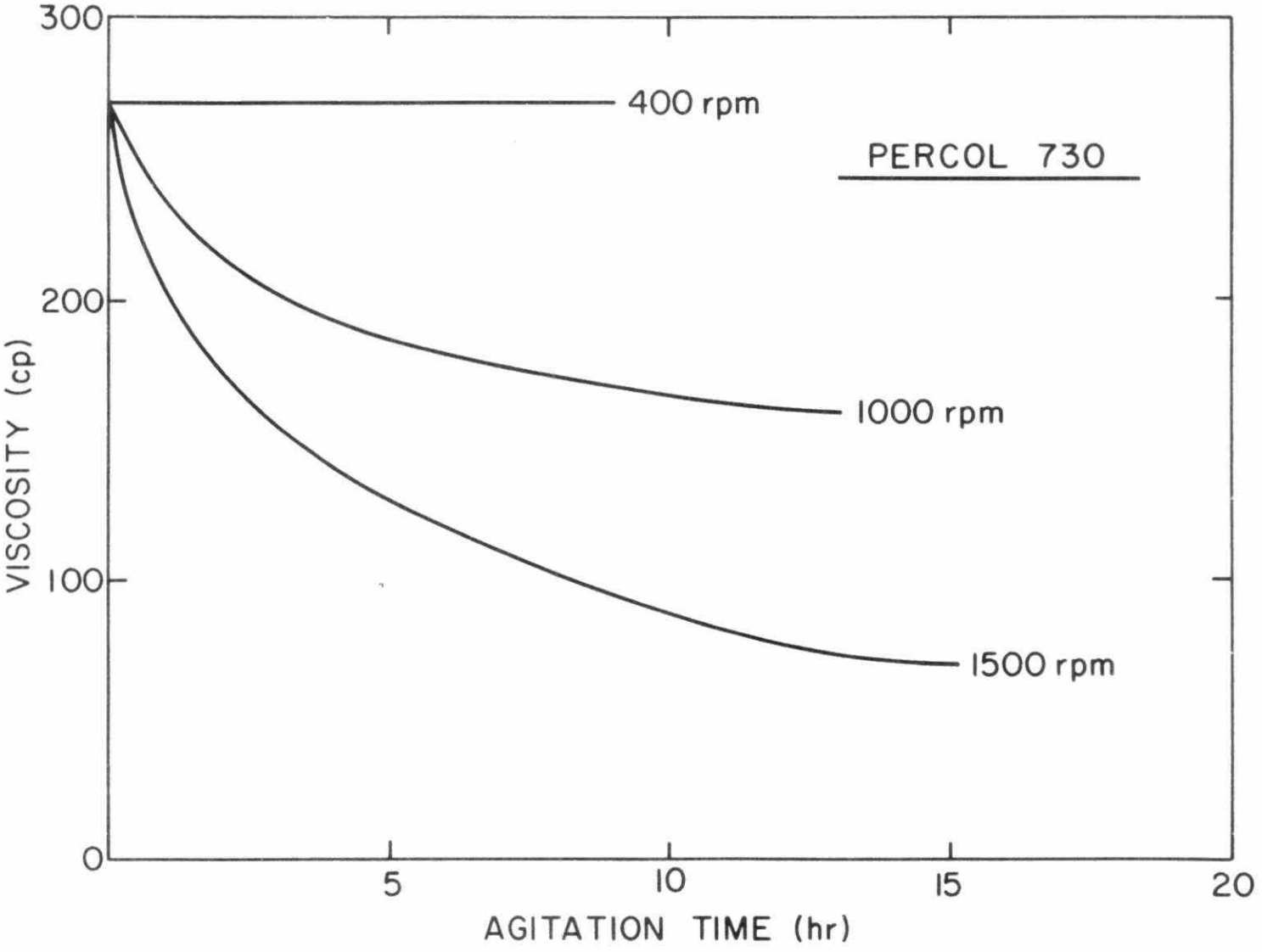

FIGURE 12. MECHANICAL SHEAR STABILITY OF PERCOL 730 - SOLUTION VISCOSITY CHANGE WITH AGITATION TIME (0.2 WT% AT 25°C, pH = 4.8)

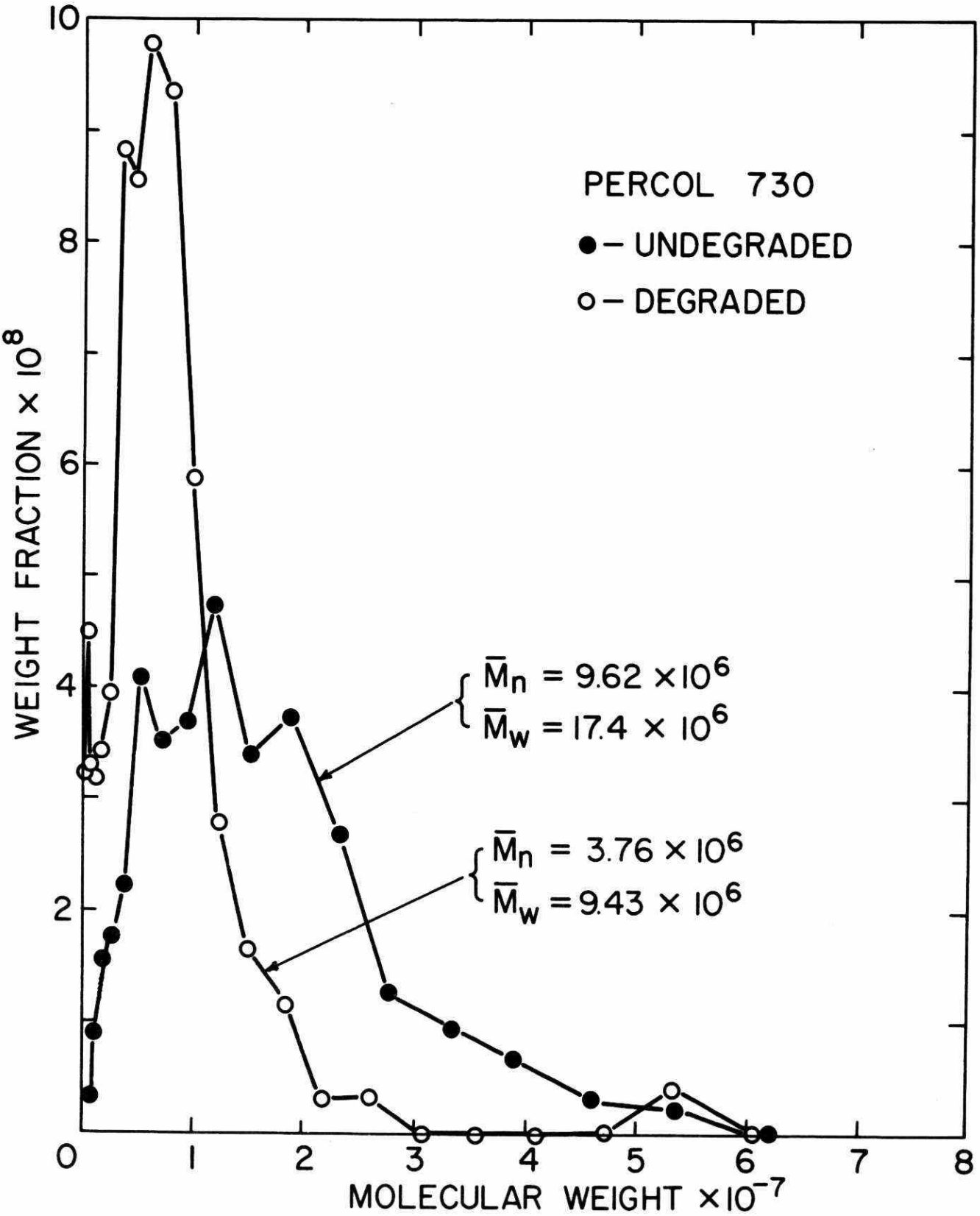

FIGURE 13. MOLECULAR WEIGHT DISTRIBUTION OF UNDEGRADED AND DEGRADED PERCOL 730 MEASURED BY ELECTRON MICROSCOPY

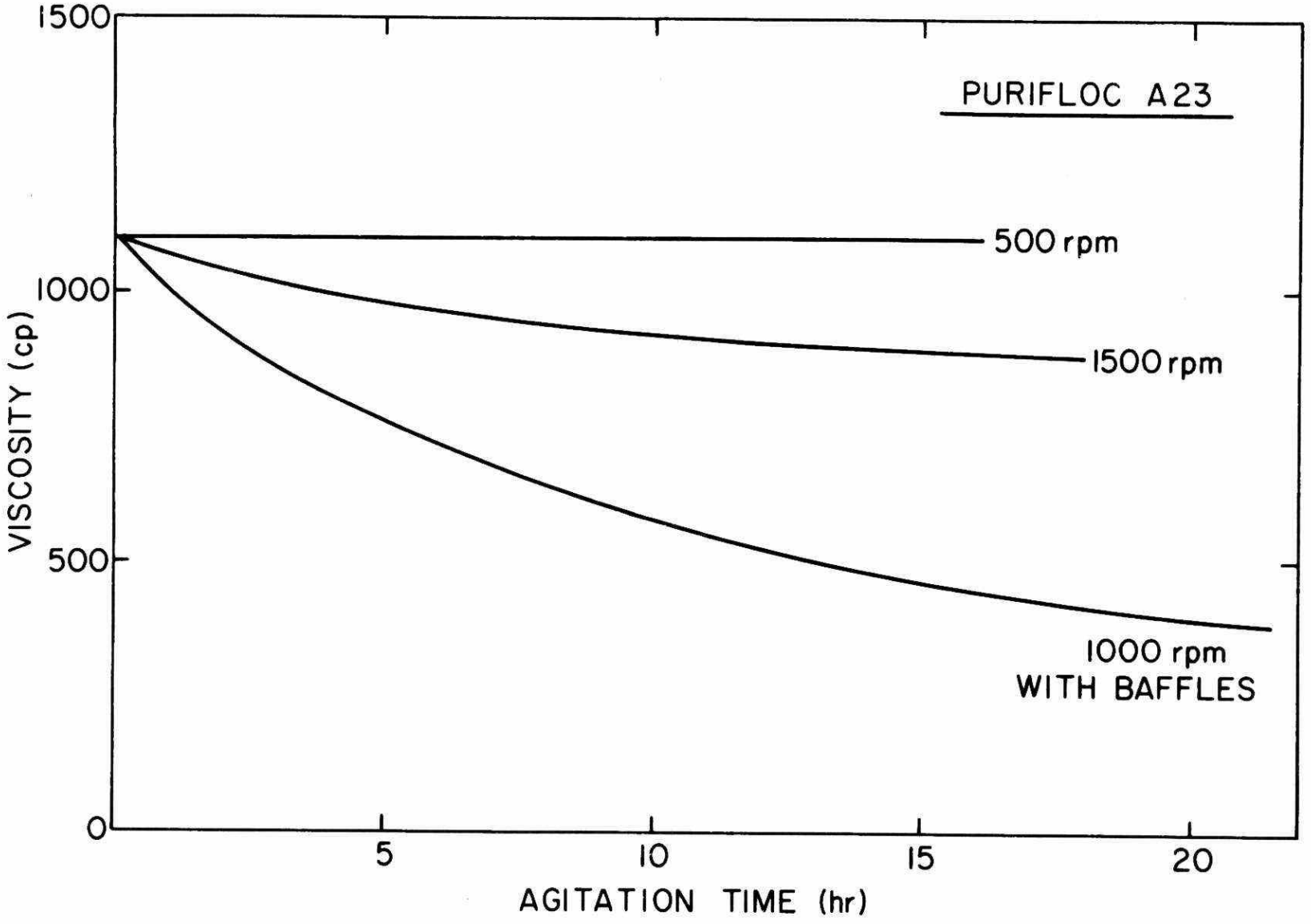

FIGURE 14. MECHANICAL SHEAR STABILITY OF PURIFLOC A23 - SOLUTION VISCOSITY CHANGE WITH AGITATION TIME (0.2 WT% AT 25°C, pH = 10)

shear. This is probably a result of a reduction in the number of chain entanglement points due to intra and interchain repulsion. To increase the degradation rate of Purifloc A23, baffles were employed to give a higher maximum shear stress.

3.3.3 Experiment B

Figures 15 and 16 show results for chemical stability of Percol 730 and Purifloc A23, as influenced by various inorganic reagents which are often used as coagulants for phosphorus removal from wastewater. The iron salts had a rather dramatic effect on the viscosity of Percol 730. This was particularly true with the ferrous salt. On the other hand, Purifloc A23 was stable for all three inorganic reagents.

It is interesting to note that in a solution free of dissolved oxygen, Percol 730 was stable in the presence of ferrous sulphate. Apparently, the degradation was associated with the oxidation of ferrous to ferric iron. Radicals formed during the oxidation may have reacted with the polymer chains. Metal ions may react with dissolved oxygen at low pH and generate radicals which would be responsible for the degradation of Percol 730 in the presence of alum and ferric sulphate. At the higher pH obtained with Purifloc A23 this may not occur. No definite statements can be made.

3.3.4 Experiment C

Figure 17 shows the effect of pH on the viscosity of an aqueous solution of Percol 730. pH was changed by adding either NaOH or HCl. Starting with the initial solution (dark circle in Figure 17), the viscosity can be increased by adding NaOH and raising the pH, or decreased by adding HCl and lowering the pH. Viscosity changes are due to changes in polymer chain conformation with an extended conformation favoured at higher pH. At higher hydrogen ion concentrations, negative charges on the polymer chain were neutralized causing chain contraction. With increase in pH the opposite was true. A significant viscosity recovery can be obtained by returning to the original pH with appropriate additions of acid or base. This is evidence for reversible chain conformation. It is not clear why more complete viscosity recovery was not obtained.

3.3.5 Experiment D

Figure 18 shows the change in viscosity of an agitated solution

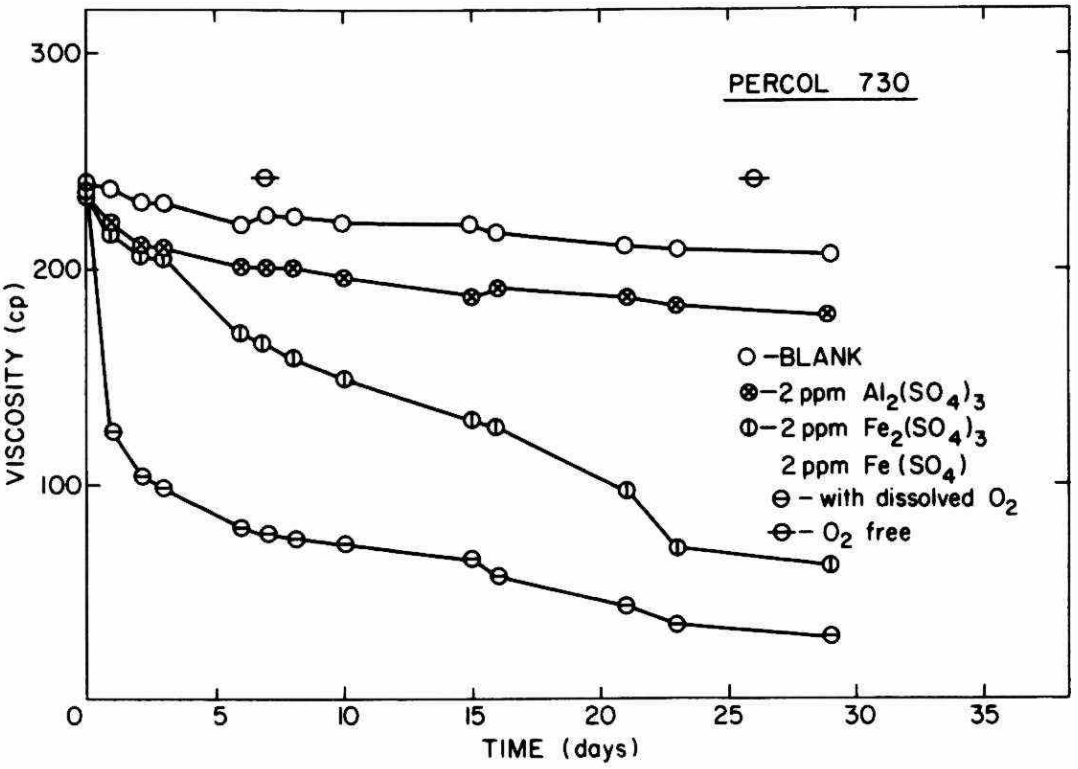

FIGURE 15. CHEMICAL STABILITY OF PERCOL 730 - SOLUTION VISCOSITY CHANGE WITH TIME (0.2 WT% AT 25°C, pH = 4.8)

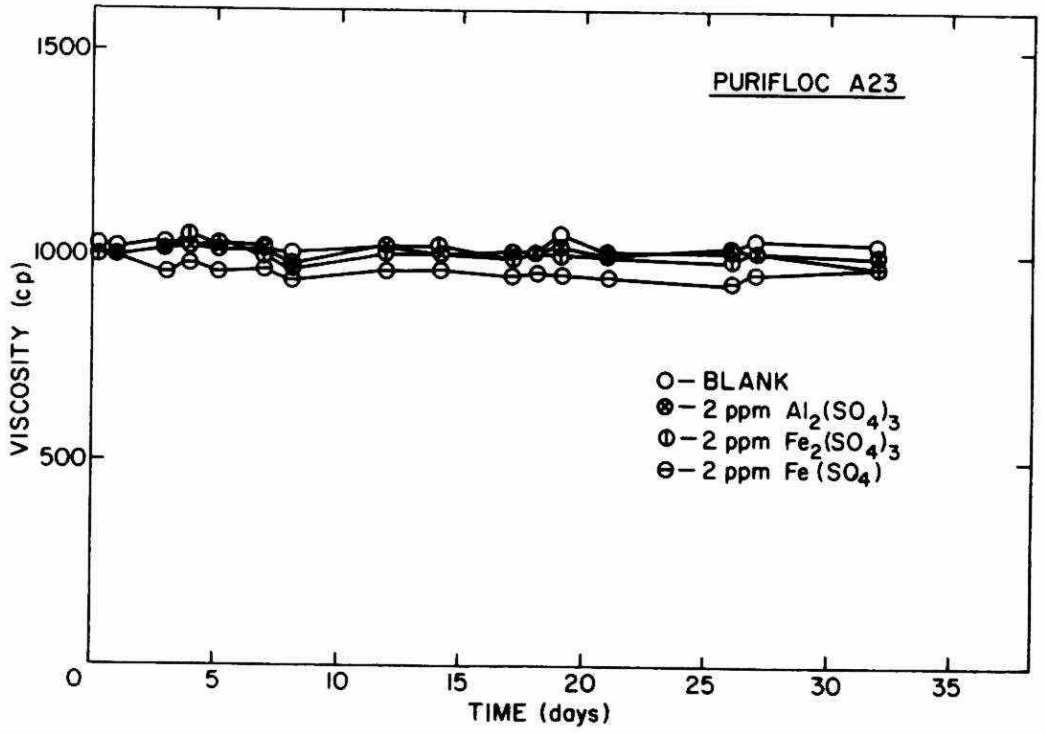

FIGURE 16. CHEMICAL STABILITY OF PURIFLOC A23 - SOLUTION VISCOSITY CHANGE WITH TIME (0.2 WT% AT 25°C, pH = 10)

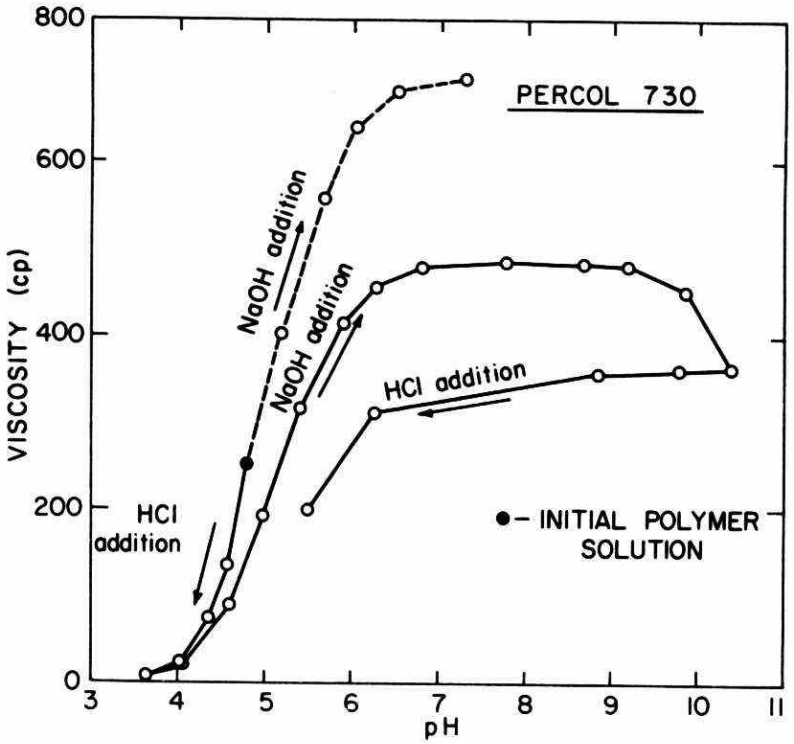

FIGURE 17. POLYMER CHAIN CONFORMATION OF PERCOL 730 - SOLUTION VISCOSITY CHANGE WITH pH (0.2 WT% AT 25°C)

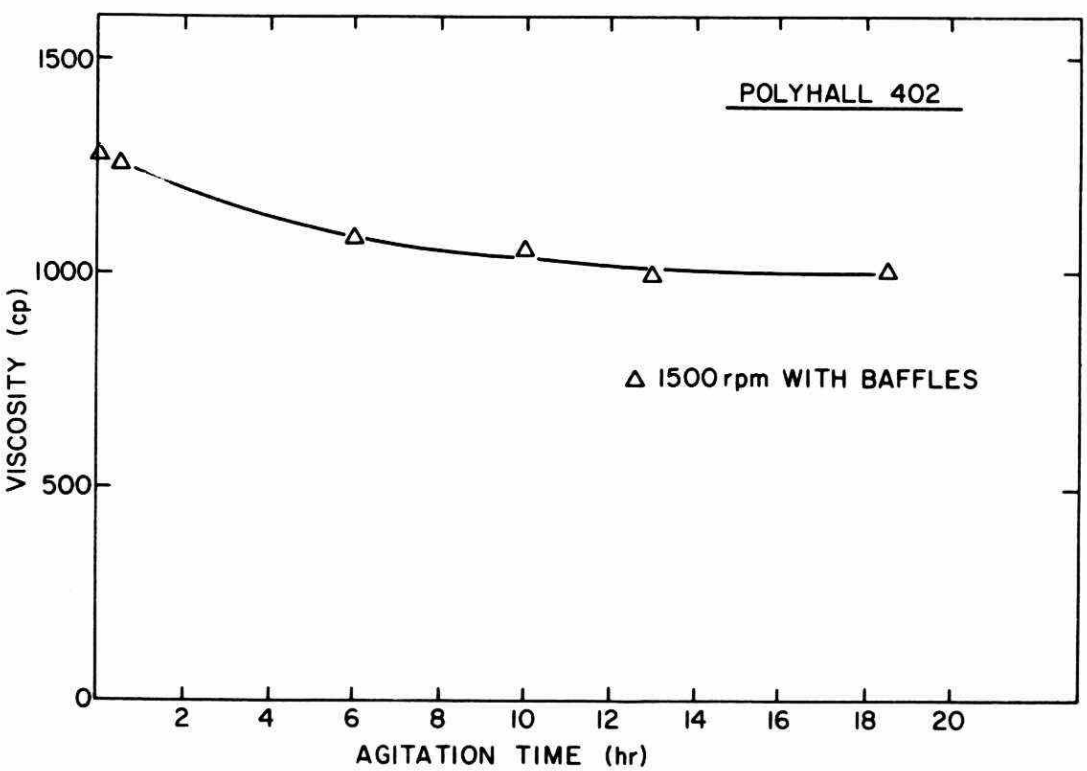

FIGURE 18. MECHANICAL SHEAR DEGRADATION OF POLYHALL 402 - SOLUTION VISCOSITY CHANGE WITH AGITATION TIME (0.2 WT% AT 25°C, pH = 7.7)

of Polyhall 402. Baffles were used to increase the maximum shear stress and thus reduce the time required to reach a limiting viscosity. A limiting viscosity is reached when all of the polymer molecules greater than a certain molecular weight have experienced the maximum shear stress applied. The molecular weight distributions of the undegraded and degraded Polyhall 402 (polymer which reached the limiting viscosity) were measured by gel permeation chromatography. The chromatograms are shown in Figure 19. The critical retention volume of 21.5 counts is equivalent to a critical molecular weight of 1.9×10^7. In other words, polymer molecules of molecular weight smaller than 1.9×10^7 were stable in a solution of limiting viscosity 1000 cp experiencing the maximum shear stress supplied by the turbine-bladed impeller at 1500 rpm in the baffled jar. An examination of the two chromatograms in Figure 19 clearly shows that polymer molecules with molecular weights smaller than 1.9×10^7 were degraded. This is a result of the higher initial solution viscosity (1300 cp) and concomitant higher maximum shear stress at zero time. In addition, during startup of the impeller, polymer chains may be broken before they can disentangle and adjust to the new shear environment. Employing the relationship for polyacrylamide:

$$M_c = \frac{3.59 \times 10^8}{\tau^{0.41}}$$

developed by Abdel-Alim and Hamielec (1973) for the stirred tank, the maximum shear stress is found to be about 1300 dynes/cm^2. Thus, a novel technique for the estimation of the maximum shear stress in a vessel with a complex mixing pattern is presented. The method should be applicable to systems involving liquids other than water. In these instances, appropriate polymers must be employed.

3.3.6 Experiment E

Figure 20 shows settling curves for undegraded and degraded Percol 730. The phosphorus concentration ratio C/C_o versus time is a measure of the floc settling rate, with a rapid reduction in C/C_o indicating a rapid settling rate. It is clear that the larger polymer chains are much more efficient flocculants (see the molecular weight distributions in Figure 13). An optimal molecular weight distribution might be monodisperse with a molecular weight of 25×10^6.

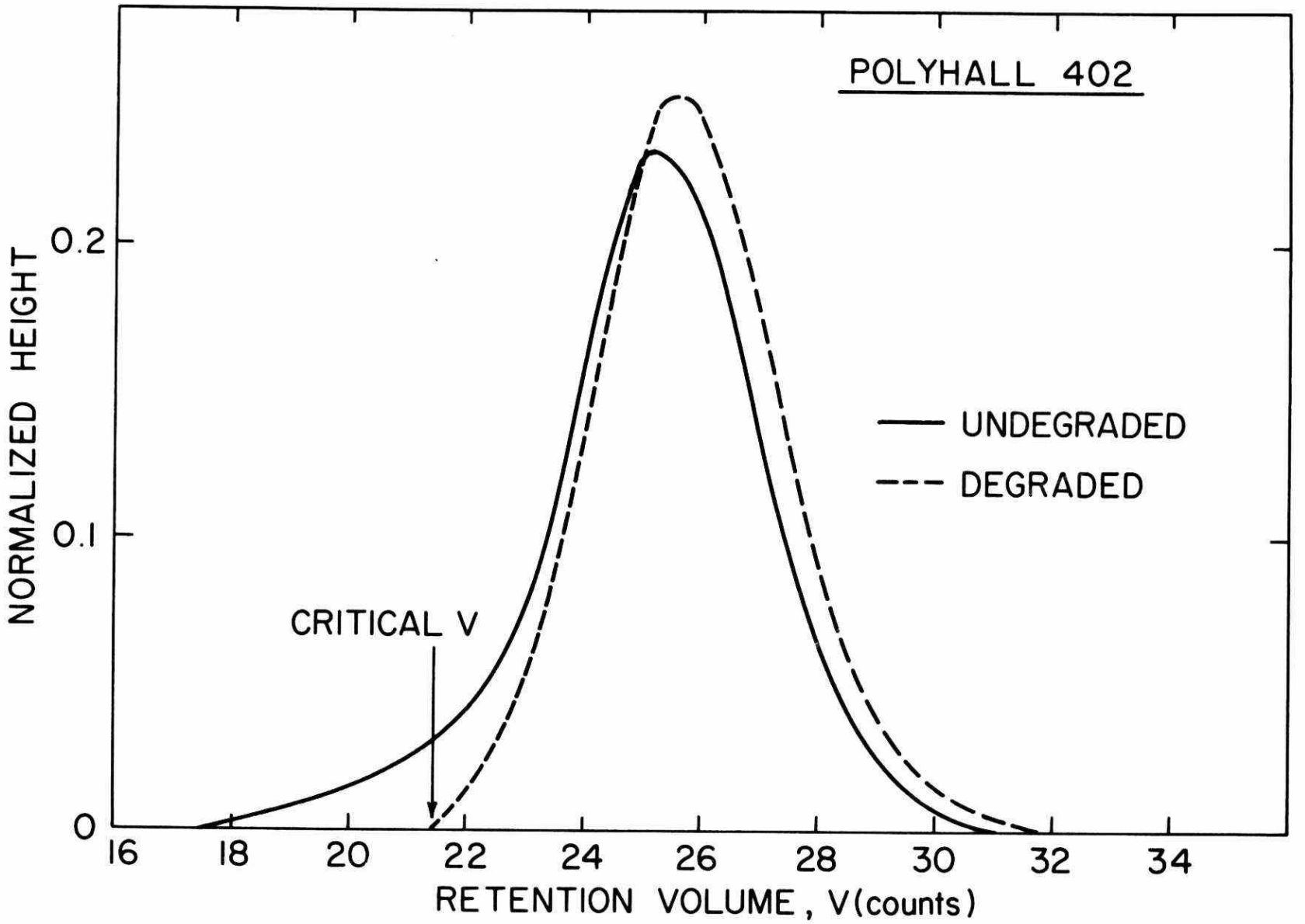

FIGURE 19. GEL PERMEATION CHROMATOGRAPHY - CHROMATOGRAPHS FOR UNDEGRADED AND DEGRADED POLYHALL 402

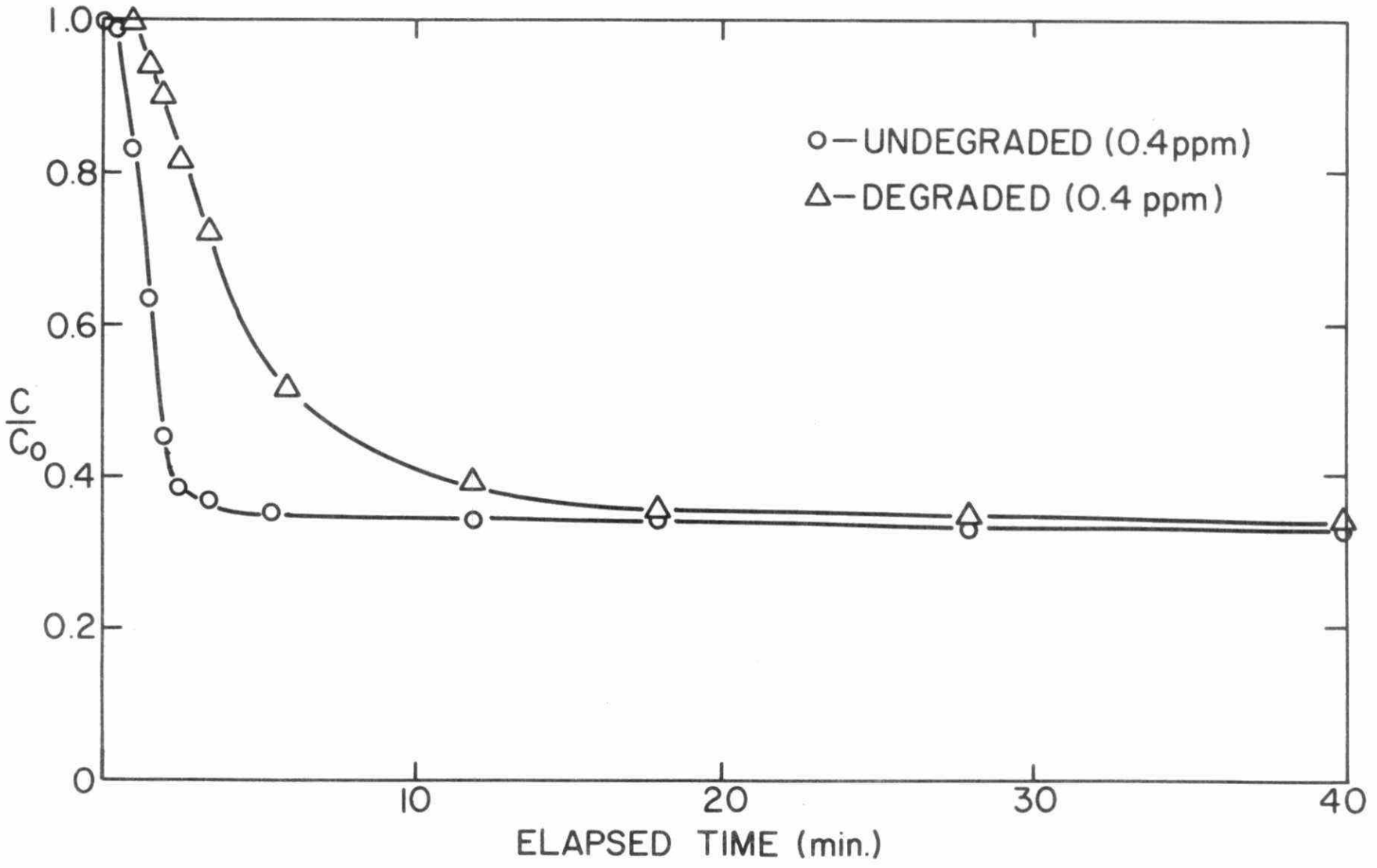

FIGURE 20. SETTLING CURVES FOR THE REMOVAL OF COLLOIDAL PHOSPHORUS COMPOUNDS BY POLYMER FLOCCULANTS - PERCOL 730 WITH DIFFERENT MOLECULAR WEIGHT DISTRIBUTIONS (ALUMINUM TO PHOSPHORUS RATIO = 1, INITIAL PHOSPHORUS CONCENTRATION: 5 PPM AS P-50% ORTHO, 10% PYRO, 40% TRIPOLY)

4. SETTLEABILITY OF METAL PHOSPHATE FLOCS

4.1 Introduction

As discussed in Section 2, the primary reason for applying polyelectrolytes in phosphorus removal is to increase the settling rate of precipitated flocs. An examination of the literature, however, revealed an almost total lack of settling rate data for precipitated phosphorus flocs in domestic wastewater. This kind of information is essential for the proper understanding and application of polyelectrolytes. Therefore, the objective of this section was to generate the base case data on phosphate precipitation in the absence of polyelectrolytes. These data will be compared, in Section 5, to similar data in the presence of polyelectrolytes.

More specifically, this section examines "ultimate" or residual phosphorus concentration and settling rate as a function of:

(i) metal coagulant precipitant type (alum, iron salts and lime) and dosage;
(ii) pH and alkalinity; and
(iii) phosphate species.

As domestic wastewater is a highly variable entity, probability plots (see Section 6) are required to establish trends. Thus, model phosphate solutions were used in the experiment of this section to avoid the extensive repetition of data points necessitated by probability plots.

4.2 Experimental

4.2.1 Overall procedure

The experimental apparatus and procedure for this experiment was the batch settling apparatus described in detail in Section 2.

The pH of each settling vessel was measured at the conclusion of each experiment. The samples collected during the tests were acidified with four drops of concentrated sulphuric acid and analyzed for total phosphate with the Technicon Auto-Analyzer according to Technicon's industrial method 4-68 W.

4.2.2 Model solutions

Two types of model wastewater solutions were utilized in these studies: an "orthophosphate" system made up in distilled water containing 15 ppm P, and a "mixed phosphate" system containing 15 ppm P of 50% ortho, 10% pyro and 40% tripoly phosphates. In addition to phosphates, the solutions contained 200 mg/l $NaHCO_3$ when alum was used, while with iron, solution buffering was provided with 100 mg/l of $CaCO_3$. When lime $Ca(OH)_2$ was used as the coagulant, the model solutions usually contained 100 mg/l as $CaCO_3$ of $NaHCO_3$ and 5 mg/l of $MgCl_2 \cdot 6H_2O$ as Mg.

4.2.3 pH control

The desired ultimate pH in each test was obtained by adding 1.2 N NaOH (6.2 N NaOH with the lime runs) or 1.0 N HCl to the model solutions prior to coagulant addition. The amount of acid or base required was determined from sets of pH control curves shown in Figures 93 to 100 in Appendix A. These curves were prepared with model jar tests to determine ultimate pH as a function of acid, base and metal coagulant dosage.

Figures 101 to 104 (Appendix A) show the initial solution alkalinity as a result of base and acid addition for several model solutions.

4.3 Results and Discussion

4.3.1 Al, Fe, and Ca equilibrium

The extent of phosphorus precipitation is a function of the solubility of the precipitate. The equilibrium solubility (Stumm and Morgan, 1970) of the most important precipitates is shown as a function of pH in Figure 21. The minimum solubility of the most important phosphate precipitates occurs near pH 6 for $AlPO_4$, near pH 5 for $FePO_4$ and in a pH range above 9 for $Ca_{10}(OH)_2(PO_4)_6$. Precipitation of the hydroxides of the cations (e.g., $Al(OH)_3$, $Fe(OH)_3$, $Mg(OH)_2$) competes with phosphorus precipitation. The metal hydroxides are highly insoluble over a wide pH range as shown in Figure 21. The hydroxide flocs are potentially important as nucleation sites for flocculation and can also enmesh near colloidal

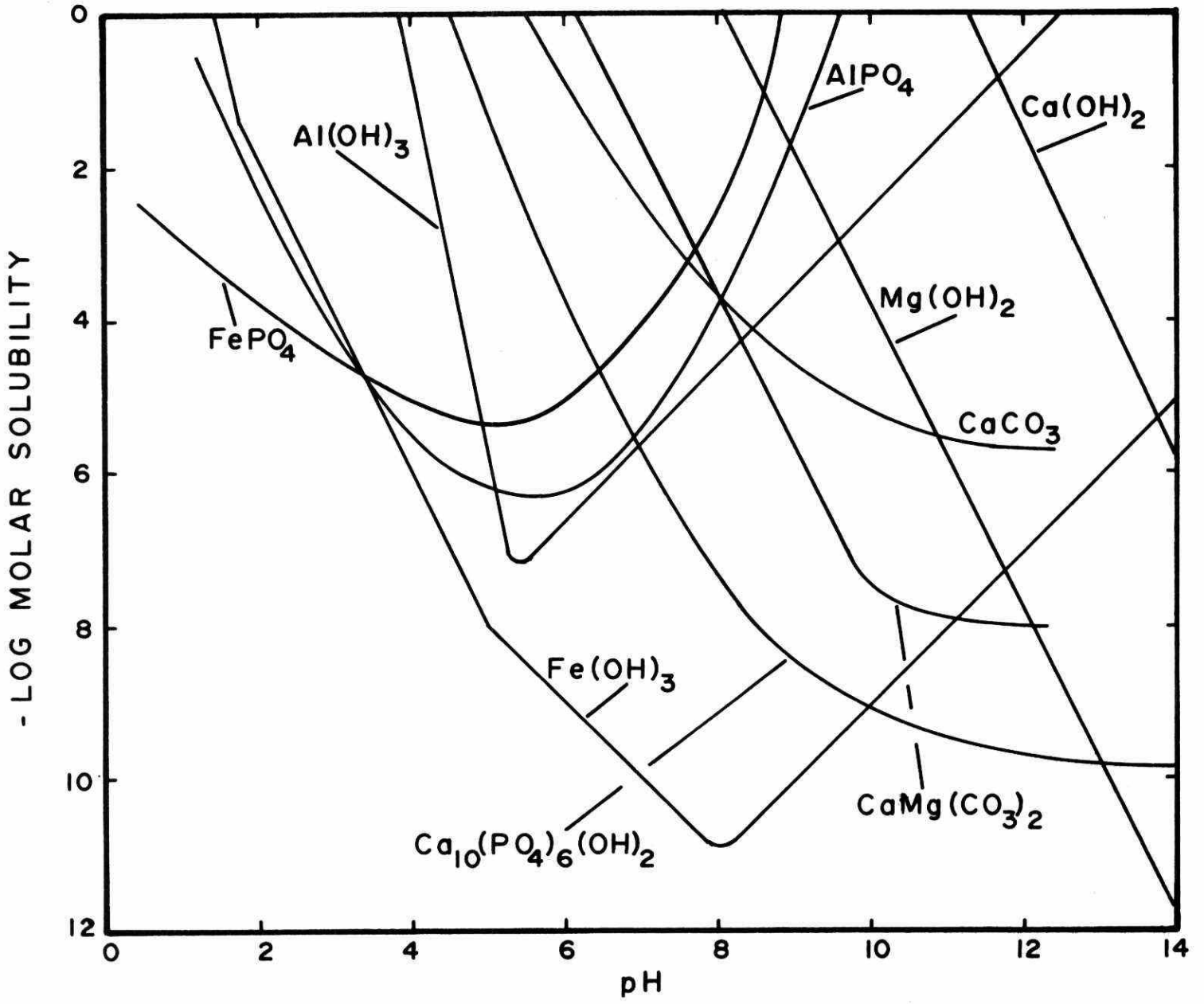

FIGURE 21. EQUILIBRIUM SOLUBILITY OF IMPORTANT PRECIPITATES IN THE METAL COAGULANT-PHOSPHATE MODEL SOLUTION SYSTEM (CALCULATED ON THE BASIS OF SOLUBILITY AND EQUILIBRIUM CONSTANTS LISTED IN STUMM AND MORGAN, 1970)

particles and adsorb PO_4^{-3} ions. The precipitation of calcium carbonate, in the lime system, interacts similarily with phosphorus precipitates.

4.3.2 Ultimate phosphorus residual

Contour diagrams of the ultimate settled phosphorus residuals as a function of M:P (metal to phosphate) molar ratio and pH are presented in Figures 22 and 23 for aluminum, 24 and 25 for iron, and 26 for calcium. There were insufficient data for a contour diagram with calcium in the orthophosphate system. The limited data obtained are shown in Figure 105 of Appendix A. The contour diagrams are based on Figures 106 to 110 for aluminum, 111 to 118 for iron and 119 to 122 for lime, in Appendix A. The ultimate phosphorus removal is defined at the point where the slope of the settling curve is zero (see Section 2).

Phosphorus removal, as shown on the contour diagrams, follows the equilibrium of aluminum phosphate, iron phosphate and calcium phosphate shown in Figure 21. The difference between the equilibrium solubility curves and the removal curves results from settling effects (i.e., the formation of nonsettleable near colloidal precipitate), the presence of miscellaneous ions in the system (see Section 4.3.7) and the formation of metal hydroxides.

The spacing between contour lines parallel to the coordinates indicates the importance of the respective coordinate.

For the aluminum - orthophosphate system in Figure 22, removal was independent of pH below an Al:P ratio of 1.5. Above Al:P = 1.5, removals were both pH and Al:P ratio dependent. Optimum pH for phosphorus removal occurred between 6 to 6.5; the sharpness of this optimum and, therefore, pH dependence increased with percent removal. Both increasing and decreasing pH from the optimum required higher Al dosages for the same removal. As the pH is raised from 6 to 8, the required Al:P ratio rises from 2 to 5 for 90% removal. 99% removal is possible with an Al:P ratio of 4.5, at the optimum pH.

Inorganic domestic wastewater phosphates in Ontario consist of a mixture of ortho and condensed phosphates. For the mixed phosphate model solution, the phosphate mixture was chosen to approximate the phosphate composition of influents to several southern Ontario wastewater treatment

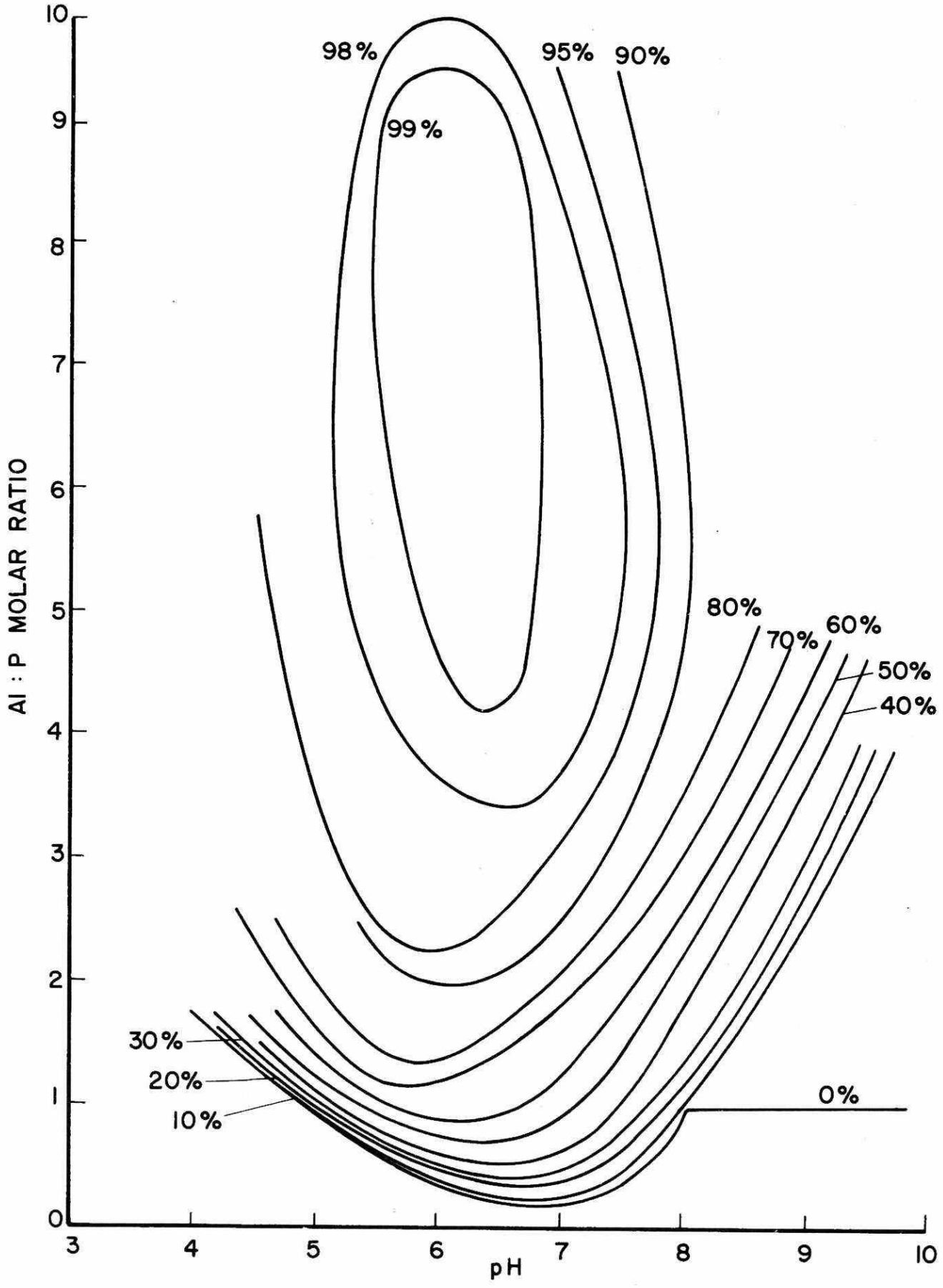

FIGURE 22. PHOSPHORUS REMOVAL CONTOUR IN THE ALUMINUM-ORTHOPHOSPHATE SYSTEM

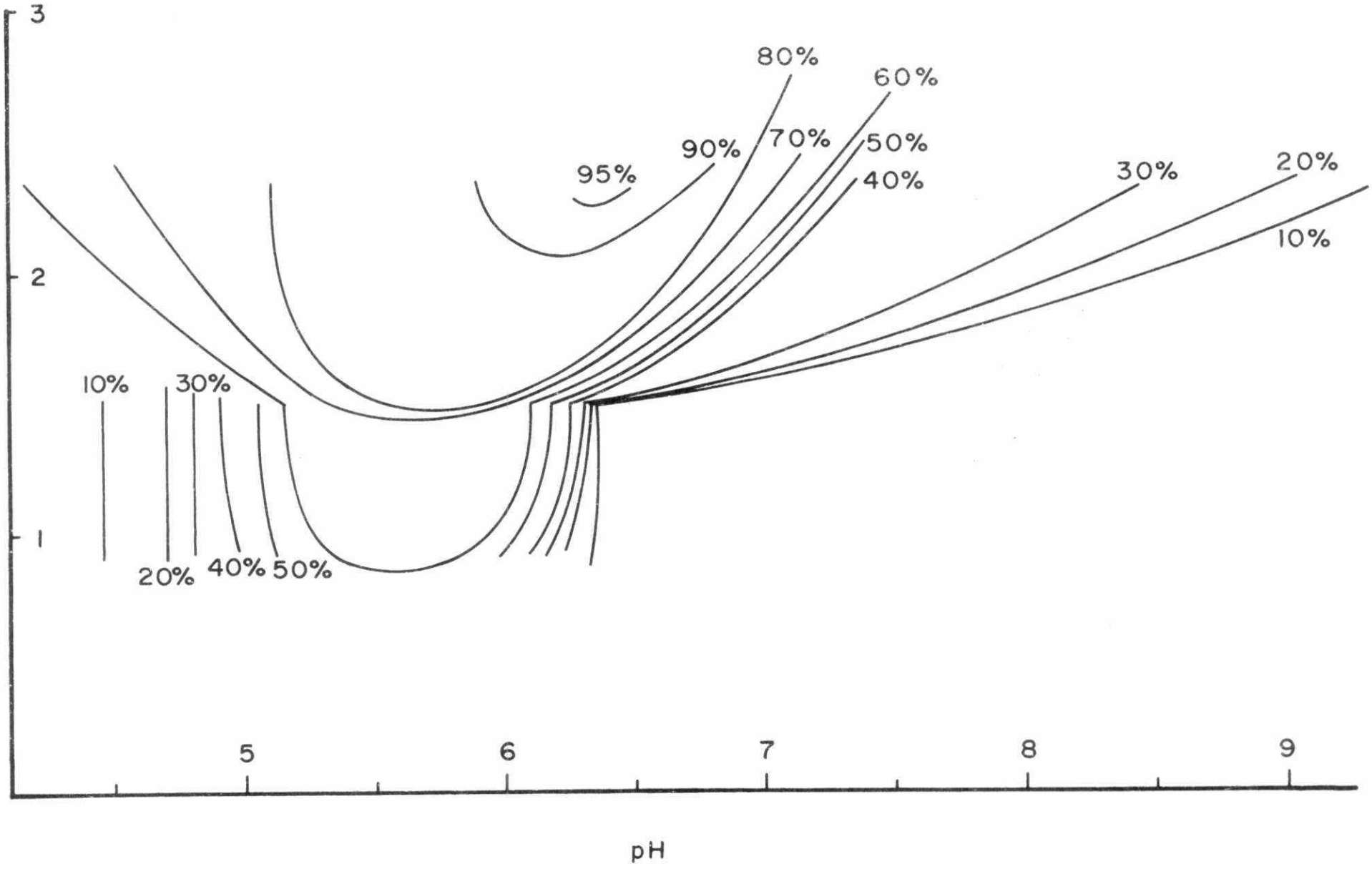

FIGURE 23. PHOSPHORUS REMOVAL CONTOUR IN THE ALUMINUM-MIXED PHOSPHATE SYSTEM

plants in 1971 (Melnyk, 1971). During the course of the present study, the percentage of the orthophosphate rose to approximately 80% (see Section 6) due to the compulsory reduction of condensed phosphates in detergents.

For the aluminum - mixed phosphate system, the phosphorus removals shown in Figure 23 were quite similar to the orthophosphate data in Figure 22. The optimum pH and the Al:P ratios required to accomplish a certain removal percentage were almost identical near the optimum pH. Thus, for example, 90% phosphorus removal is possible with Al:P = 2.3 in the pH range of 5.9 to 6.6. The major difference between Figures 23 and 22 is the apparent narrowing of the favourable pH range in the presence of condensed phosphates. This narrowing of the pH range for equal phosphorus removal in the presence of condensed phosphates was also observed by Nilsson (1969) in an alum - domestic wastewater system.

Phosphorus removal in the iron - orthophosphate system, shown in Figure 24, was independent of pH below the Fe:P ratio of 1.5, as shown by contour lines nearly parallel to the pH axis. Above Fe:P = 1.5, the pH exerts increasing influence and a broad optimum pH range develops around pH 6, if the peculiarity exhibited at Fe:P ratios of 1.5 to 2 below pH 6 is neglected. This peculiarity is probably related to the fact that the optimum pH from equilibrium considerations (see Figure 21) occurs at pH 5 rather than 6. A phosphorus removal of 90% is possible with an Fe:P ratio of 1.5 in the pH range of 5 to 6.5. As the pH is raised to 8, the Fe dosage required is raised to 2 as Fe:P. At an Fe:P ratio of 3, 99% removal is possible at pH 6, indicating the advantage of iron (on stoichiometric bases) if high phosphorus removal is under consideration.

The iron data also indicate comparable phosphorus removals in the ortho and mixed phosphate systems. In Figure 25 for removals below 90%, however, the pH range shifted toward the acid side and below pH 5, the required Fe dosage for equal removal was slightly reduced. For example, at an Fe:P ratio of 2.0, the pH range for 90% removal was 4.7 to 7.4 for the mixed phosphate system and 5.1 to 8.0 for the orthophosphate system.

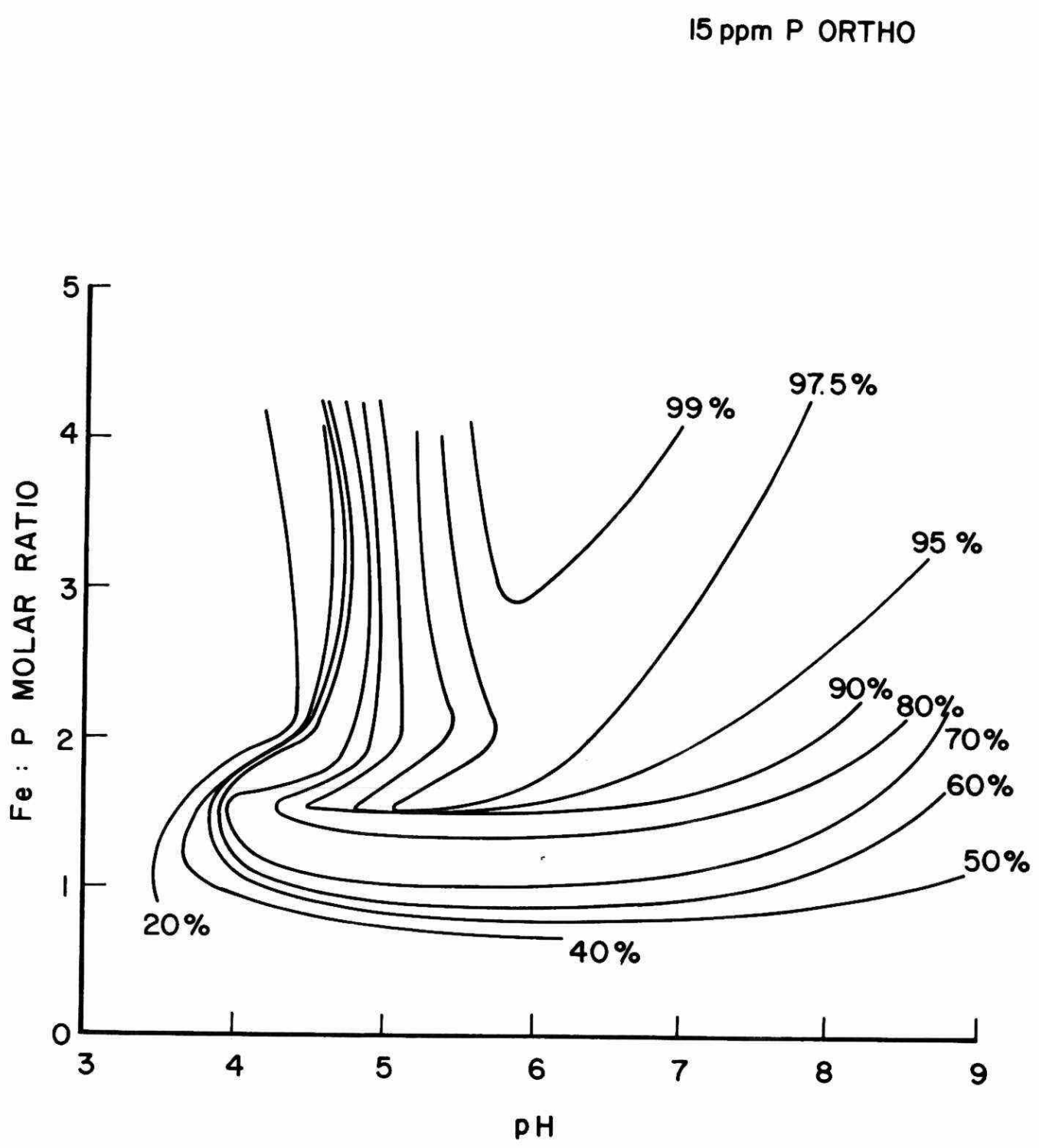

FIGURE 24. PHOSPHORUS REMOVAL CONTOUR IN THE IRON-ORTHOPHOSPHATE SYSTEM

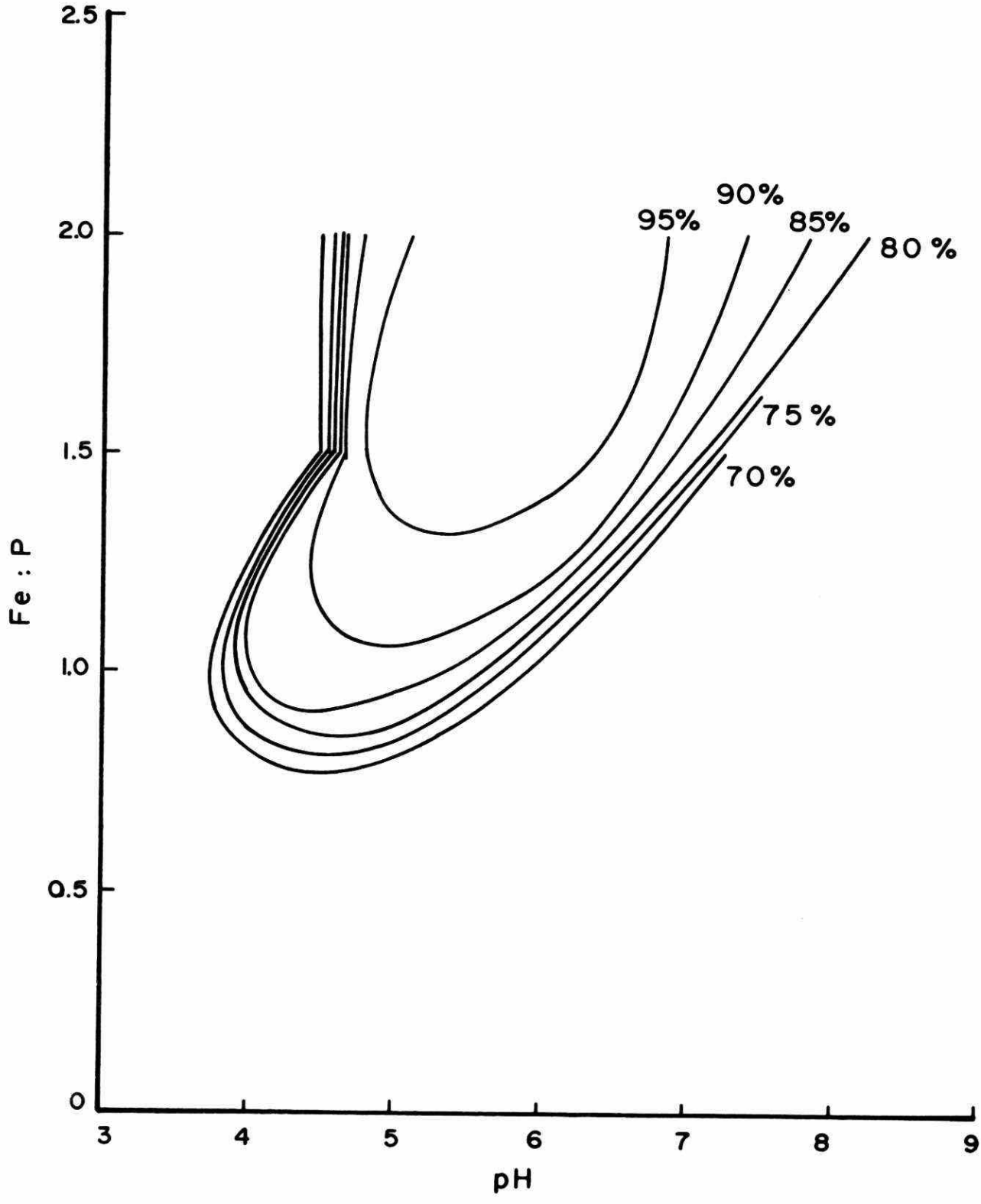

FIGURE 25. PHOSPHORUS REMOVAL CONTOUR IN THE IRON-MIXED PHOSPHATE SYSTEM

Calcium (lime) precipitation of phosphorus generated a contour diagram (Figure 26) different from those generated by aluminum and iron in that the removal curves do not exhibit a limiting upper pH and a 90% removal plateau exists around pH 10. Figure 26 also exhibits a threshold Ca:P ratio of 1.5, below which phosphate precipitation is minimal regardless of pH. The four most probable precipitates (see Figure 21) in the model solution would by hydroxyl apatite ($Ca_{10}[PO_4]_6[OH]_2$), calcium carbonate ($CaCO_3$), dolomite ($CaMg[CO_3]_2$) and magnesium hydroxide ($Mg[OH]_2$). The threshold concentration noted in Figure 26 is believed to result from the competition for calcium by the carbonate and the apatite precipitates. The carbonate calcium requirement in this model solution is:

$$100 \text{ mg/l } CaCO_3 \times \frac{\text{m mole}}{100 \text{ mg}}$$

$$= 1 \text{ m mole } Ca^{++}$$

$$= 2.07 \text{ in terms of Ca:P}$$

and the phosphorus requirement is:

$$15 \text{ mg/l} \times \frac{\text{m mole}}{31 \text{ mg}} \times \frac{5 \text{ m mole } Ca^{++}}{3 \text{ m mole P}} =$$

$$= 0.807 \text{ in terms of Ca:P.}$$

Thus, up to the threshold Ca:P ratio, carbonate precipitation appears to be dominated, and apparently, 72.5% (1.5 x 100/2.07) of the carbonate must be precipitated prior to the initiation of phosphorus removal. As noted in Section 4.3.3, below, at this low dosage kinetics may interfere with the results as well.

A slight increase in Ca dosage above the threshold Ca:P ratio rapidly increases removals above pH 9. Below pH 9, the pH exerts a strong influence, while above pH 9, both Ca dosage and pH are important variables. Ninety percent phosphorus removal is possible on the plateau bordered by the pH range of 9.3 to 11.3 and Ca:P ratios of 2.5 to 6, and 99% removal can be achieved at pH 12.2 with a Ca:P ratio of 4.

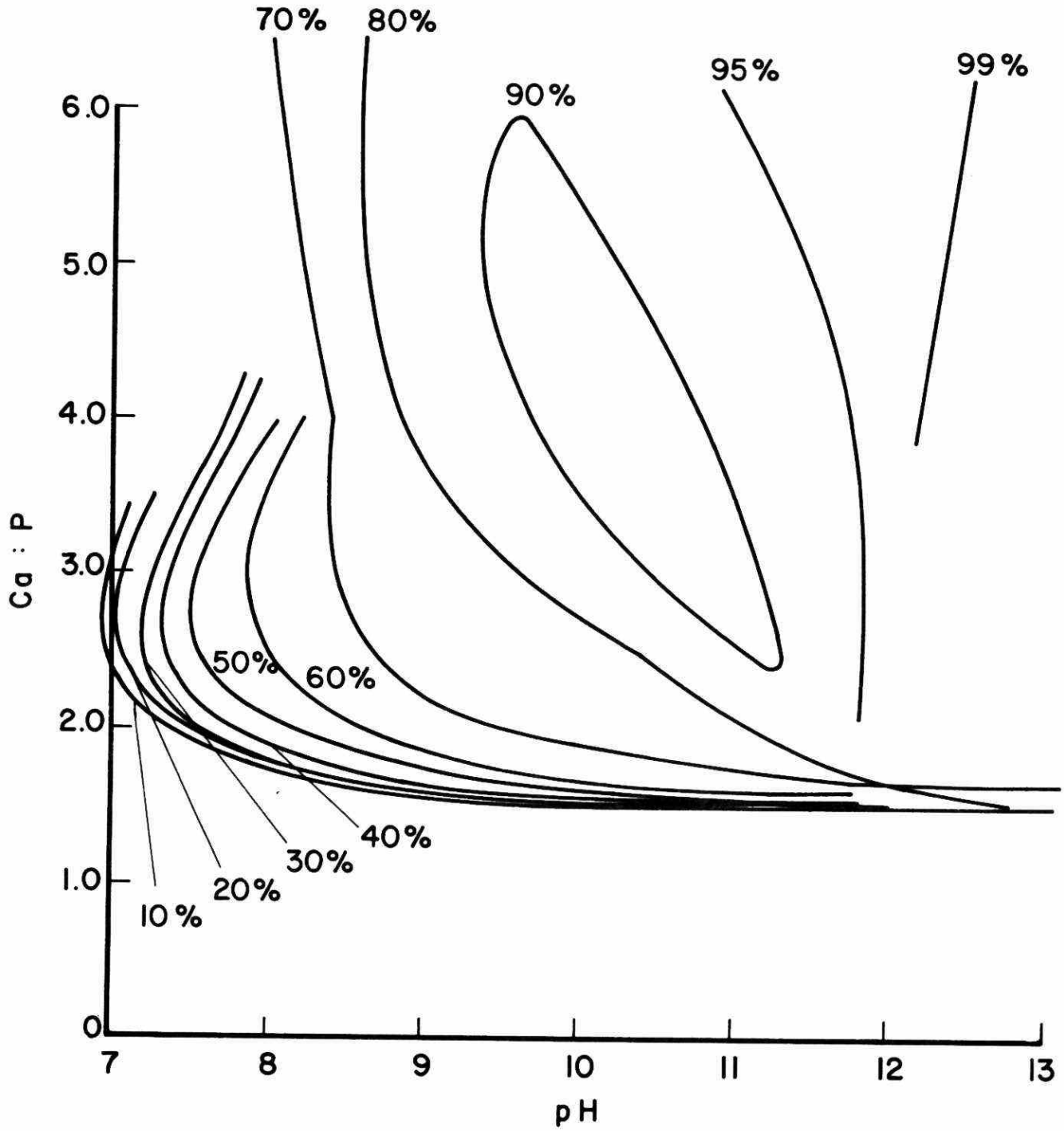

FIGURE 26. PHOSPHORUS REMOVAL CONTOUR IN THE CALCIUM-MIXED PHOSPHATE SYSTEM

4.3.3 Formation of near colloidal particles

In the aluminum - mixed phosphate system, a considerable amount of near colloidal particles were formed at all dosages, especially at pH levels above 6.5, as shown in Figure 27. The presence of near colloidal particles is shown by the difference in phosphorus removal between the curves in Figure 27 representing settled and 0.45μ membrane filtered samples. The charge on the near colloidal particles is strongly negative, especially at the higher pH levels, as shown in Figure 28. The lower electrolyte mobility of the orthophosphate system in Figure 28, particularly at higher pH, confirms the shift in precipitation toward lower pH with condensed phosphates. Furthermore, in both systems the electrophoretic mobility should be less negative than -25 μ/sec/volt/cm for effective phosphorus removal.

The iron system behaved similarly to the aluminum system in terms of the pH range of near colloidal particle formation; however, fewer such particles were formed with iron, particularly at low pH as shown in Figure 29. As shown in Figure 30, phosphorus precipitation and the formation of near colloidal particles was strongly influenced by reaction time at the lowest lime dosage (Ferguson et al, 1973; Ferguson and McCarty, 1969). At both 90 minutes and 17 hours, a large fraction of near colloidal particles formed below pH 11.5. The gap in phosphorus removal at the two times indicates a slow reaction rate and possibly a slow particle aggregation rate as well. At a higher calcium dosage, the reaction proceeded to essential completion by the end of the usual sampling period.

4.3.4 Settling

The maximum permissible overflow rates for 90% of the ultimate phosphorus removal (i.e., 90% of the settleable flocs) with aluminum and iron in the orthophosphate system are shown in Figures 31 and 32. Permissible overflow rates are a function of coagulant dosage. Typical clarifier design overflow rates (600-800 lgpd/ft^2) are exceeded at an Al:P ratio of 9.2 only for aluminum and an Fe:P ratio of $\geq$ 2 for iron at pH between 5 to 7.5. While the overflow rate curve for aluminum is fairly flat (particularly as the dosage is increased) a sharp rise in overflow rate is observed at about pH 5 with iron. This point coincides

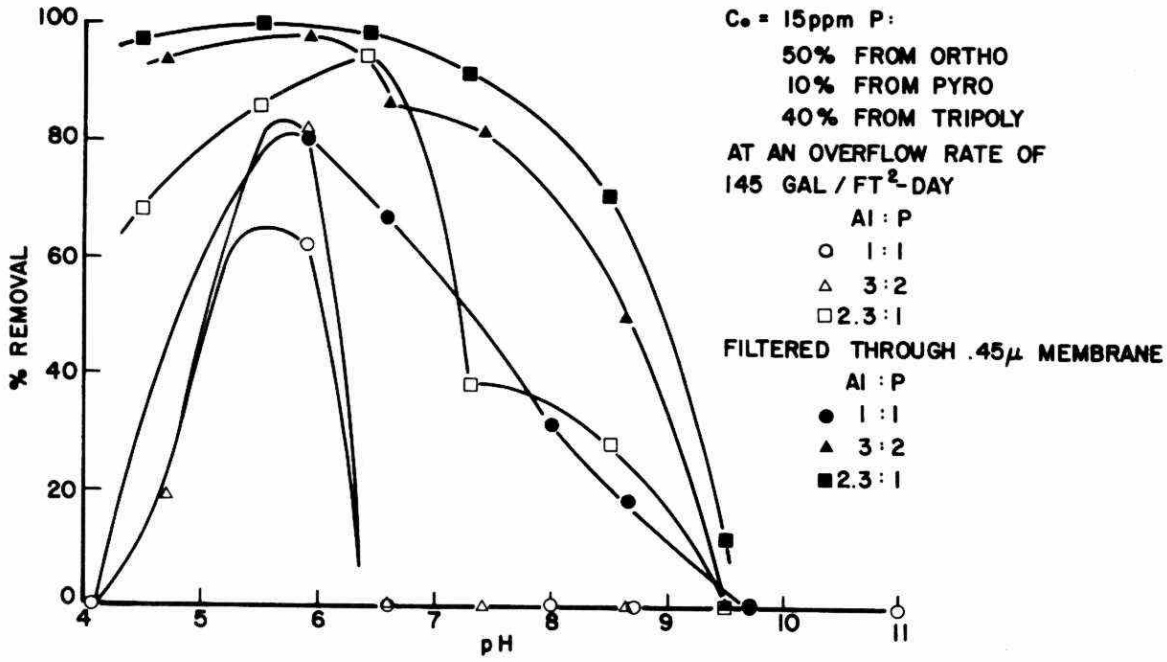

FIGURE 27. UNSETTLEABLE FLOCS IN THE ALUMINUM-MIXED PHOSPHATE SYSTEM

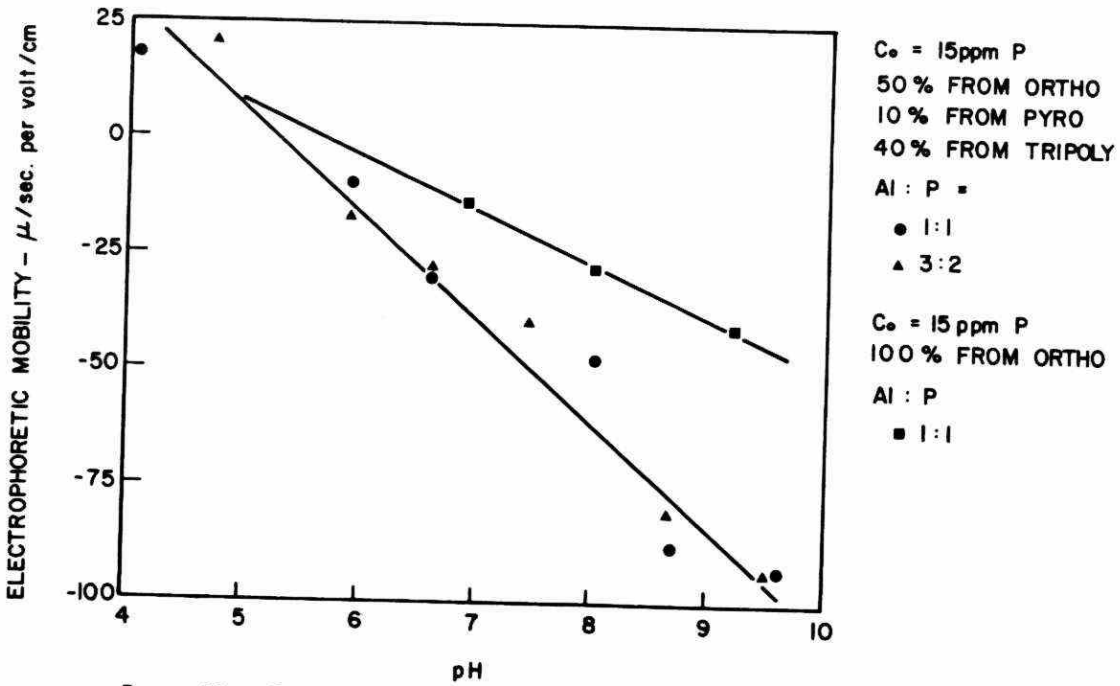

FIGURE 28. ELECTROPHORETIC MOBILITY OF PRECIPITATE IN THE ALUMINUM-PHOSPHATE SYSTEM

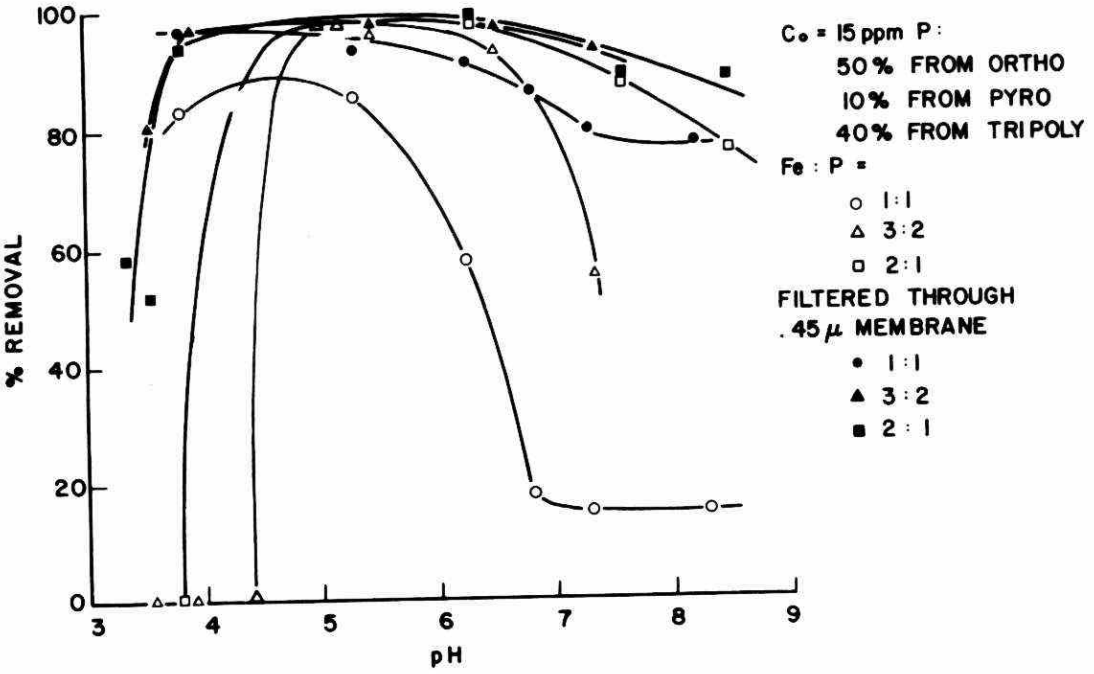

FIGURE 29. UNSETTLEABLE FLOCS IN THE IRON-MIXED PHOSPHATE SYSTEM

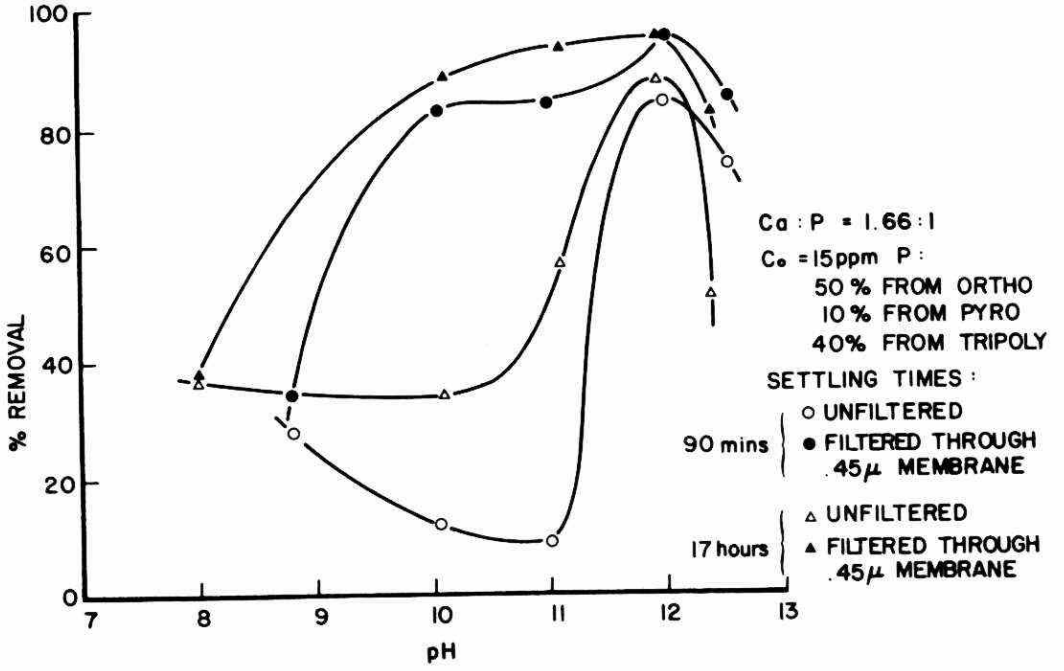

FIGURE 30. UNSETTLEABLE FLOCS IN THE CALCIUM-MIXED PHOSPHATE SYSTEM

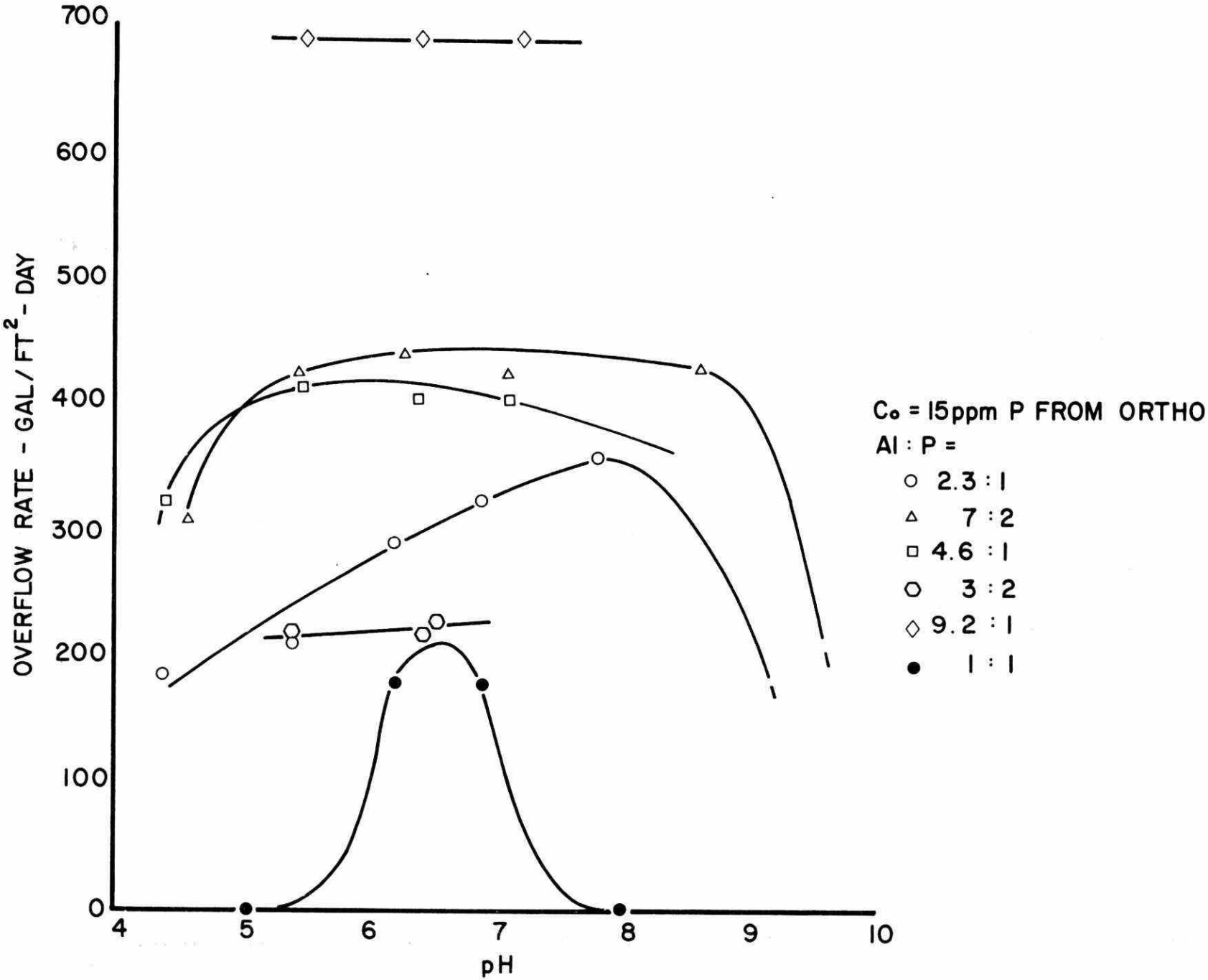

FIGURE 31. MAXIMUM PERMISSIBLE OVERFLOW RATES FOR 90% FLOC REMOVAL IN THE ALUMINUM-ORTHOPHOSPHATE SYSTEM

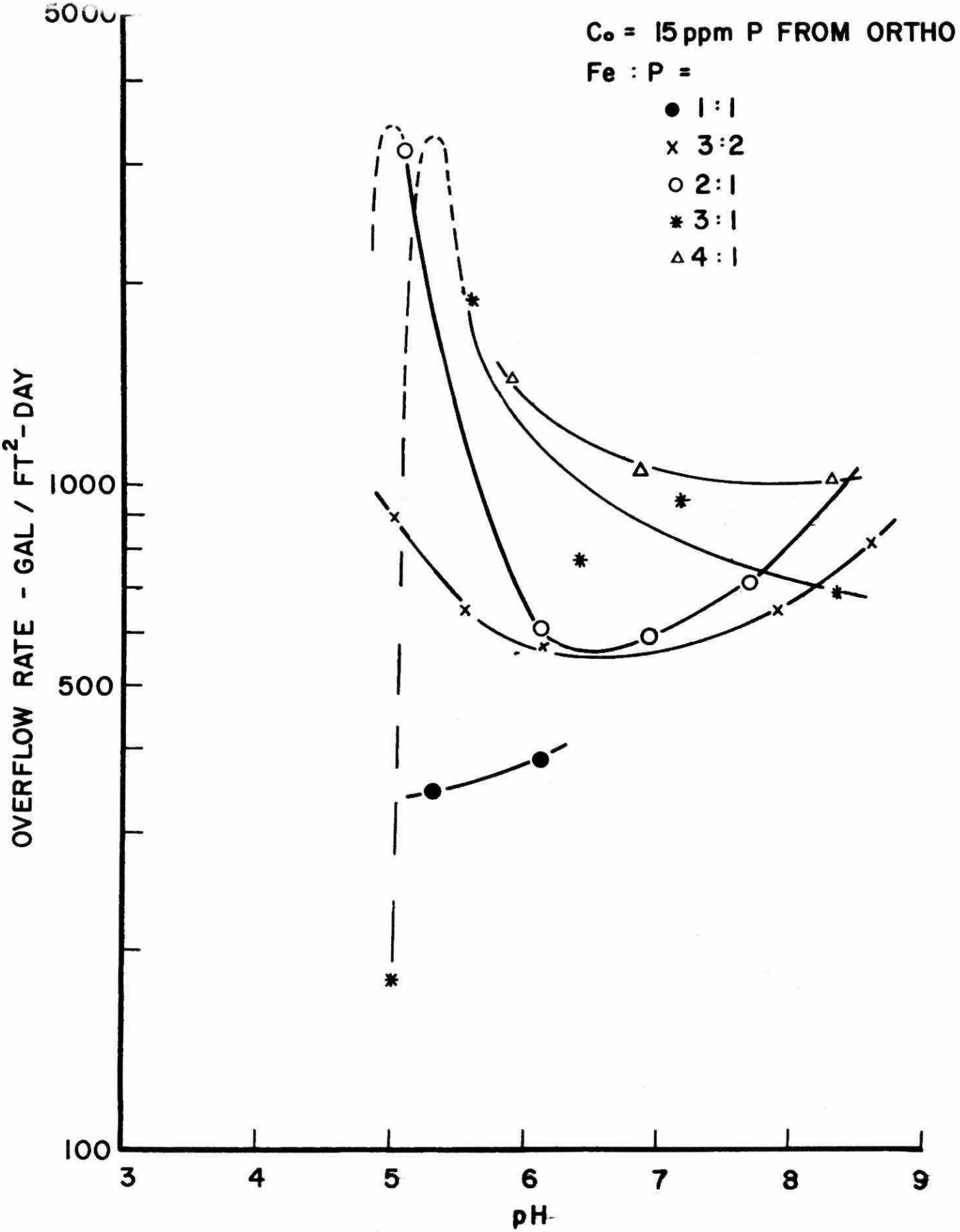

FIGURE 32. MAXIMUM PERMISSIBLE OVERFLOW RATES FOR 90% FLOC REMOVAL IN THE IRON-ORTHOPHOSPHATE SYSTEM

with the minimum solubility of $FePO_4$ and the region of peculiarities noted during the discussion of the ultimate removal contour diagram.

The settling rate of flocs in the mixed phosphate system was a strong function of pH, as shown in Figures 33 (for Fe), 34 (for Ca) and 47 (for Al).

There were relatively limited mixed phosphate data for iron and aluminum. In general, settling rates appear to be very similar to those in the orthophosphate model solution. In the case of iron, mixed phosphate sedimentation appears to be somewhat poorer at pH below 7.5, while the sharp rise in sedimentation rate around pH 5, observed in the orthophosphate system, is maintained in the mixed phosphate system as well.

Permissible overflow rates were very low with lime at pH below 10.5 (see Figure 34). At a Ca:P ratio of 2.5, a peak overflow rate is achieved at pH 11.5. Such a peak, however, is not observed at higher calcium dosages. At higher dosages, permissible overflow rates start to improve at pH greater than 11.5 only. Lime addition to wastewater usually results in an operating pH of 10.5-12.0 (Culp and Culp, 1971; Domtar Ltd., 1973). In this pH range, permissible overflow rates still appear to be too low, except in the special case of a Ca:P ratio of 2.5, for conventionally designed clarifiers.

The slow settling in the mixed phosphate system is a result of the formation of near colloidal particles as discussed in Section 4.3.3.

4.3.5 Coagulant dosage

Phosphorus removal is examined directly as function of M:P (metal to phosphorus) molar ratio at a number of pH values and overflow rates in Figure 35 for aluminum and Figure 36 for iron in the orthophosphate model solution. The overflow rates were chosen to represent typical primary clarifier overflow rates (e.g., 600 and 1,000 $lgpd/ft^2$) and to bracket the sedimentation period in the experimental runs. Thus, the overflow rate of 145 $lgpd/ft^2$ corresponds to the end of the sedimentation period, and 2,100 $lgpd/ft^2$ represents a very high overflow rate near the beginning of the sedimentation period. An optimum coagulant dosage can be determined from Figures 35 and 36 at a point where tangents of the

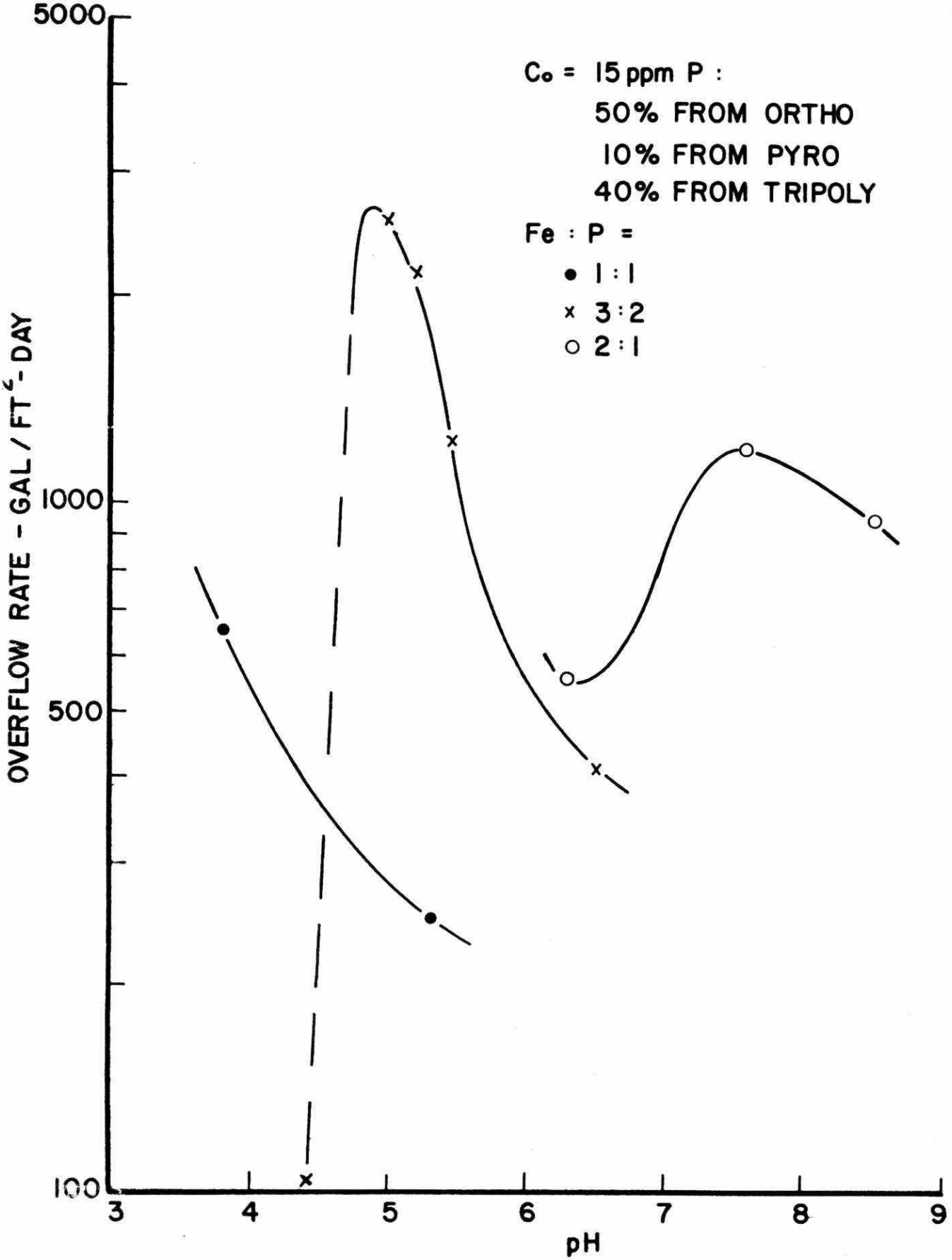

FIGURE 33. MAXIMUM PERMISSIBLE OVERFLOW RATES FOR 90% FLOC REMOVAL IN THE IRON-MIXED PHOSPHATE SYSTEM

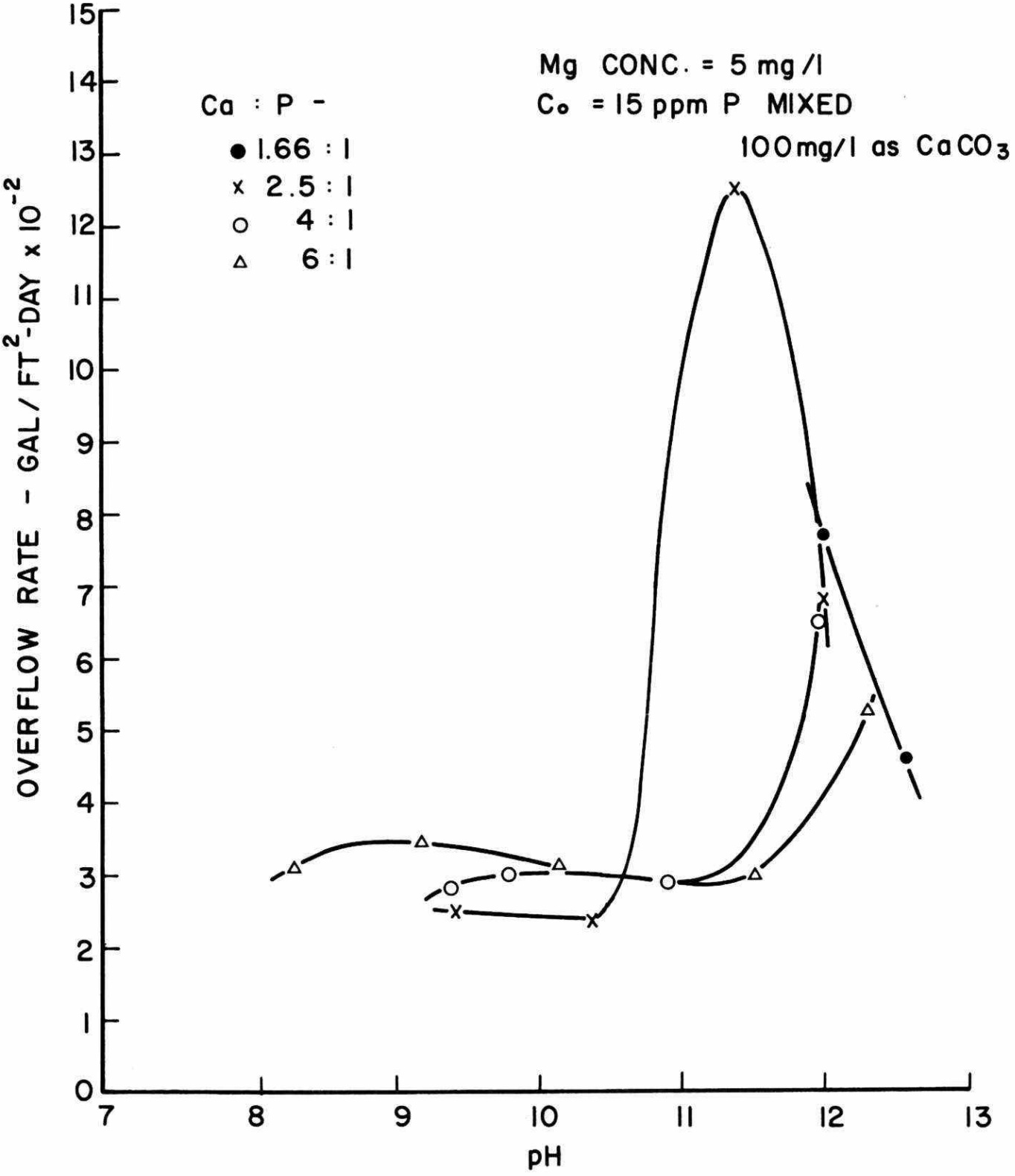

FIGURE 34. MAXIMUM PERMISSIBLE OVERFLOW RATES FOR 90% FLOC REMOVAL IN THE CALCIUM-MIXED PHOSPHATE SYSTEM

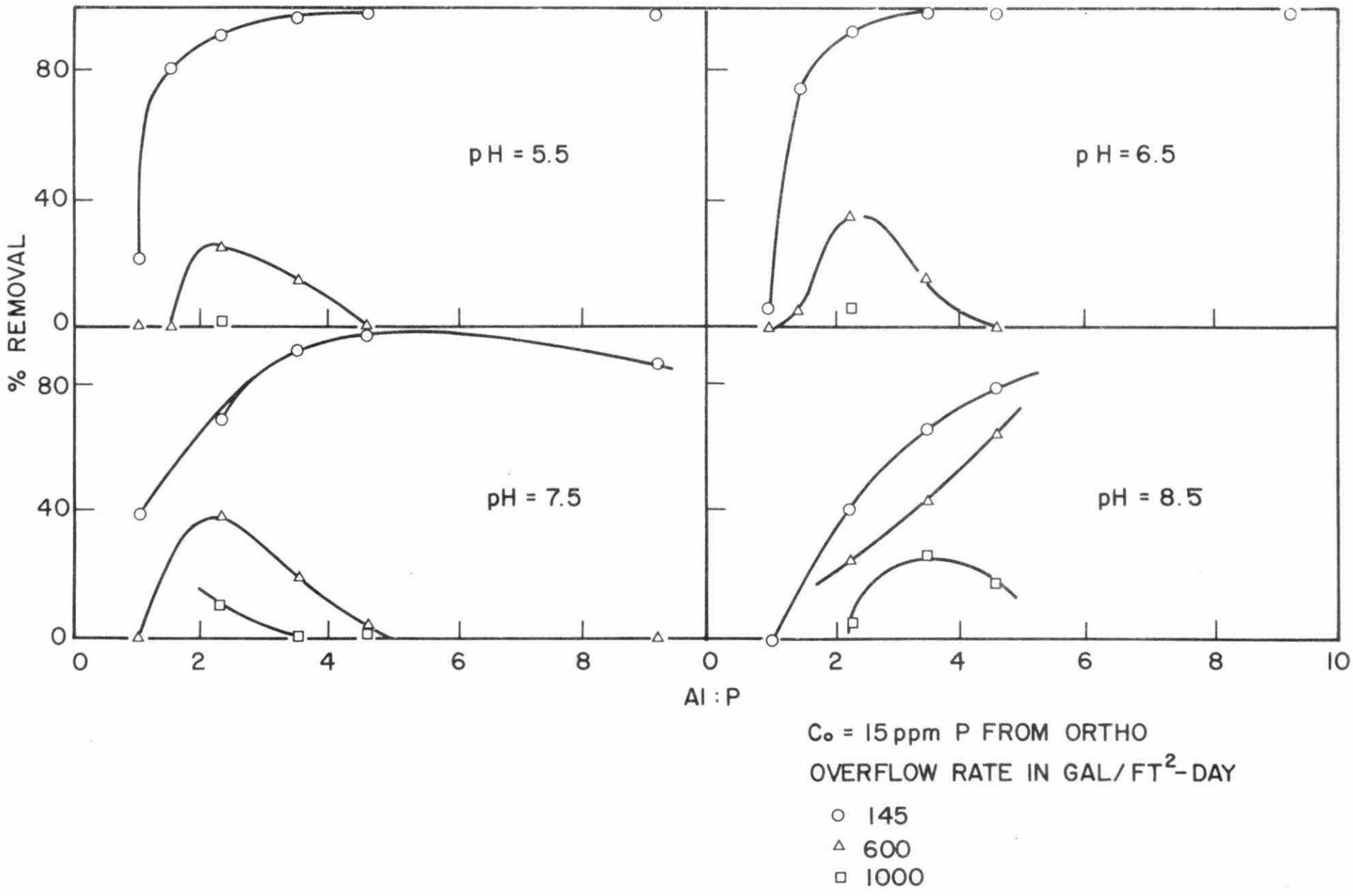

FIGURE 35. ULTIMATE PHOSPHORUS REMOVAL AS A FUNCTION OF Al:P RATIO IN THE ALUMINUM-ORTHOPHOSPHATE SYSTEM

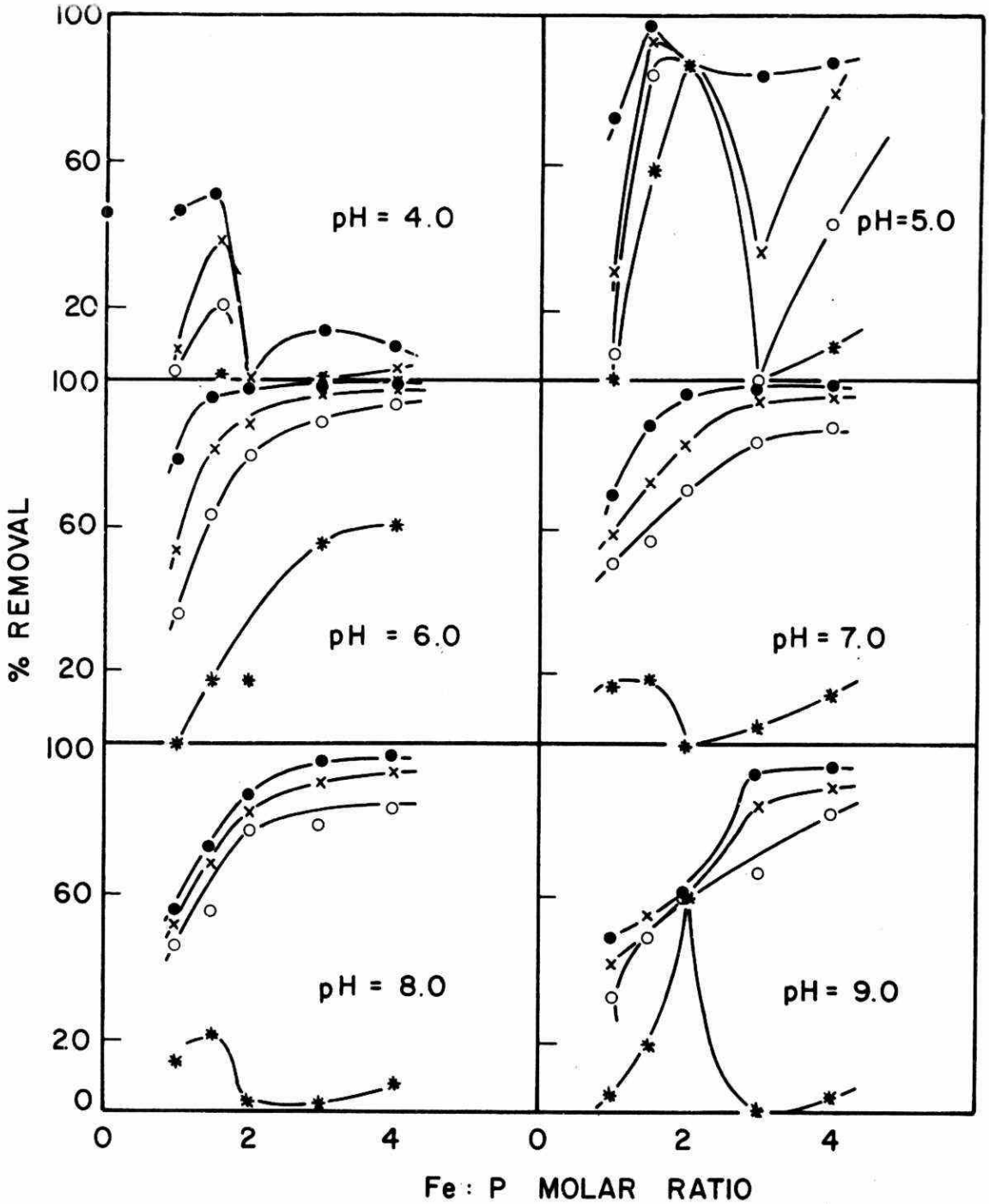

C_o = 15ppm P FROM ORTHO

OVERFLOW RATE
GAL / FT^2 - DAY

- • 145
- × 600
- ○ 1000
- ✱ 2100

FIGURE 36. ULTIMATE PHOSPHORUS REMOVAL AS A FUNCTION OF FE:P RATIO IN THE ALUMINUM-MIXED PHOSPHATE SYSTEM

vertical and horizontal sections of the ultimate phosphorus removal curves (145 lgpd/ft^2) intersect. Thus, the optimum metal dosage is about 2 as Al:P for aluminum at pH 6.5 and 1.5 as Fe:P for iron at pH 6.

In the mixed phosphate system, at pH 6.5, the optimum aluminum dosage in Figure 37 is 2.5 as Al:P, and for iron in Figure 38 is 1.4 as Fe:P. At pH 11.5, the optimum calcium dosage in Figure 39 is 2.5 as Ca:P.

The optimum Al:P molar ratio of 2 for the orthophosphate system compares well with the Al:P molar ratio 2.65 found in domestic wastewater in Section 6. Lang et al found 2.53 as the "optimum" Al:P ratio for domestic wastewater. The slightly higher aluminum dosage required in domestic wastewater is due to the presence of organic matter not present in the model solutions.

The Fe:P molar ratios of 1.5 obtained in the orthophosphate system and 1.4 in the mixed phosphate system are lower than the Fe:P ratio of 2 suggested by Recht and Ghassemi (1970).

4.3.6 Alkalinity effects

Initial solution alkalinity can have a very strong effect on phosphorus removal as shown in Figure 40 for aluminum and 41 for iron. As the metal dosage is increased beyond a certain point, a sharp drop in phosphorus removal occurs. This drop is explained in terms of a drop in pH to levels where the precipitate is more soluble, as a result of H^+ ion release from metal hydroxide formation, e.g.,

$$Al^{3+} + 3H_2O \rightarrow Al(OH)_3 \downarrow + 3H^+ \quad (1)$$

or

$$Fe^{3+} + 3H_2O \rightarrow Fe(OH)_3 \downarrow + 3H^+ \quad (2)$$

and by metal phosphate formation as

$$Al^{3+} + H_2PO_4^- \rightarrow AlPO_4 \downarrow + 2H^+ \quad (3)$$

or

$$Fe^{3+} + H_2PO_4^- \rightarrow FePO_4 \downarrow + 2H^+ \quad (4)$$

At the prevailing pH for aluminum and iron precipitation, phosphates are expected to be in the dibasic form.

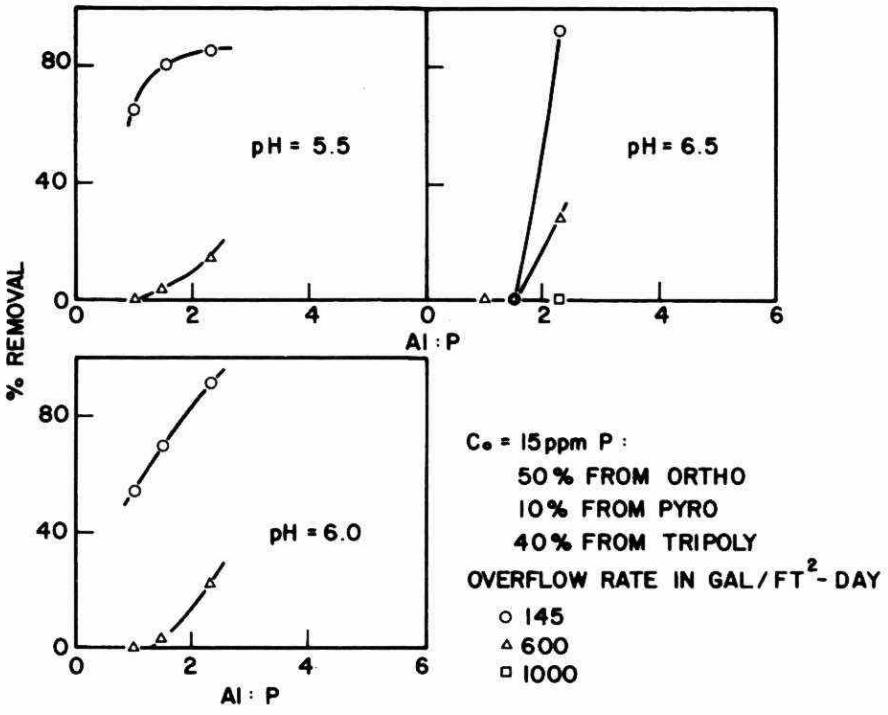

FIGURE 37. ULTIMATE PHOSPHORUS REMOVAL AS A FUNCTION OF Al:P RATIO IN THE ALUMINUM-MIXED PHOSPHATE SYSTEM

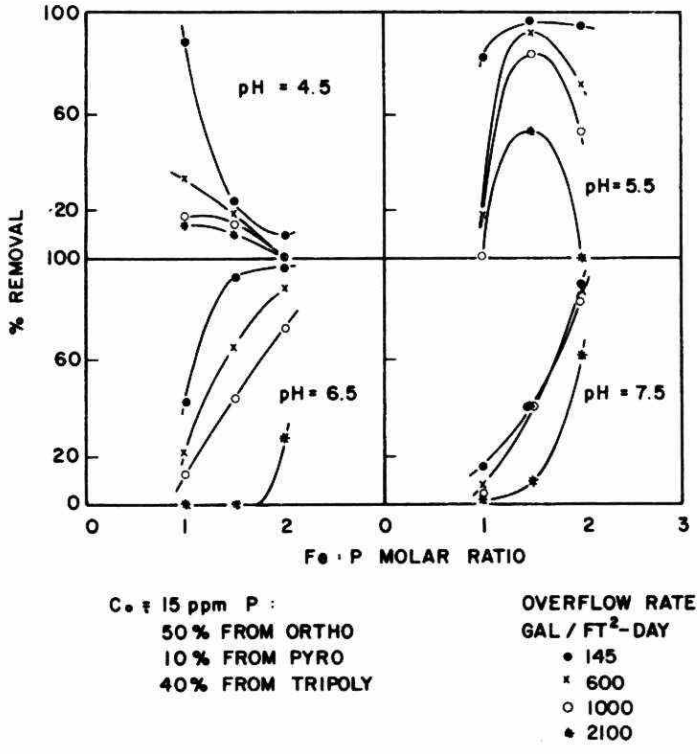

FIGURE 38. ULTIMATE PHOSPHORUS REMOVAL AS A FUNCTION OF Fe:P RATIO IN THE IRON-MIXED PHOSPHATE SYSTEM

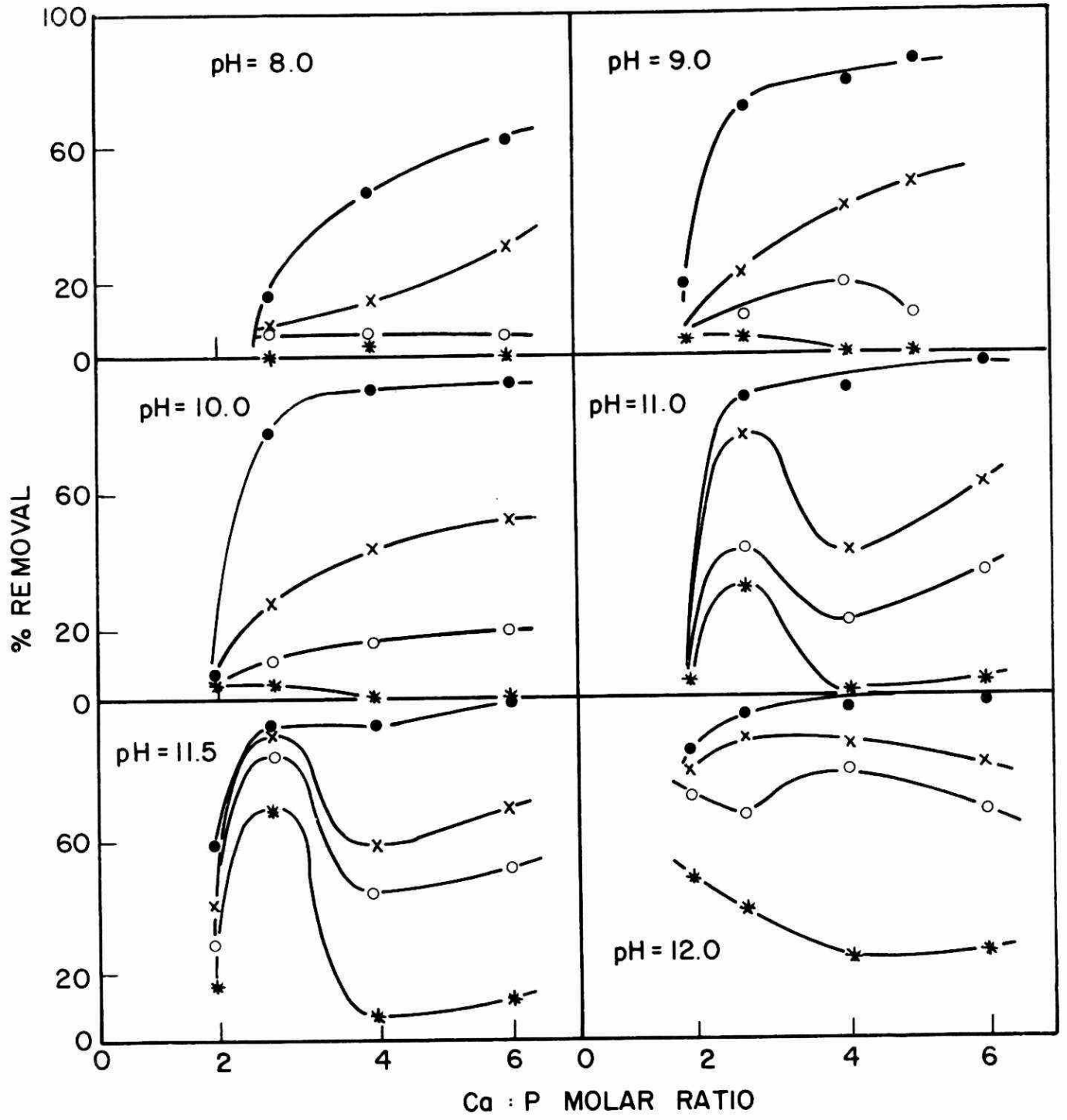

C_o = 15 ppm P =
50 % FROM ORTHO
10 % FROM PYRO
40 % FROM TRIPOLY

OVERFLOW RATE IN GAL / FT^2 - DAY
● 145
× 600
○ 1000

FIGURE 39. ULTIMATE PHOSPHORUS REMOVAL AS A FUNCTION OF CA:P RAT IN THE CALCIUM-MIXED PHOSPHATE SYSTEM

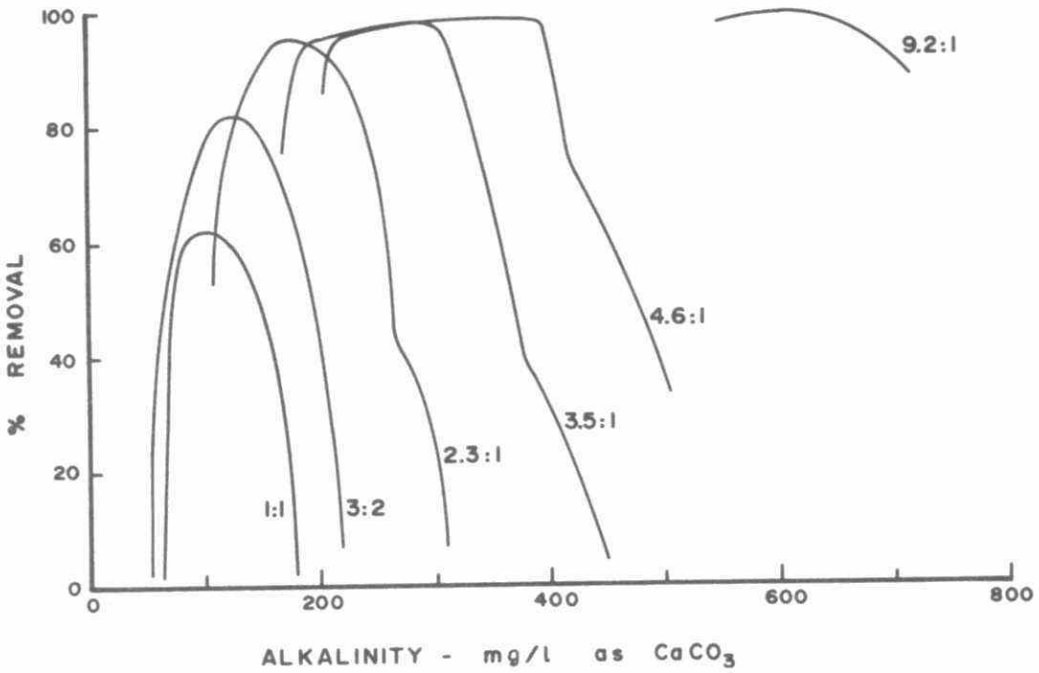

FIGURE 40. ULTIMATE PHOSPHORUS REMOVAL AS A FUNCTION OF Al:P RATIO AND INITIAL SOLUTION ALKALINITY IN THE ALUMINUM-ORTHOPHOSPHATE SYSTEM

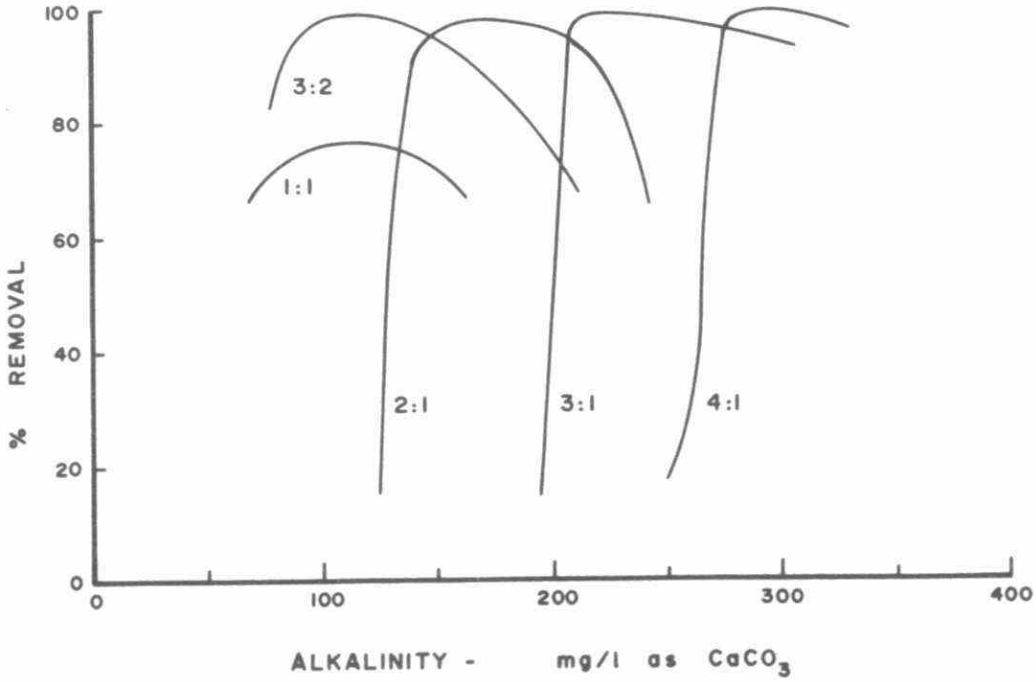

FIGURE 41. ULTIMATE PHOSPHORUS REMOVAL AS A FUNCTION OF Fe:P RATIO AND INITIAL SOLUTION ALKALINITY IN THE IRON-ORTHOPHOSPHATE SYSTEM

The crossing of tangents of the nearly vertical and horizontal sections of each M:P ratio line in Figures 40 and 41 defines the maximum permissible metal dosage at a particular alkalinity. At this point, the concentration of H^+ ions released is given by:

$$[H^+] = 3P\left[\frac{M}{P} - 1\right] + 2P \qquad (5)$$

where $[H^+]$ = molar concentration of H^+ ions released

P = molar phosphorus concentration

and M = molar metal ion (Al or Fe) concentration

The H^+ ion released at maximum permissible coagulant dosage, $[H^+]_P$, is plotted against the initial solution alkalinity in Figure 42 for aluminum and Figure 43 for iron. The equation describing $[H^+]_P$ in terms of initial solution alkalinity is, for aluminum:

$$[H^+]_P = 0.02\ Alk - 0.5 \qquad (6)$$

and for iron:

$$[H^+]_P = 0.0236\ Alk - 1.2 \qquad (7)$$

The solution of Equation (5) in terms of Equations (6) and (7) describes the maximum permissible metal dosage for a given initial solution alkalinity and phosphorus concentration. Thus, the maximum permissible dosage for aluminum is:

$$Al = 0.373\ Alk - 9.32 + 0.602P \qquad (8)$$

and for iron is:

$$Fe = 0.44\ Alk - 20.9 + 0.602P \qquad (9)$$

where Al or Fe = metal concentration in mg/l

P = phosphorus concentration in mg/l

and Alk = initial solution alkalinity in mg/l as $CaCO_3$.

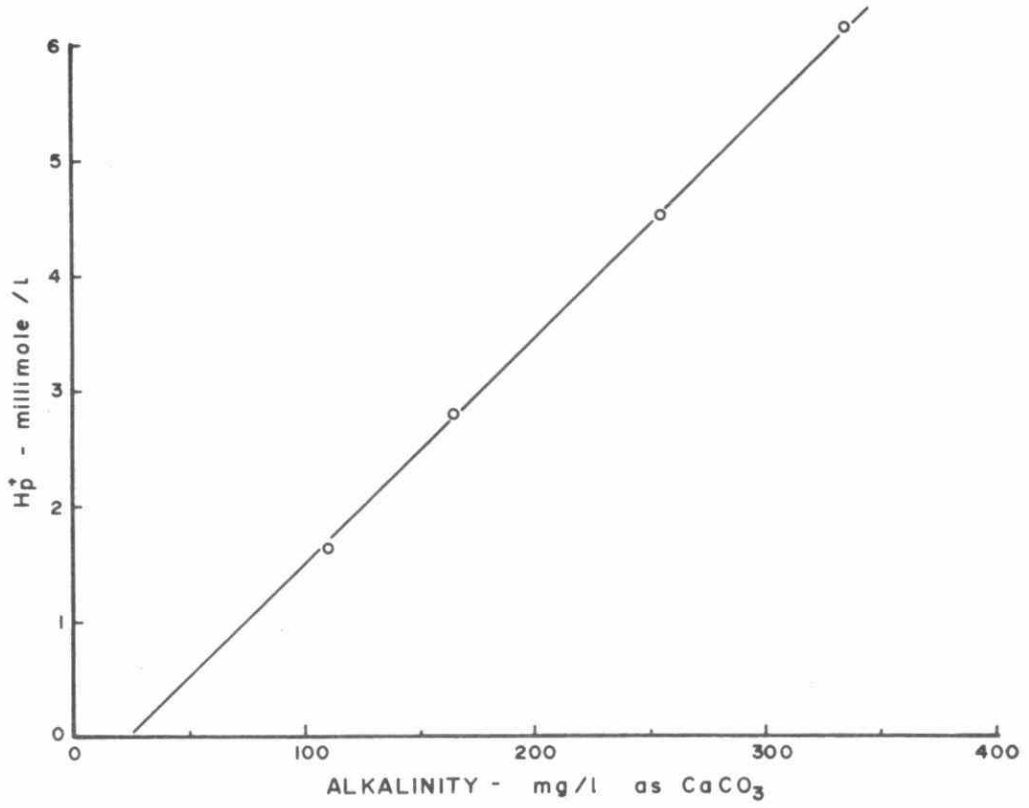

FIGURE 42. MAXIMUM PERMISSIBLE HYDRONIUM ION RELEASED AS A FUNCTION OF ALKALINITY IN THE ALUMINUM-ORTHOPHOSPHATE SYSTEM

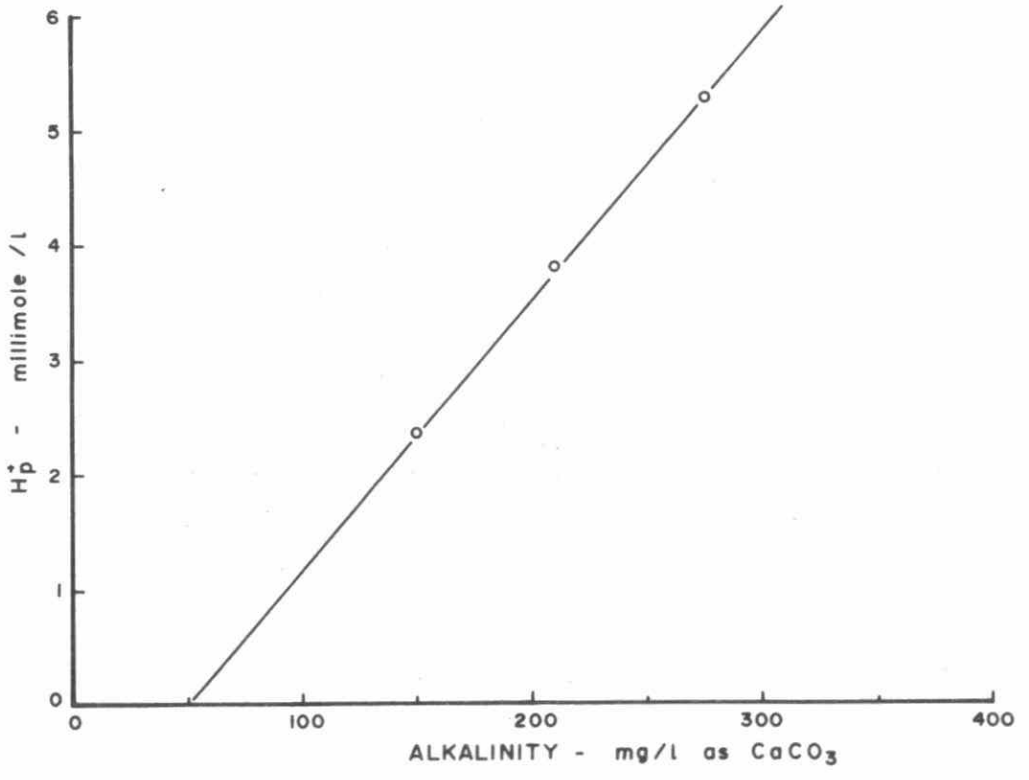

FIGURE 43. MAXIMUM PERMISSIBLE HYDRONIUM ION RELEASED AS A FUNCTION OF ALKALINITY IN THE IRON-ORTHOPHOSPHATE SYSTEM

The effect of carbonate concentration on phosphorus removal with calcium is shown in Figure 44 as function of pH and overflow rate. The best performance is shown in the presence of 100 mg/l $NaHCO_3$ as $CaCO_3$. In the presence of only 20 mg/l $NaHCO_3$ as $CaCO_3$, the quantity of $CaCO_3$ precipitation may be insufficient to ensure good settling. On the other hand, in the presence of 240 mg/l $NaHCO_3$ as $CaCO_3$ higher Ca dosage is required due to the competition of $CO_3^{=}$ ions for Ca^{2+} with phosphates, and thus a threshold is apparent.

4.3.7 Miscellaneous ion effects

4.3.7.1 Presence of $SO_4^{=}$. $Fe_2(SO_4)_3$ is a potential coagulant for phosphorus precipitation; therefore, a few experiments were undertaken to evaluate it. The results are compared in Figure 45 with $FeCl_3$ data. The ultimate phosphorus removal has been extended to a lower pH region by the presence of $SO_4^{=}$. Removals above pH 4.6, however, were lower with $Fe_2(SO_4)_3$ than with $FeCl_3$. Although equal or greater amounts of precipitate were formed, with $Fe_2(SO_4)_3$ (based on filtered phosphorus concentration data), a larger fraction was near colloidal in size as shown by the differences between the filterable and settleable curves. The relatively slow settling rates observed with $Fe_2(SO_4)_3$ throughout the pH range investigated (particularly at pH 5) also illustrate that smaller flocs are formed by $Fe_2(SO_4)_3$. A similar extension of the coagulation region toward the acid side was shown by Bartow et al (1935) for $SO_4^{=}$.

4.3.7.2 Presence of Ca^{++}. In a few experiments with Al, the $NaHCO_3$ buffer was replaced with $CaCO_3$. The ultimate phosphorus removal with the two buffers is shown in Figure 46. Some removal was achieved with $CaCO_3$ alone. Improvement in phosphorus removal was shown with Al in the presence of $CaCO_3$, instead of $NaHCO_3$, in the pH range above 5 and especially above pH 6.5. The maximum permissible overflow rates for 90% floc removal as shown in Figure 47 were increased from 190 lgpd/ft^2 to 800 lgpd/ft^2 at pH 5 ± 0.25 in the presence of $CaCO_3$. At other pH values, however, settling did not increase substantially.

The improvement in ultimate phosphorus removal with $CaCO_3$ over that with $NaHCO_3$ may be attributed to the additional metal available

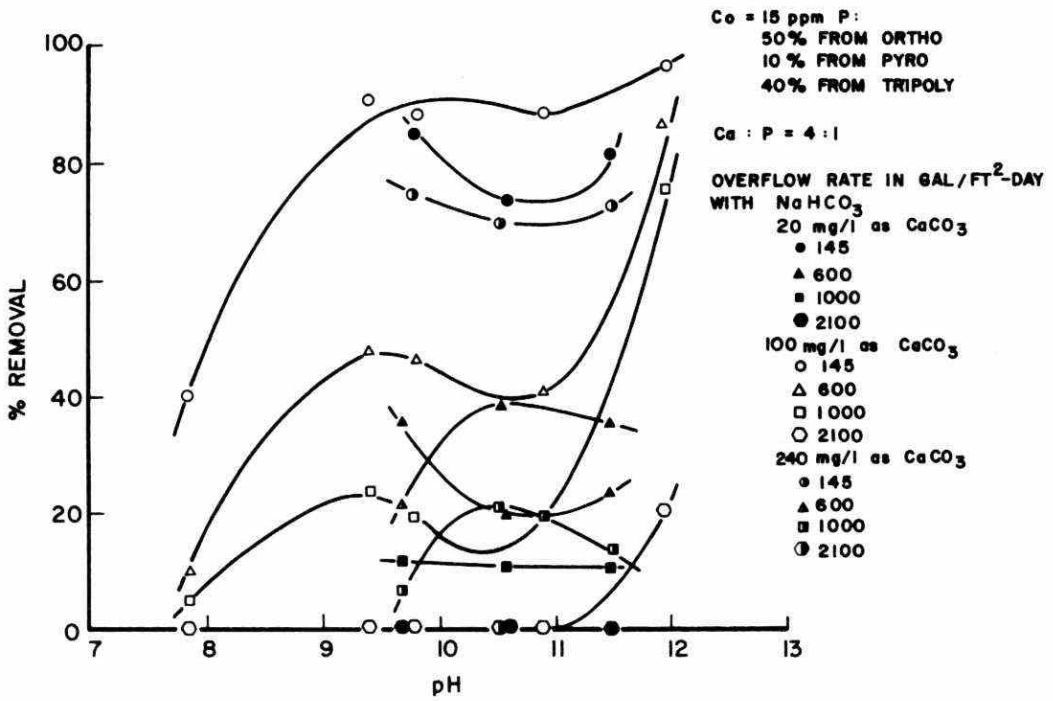

FIGURE 44. PHOSPHORUS REMOVAL AS A FUNCTION OF $CO_3^=$ CONCENTRATION IN THE CALCIUM-MIXED PHOSPHATE SYSTEM

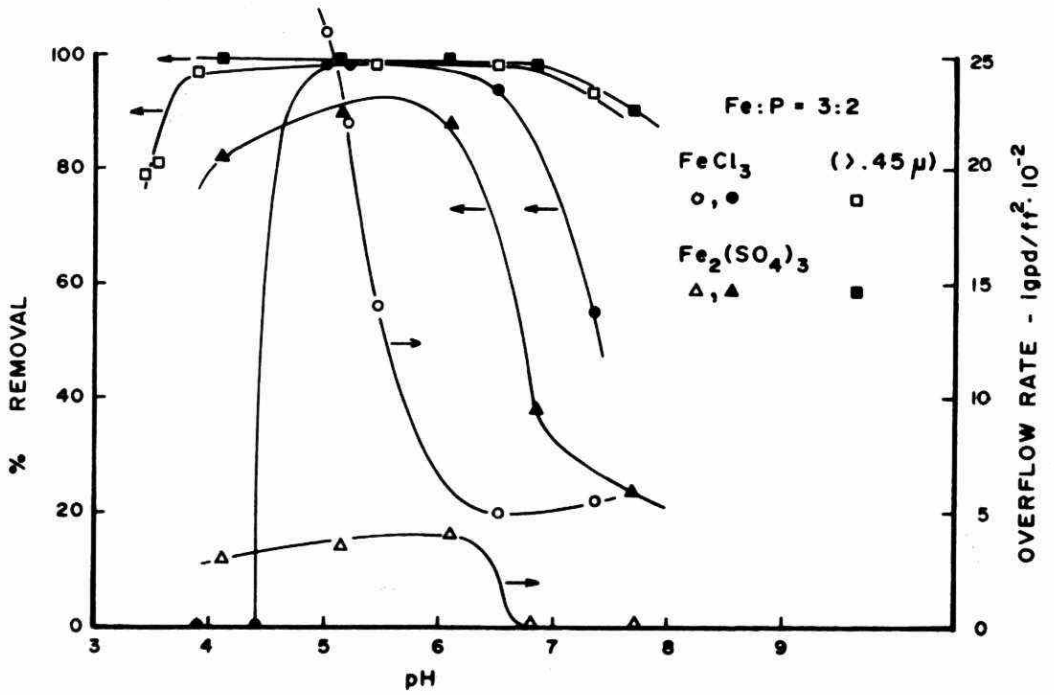

FIGURE 45. COMPARISON OF PHOSPHORUS REMOVAL WITH $FeCl_3$ AND $Fe(SO_4)_3$

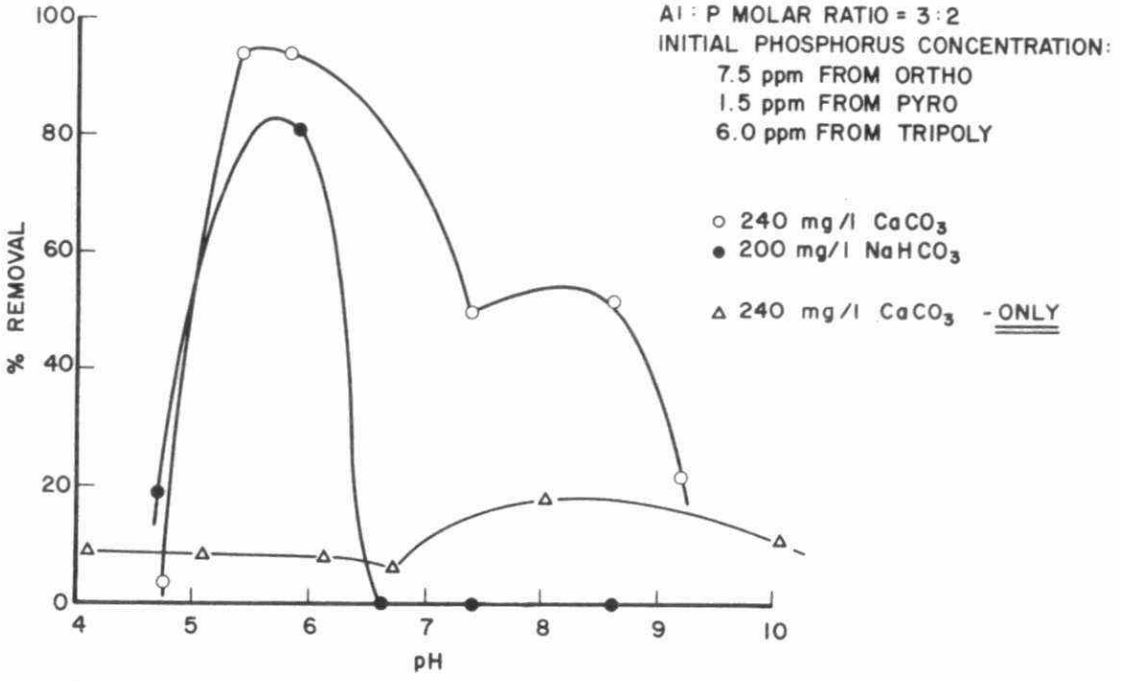

FIGURE 46. PHOSPHORUS REMOVAL IN THE PRESENCE AND ABSENCE OF $CaCO_3$ IN THE ALUMINUM-MIXED PHOSPHATE SYSTEM

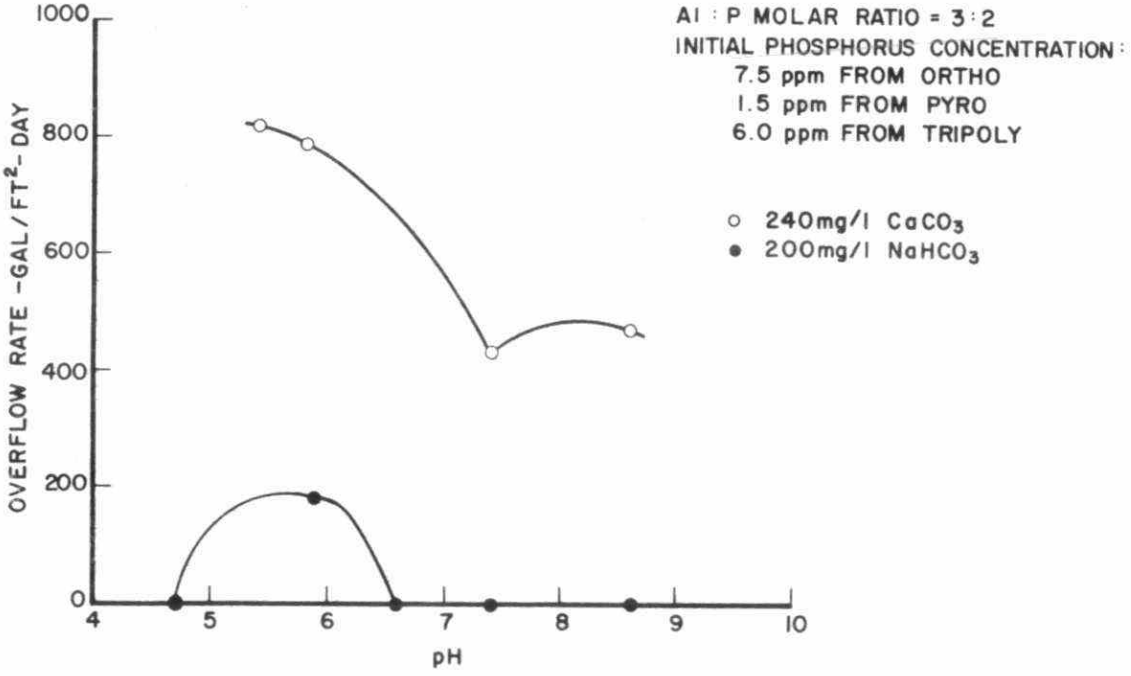

FIGURE 47. MAXIMUM PERMISSIBLE OVERFLOW RATES FOR 90% FLOC REMOVAL IN THE PRESENCE AND ABSENCE OF $CaCO_3$ IN THE ALUMINUM-MIXED PHOSPHATE SYSTEM

for precipitation, even though Ca^{++} was more effective above pH 7.5. The concentrations of Ca^{++} were unusually high in these experiments and accentuate the probable differences to be anticipated with typical southern Ontario wastewaters.

4.3.7.3 Presence of Mg^{++}. Magnesium is present in wastewater and it is generally expected to start precipitating at about pH 11 (Convery, 1970; Domtar Ltd., 1973; Ferguson et al, 1973; Ferguson and McCarty, 1969). Its presence would affect phosphorus precipitation with lime. The results from runs with three Mg^{++} dosages are shown in Figure 48.

The ultimate phosphorus removal was not appreciably affected by the presence of Mg^{++}. The settling rates were also unaffected below pH 11 (Convery, 1970; Ferguson et al, 1973; Ferguson and McCarty, 1969). At pH 11.5, however, the addition of 10 mg/l Mg^{++} showed a strong and sudden effect on settling rates, indicating 85% removal at a settling rate of 1,000 lgpd/ft^2. As the Mg^{++} concentrations in most natural waters are expected to be 10 mg/l or higher, lime flocs are expected to show excellent settling characteristics (in agreement with full scale plant observation, Domtar Ltd., 1973), however, the data obtained in this study indicate that this would only occur at pH > 11.

4.4 Conclusions

The following conclusions can be drawn from this study:

1) 90% phosphorus removal is possible with the following metal coagulant dosages at specified pH ranges, in the orthophosphate model solution:

Al^{3+}: Al:P = 2.3, pH 5.4 - 6.9

Fe^{3+}: Fe:P = 1.5, pH 4.5 - 6.5

and, in the mixed phosphate model solution:

Al^{3+}: Al:P = 2.3, pH 5.9 - 6.6

Fe^{3+}: Fe:P = 1.25, pH 4.4 - 6.1

Ca^{2+}: Ca:P = 2.56, pH 11.3 - 9.3.

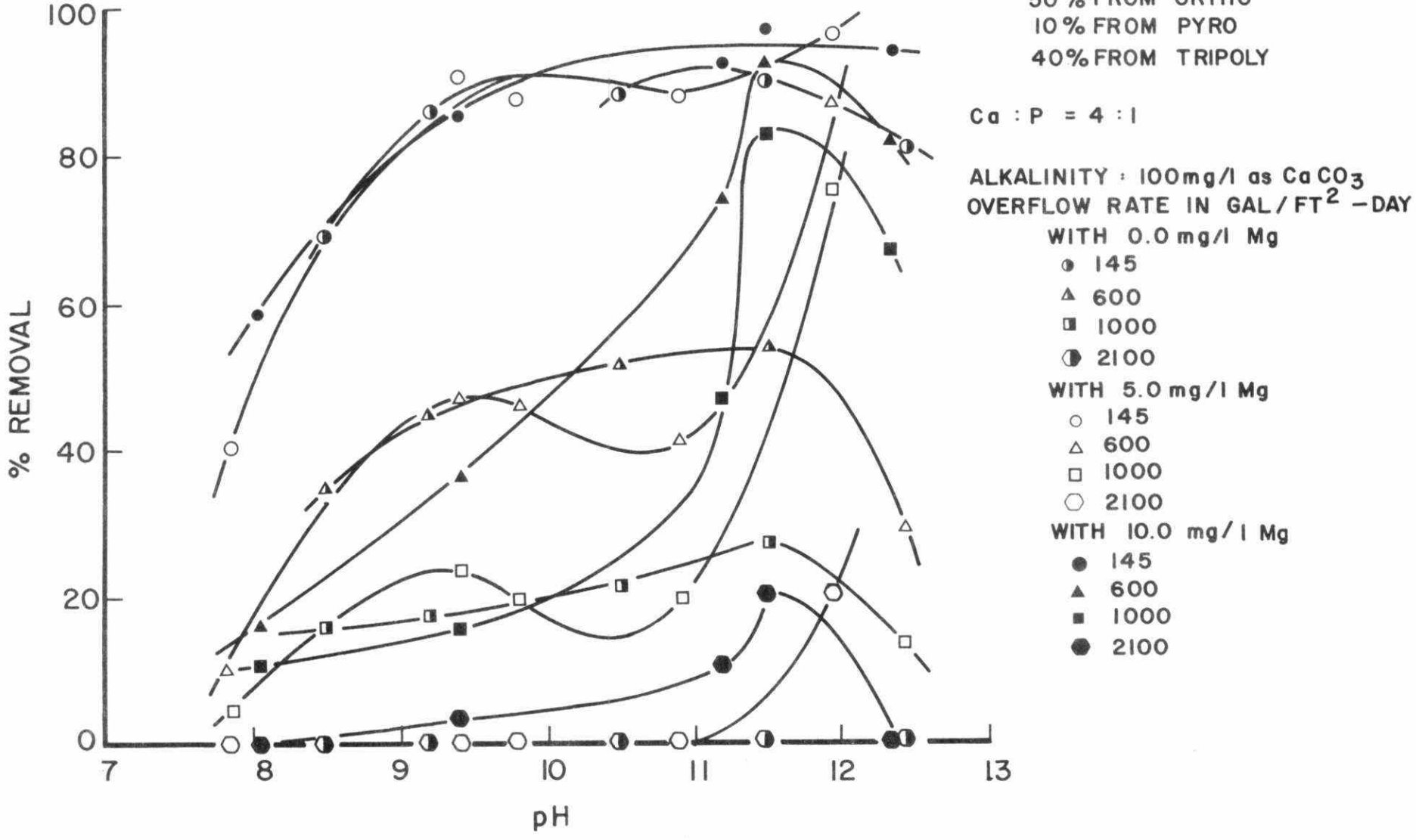

FIGURE 48. PHOSPHORUS REMOVAL AS A FUNCTION OF Mg^{++} DOSAGE IN THE CALCIUM-MIXED PHOSPHATE SYSTEM

2) All three metals formed relatively slow settling flocs. In general, iron appeared to settle better than aluminum which, in turn, appeared to settle better than lime (except at pH > 11.5 in the presence of 10 mg/l of Mg^{++}).

3) The presence of condensed phosphates reduced floc settling rates and, for aluminum and iron, moved the optimum pH range toward lower pH.

4) The maximum permissible metal dosage with any initial solution alkalinity and phosphorus concentration for Al was:

$$Al = 0.373\ Alk - 9.32 + 0.602P$$

and for Fe:

$$Fe = 0.44\ Alk - 20.9 + 0.602P$$

5) The presence of Ca^{2+} enhanced phosphorus removal with Al^{3+} and Fe^{3+}.

6) The presence of Mg^{2+} enhanced phosphorus removal with lime at pH > 11.5.

7) The presence of $SO_4^{=}$ in wastewater detrimentally affected phosphorus removal with Fe^{3+}.

5. POLYELECTROLYTES IN WASTEWATER TREATMENT: THE SETTLEABILITY OF METAL PRECIPITATED PHOSPHATE FLOCS

5.1 Introduction

The results of Section 4 indicated that metallic coagulant precipitated flocs settle relatively slowly. The resulting poor clarifier performance could be considerably improved by the use of polyelectrolytes (Rocheleau et al, 1970; Wukasch, 1968). A review of the literature, however, did not locate specific investigations on the settling rate or, more particularly, the design overflow rates of phosphate flocs.

The objectives of this investigation were:

(i) to determine the effect of polyelectrolytes on settling and predict maximum permissible clarifier overflow rates in the presence of polyelectrolytes;

(ii) to determine the effect of polyelectrolytes on ultimate residual or equilibrium phosphorus concentrations;

(iii) to estimate and compare the required polyelectrolyte dosages in conjunction with alum, ferric chloride and lime; and,

(iv) to examine the effect of operating variables such as pH, phosphate type and divalent cation concentrations on polyelectrolyte effectiveness.

5.2 Experimental

5.2.1 Overall procedure

The apparatus used in these experiments was the batch settling apparatus described in detail in Section 2.

The experimental procedure was described in detail in Sections 2 and 4.

5.2.2 Polyelectrolyte solutions

The polyelectrolytes used were Purifloc A23 (Dow Chemical), Percol 730, and Percol 728 (Allied Colloids). Purifloc A23 and Percol 730 are both anionic polyacrylamides with different degrees of hydrolysis

(see Section 3). Percol 728 is a cationic polyelectrolyte. All three possess similarly high molecular weights and are sold in a dry form.

Polyelectrolyte stock solutions were prepared by gradually dissolving the required polyelectrolyte to a concentration of 300 mg/l in (stirred) distilled water.

5.3 Results and Discussion

5.3.1 Effects on ultimate removal

Ultimate phosphorus removal in the presence of polyelectrolytes followed, with small improvement, the removal envelope generated by the metallic coagulants alone, as typically shown in Figure 49. (For specific cases, see Figures 123 to 129 for the aluminum system, Figures 130 to 147 for the iron system and Figures 148 to 154 for the lime system in Appendix A.)

The improvement in phosphorus removal by polyelectrolyte addition over removal by metallic coagulant addition alone can be defined in terms of the "percentage removal enhancement due to polyelectrolyte addition" (REP). REP is calculated by the equation:

$$REP = Rp - R \qquad (1)$$

where Rp = percent phosphorus removal with polyelectrolyte addition, and

R = percent phosphorus removal with metallic coagulant addition only.

REP for selected combinations of metal precipitant and polyelectrolyte are shown as a function of pH in Figure 50 for the orthophosphate system with aluminum and iron, and Figure 51 for the mixed phosphate system with lime. With all three metals, the ultimate REP was strongly pH dependent. The optimum pH for maximum removal ranges from 6 to 6.5 in Figure 49. Polyelectrolytes did not alter significantly the optimum removal pH; however, maximum removal enhancement (REP) usually occurred at pH values other than the optimum.

Thus for aluminum (Figure 50A), REP values were quite low in the optimum removal pH range of 6-6.5; however, REP rose sharply on both sides of this pH range. As explained in Section 4, the fraction

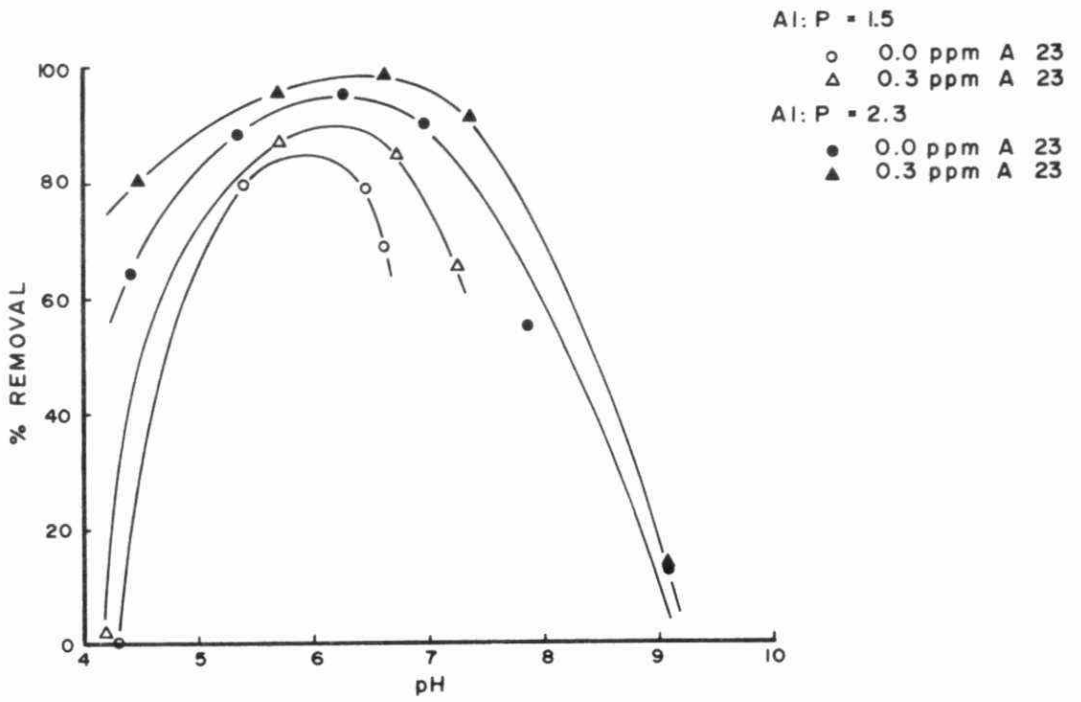

FIGURE 49. ULTIMATE PHOSPHORUS REMOVAL AS FUNCTION OF pH, Al:P RATIO AND POLYELECTROLYTE ADDITION

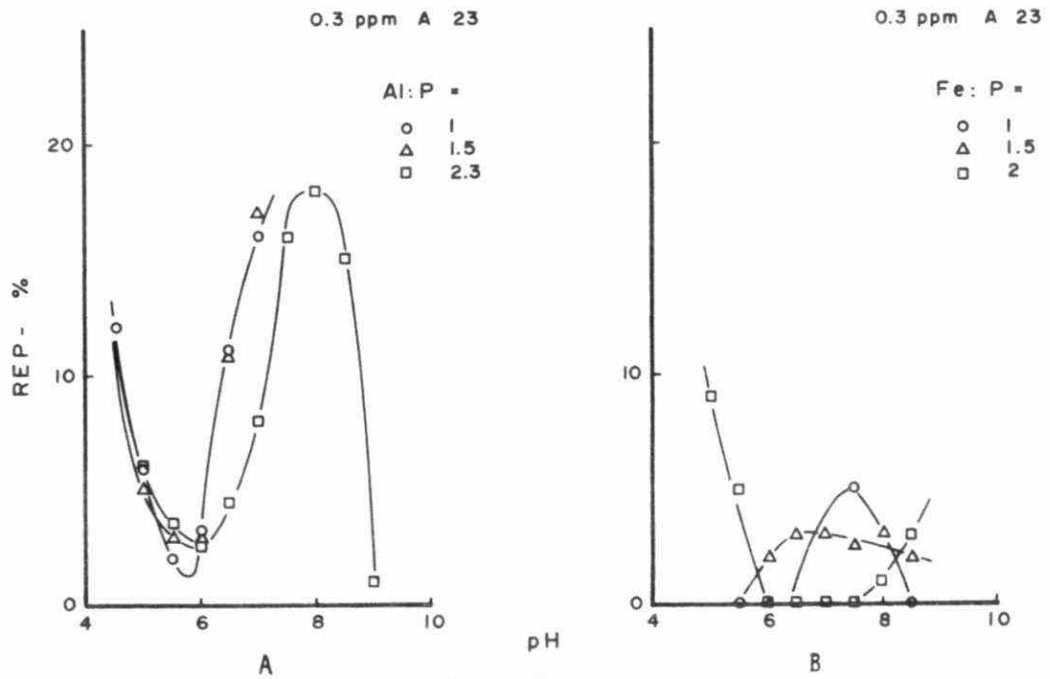

FIGURE 50. ULTIMATE PHOSPHORUS REMOVAL ENHANCEMENT FROM POLYELECTROLYTE ADDITION, REP, (CALCULATED FROM RESIDUAL CONCENTRATIONS)
A) IN THE ALUMINUM-ORTHOPHOSPHATE SYSTEM
B) IN THE IRON-ORTHOPHOSPHATE SYSTEM

of unsettleable flocs becomes significant as one moves away from the optimum pH range. Hence, polyelectrolytes appear to be successful in removing a sizeable fraction of these flocs. The data for iron (Figure 50B) are very similar, although the degree of enhancement by polyelectrolytes was smaller and, due to the broader effective pH range of this coagulant, the sharp increases in REP at low and high pH were not observed. With lime (Figure 51) maximum REP occurred around pH 10. The dip in REP around pH 11.5 was expected, as this is the optimum pH for phosphorus removal with lime.

In general, REP values tended to be greatest at the lowest metal coagulant dosage, particularly in the region of maximum REP values.

5.3.2 Settling rates

The maximum permissible overflow rates for 90% floc removal are shown in Figure 52 for aluminum and Figure 53 for iron in the orthophosphate system (overflow rates at other metal dosages are shown in Figures 160 to 170 in Appendix A). In the aluminum system, at pH 7, the overflow rates increased from 330 lgpd/ft^2 to 1350 lgpd/ft^2, and to 2000 lgpd/ft^2 with 0.15 and 0.3 ppm of polyelectrolyte, respectively. In the iron system, at the same pH, the addition of polyelectrolyte increased overflow rates from 550 lgpd/ft^2 to 2900 lgpd/ft^2, and to 4000 lgpd/ft^2 with 0.15 and 0.3 ppm, respectively. The overflow rates at either polyelectrolyte dosages were much higher than those required for sedimentation in typical clarifiers, thus indicating that 0.15 ppm or an even lower polyelectrolyte dosage would be sufficient. In domestic wastewater, however, the presence of other (non-phosphate flocs) would require higher polyelectrolyte dosages. On the other hand, the magnitude of the overflow rates obtained in model solutions should be indicative of the overflow rates obtainable in real systems.

Settling rates were relatively insensitive to pH with polyelectrolytes in the iron system (Figure 53).

In the mixed phosphate system, the maximum permissible overflow rates were considerably reduced from values obtained in the orthophosphate system as shown in Figure 54 for iron and Figure 62 for aluminum. Settling

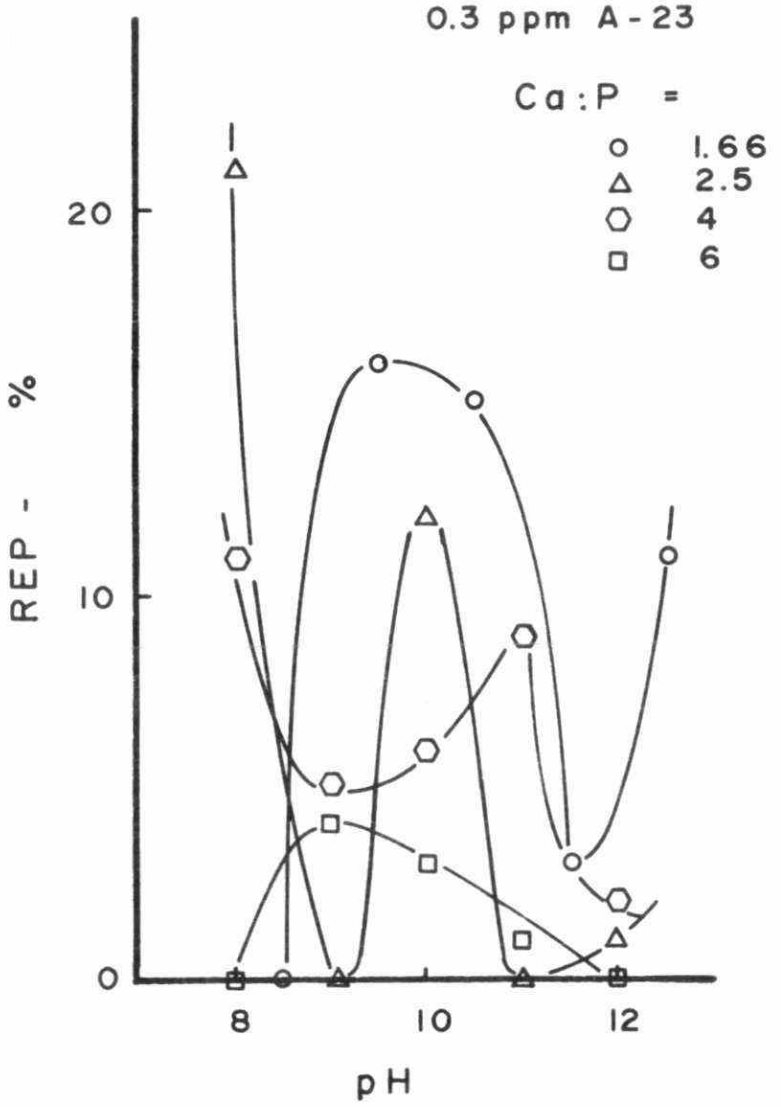

FIGURE 51. REP IN THE CALCIUM-MIXED PHOSPHATE SYSTEM

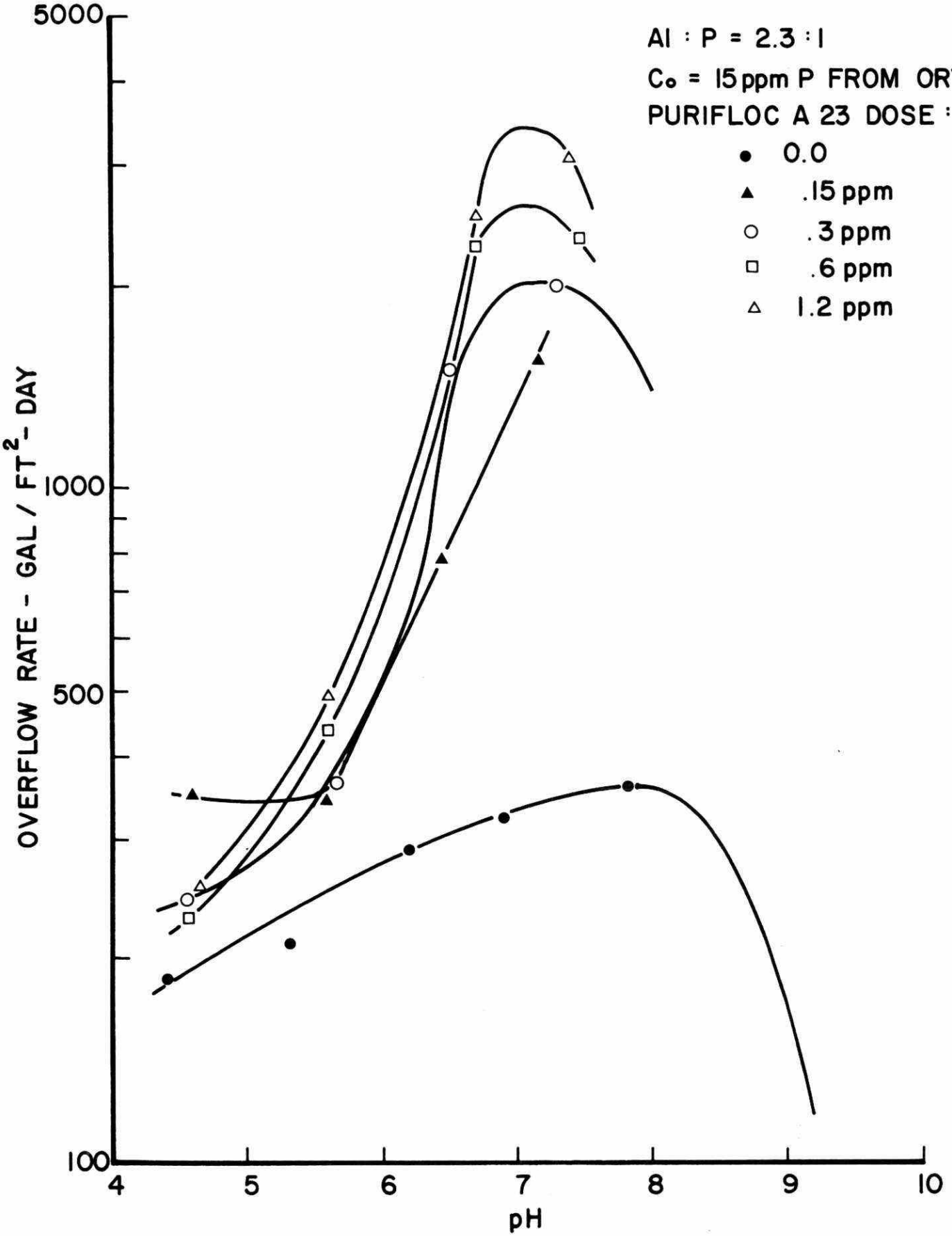

FIGURE 52. MAXIMUM PERMISSIBLE OVERFLOW RATES FOR 90% FLOC REMOVAL IN THE ALUMINUM-ORTHOPHOSPHATE SYSTEM WITH POLYELECTROLYTE ADDITION

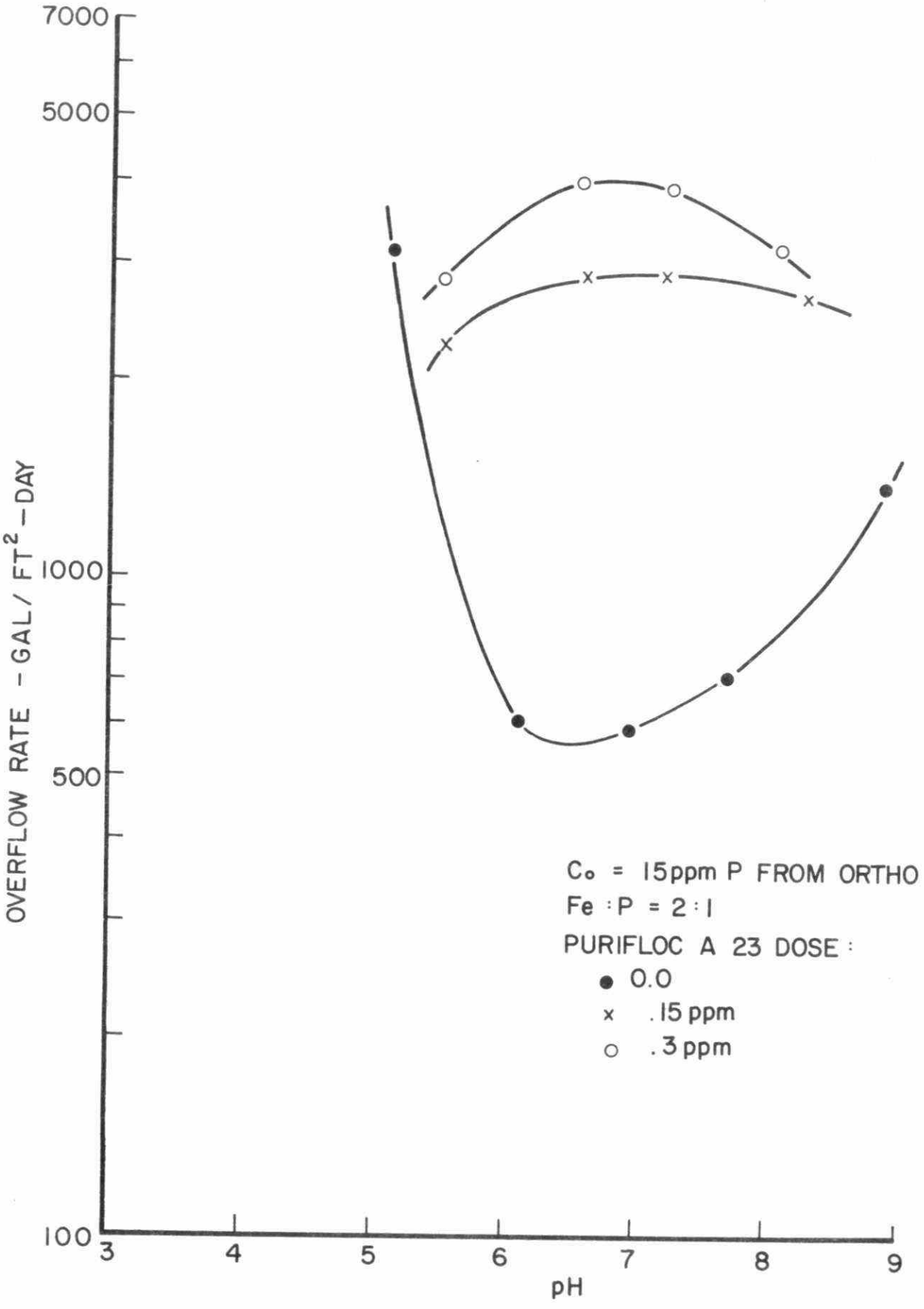

FIGURE 53. MAXIMUM PERMISSIBLE OVERFLOW RATES FOR 90% FLOC REMOVAL IN THE IRON-ORTHOPHOSPHATE SYSTEM WITH POLYELECTROLYTE ADDITION

rates were strongly pH dependent and a peak appeared around pH 5, corresponding to the minimum solubility of $FePO_4$.

With lime addition, the overflow rates were insensitive to pH at all polyelectrolyte dosages as shown in Figure 55. At pH 11, overflow rates increased from 300 lgpd/ft^2 to 680 lgpd/ft^2, and to 1250 lgpd/ft^2 with 0.15 and 0.3 ppm of polyelectrolyte.

Selected plots of REP as function of overflow rate and pH are shown in Figures 56, 57 and 58. Plots illustrating REP at other metal to phosphorus ratios and polyelectrolyte dosages are shown in Figures 159 to 168, and the corresponding absolute removals are shown in Figures 123 to 154 in Appendix A. As explained in Section 4, the overflow rates shown in these figures were chosen to represent usual clarifier overflow rates (600 and 1000 lgpd/ft^2) and to bracket the sedimentation period in the tests conducted, i.e., the 145 lgpd/ft^2 corresponds to the ultimate residual concentration at the end of the sedimentation period (this is usually the point where the ultimate residual concentration is calculated), and the 2100 lgpd/ft^2 represents a relatively high overflow rate obtained near the beginning of the sedimentation period.

All three figures show that the greatest benefit from polyelectrolyte addition would be realized at high clarifier overflow rates.

In the orthophosphate system with aluminum in Figure 56, the REP is pH dependent at all overflow rates and a maximum REP apparently moves progressively to lower pH values, but not towards the optimum precipitation pH, as the overflow rate is increased.

With iron, on the other hand, pH is once again a less important factor. Furthermore, maximum REP's occur at pH 7, and shift very little as settling rates increase. Better than 93% removal can be obtained at pH 7 at an overflow rate of 2100 lgpd/ft^2.

In the mixed phosphate system with iron, the REP is strongly pH dependent and above pH 7 almost no benefit is gained from the addition of anionic polyelectrolyte, as shown in Figure 58A. As the pH is lowered toward the minimum equilibrium solubility pH, there is a dramatic gain obtained from polyelectrolyte addition, especially at the overflow rate of 2100 lgpd/ft^2.

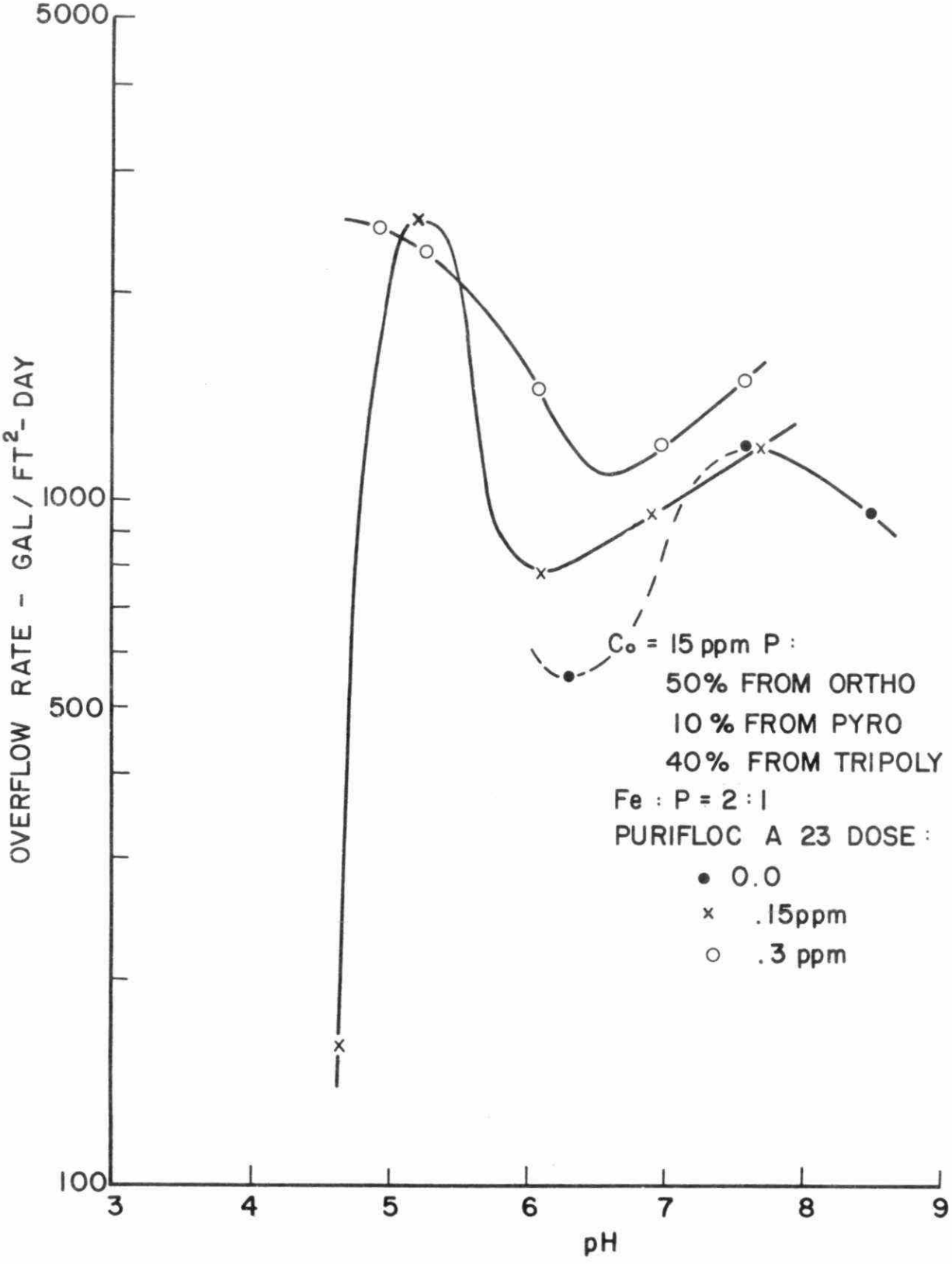

FIGURE 54. MAXIMUM PERMISSIBLE OVERFLOW RATES FOR 90% FLOC REMOVAL IN THE IRON-MIXED PHOSPHATE SYSTEM WITH POLYELECTROLYTE ADDITION

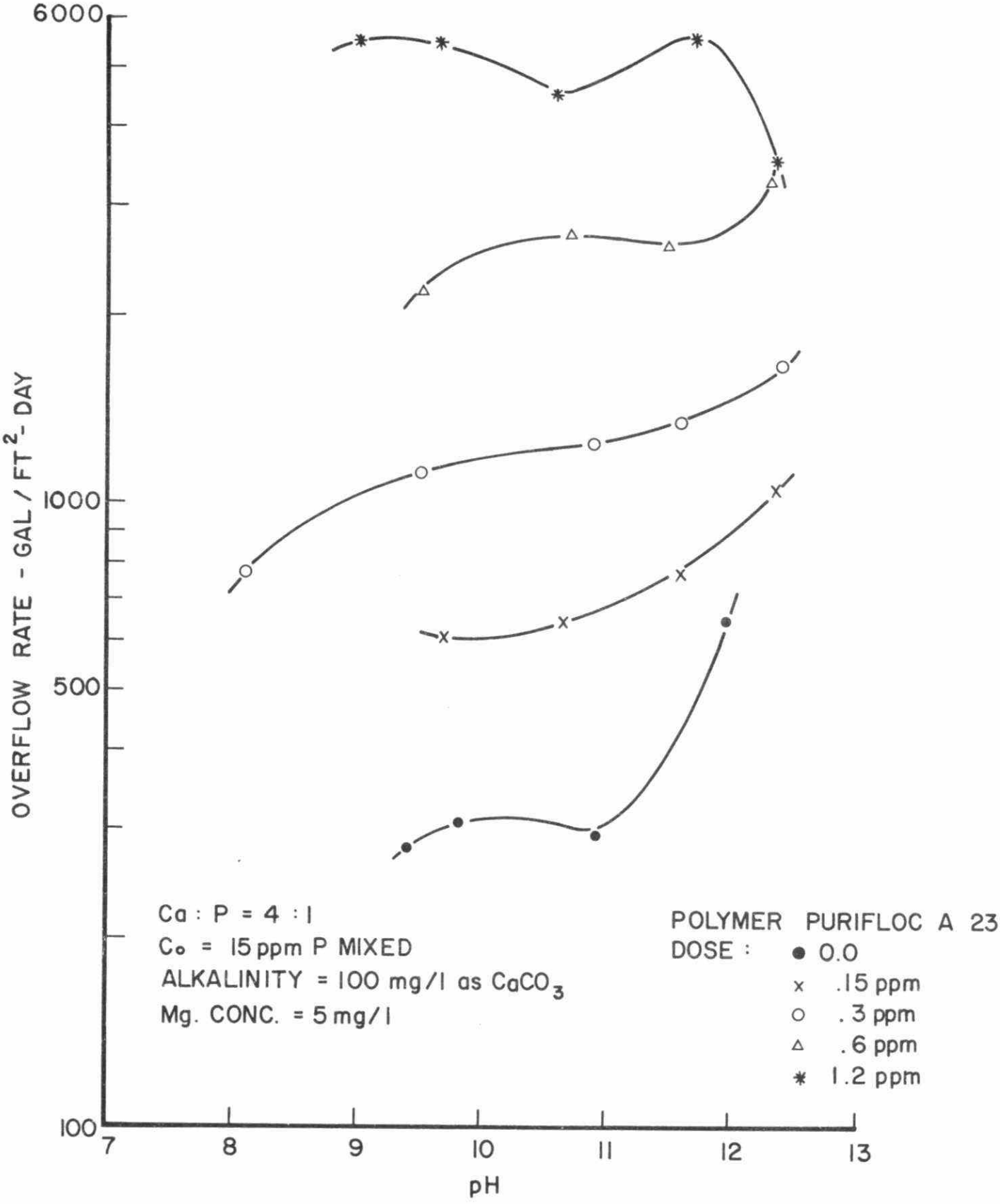

FIGURE 55. MAXIMUM PERMISSIBLE OVERFLOW RATE FOR 90% FLOC REMOVAL IN THE CALCIUM-MIXED PHOSPHATE SYSTEM WITH POLYELECTROLYTE ADDITION

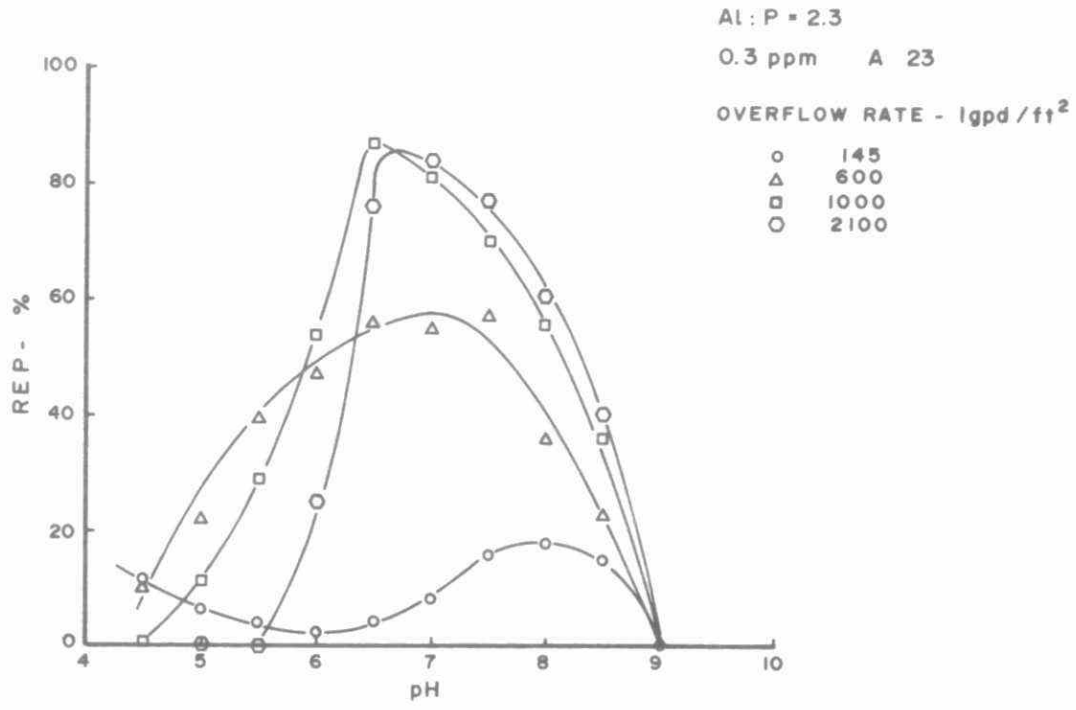

FIGURE 56. REP IN THE ALUMINUM-ORTHOPHOSPHATE SYSTEM

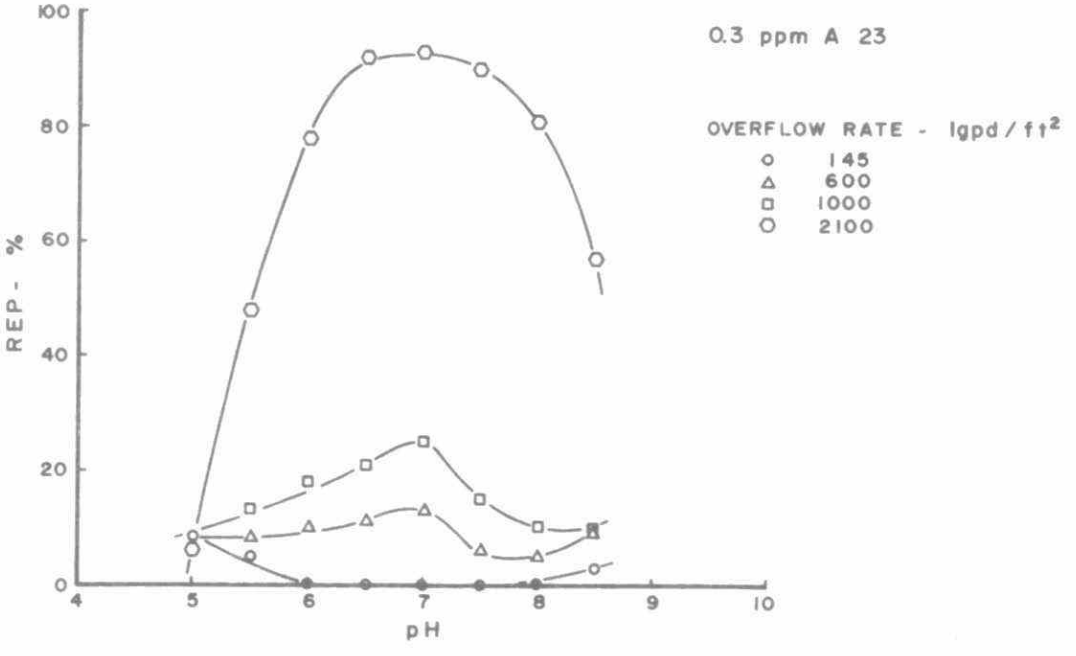

FIGURE 57. REP IN THE IRON-ORTHOPHOSPHATE SYSTEM

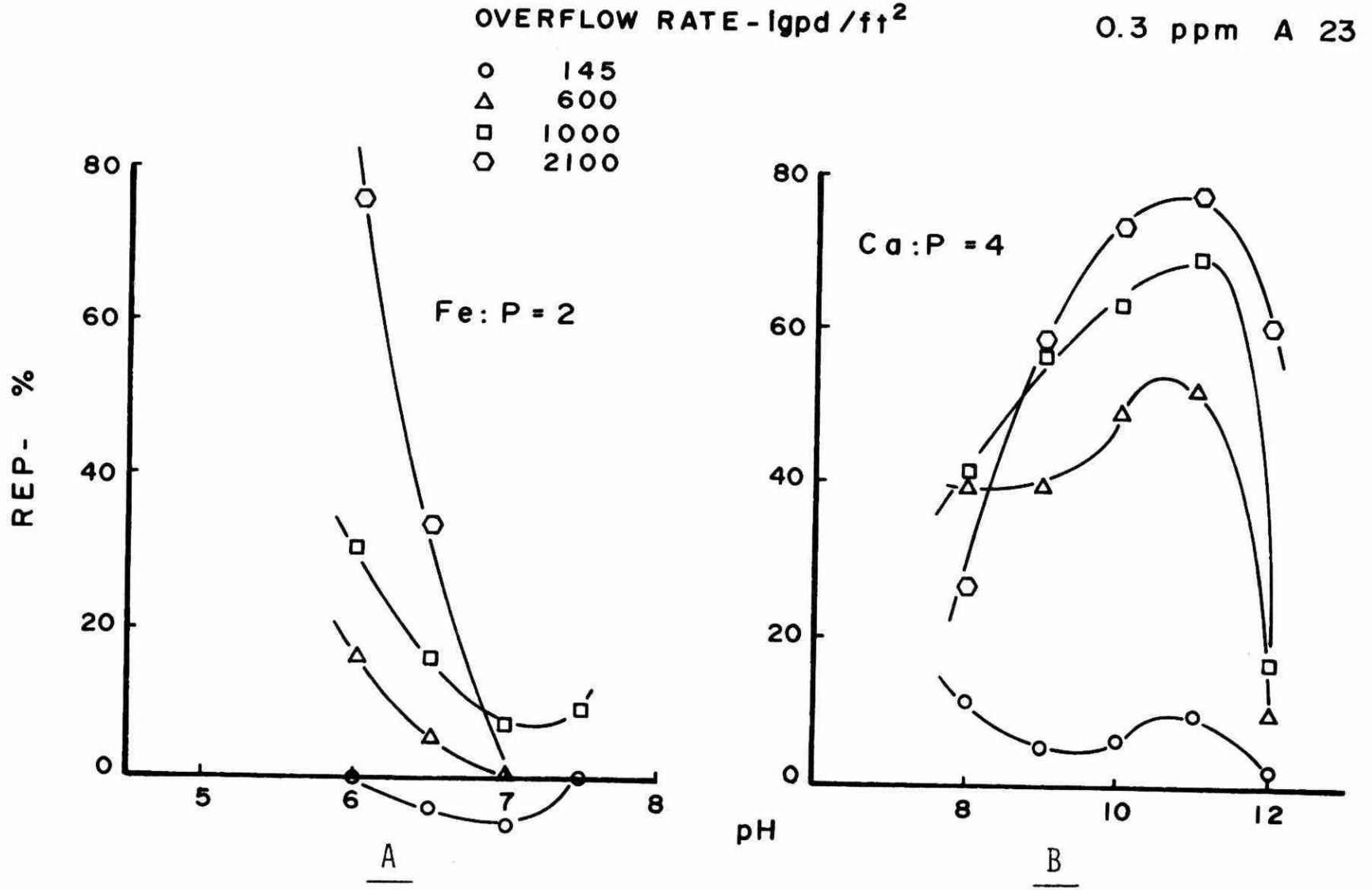

FIGURE 58. REP IN THE A) IRON-MIXED PHOSPHATE SYSTEM
B) CALCIUM-MIXED PHOSPHATE SYSTEM

With lime, in Figure 58B, REP is again strongly pH dependent and peaks occur near pH 11 at overflow rates of 600 lgpd/ft^2 and higher. The sharp drop at pH 12 is due to the relatively good settleability of the calcium phosphate precipitate without polyelectrolytes at pH 12.

5.3.3 Polyelectrolyte dosage

Phosphorus removal as a function of polyelectrolyte dosage, overflow rate and pH is shown in Figure 59 for aluminum, Figure 60 for iron and Figure 61 for lime. Additional curves are presented in Figures 171 to 176 in Appendix A.

These figures show that the first increment in polyelectrolyte dosage, in this case 0.15 ppm, gave the greatest improvement in phosphorus removal over the addition of metal only. Further increase in polyelectrolyte dosage did not appreciably increase phosphorus removals, except at high overflow rates or pH values outside the optimum range.

In the mixed phosphate systems with aluminum and iron, below pH 6.5, the required anionic polyelectrolyte dosages were identical with the dosages determined for the orthophosphate systems. Above pH 6.5, the anionic polyelectrolytes were not as useful (see Figures 172, 173 and 174 in Appendix A) due to the formation of excessive amounts of negatively charged near colloidal particles. The usefulness of cationic polyelectrolytes in this pH region will be shown in Section 5.3.4.

The optimum polyelectrolyte dosage may be determined from Figures 59, 60 and 61 at the point where the tangents to the nearly vertical and horizontal sections of the curves intersect. Thus, the optimum polyelectrolyte dosage is approximately 0.3 ppm for all three metal systems.

5.3.4 Polyelectrolyte characteristics

5.3.4.1 Anionic polyelectrolytes. The first indication in this project of differences in performance between anionic polyelectrolytes of different degrees of hydrolysis is shown in Figure 62. At pH 5.9, the addition of 0.6 ppm Percol 730 resulted in an overflow rate of 6500 lgpd/ft^2, while with 0.6 ppm Purifloc A23, an overflow rate of 850 lgpd/ft^2 was obtained. The performance of a large number of polyelectrolytes and the effect of parameters such as hydrolysis are further evaluated in Section 8.

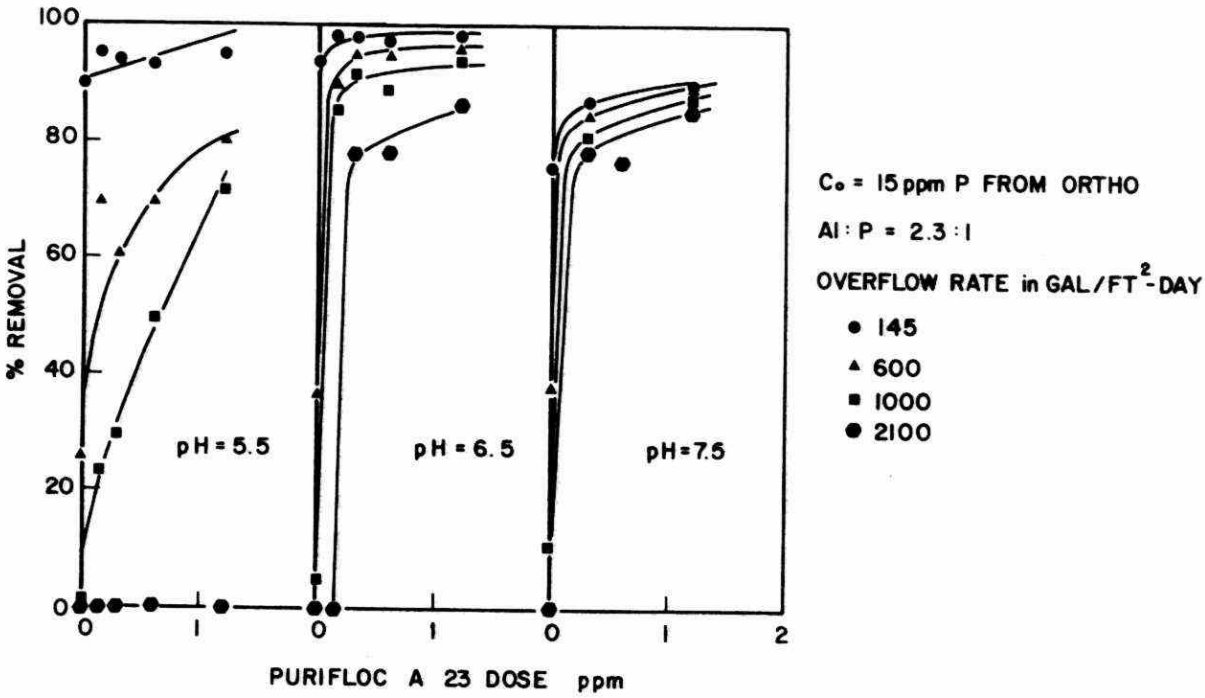

FIGURE 59. PHOSPHORUS REMOVAL AS FUNCTION OF POLYELECTROLYTE DOSAGE IN THE ALUMINUM-ORTHOPHOSPHATE SYSTEM

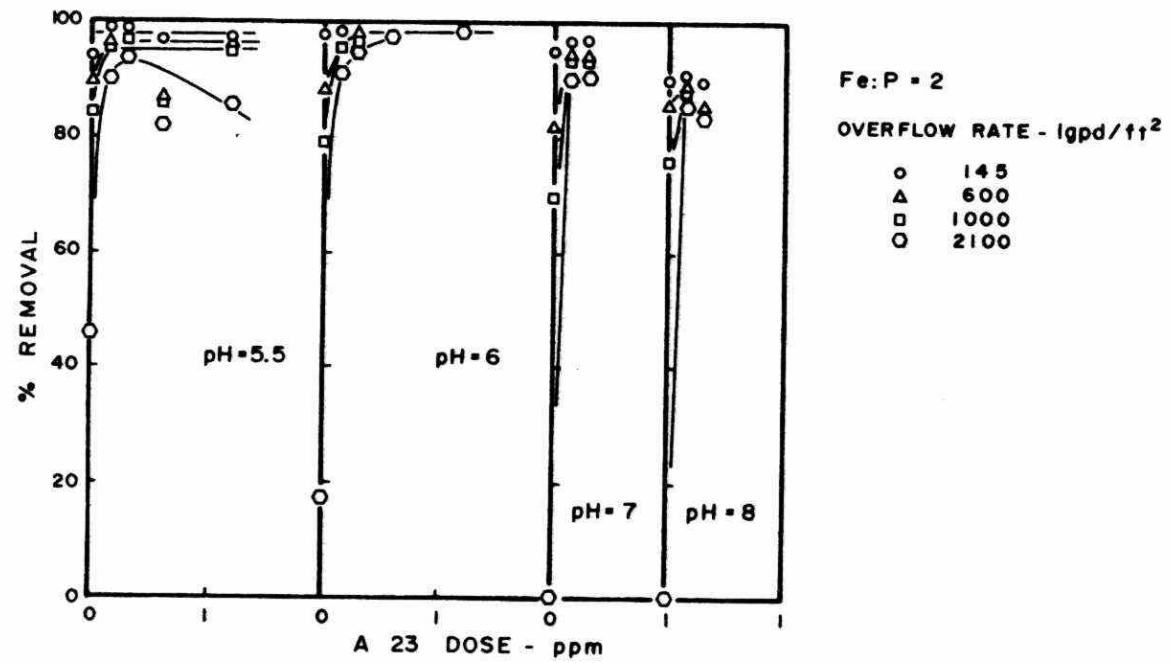

FIGURE 60. PHOSPHORUS REMOVAL AS FUNCTION OF POLYELECTROLYTE DOSAGE IN THE IRON-ORTHOPHOSPHATE SYSTEM

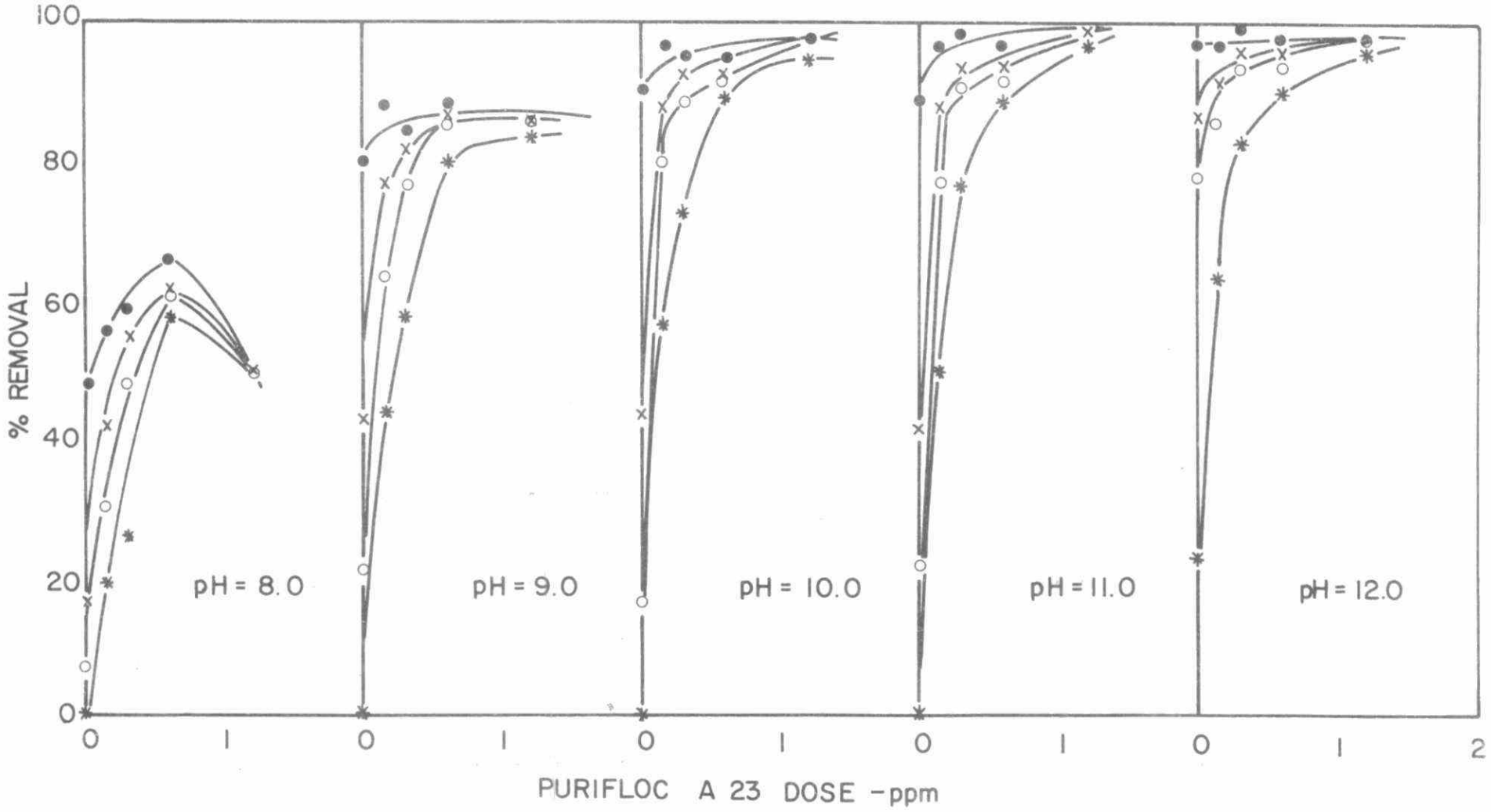

C_o = 15 ppm P :
50 % FROM ORTHO
10 % FROM PYRO
40 % FROM TRIPOLY

Ca : P = 4 : 1

OVERFLOW RATE
GAL / FT^2 – DAY
● 145 ○ 1000
× 600 * 2100

FIGURE 61. PHOSPHORUS REMOVAL AS FUNCTION OF POLYELECTROLYTE DOSAGE IN THE CALCIUM-MIXED PHOSPHATE SYSTEM

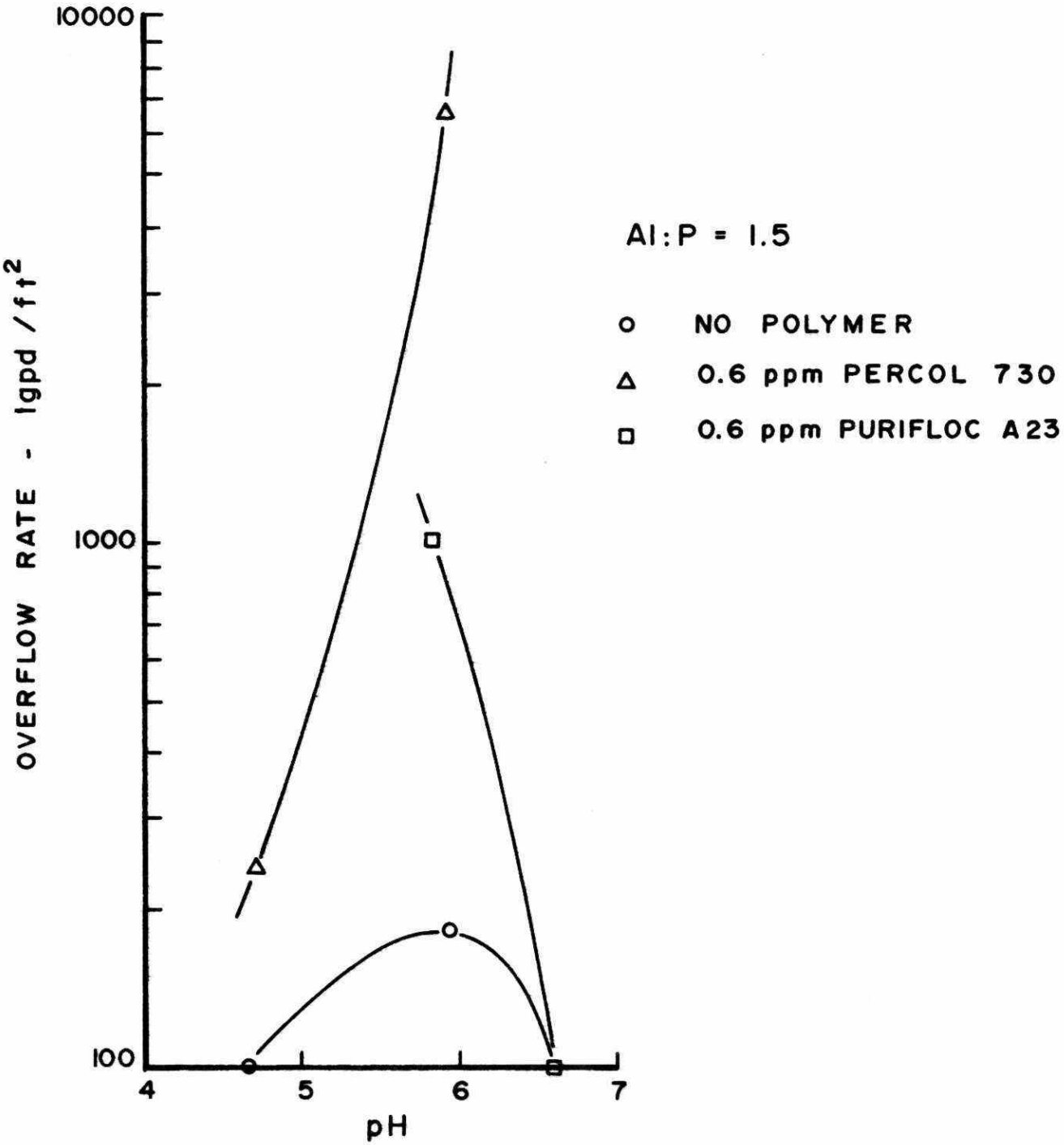

FIGURE 62. MAXIMUM PERMISSIBLE OVERFLOW RATES FOR 90% FLOC REMOVAL WITH PERCOL 730 AND PURIFLOC A23

5.3.4.2 Cationic polyelectrolytes. The presence of condensed phosphates with anionic polyelectrolytes was shown to be detrimental to phosphorus removal in Sections 4 and 5.3.3. Phosphorus removal with aluminum was most seriously affected (Figures 27 and 28). The fraction of near colloidal particles is blamed for the slow settling flocs resulting in incomplete phosphorus removal. The charge on these particles is increasingly negative with pH; thus, a cationic polyelectrolyte is expected to successfully flocculate the particles as pH is increased. Phosphorus removals with aluminum and anionic (Percol 730) and cationic (Percol 728) polyelectrolytes are presented in Figure 63. Below pH 6.5, the anionic polyelectrolyte increased phosphorus removals at all overflow rates, as shown by the closely spaced data points. Above pH 6.5, however, the cationic polyelectrolyte became predominant, as expected. Removals as high as 80% and very fast settling were achieved, as shown by the identical positions of the data points, where no removals were evident without polyelectrolyte addition. It is possible (but not probable on the basis of the data presented in Section 5.3.5) that a cationic polyelectrolyte in this region acts as a primary coagulant.

5.3.5 Presence of divalent cations (Ca^{++})

The effect of the presence of Ca^{++} on ultimate phosphorus removal is examined in Figure 64.

With the replacement of $NaHCO_3$ by $CaCO_3$ as the source of carbonate alkalinity, phosphorus removal was greatly increased throughout the pH range of 5 to 9 and especially above 6.5. The ultimate phosphorus removal with polyelectrolyte addition again follows, with some improvement, the removal envelope defined by alum addition alone. At pH 7, the addition of 0.3 ppm A23 obtained 75% phosphorus removal in the presence of $CaCO_3$, while 0.6 ppm A23 obtained only 2% removal in the presence of $NaHCO_3$. At pH 7, however, the addition of 0.3 ppm Percol 728 obtained 78% phosphorus removal in the presence of $CaCO_3$, while 3.0 ppm Percol 728 obtained only 70% removal in the presence of $NaHCO_3$.

This may indicate that, as the precipitate becomes increasingly negative, the presence of a divalent cation, such as Ca^{++}, improves the attachment of negatively charged electrolytes. It is also possible,

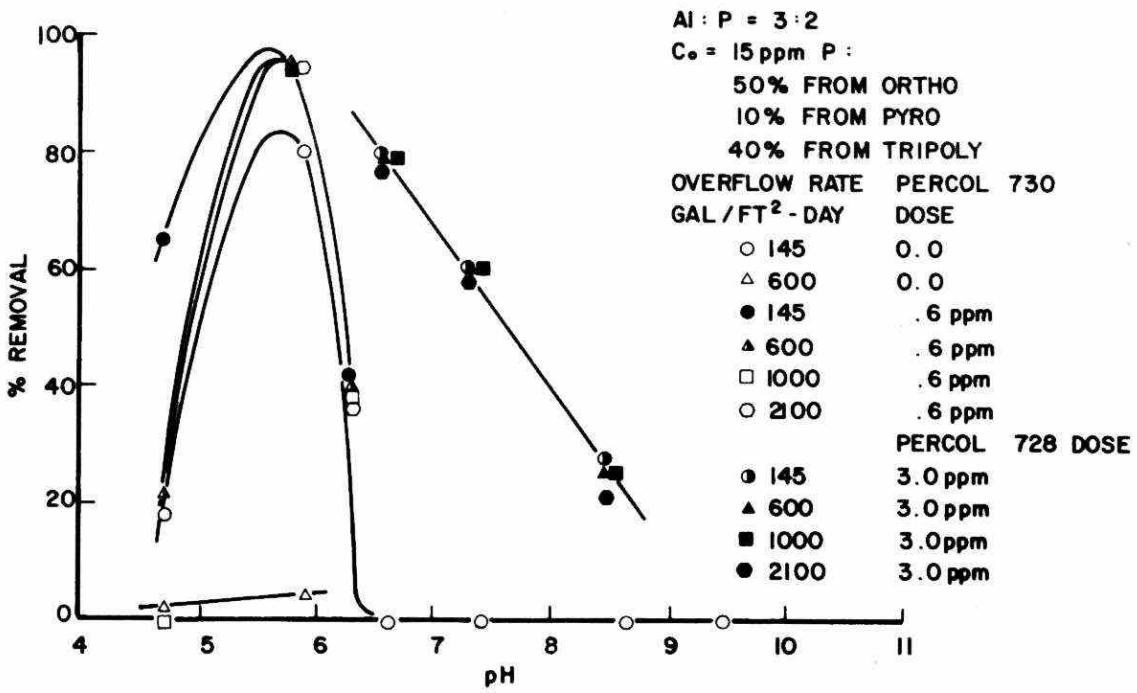

FIGURE 63. PHOSPHORUS REMOVAL WITH ANIONIC (P-730) AND CATIONIC (P-728) POLYELECTROLYTES IN THE ALUMINUM-MIXED PHOSPHATE SYSTEM

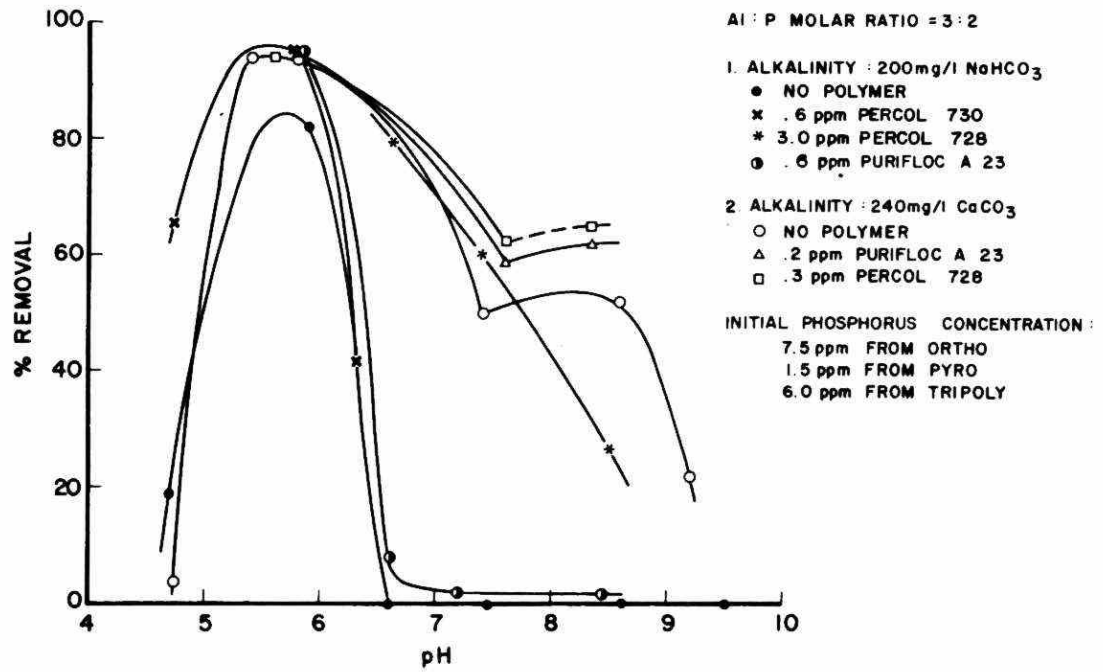

FIGURE 64. PHOSPHORUS REMOVAL IN THE PRESENCE AND ABSENCE OF $CaCO_3$ WITH POLYELECTROLYTE ADDITION

as discussed in Section 4, that a calcium may react with phosphate to bring about further removal.

Removals in the presence of a cationic polyelectrolyte appeared to be similar to those with calcium and anionic polyelectrolyte. This indicates that the cationic polyelectrolyte was not acting as a primary coagulant.

5.4 Conclusions

The following conclusions can be drawn from this study:

1) Phosphorus removal with polyelectrolyte addition followed, with some improvement, the ultimate removal envelope defined by metallic coagulant addition alone.

2) Polyelectrolyte addition substantially improved settling at all pH levels where a precipitate formed. Maximum settling usually occurred at the optimum precipitation pH.

3) Maximum permissible overflow rates for 90% floc removal were increased by polyelectrolyte dosages as low as 0.15 ppm to well above typical clarifier design overflow rates (600-800 lgpd/ft^2) at near optimum pH. As pH moved away from the optimum pH, higher polyelectrolyte dosages were required.

4) At pH greater than 6.5, in the aluminum system, if calcium ions are present, anionic polyelectrolytes can be used. In the absence of calcium, cationic polyelectrolytes are recommended.

6. LABORATORY STUDIES ON DOMESTIC WASTEWATER

The techniques developed in Section 2 and tested on model solutions, i.e., Sections 4 and 5, were applied to pretreated raw sewage in these studies. The objectives were as follows:

i) to establish the settleability of alum precipitated sewage at different polyelectrolyte dosages;

ii) to determine the validity of model solution studies; and,

iii) to establish the ideal sedimentation tank framework for the full scale studies described in Section 7.

6.1 Experimental

6.1.1 Apparatus and procedure

The batch settling apparatus tests were conducted (as described in Section 2) on raw sewage samples collected at either the Napanee, Ontario or the Dundas, Ontario, Water Pollution Control Plants.

Due to the random variations in sewage composition, ten tests were carried out for each chemical dosage in accordance with the Ministry of the Environment guidelines (Van Fleet, 1972).

Enough raw sewage, about 20 litres, was collected to conduct a full set of batch settling apparatus tests.

Normally, a 250 ml sample was taken from the fully mixed sewage sample for analysis. The samples for differential phosphorus analysis were frozen in dry ice immediately after collection.

6.1.2 Analysis

The samples destined for soluble phosphorus analysis were filtered through 0.45μ sartorious membranes, and were then acidified and analyzed with the Technicon Auto-Analyzer.

The samples destined for total phosphorus analysis were acidified with five drops of concentrated sulphuric acid (the samples collected during the batch settling apparatus tests were acidified immediately following the completion of the tests), filtered through the 0.45μ membrane and analyzed with the Technicon Auto-Analyzer in accordance with Technicon's method 3-68 W.

The filtered unacidified portion of the raw sewage was analyzed for ortho, pyro and tripoly phosphates by ion exchange chromatography and continuous phosphorus analysis as described in detail by Melnyk (1974).

6.2 Results and Discussion

6.2.1 The nature and occurrence of phosphorus

The probability distributions of the various types of phosphates in raw municipal wastewater are presented in Figures 177 and 178 in Appendix A, and summarized in Table 2 below.

TABLE 2. PHOSPHORUS OCCURRENCE IN DOMESTIC WASTEWATERS
(As determined from probability plots, Figures 177 and 178)

Phosphorus	Dundas			Napanee		
	Av. mg/l	S.D.	% of + soluble	Av. mg/l	S.D.	% of + soluble
Total	6.6	1.3	-	4.0	1.0	-
Soluble	5.1	1.45	100	3.15	.65	100
Ortho	4.05	.95	79	2.45	.7	78
Pryo	.1	.07	2	.2	.1	6
Tripoly	.7	.5	14	.85	.45	27

Total phosphorus levels were relatively low due to infiltration problems at both plants, although unusually high phosphorus levels were occasionally encountered in the Napanee samples, due to sporadic milky waste slugs.

Table 2 shows that, on the percent soluble basis, the Napanee sewage contained higher levels of condensed phosphates than the Dundas sewage. Condensed phosphates were relatively low at both plants due to the gradual reduction of detergent phosphates in Canada (Canada Water Act Annual Report, 1973-74).

Figure 65 shows the seasonal variation of phosphorus in the Dundas raw sewage. The differences in sewage used for the tests with 130 and 160 mg/l alum, and 190 mg/l alum plus 0.3 and 0.8 ppm Percol 730 were encountered in a period of about six weeks, while the sewage for the 190 mg/l alum plus 1.2 ppm Percol 730 tests was collected four months later.

6.2.2 Alum dosage

Figures 66 and 67 show the ultimate residual phosphorus concentrations obtained in Napanee and Dundas. The ultimate phosphorus residual is determined at the point where the slope of the settling curves is zero in Figure 179 in Appendix A.

In Napanee, one of the alum dosages used was 150 mg/l as $Al_2(SO_4)_3 \cdot 14H_2O$, based on recommendations by Love Associates (1972), and the other dosage used was 110 mg/l. The second alum dosage was chosen because the studies described in Section 5 showed that when polyelectrolytes are used, alum dosages can be somewhat reduced without sacrificing effluent quality. As shown in Figure 66, there was only a slight lowering of the phosphorus residual with increased alum dose. The milky wastewater samples, however, could not be treated successfully at these dosages.

In Dundas, a different situation appeared. The alum dosage suggested by Underwood McLellan and Associates (1972) was 150 mg/l as $Al_2(SO_4)_3 \cdot 16H_2O$. Based on this, alum dosages of 130 and 160 mg/l were initially chosen. As shown in Figure 67, both dosages were inadequate for the samples. In this case, a relatively high alum dosage of 190 mg/l was required to effect precipitation below 1 mg/l of phosphorus.

6.2.3 Al:P molar ratio

All ultimate residual data in the alum-sewage system are plotted in Figures 68 and 69 for Napanee and Dundas, respectively. There are apparent trends in these figures. First, up to a certain point, removal improved with increasing Al:P ratio. After this point, however, increasing Al:P ratio did not appear to change the percent removal. This "break" point between the two regions could be considered in determining the optimum Al:P ratio.

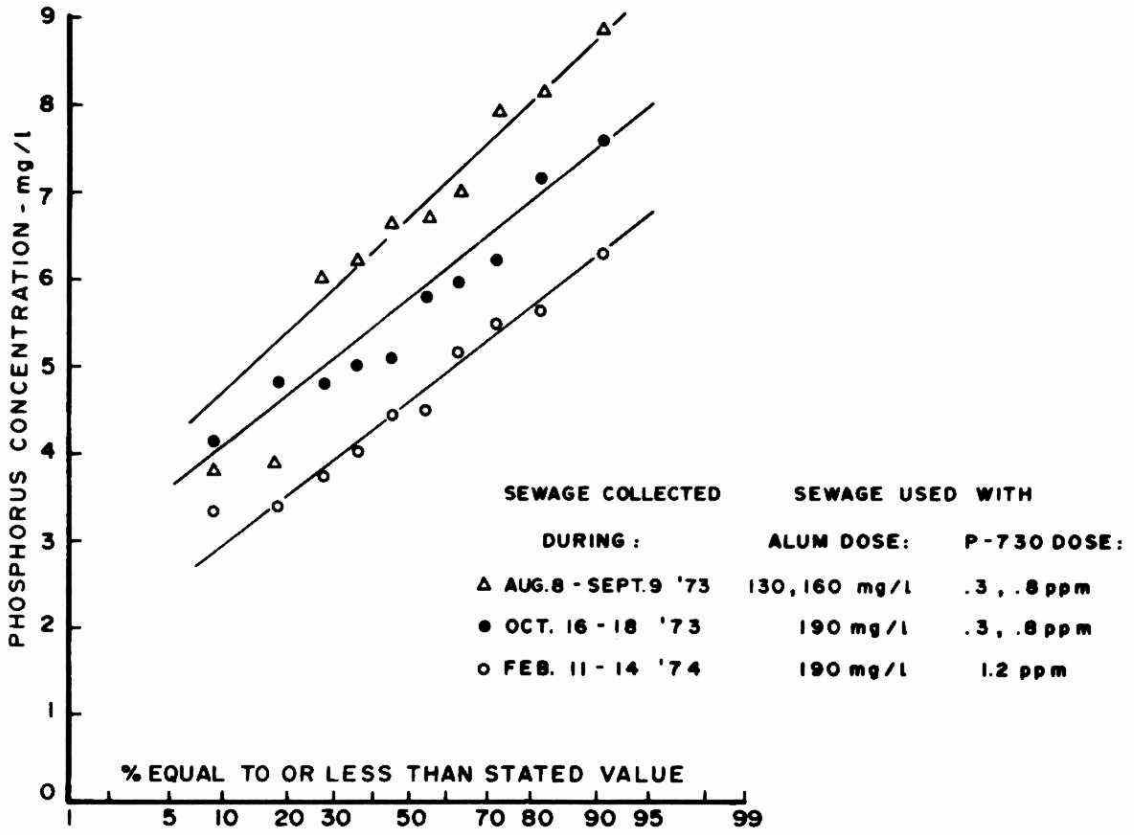

FIGURE 65. OCCURRENCE OF PHOSPHORUS IN DUNDAS RAW SEWAGE

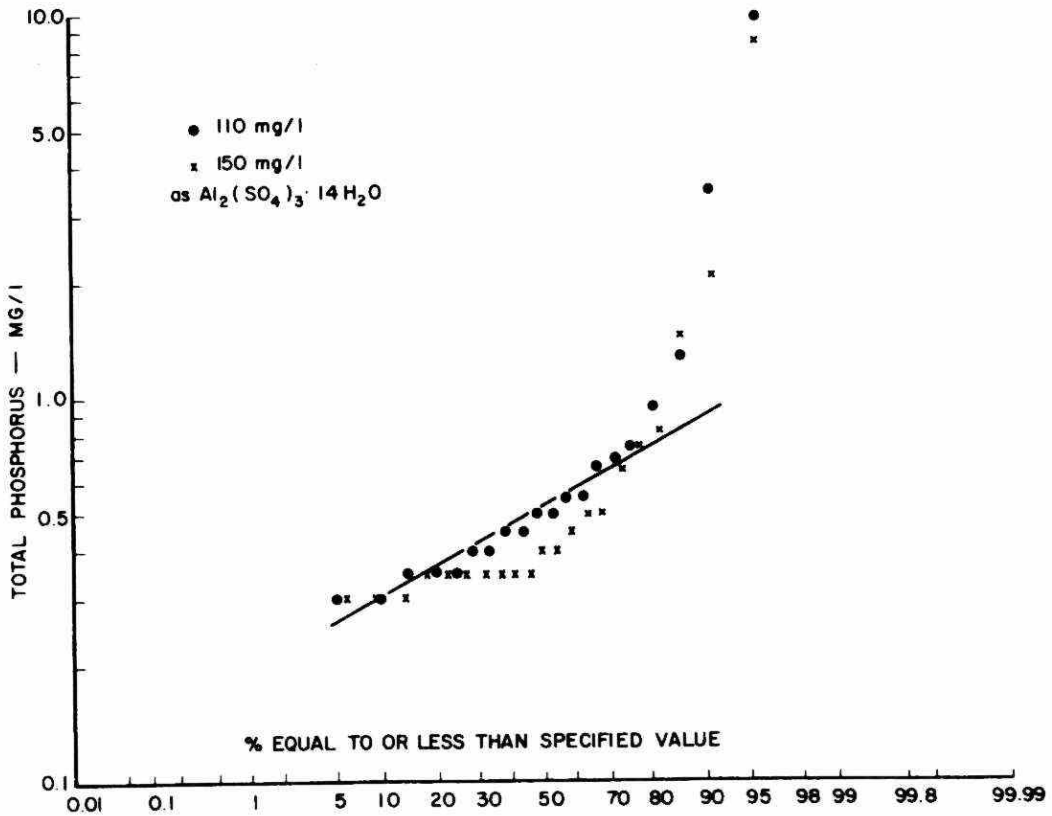

FIGURE 66. ULTIMATE RESIDUAL PHOSPHORUS LEVELS RESULT OF ALUM ADDITION TO NAPANEE RAW SEWAGE

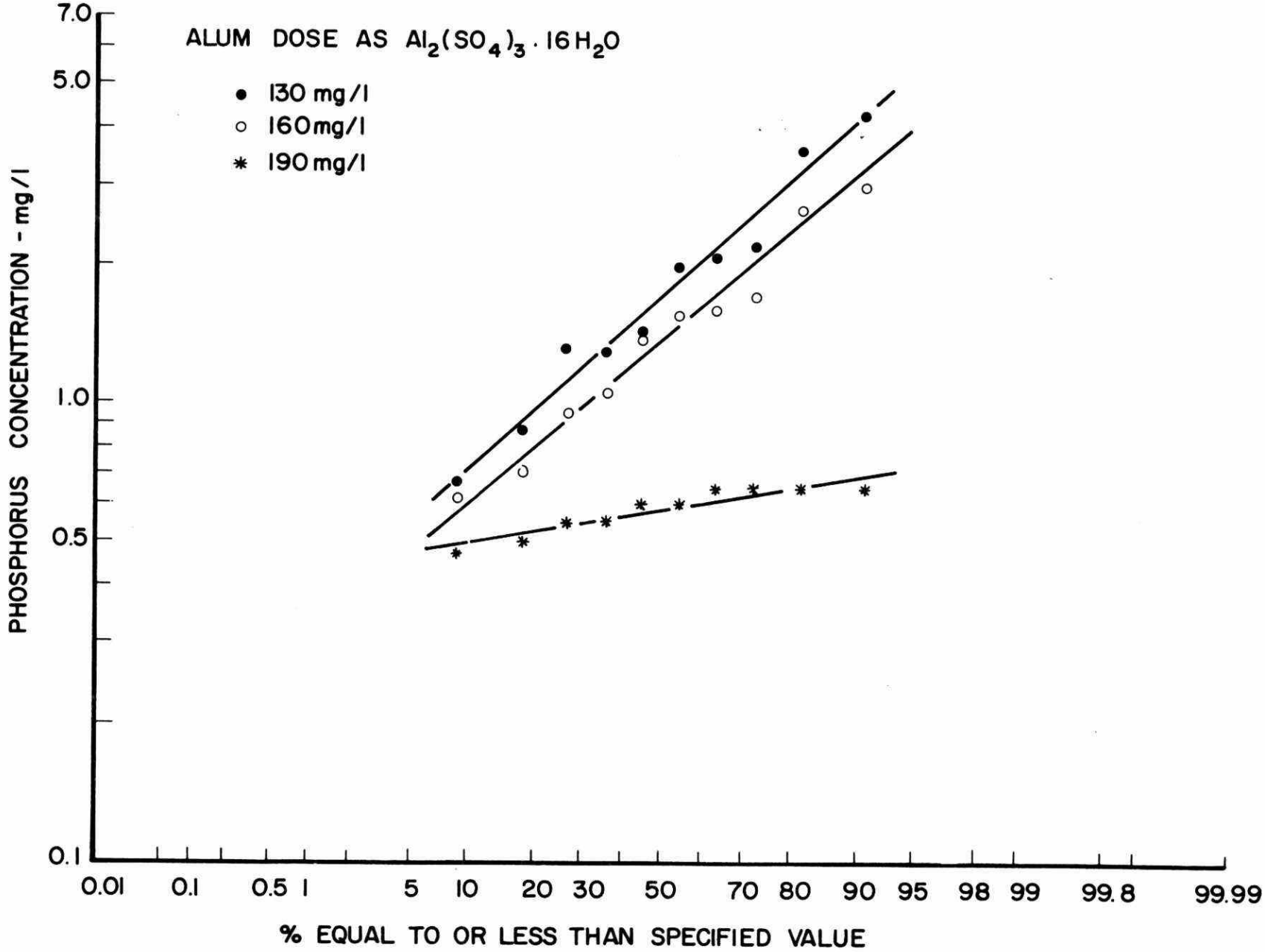

FIGURE 67. ULTIMATE RESIDUAL PHOSPHORUS LEVELS RESULT OF ALUM ADDITION TO DUNDAS RAW SEWAGE

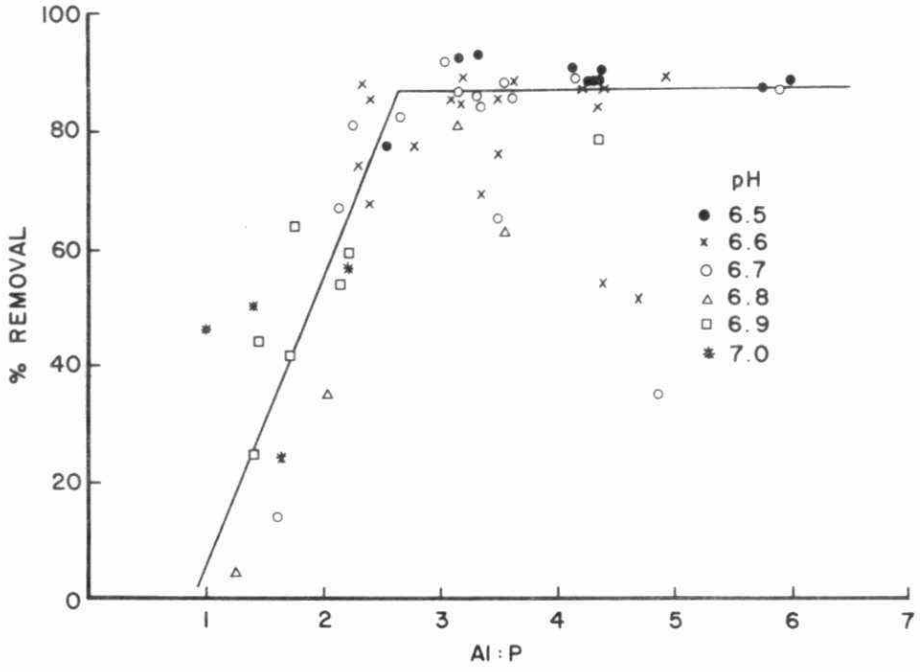

FIGURE 68. PHOSPHORUS REMOVAL AS FUNCTION OF AL:P MOLAR RATIO IN NAPANEE RAW SEWAGE

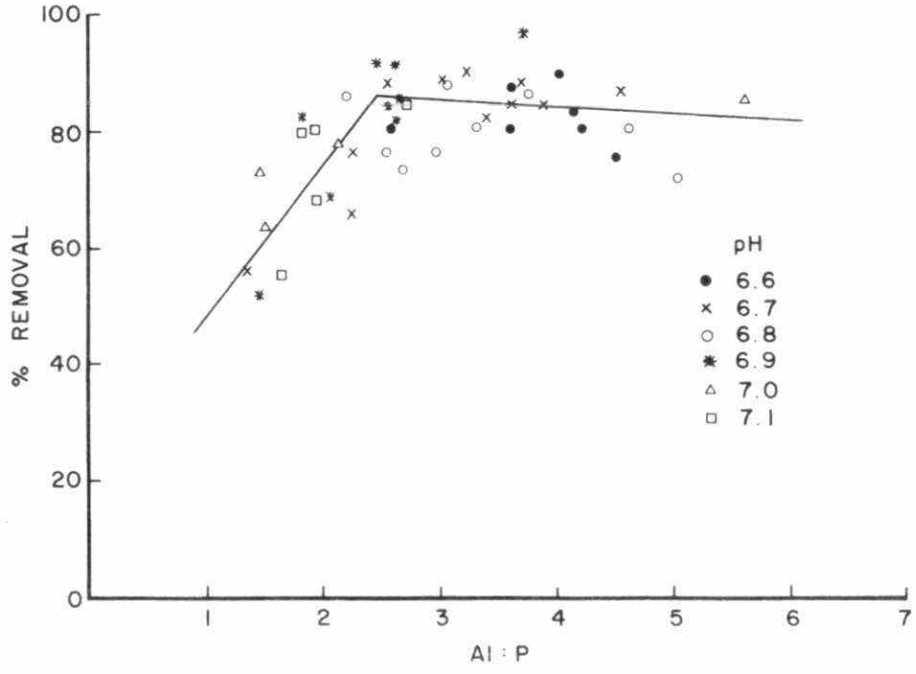

FIGURE 69. PHOSPHORUS REMOVAL AS FUNCTION OF AL:P MOLAR RATIO IN DUNDAS RAW SEWAGE

Unfortunately, data scatter does not permit the accurate identification of the optimum point, although its location can be estimated by the intersection of the least square lines fitted to the lower and upper section of the data in Figures 68 and 69. Thus, the estimated optimum Al:P molar ratio was 2.63 for the Napanee sewage and 2.45 for the Dundas sewage. In the model studies, this optimum ratio was between 1.6-3, depending on pH. The effect of pH over the narrow range of 6.5-7.0 does not appear to be significant in Figures 68 and 69; however, weak trends would be masked by data scatter.

The aluminum-phosphate flocs settled very slowly at all alum doses. Both in Napanee and Dundas, the overflow rate permitted for 90% of the ultimate phosphorus removal was 400 Igpd/ft^2 in Napanee and 350 Igpd/ft^2 in Dundas (see Figures 178, 179, 180, 181, 191, and 192 in Appendix A).

Figure 70 indicates that, with identical pH and Al:P molar ratios, the floc settling velocities in sewage were very similar to floc settling velocities in model solutions. This indicates that the inorganic precipitate (mostly aluminum hydroxide) settling velocity is insignificantly altered by the presence of organic wastewater colloids.

6.2.4 Comparison to Ministry of the Environment Data

The Ontario Ministry of the Environment researchers summarized their extensive jar test results (ultimate residual concentrations), indicating the range of alum dosages required for a 1 ppm residual as function of initial phosphorus concentration (Boyko and Rupke, 1973).

The 190 mg/l as $Al_2(SO_4)_3 \cdot 16H_2O$, or 179 mg/l as $Al_2(SO_4)_3 \cdot 14\ H_2O$, alum dosage used with the Dundas sewage with an average phosphorus concentration of 5.2 mg/l corresponds to the alum dosage required for similar sewage in the Ministry data. At Napanee, 150 mg/l as $Al_2(SO_4)_3 \cdot 14\ H_2O$ alum dosage (with an average raw sewage phosphorus concentration of 4 mg/l) also corresponds quite well to the Ministry average and the 110 mg/l dosage is about 30% below the average.

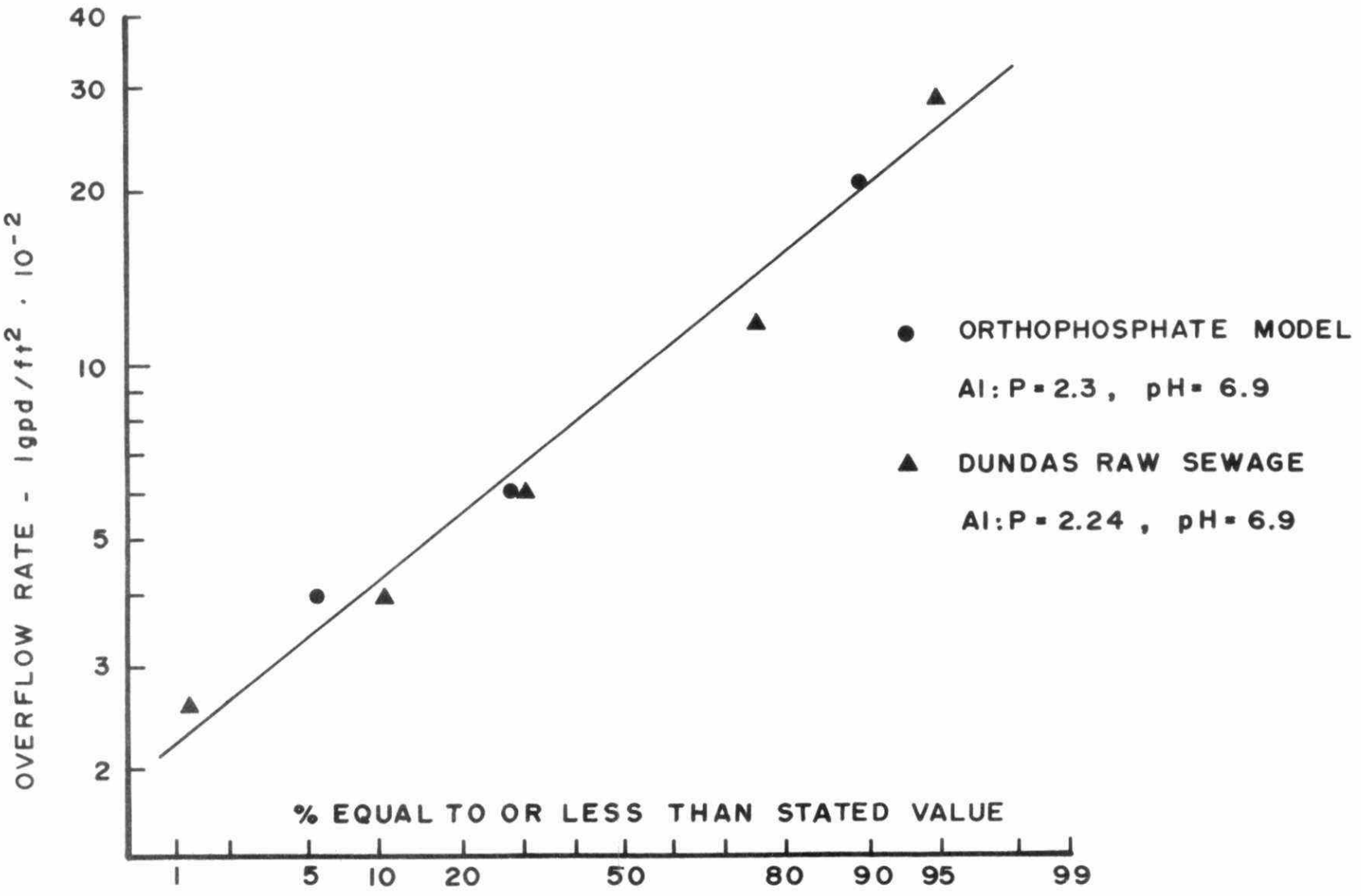

FIGURE 70. FLOC SIZE DISTRIBUTION IN ORTHOPHOSPHATE SOLUTION AND IN DUNDAS RAW SEWAGE UNDER SIMILAR CONDITIONS

6.2.5 Polyelectrolyte choice

The polyelectrolytes considered for use were Purifloc A23 (Dow Chemical), Percol 726, 728, 730 (Allied Colloids), and Praestol 444K (Bayer Dyestuffs and Chemicals), in Napanee, and Purifloc A23 WT-3000 (Calgon Corporation), Hercofloc 822.2 (Hercules Inc.), Percol 728 and Percol 730 in Dundas. Preliminary tests showed that Percol 730 Purifloc A23 and WT-3000 were the most effective and further evaluations were undertaken for these three polyelectrolytes.

Figures 71 and 72 compare the effectiveness of Percol 730 and Purifloc A23 in settling alum-phosphate flocs from Napanee raw sewage at 0.45 mg/l polyelectrolyte dosage. Figures 182 to 185 in Appendix A compare the effectiveness of these polyelectrolytes at other dosages. The ultimate phosphorus residuals were quite similar for both polyelectrolytes. Sharp differences between polyelectrolytes become evident, however, when floc settling rates are examined. For example at 0.45 ppm Percol 730, the average permissible overflow rate of 1 ppm residual phosphorus was 2000 $lgpd/ft^2$ (with a standard deviation of 650) while for Purifloc A23, an overflow rate of only 550 $lgpd/ft^2$ (with a standard deviation of 380) was permissible.

Polyelectrolytes Percol 730 and WT-3000 were compared through a similar set of data (see Appendix A, Figures 186 to 190) using Dundas wastewater. Once again, Percol 730 proved superior. The major difference between Percol 730 and the other two polyelectrolytes was in degree of hydrolysis. The effect of the degree of hydrolysis and the molecular weight is examined further in Section 9 for a wide variety of commercial polyelectrolytes. Percol 730's degree of hydrolysis was at least 15% lower than that of the other two polyelectrolytes (A23 and WT-3000) and, according to Section 9, this is the reason for the better performance.

6.2.6 Polyelectrolyte enhancement

Figures 73 and 74, along with Appendix Figures 182, 184, 186, 188, and 190, show that the ultimate phosphorus removal from sewage with polyelectrolyte addition follows, with some improvement, the removal envelope defined by the alum addition alone. In the Napanee study (Figure 72) some data points with alum alone were well below the majority of data points for similar Al:P ratios (see Section 6.2.2). Polyelectrolyte addition moved up the residual concentrations found in such cases to

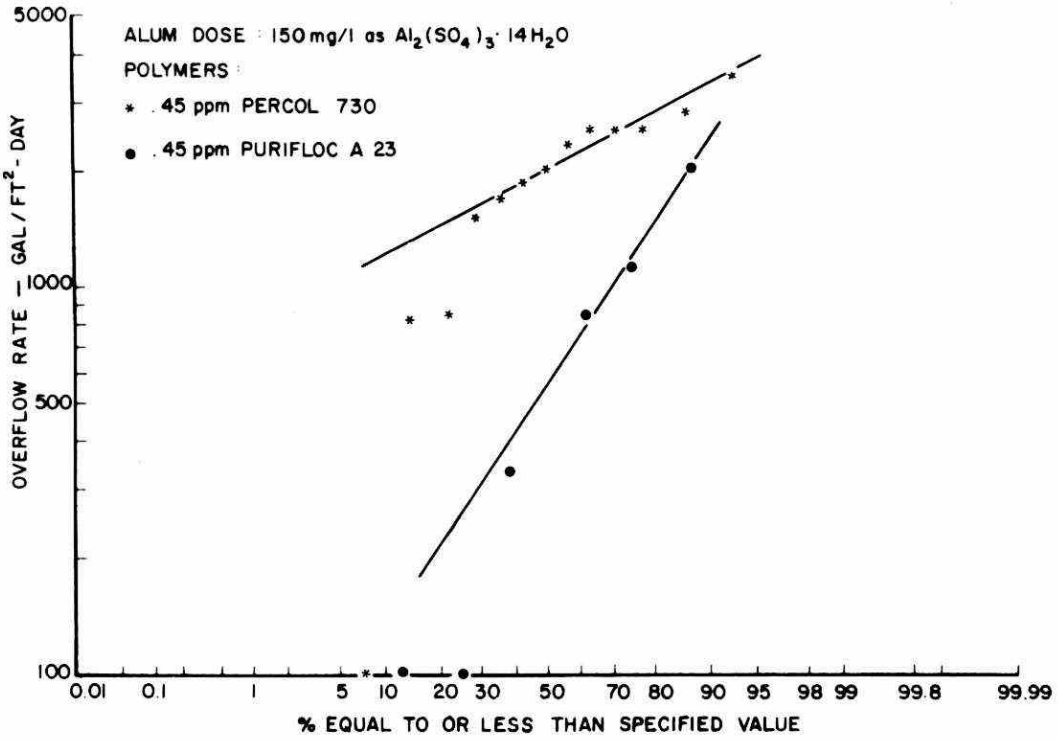

FIGURE 71. PERMISSIBLE OVERFLOW RATES FOR 90% FLOC REMOVAL WITH ALUM, PURIFLOC A23, AND PERCOL 730 IN NAPANEE RAW SEWAGE

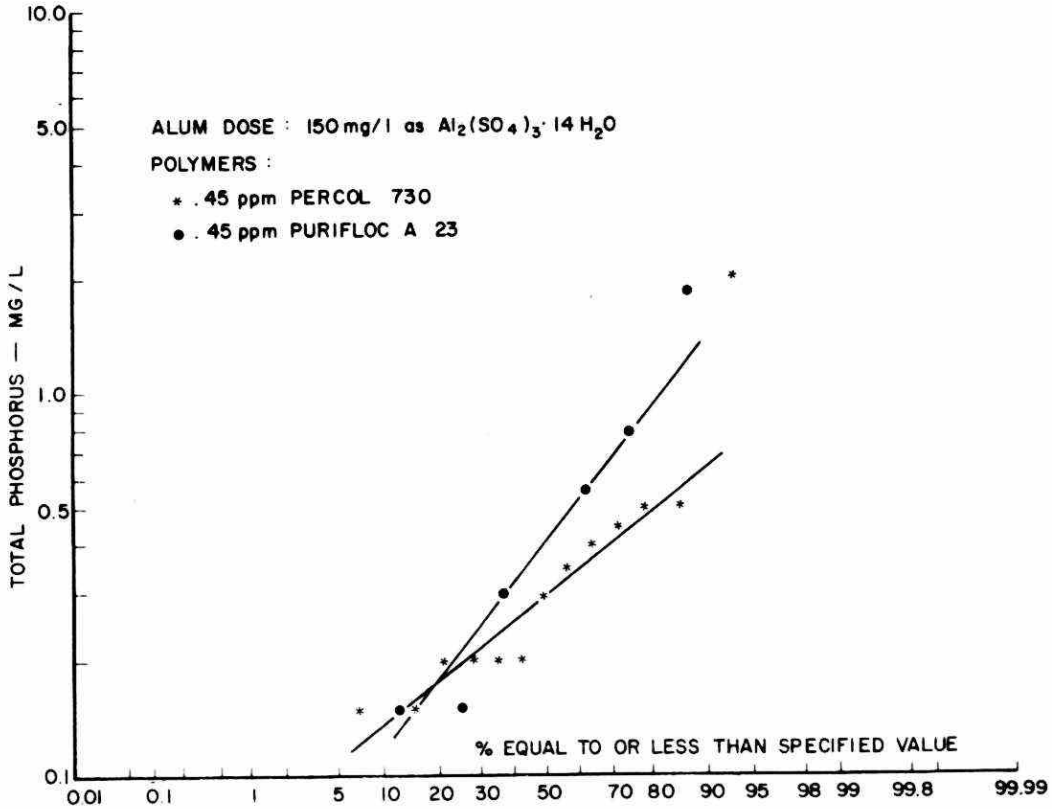

FIGURE 72. ULTIMATE PHOSPHORUS RESIDUALS OBTAINED WITH ALUM, PURIFLOC A23 AND PERCOL 730

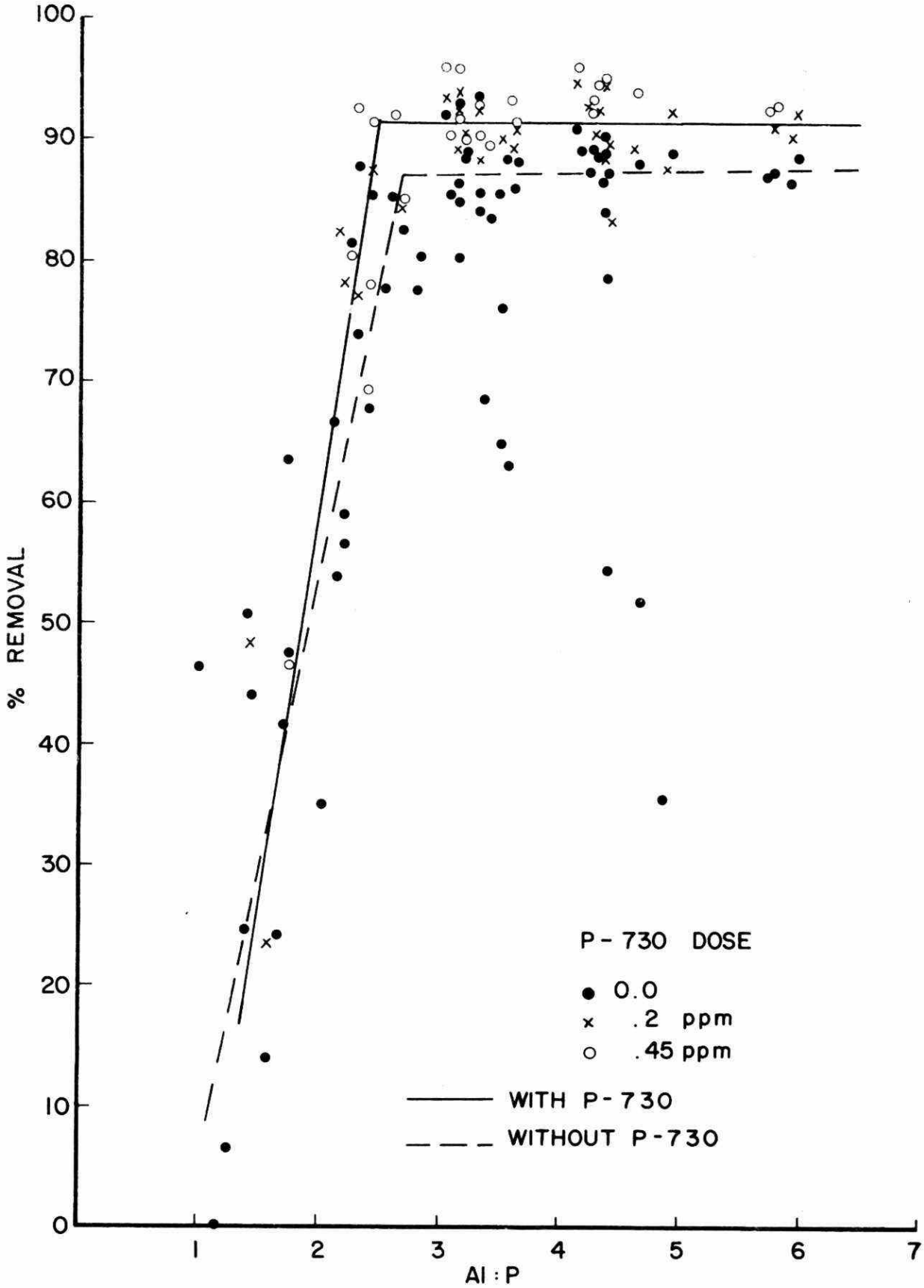

FIGURE 73. PHOSPHORUS REMOVAL AS FUNCTION OF AL:P MOLAR RATIO WITH PERCOL 730 IN NAPANEE RAW SEWAGE

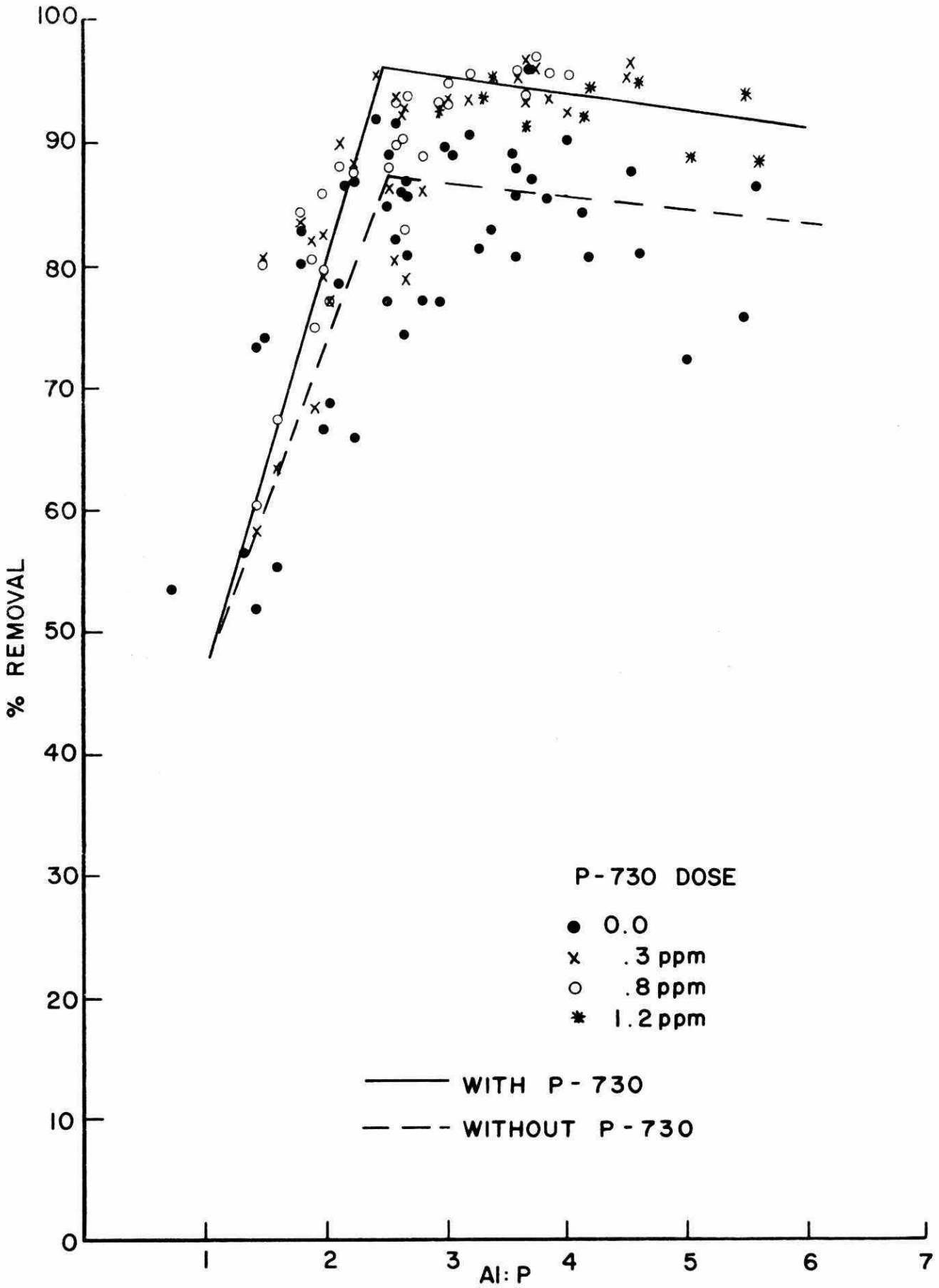

FIGURE 74. PHOSPHORUS REMOVAL AS FUNCTION OF Al:P MOLAR RATIO WITH ALUM AND PERCOL 730 IN DUNDAS RAW SEWAGE

blend with other data points. Thus, poor removals at high Al:P ratios were probably caused by difficult to settle colloidal precipitates.

Residual concentrations appear to be a weak function of increased polyelectrolyte dosage.

The optimum Al:P molar ratios were slightly reduced with polyelectrolyte addition, in Napanee sewage from 2.63 to 2.5, and in Dundas sewage from 2.5 to 2.45. The phosphorus removal with the optimum Al:P ratio was increased with polyelectrolyte addition by 4 percentage points in Napanee sewage, and by 9 percentage points in Dundas sewage for the optimum Al:P ratios with alum alone. These increases in removal apparently remain constant above the alum-only line. Figure 75, and Figures 183, 185, 187, 189, 191 and 192 in Appendix A, present the maximum permissible overflow rates for 90% floc removal.

In Napanee, the average overflow rates were raised from 400 Igpd/ft^2 to 600 Igpd/ft^2 with the addition of 0.2 ppm Percol 730, and to 1100 Igpd/ft^2 with the addition of 0.45 ppm Percol 730.

In Dundas, the average overflow rates were raised from 350 Igpd/ft^2 to 1550 Igpd/ft^2 with the addition of 0.3 ppm Percol 730, and to 3500 Igpd/ft^2 with the addition of 0.8 ppm Percol 730. A further increase of polyelectrolyte dosage to 1.2 ppm apparently did not increase overflow rates. The probable cause for this phenomenon is that the 1.2 ppm polyelectrolyte addition was done at a different time of the year (see Section 6.2.1 for a discussion of seasonal variations).

Figures 191 and 192 in Appendix A show that at all Al:P molar ratios, the floc settling velocities were increased with polyelectrolyte addition. Above an Al:P molar ratio of 3.5, however, a decline in overflow rates was observed with all polyelectrolyte dosages in both Napanee and Dundas sewages.

The comparison, in Table 3, of maximum permissible overflow rates for 90% floc removal with polyelectrolyte addition shows that in sewage, the average overflow rates observed were half those observed in the model solution. The presence of organic material in the sewage that was not included in the model solution is the apparent cause of this discrepancy.

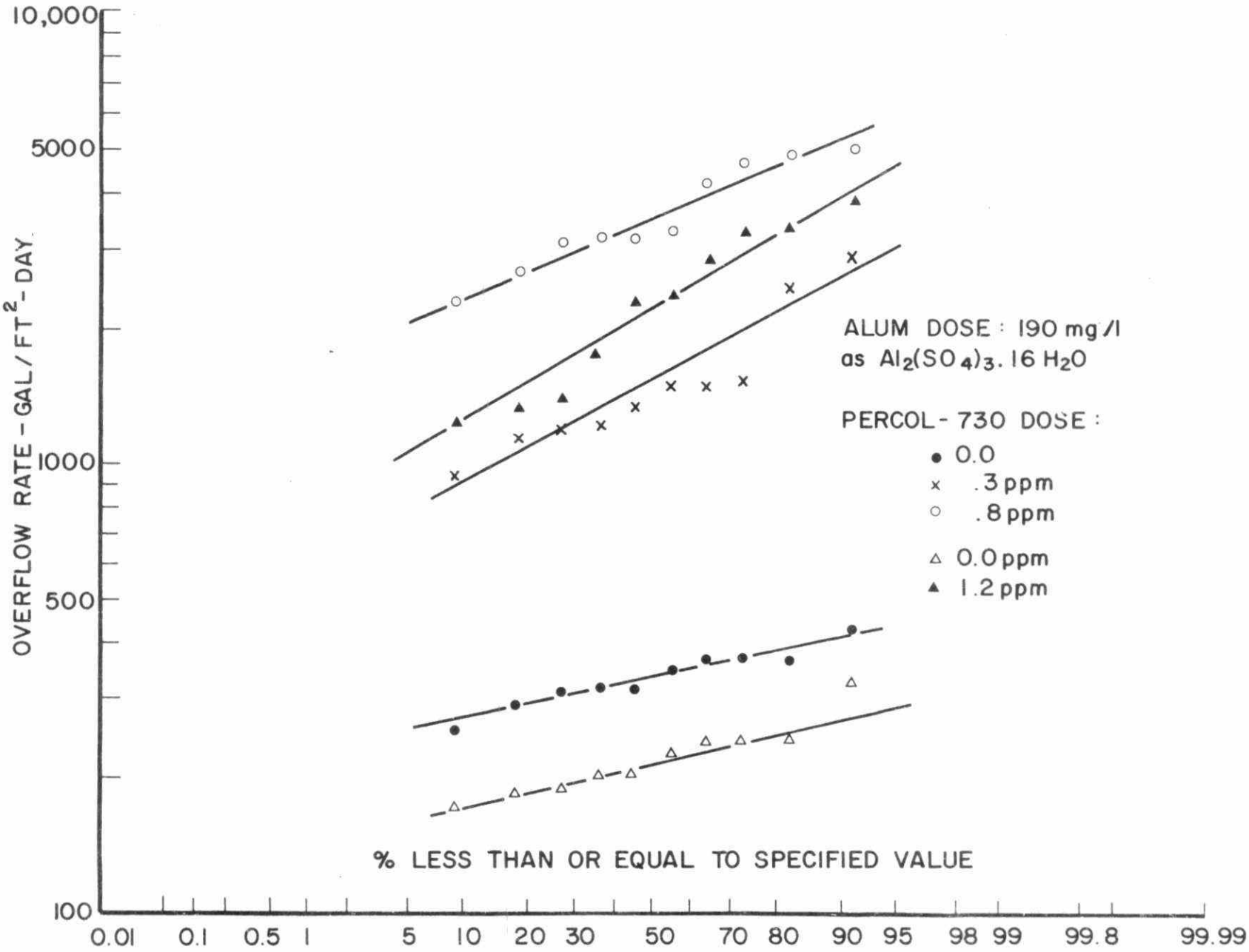

FIGURE 75. PERMISSIBLE OVERFLOW RATES FOR 90% FLOC REMOVAL WITH ALUM AND PERCOL 730 IN DUNDAS RAW SEWAGE

TABLE 3. COMPARISON OF THE MAXIMUM PERMISSIBLE OVERFLOW RATES FOR 90% FLOC REMOVAL OBSERVED IN THE MODEL SOLUTION AND IN SEWAGE

MODEL SOLUTION		NAPANEE SEWAGE as $Al_2(SO_4)_3 \cdot 14H_2O$	
Al:P=2.3 pH=6.5		Alum Dose 150 mg/l pH∿6.5	
A23 dose ppm	Overflow Rate lgpd/ft^2	A23 dose ppm	Av. Overflow Rate lgpd/ft^2
0	310	0	400
.15	850	.2	470
.3	1350	.45	700
.6	1500		
1.2	1700		

6.3 Conclusions

The following conclusions can be drawn from this study:

1) Average total phosphorus levels in two moderately weak Ontario sewages ranged from 4-6 mg/l with approximately 80% of this soluble and 80% of the soluble as orthophosphate. The bulk of the remaining soluble phosphorus was tripoly phosphate.

2) The optimum Al:P molar ratio for sewage was approximately 2.5. This agrees with the optimum Al:P molar ratio for the model solutions.

3) In the narrow pH range from 5.5-7.0 observed in sewage the pH had no effect on phosphorus removal.

4) Alum precipitate phosphate flocs were relatively difficult to settle. Batch tests predict that the maximum permissible overflow rate for 90% floc removal is 400 lgpd/ft^2.

5) Percol 730, a 10% hydrolysis polyelectrolyte, showed consistently better settling rates than the two other polyelectrolytes with similar molecular weight but greater percent hydrolysis.

6) In sewage, as in the model solutions, the phosphorus removal with polyelectrolyte addition followed, with some improvement, the removal envelope defined by alum addition alone.

7) The permissible overflow rates for 90% floc removal increased from 350 lgpd/ft^2 to 1550 lgpd/ft^2 with the additon of 0.3 ppm Percol 730, and to 3500 lgpd/ft^2 with the additon of 0.8 ppm Percol 730 in Dundas sewage, and in Napanee sewage from 400 lgpd/ft^2 to 600 lgpd/ft^2 with the addition of 0.2 ppm Percol 730, and 1100 lgpd/ft^2 with the addition of 0.45 ppm Percol 730.

8) The average maximum permissible overflow rates for 90% floc removal with polyelectrolyte addition observed for the sewage were half of those observed for the model solution.

7. THE USE OF POLYELECTROLYTES FOR OVERLOADED CLARIFIERS

7.1 Introduction

This section relates the batch studies reported earlier to plant results through the following three sequential objectives:

i) to examine the batch settling properties of an alum-polyelectrolyte sewage system at a chosen Water Pollution Control Plant and, from the settling data, to predict clarifier performance in full scale;

ii) to obtain full scale data for primary alum and polyelectrolyte addition on the chosen Water Pollution Control Plant at controlled overflow rates and, thereby, predict the maximum permissible hydraulic loadings for a primary clarifier under these conditions; and,

iii) to compare the laboratory predictions and the results of full scale study.

7.2 Experimental

The laboratory studies were based on the batch settling apparatus described in detail in Sections 2 and 6.

The full scale trials were conducted at the Water Pollution Control Centre located in Dundas, Ontario, during November and December of 1973. The Dundas Water Pollution Control Plant is designed for a 2 mlgpd flow. The plant pretreatment facilities consist of a mechanically cleaned bar screen and an aerated grit chamber, while primary treatment consists of two parallel rectangular clarifiers. Primary settling is followed by conventional activated sludge treatment. Figure 76 shows the layout of the plant.

During the study, the alum was added at a baffled manhole ahead of the screens where the joining of a force main and a gravity sewer created intense turbulence. Polyelectrolyte solution was added to the final section of the grit chamber. The solution makeup, delivery and addition system is shown in Figure 77.

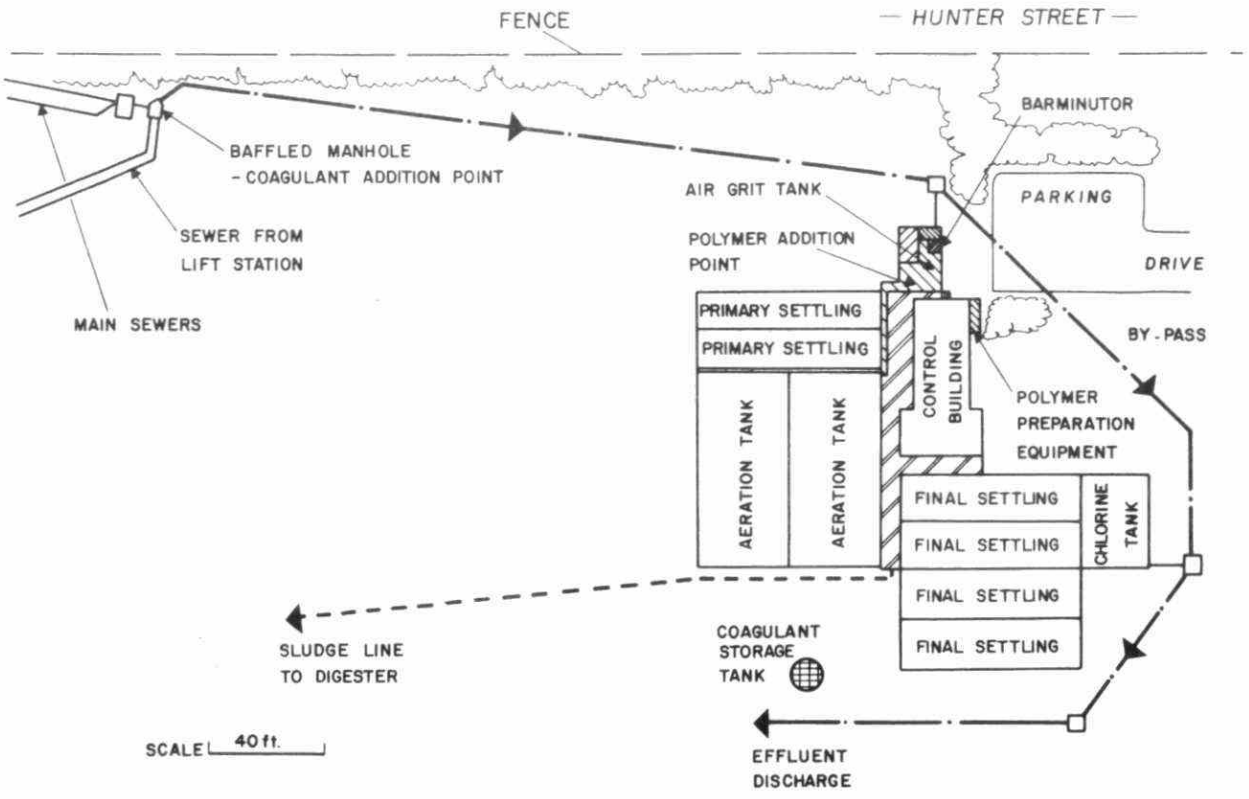

FIGURE 76. DUNDAS POLLUTION CONTROL CENTRE

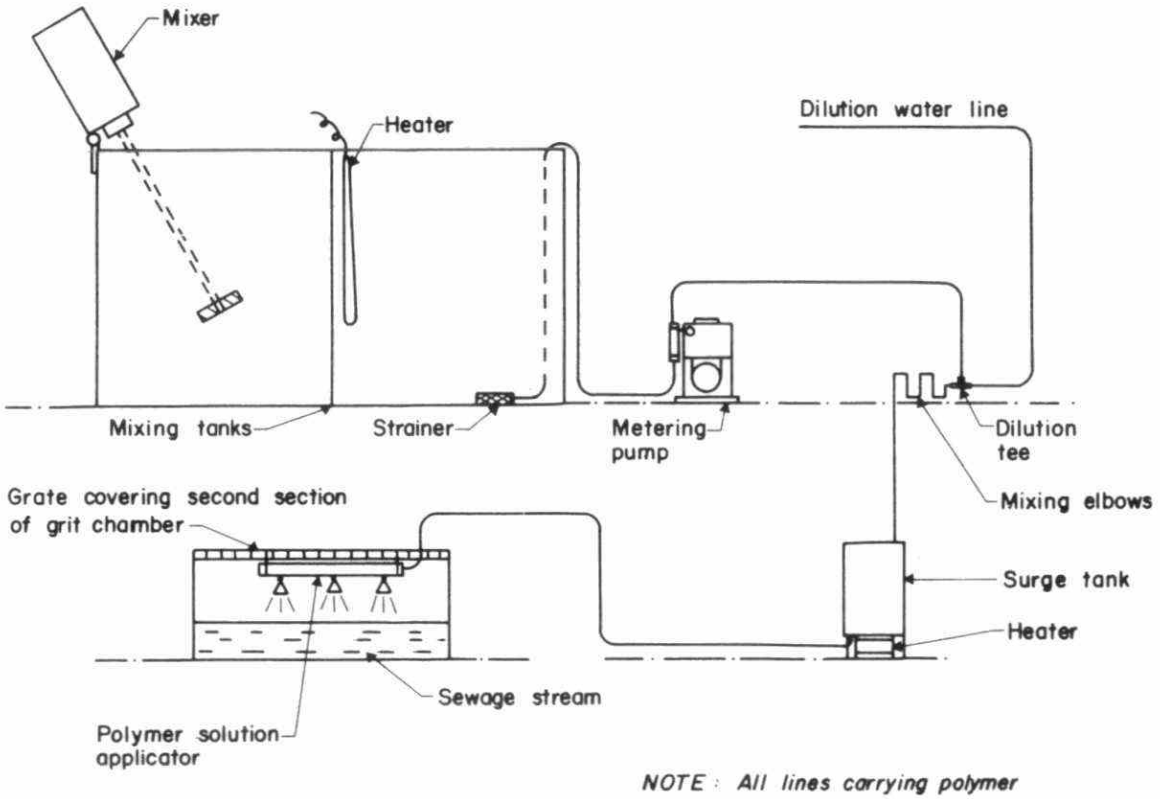

NOTE : All lines carrying polymer solution were insulated.

FIGURE 77. POLYMER SOLUTION PREPARATION AND APPLICATION SYSTEM

The flow through the individual clarifiers was controlled by inlet sluice gates and monitored through level measurements in the spillways at the outlet end of the clarifier as discussed by Camp (1940). The total flow through the plant was determined with a weir placed into the entire primary effluent stream.

The clarifier performance was based on two daily eight-hour composite samples. The samples were analyzed for total and filtered phosphorus and filtered COD according to automated Technicon methods, while suspended solids and total COD were analyzed according to Standard Methods (APHA et al, 1971). The samples were frozen immediately after composition for preservation. A separate study (Najak et al, 1974) showed that freezing introduced errors of about forty percent into suspended solids determinations; therefore, the suspended solids data must be considered with caution.

7.3 Results and Discussion

7.3.1 Laboratory study

The batch settling apparatus generates settling curves such as the ones shown in Figure 78. From the settling curves, graphs of overflow rates versus residual concentrations can be calculated using the Hazen-Camp ideal sedimentation tank theory (see Figure 79). The maximum permissible overflow rate to ensure sedimentation of any desired fraction of the flocs can be directly determined from plots such as those shown in Figure 79, (e.g., see Figure 82). Conversely, one can also determine the anticipated effluent concentration at a given clarifier overflow rate (see Section 2).

Data shown in Figure 78 or 79, together with some additional curves (See Appendix A, Figures 193 to 197), were used to choose one of the more promising polyelectrolytes for further study.

Figure 80 shows the probability distribution of the ultimate phosphorus residual concentrations as a function of alum dosage (without polyelectrolye addition). These ultimate residuals are read from Figure 78 after the slope approaches zero (usually this happened well before the end of the sampling period). In Ontario, the Ministry of the Environment (Boyko and Rupke, 1973), recommends that ten

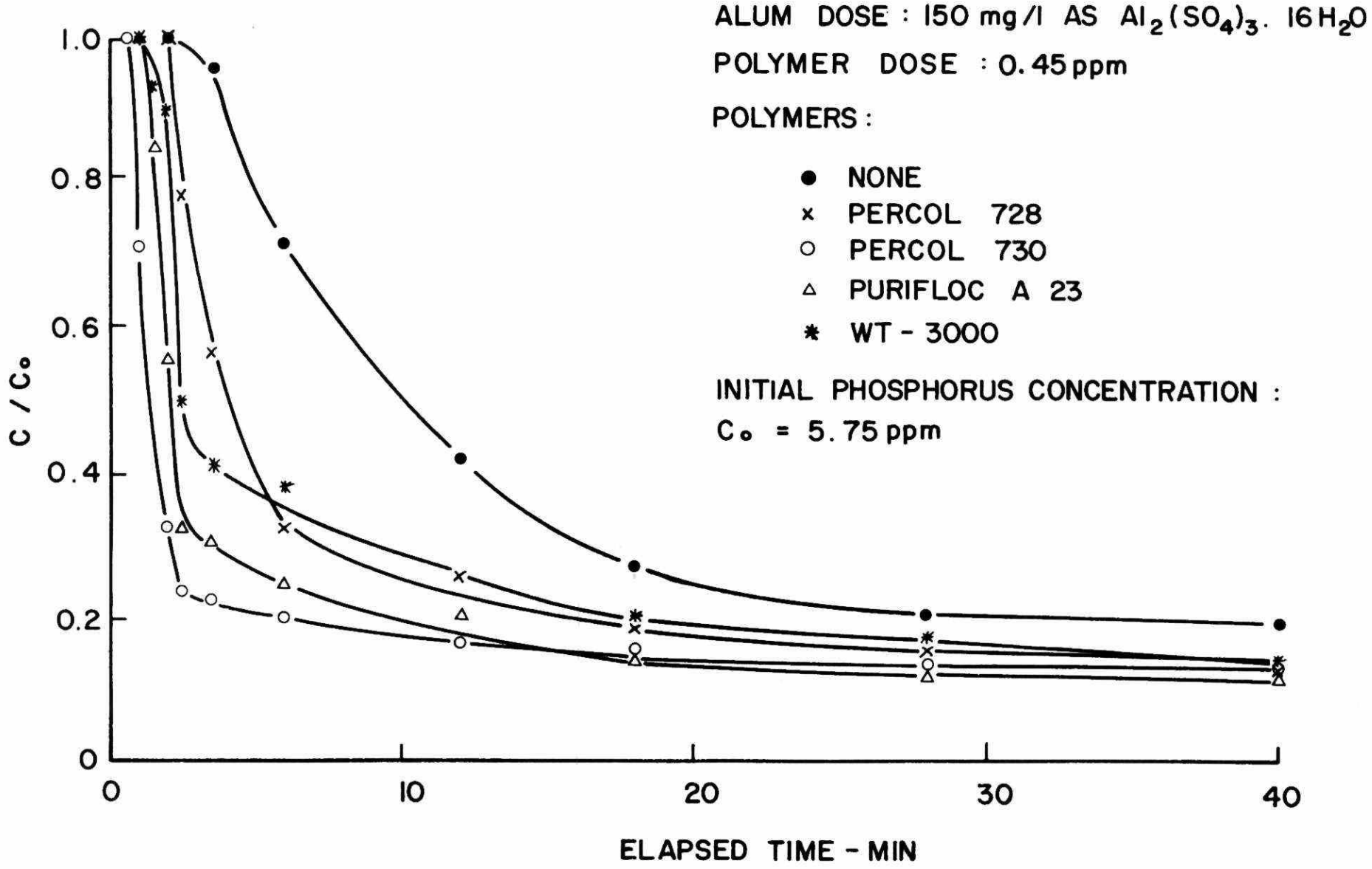

FIGURE 78. TYPICAL SEDIMENTATION CURVES FOR THE SEWAGE-ALUM-POLYELECTROLYTE SYSTEM

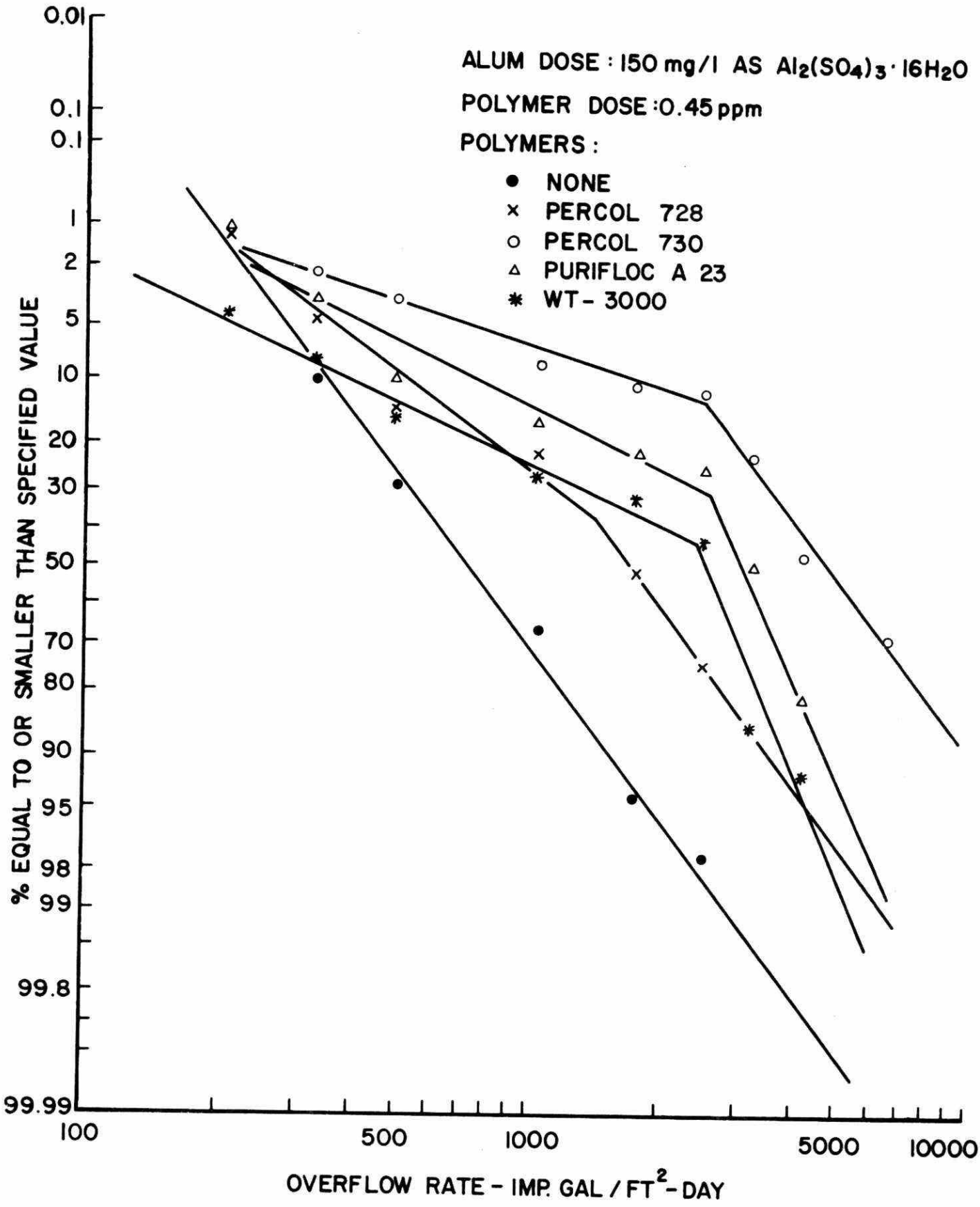

FIGURE 79. OVERFLOW RATE DISTRIBUTION FOR FIGURE 78 DATA

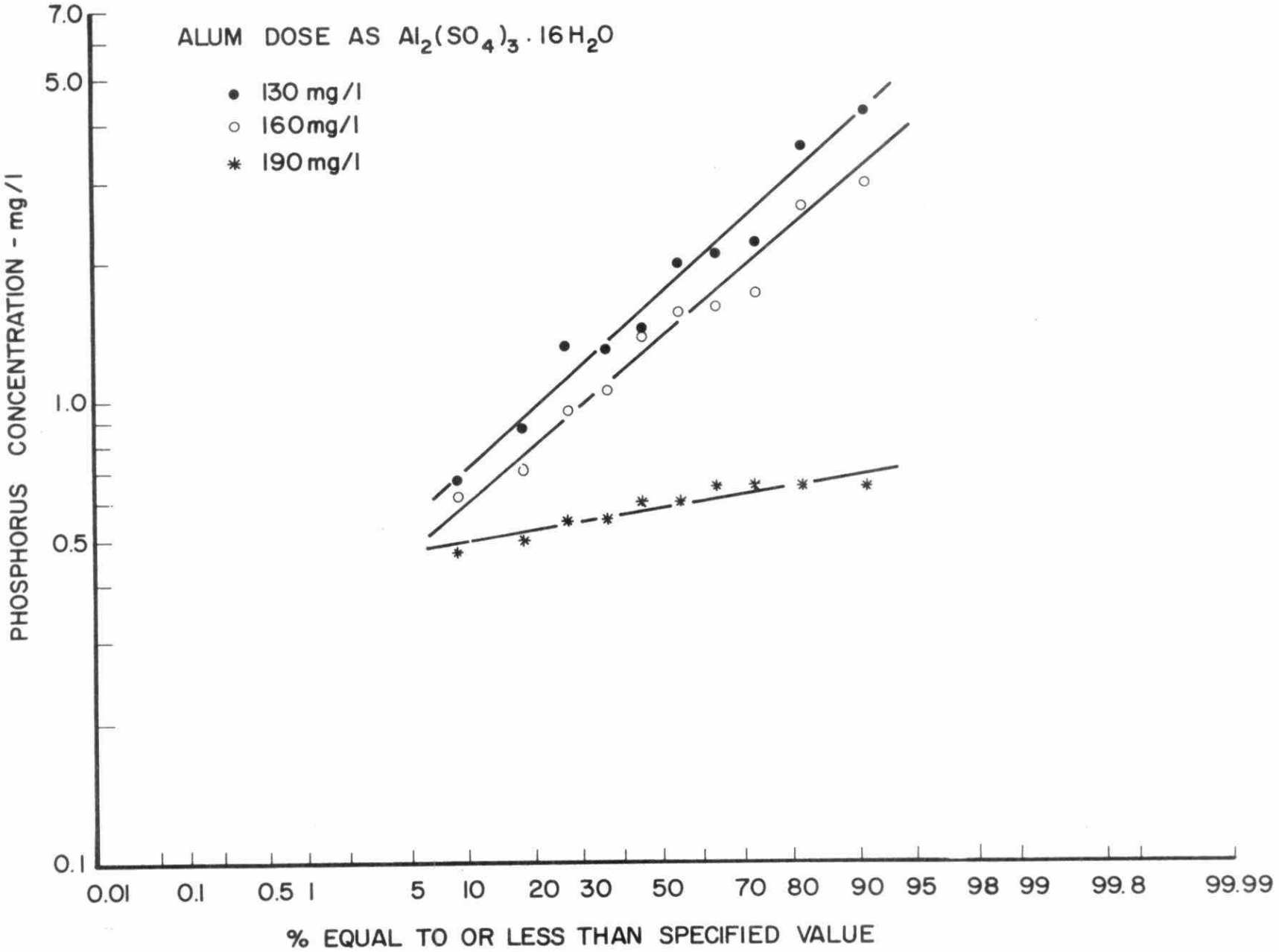

FIGURE 80. ULTIMATE PHOSPHORUS RESIDUAL CONCENTRATIONS OBTAINED IN THE BATCH SETTLING APPARATUS WITH ALUM ALONE

different sewage samples should be tested, such that chemical dosages for plant scale use can be estimated on a probability basis. The 1975 U.S./ Canada standards for sewage treatment plants located in the Lower Great Lakes drainage basin call for effluent phosphorus concentrations below 1 ppm, 80 percent of the time in jar tests, and 50 percent of the time in plant operation.

Figure 80 indicates that, in Dundas sewage, this standard is easily attained with 190 mg/l alum as $Al_2(SO_4)_3 \cdot 16H_2O$, but not with 160 mg/l.

With the addition of a polyelectrolyte, in this case Percol 730 (Allied Colloids Ltd.), the ultimate phosphorus residuals were further reduced as shown in Figure 81. As shown in Figure 82, the maximum permissible overflow rate for 1 ppm phosphorus residual was increased from 300 lgpd/ft^2 (360 gpd/ft^2, 14.4 m^3/day/m^2) to 1650 lgpd/ft^2 (1980 gpd/ft^2, 80.5 m^3/day/m^2) with the addition of 0.3 ppm (ppm ½ mg/l) Percol 730. Increasing the polyelectrolyte dosage tended to alter the ultimate phosphorus removals very little while the effect on overflow rate was quite strong. There appears to be an inconsistency on going from the 0.8 ppm to the 1.2 ppm dosage. The reason for this inconsistency is not clear. However, as the sewage used in the 1.2 ppm runs was obtained some four months after all the other runs were completed, this inconsistency was most likely caused by seasonal variations in sewage characteristics.

7.3.2 Full scale study

Table 4 summarizes the plant measurements of the Ontario Ministry of the Environment on the Dundas Water Pollution Control Plant for a four month period including the duration of this study. Without chemical treatment the phosphorus removal requirements were not met.

The very poor suspended solids removal in the primary clarifier in the absence of chemicals in Table 4 was probably due to the practice of collecting raw sewage samples before the point where the activated sludge was wasted.

The average overflow rate for the primary clarifiers was 1200 lgpd/ft^2 (1440 gpd/ft^2, 58.8 m^3/day/m^2). At this overflow rate, the clarifiers obviously do not fulfill their function, and this is

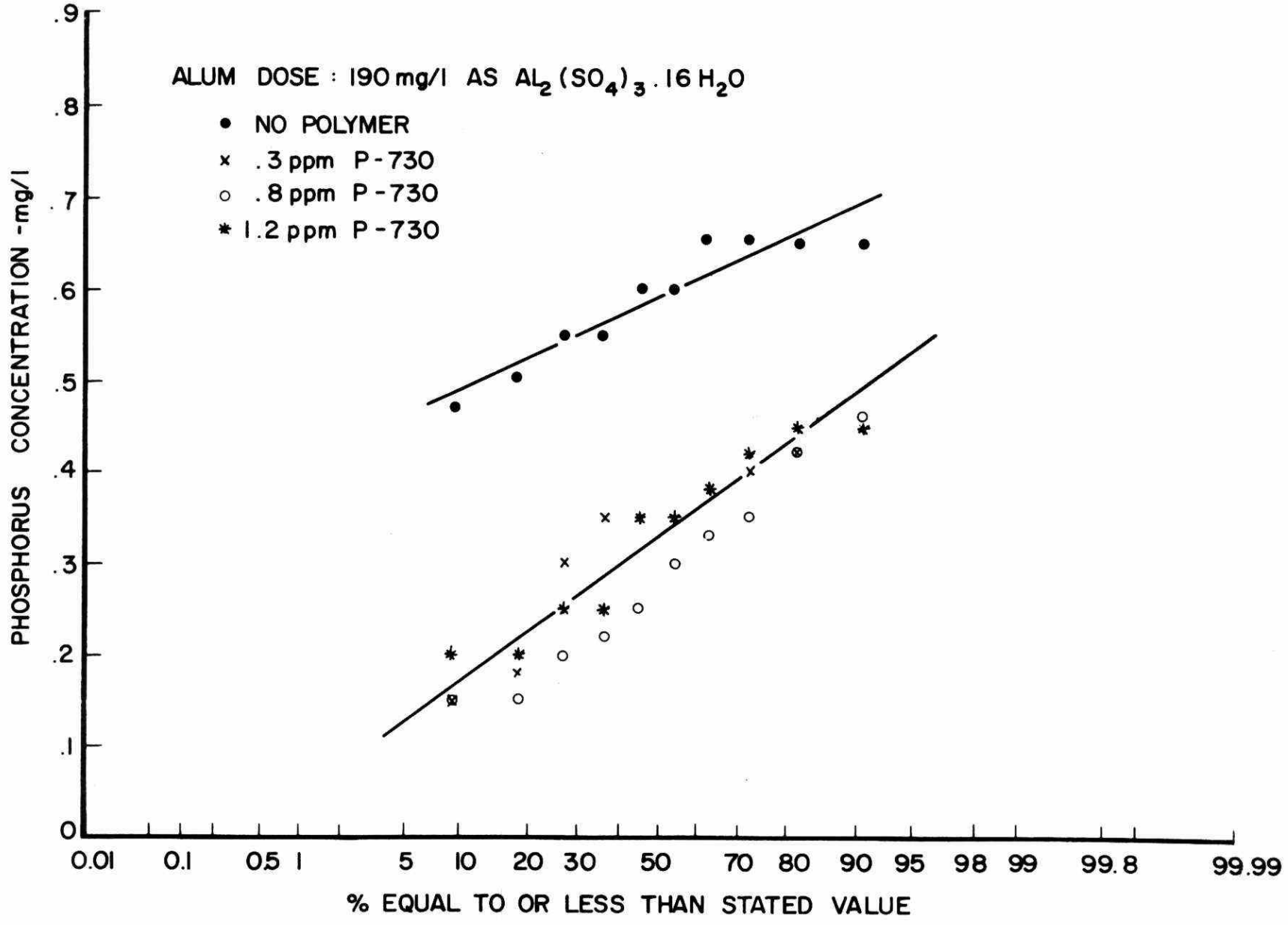

FIGURE 81. ULTIMATE PHOSPHORUS RESIDUAL CONCENTRATIONS OBTAINED IN THE BATCH SETTLING APPARATUS WITH ALUM AND PERCOL 730

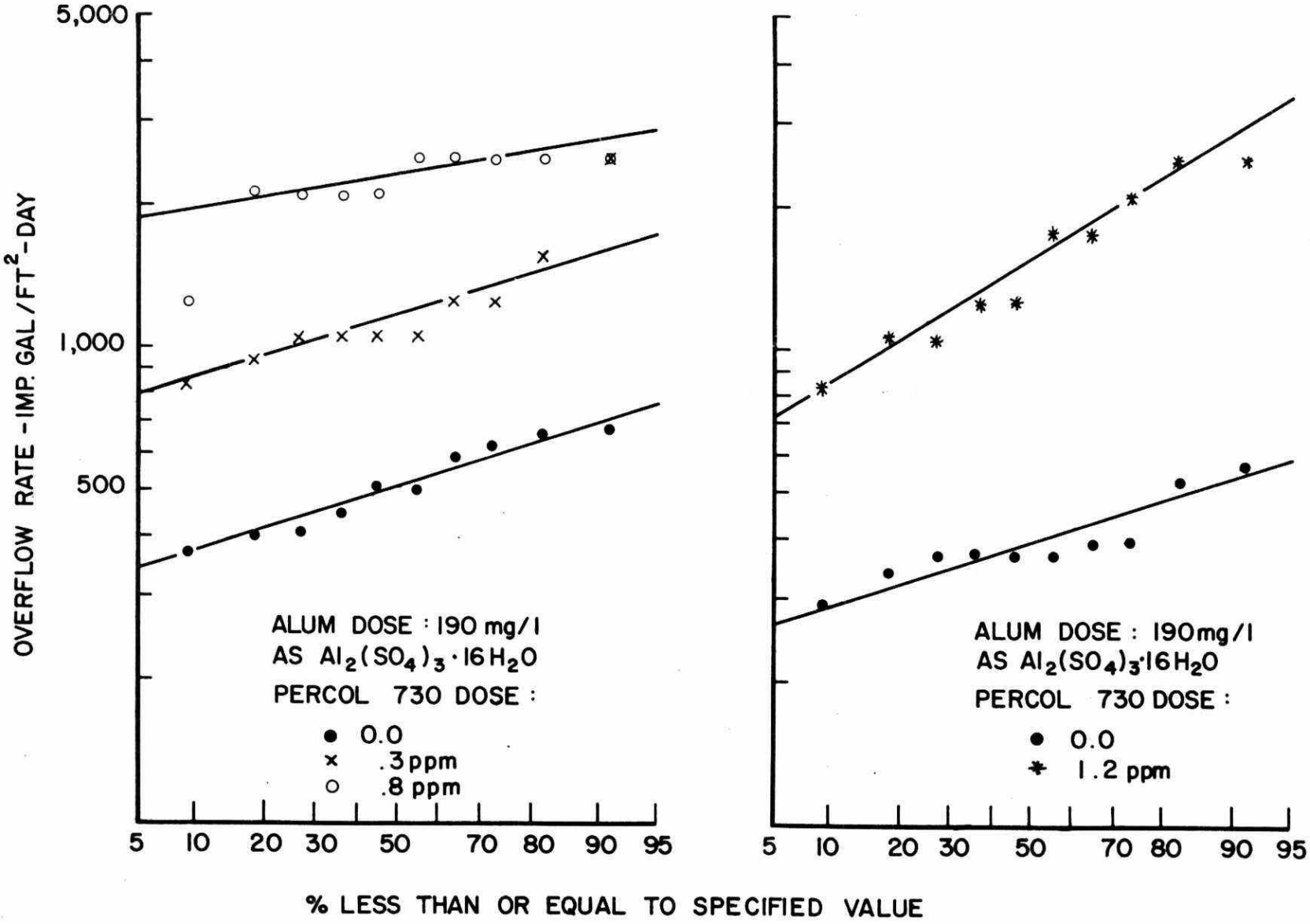

FIGURE 82. PERMISSIBLE OVERFLOW RATES FOR 1 PPM PHOSPHORUS RESIDUAL IN THE BATCH SETTLING APPARATUS WITH ALUM AND PERCOL 730

TABLE 4. ONTARIO MINISTRY OF THE ENVIRONMENT ANALYSIS OF DUNDAS WPCP GRAB SAMPLES

DATE	PHOSPHORUS mg/l		SUSPENDED SOLIDS mg/l			BOD_5 mg/l			TKN mg/l AS N	
	Raw Influent	Final Effluent	Raw Influent	Primary Effluent	Final Effluent	Raw Influent	Primary Effluent	Final Effluent	Raw Influent	Final Effluent
73/10/17	7.3	5.5	110	160	20	140	150	26	37	18
73/11/14	5.7	1.4	85	75	15	110	90	14	27	21
73/12/19*	6.8	.4	320	40	20	120	55	10	34	9.2
74/1/21	8.2	2.1	280	100	20	180	120	24	23	3.0
74/2/20	4.8	1.8	120	150	10	150	200	16	27	1.4

* Alum and Polymer addition prior to primary clarification by McMaster University.

understandable, since the maximum design overflow rate recommended by the Ten State Standard (Health Education Services, 1971) is 840 Igpd/ft^2 (1000 gpd/ft^2, 40.8 m^3/day/m^2).

With chemical treatment, phosphorus removal requirements were always met in the final effluent as shown in Table 5. Figures 83 and 84 (additional Figures 193 - 197 found in Appendix A) show a typical set of results for phosphorus and COD removal across the treatment plant. In addition, chemical treatment eliminated continual odour and grease build-up problems.

7.3.3 Primary clarifier

The operating conditions for the flow rate controlled clarifier are listed in Table 5.

Figure 85 showing effluent phosphorus concentrations indicates three noteworthy phenomena:

i) Different polyelectrolyte dosages tended to reduce the effluent phosphorus to the same level. Thus a single line can be drawn through the three sets of polymer data. Some small differences in behaviour are observable between the different sets if the removals are examined (see Figure 88).

ii) With polyelectrolyte, phosphorus levels were reduced by a further 50 percent from 1.6 to 0.8 ppm.

iii) Primary clarification with alum only at these relatively high overflow rates will not meet phosphorus removal standards. With polyelectrolyte addition, the effluent phosphorus level was less than 1 ppm approximately 66 percent of the time. This meets the 1975 plant effluent standards.

The suspended COD removal data in Figure 86 highlight the importance of polyelectrolyte in the removals of suspended organic matter. Only 40 percent removals were obtained with alum alone, (at the 50 percent probability) whereas average removals ranged from 63 to 74 percent with the addition of the different dosages of polyelectrolyte.

TABLE 5. OVERALL PERFORMANCE OF THE DUNDAS WATER POLLUTION CONTROL PLANT

OVERFLOW RATE						Percol 730	RAW INFLUENT mg/l			PRIMARY EFFLUENT mg/l			FINAL EFFLUENT mg/l		
$lgpd/ft^2$	SD*	gpd/ft^2	SD*	$m^3/day/m^2$	SD*	dose ppm	P	S. COD	SS**	P	S. COD	SS**	P	COD	SS**
945	90	1135	108	44.5	4.39	0.0	2.95	175	120	1.65	100	50	.3	17	50
840	35	1010	42	40.8	1.68	0.3	3.65	190	123	.85	55	36	.4	20	28
1270	75	1525	90	61.6	4.15	0.8	3.6	245	115	.6	90	30	.35	17	17
1690	100	2030	120	81.5	4.92	1.2	4.65	275	180	.8	75	30	.85	20	30

Alum dose: 190 mg/l as $Al_2(SO_4)_3 \cdot 16H_2O$

---

* SD - one standard deviation

** SS - possible error: ± 40%

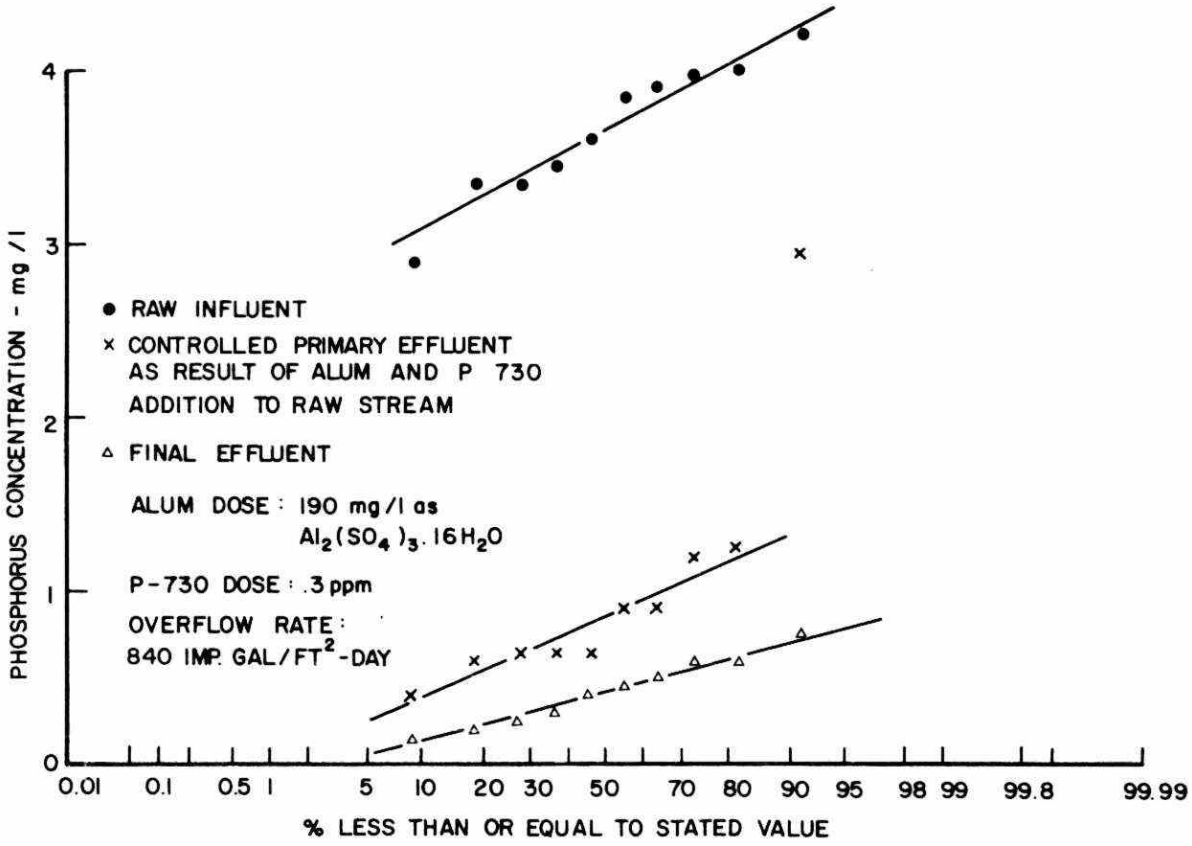

FIGURE 83. PHOSPHORUS CONCENTRATIONS ACROSS THE DUNDAS WPCP

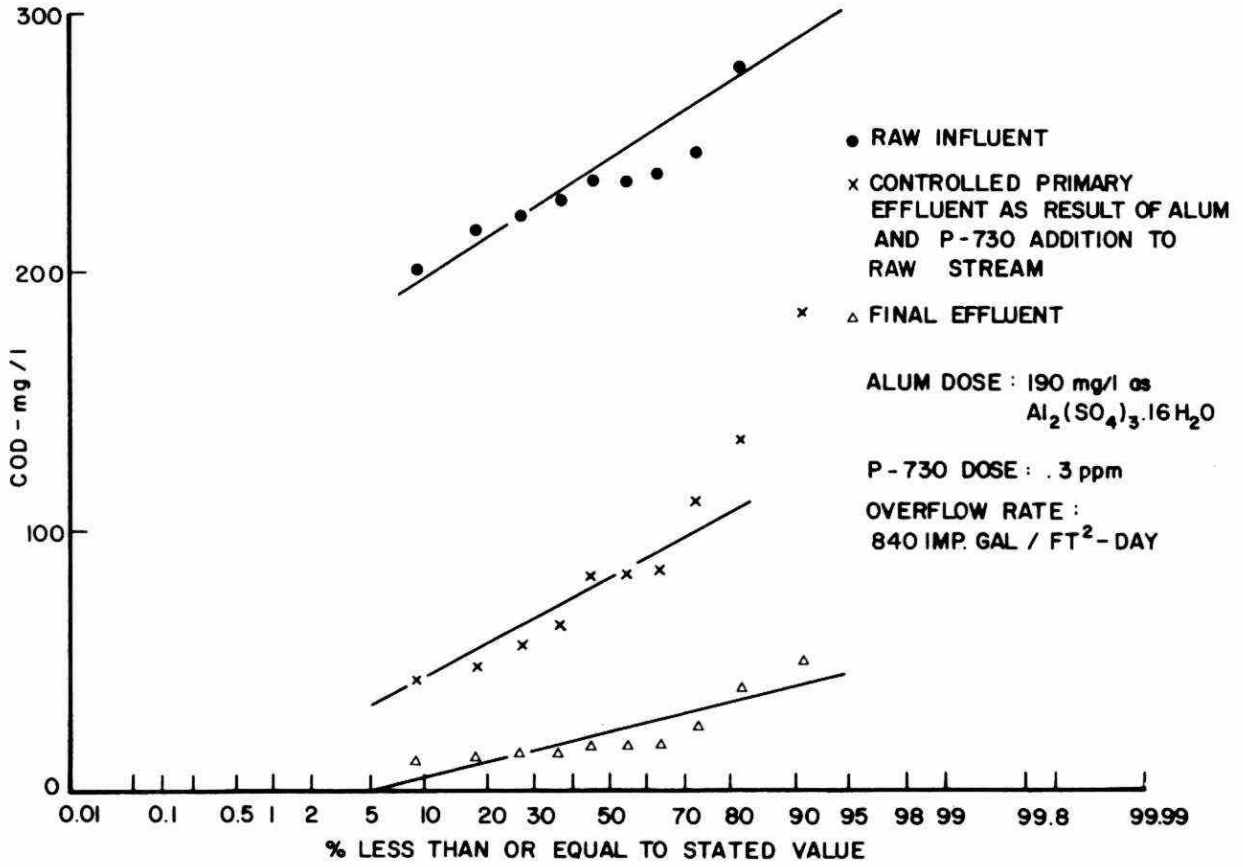

FIGURE 84. COD CONCENTRATIONS ACROSS THE DUNDAS WPCP

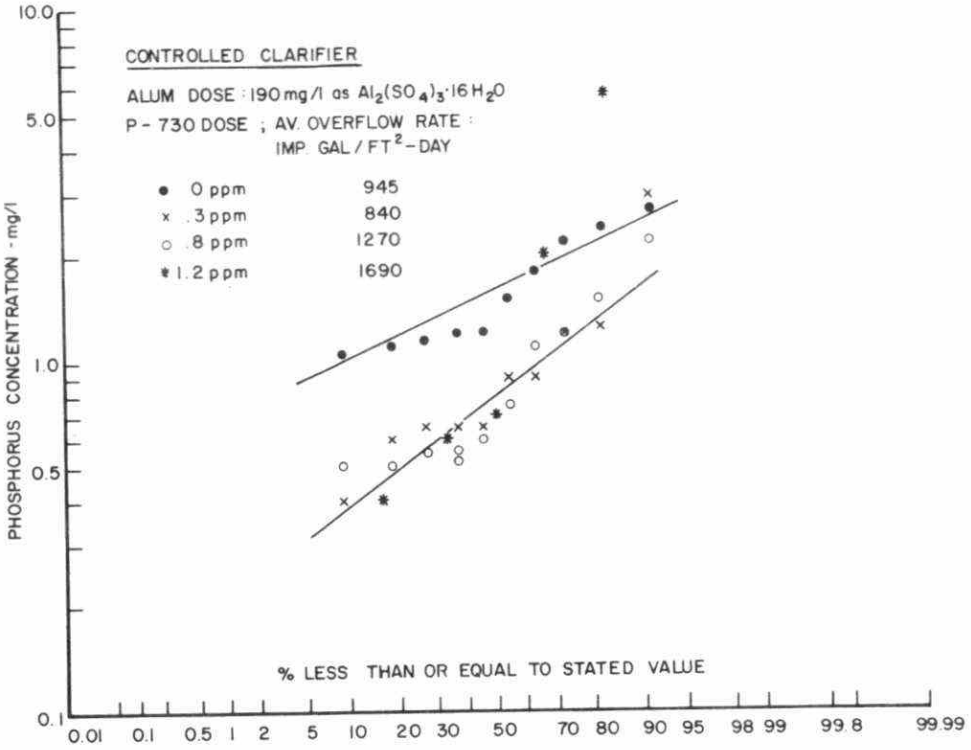

FIGURE 85. CONTROLLED PRIMARY EFFLUENT PHOSPHORUS CONCENTRATIONS

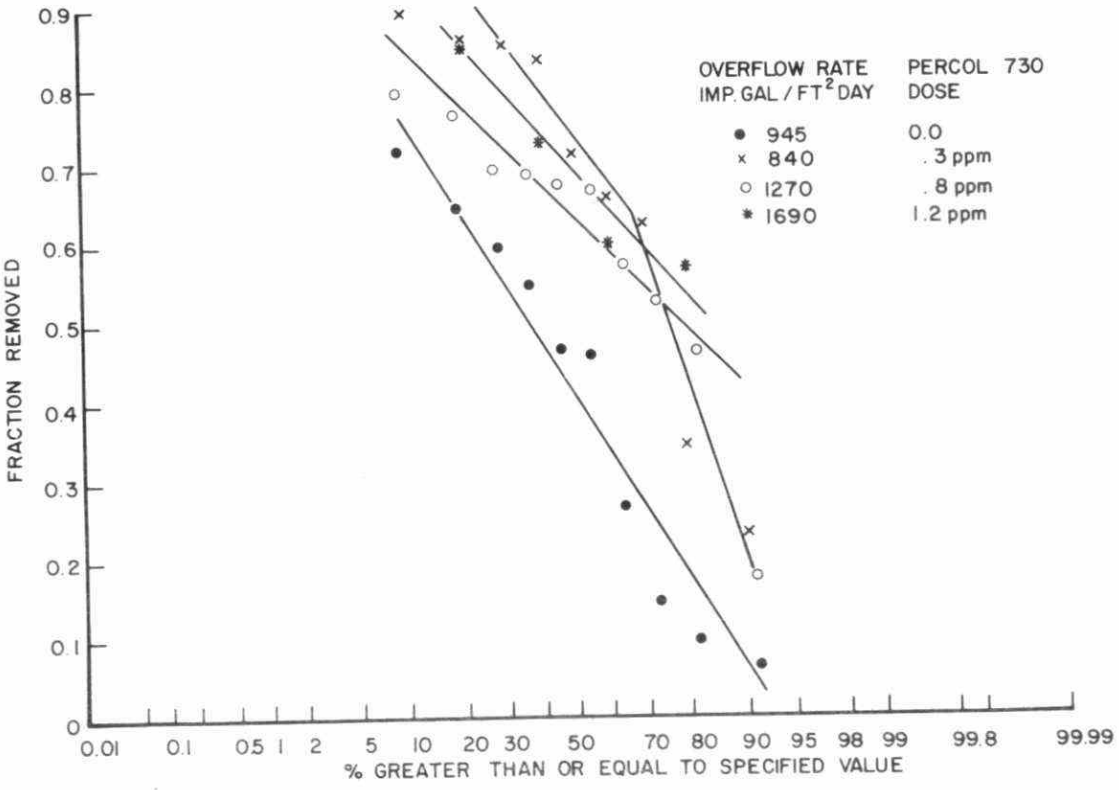

FIGURE 86. SUSPENDED COD REMOVALS IN THE CONTROLLED PRIMARY CLARIFIER

The effluent phosphorus concentrations from both the controlled and uncontrolled clarifiers are presented in Figure 87.

For the controlled clarifier, only one point per condition, the average of about ten data points is shown in Figure 87. The three averaged points with polyelectrolyte addition establish a straight line independent of overflow rate.

The alum only data points are well above this base line. A least square fit line to the data indicates a strong dependence on overflow rate.

As the overflow rate is increased beyond the level chosen for the controlled clarifier run with the 0.3 ppm polyelectrolyte dosage, the effluent concentrations start to increase indicating gradual clarifier failure or significant floc washout. A least square line, with a standard deviation of 260, to the data points crosses the polyelectrolyte base line at 1000 lgpd/ft^2 (1200 gpd/ft^2, 49.2 m^3/day/m^2). It is believed that this is the floc washout break point with 0.3 ppm polyelectrolyte dosage. Extending the alum only data to the polyelectrolyte baseline indicates a similar floc washout break point at 600 lgpd/ft^2 (720 gpd/ft^2, 28.8 m^3/day/m^2).

7.3.4 Comparison to other clarifiers

Table 6 compares the performance of the primary clarifiers located at Dundas and at Sarnia, Ontario (Gray, 1974). Only $FeCl_3$ data are available on the performance of the Sarnia primary clarifiers. Under these conditions, the Sarnia primary clarifier apparently starts to fail at an overflow rate of 700 lgpd/ft^2 (840 gpd/ft^2, 34.8 m^3/day/m^2) with only $FeCl_3$ addition, and 900 lgpd/ft^2 (1080 gpd/ft^2, 44.0 m^3/day/m^2) with an addition of 0.3 ppm Purifloc A23 (Dow Chemical) polyelectrolyte. The floc washout break point overflow rate appears at a higher value in the Sarnia clarifier than in the Dundas clarifier when only metallic coagulant was added, and at a lower value when polyelectrolyte was added in addition to the metallic coagulant. This was not unexpected, since one of the other batch settling apparatus studies (Sections 4 and 5) indicated that the $FeCl_3$ flocs tend to have slightly higher while Purifloc A23 flocs somewhat lower settling properties than those of the chemicals chosen for this study at Dundas. Furthermore, differences in

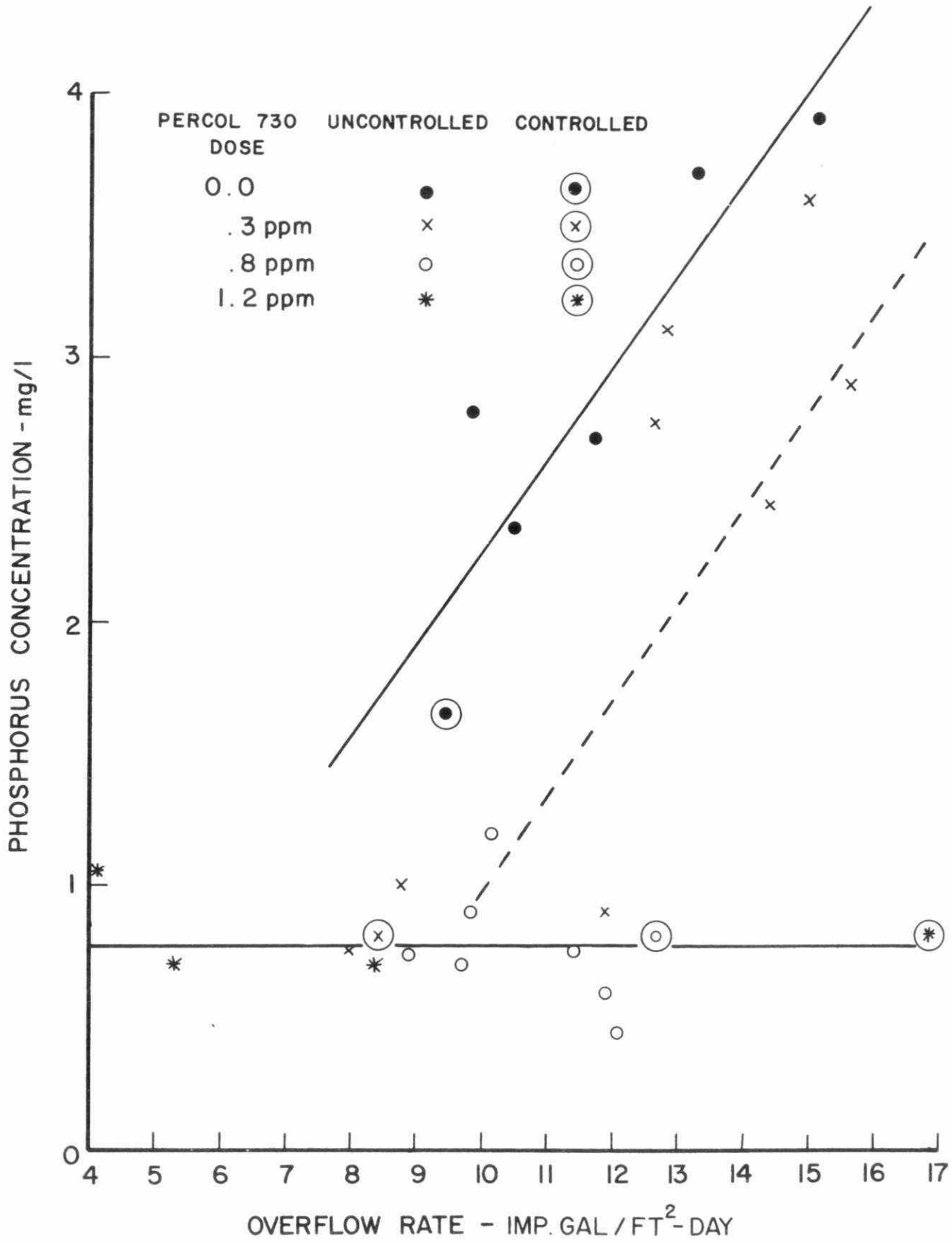

FIGURE 87. EFFLUENT PHOSPHORUS CONCENTRATIONS AS A FUNCTION OF OVERFLOW RATES IN THE CONTROLLED AND UNCONTROLLED PRIMARY CLARIFIER

TABLE 6. PERFORMANCE OF THE DUNDAS AND SARNIA WATER POLLUTION CONTROL PLANTS

DUNDAS Alum dose: 190 mg/l as $Al_2(SO_4)_3 \cdot 16H_2O$								SARNIA Fe^{+3} dose = 17 ppm							
Overflow Rate			P-730 dose:	Raw Influent		Primary Effluent		Overflow Rate			A23 dose:	Raw Influent		Primary Effluent	
lgpd/ft^2	gpd/ft^2	m^3/day/m^2	ppm	P	SS	P	SS	lgpd/ft^2	gpd/ft^2	m^3/day/m^2	ppm	P	SS	P	SS
								640	725	2.96	---	6.2	109	.94	30
								834	1000	40.8		6.4	125	1.4	28
								919	1100	44.9	---	6.6	212	1.1	31
945	1135	44.5	--	2.95	120	1.65	50								
								607	728	29.6	.3	3.8	116	.5	22
								617	740	30.0	.3	6.0	102	.8	14
840	1010	40.8	.3	3.65	123	.85	36								
								1234	1480	60.0	.3	6.0	102	1.5	32
1270	1525	61.6	.8	3.6	115	.6	30								
1690	2030	81.5	1.2	4.65	180	.8	30								

sewage and clarifier construction could equally well account for these differences.

7.3.5 Comparisons of batch settling apparatus and full scale studies

Figure 88 shows the phosphorus removals in the Dundas Water Pollution Control Plant, and those estimated from the batch settling apparatus curves, using overflow rates chosen for the plant study.

With the 1.2 ppm Percol 730 dosage at the overflow rate of 1690 Igpd/ft^2 (2030 gpd/ft^2, 81.5 m^3/day/m^2), there appears to be good agreement between the plant and the batch settling apparatus studies. At 0.3 and 0.8 ppm Percol 730 dosages and corresponding overflow rates of 840 Igpd/ft^2 (1010 gpd/ft^2, 40.8 m^3/day/m^2) and 1270 Igpd/ft^2 (1525 gpd/ft^2, 61.6 m^3/day/m^2), the plant phosphorus removal was, on the average, 10 percent below the batch settling apparatus removal. Without polyelectrolyte addition, the plant study shows considerably higher phosphorus removals than the batch settling apparatus tests.

For the laboratory data to be valid for the full scale clarifier, the following assumptions must be made:

i) Clarifier operation conforms to ideal sedimentation tank theory (no short circuiting or density currents, adequate sludge removals, etc.).

ii) Flocculation does not occur during settling (flocculation was disregarded in the analysis of the batch settling apparatus data).

Neither of these conditions were fully met. First, pronounced short circuiting in the Dundas clarifiers has been carefully documented by Tan (1972). Second, flocculation is well known to be important during settling in primary clarifiers although, with a polyelectrolyte flocculated system, extensive additional flocculation during settling is unlikely.

Thus, in Figure 88, the full scale polyelectrolyte results are more likely to be lower than the batch data, in view of short circuiting. Short circuiting was also important in the alum-only run but, in this case, flocculation during settling apparently overshadowed short circuiting.

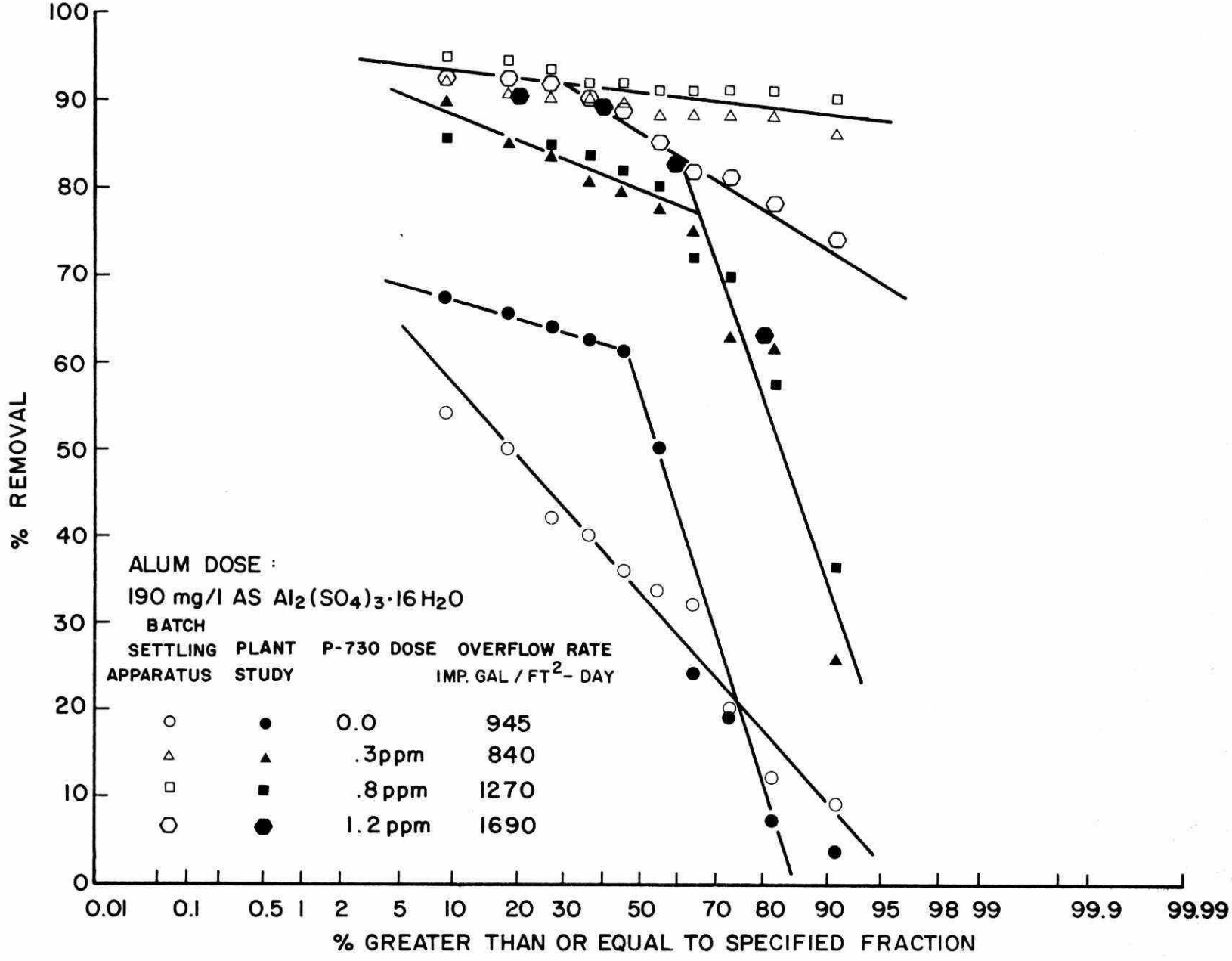

FIGURE 88. PHOSPHORUS REMOVAL IN THE BATCH SETTLING APPARATUS TESTS AND THE CONTROLLED PRIMARY CLARIFIER

The batch settling apparatus studies also have been used to predict floc washout break point overflow rates as listed in Table 7 and shown in Figure 89. For systems with polyelectrolyte added, this washout break point occurs quite close to the 90 percent floc removal, while with alum alone, the washout point is derived by the crossing of tangents to the initial and final portions of the settling curve. Full scale washout break points for the alum only and the 0.3 ppm polyelectrolyte studies were 600 lgpd/ft^2 (720 gpd/ft, 28.8 m^3/day/m^2) and 1000 lgpd/ft^2 (1200 gpd/ft^2, 49.2 m^3/day/m^2). For these conditions, the agreement between the predicted and the observed washout break point is surprisingly good.

At this point, it must be stated that caution will always have to be exercised when comparing batch and full scale studies because of the complexity of flow behaviour in full scale structures which no simple batch test can imitate. On the other hand, the batch settling apparatus test essentially evaluates the most basic properby of a floc, its settling velocity. This property should always be useful at the very least to indicate the most effective chemical dosages and general floc settling trends independent of clarifier construction.

TABLE 7. FLOC WASHOUT BREAKPOINTS AND CORRESPONDING PHOSPHORUS REMOVALS PREDICTED BY THE BATCH SETTLING APPARATUS

Alum dose: 190 mg/l as $Al_2(SO_4)_3 \cdot 16H_2O$

Percol 730 Dose: ppm	Overflow Rates			Percent Removal
	lgpd/ft^2	gpd/ft^2	m^3/day/m^2	
0.0	505	610	24.6	74.0
0.3	1150	1380	55.9	87.5
0.8	2300	2560	112.9	91.3
0.0*	395	480	19.2	53.0
1.2	1600	1920	78.0	90.0

* conducted four months later

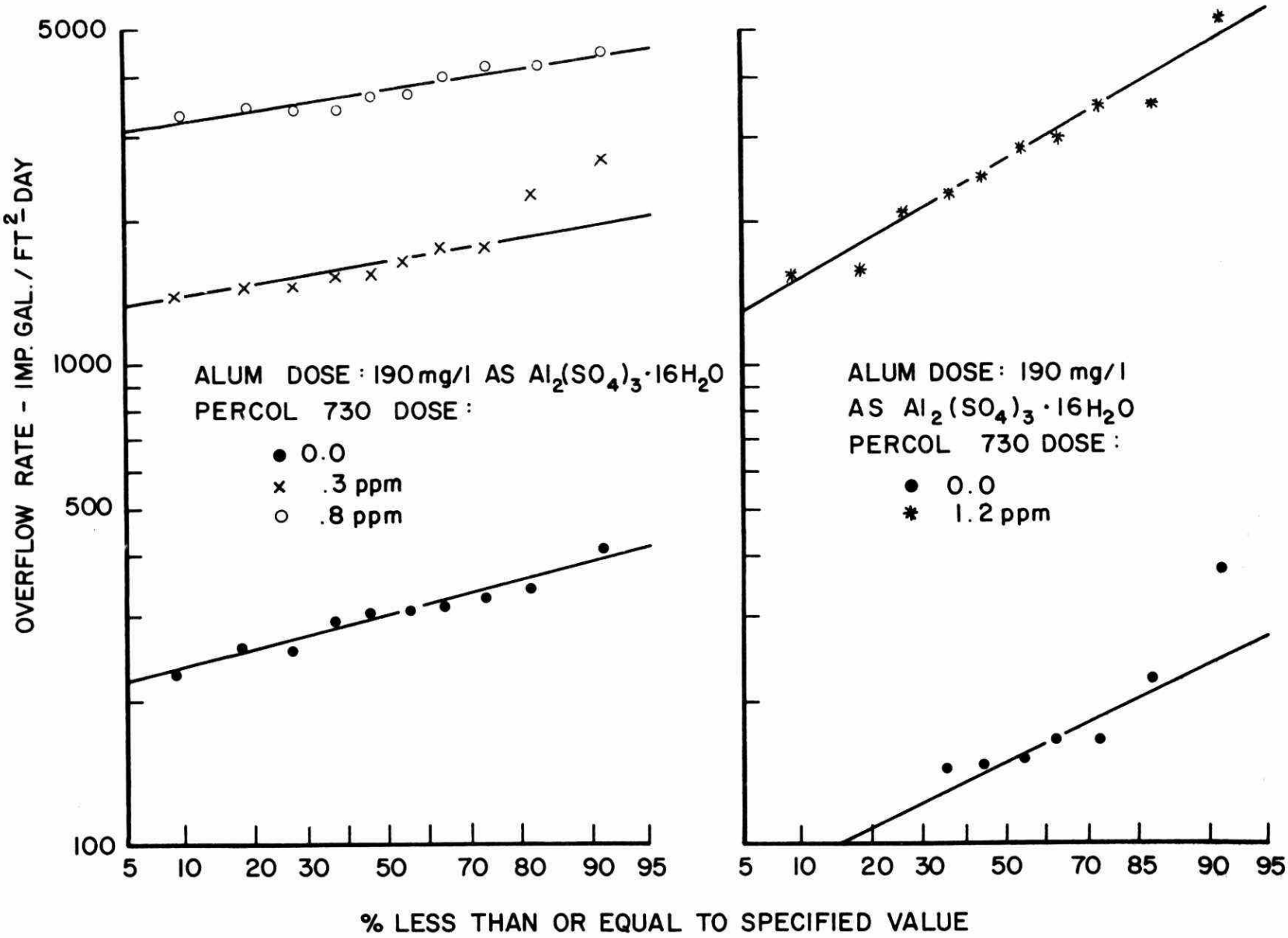

FIGURE 89. FLOC WASHOUT OVERFLOW RATES ESTIMATED WITH THE BATCH SETTLING APPARATUS

7.4 Conclusions

The following conclusions can be drawn from this study:

1) In the batch settling apparatus tests, the addition of polyelectrolyte reduced the residual phosphorus concentrations by 44% more than alum alone. The permissible overflow rates for 1 ppm phosphorus residual were increased from 300 lgpd/ft^2 (360 gpd/ft^2, 14.4 m^3/day/m^2) to 1650 lgpd/ft^2 (1980 gpd/ft^2, 80.5 m^3/day/m^2) with addition of 0.3 ppm Percol 730, and to 3800 lgpd/ft^2 (4560 gpd/ft^2, 1860 m^3/day/m^2) with 0.8 ppm Percol 730.

2) In the full scale activated sludge plant, the phosphorus concentrations in the final effluent were extremely low. They averaged around 0.5 ppm and never exceeded 1 ppm when coagulant and flocculants were added to the influent. In addition to phosphorus removal, both the suspended solids and COD levels were reduced, and the continual odour and grease build up problems were eliminated.

3) The primary clarifier effluent phosphorus concentrations were below 1 ppm 66% of the time with alum and polyelectrolyte addition. Without polyelectrolyte, the primary effluent concentration was always above 1 ppm.

4) The floc washout break point in the primary clarifier occurred at overflow rates of 600 lgpd/ft^2 (720 gpd/ft^2, 28.8 m^3/day/m^2) with alum addition alone, and at 1000 lgpd/ft^2 (1200 gpd/ft^2, 49.2 m^3/day/m^2) with the addition of 0.3 ppm Percol 730. The addition of 0.8 and 1.2 ppm Percol 730 prevented floc washout within the overflow rate range investigated up to 1800 lgpd/ft^2 (2160 gpd/ft^2, 88.2 m^3/day/m^2).

5) A comparison of the full scale data and batch settling apparatus data indicated relatively poor agreement in the prediction of absolute removal efficiencies, while floc washout break points agreed quite well.

8. COMPARISON OF COMMERCIAL POLYELECTROLYTES

There is a very wide variety of synthetic and natural polyelectrolytes available commercially. Furthermore, polyelectrolytes are sold under trade names with very little chemical or structural information supplied by the many different manufacturers. Thus, a prospective user is confronted with a difficult task when he tries to select the best polyelectrolyte for his requirements. The purpose of this section is to establish the most efficient type of polyelectrolyte for the flocculation of phosphate precipitate bearing domestic wastewater flocs and, thereby, to simplify the evaluation task of prospective users.

At the beginning of this study, eight major manufacturers of synthetic polyelectrolytes were asked to submit up to four polyelectrolytes deemed suitable for precipitated wastewater flocs. The eight manufacturers were: Alchem Ltd., Allied Colloids (Canada) Ltd., Bayer Dyestuffs and Chemicals Ltd., Calgon Canada, Cyanamid of Canada Ltd., Dow Chemical of Canada Ltd., Hercules Incorporated, and Polyhall Ltd. Chemical structure and property information was also requested of manufacturers (see request letter in Appendix B). The requested information was used to group the received polyelectrolytes and, subsequently, to interpret results. Unfortunately, most of the revealed information was confidential and, therefore, polyelectrolytes are identified by chemical properties and not trade names in this study.

8.1 Nature of Synthetic Polyelectrolytes

All of the nonionic and anionic polyelectrolytes received from manufacturers were linear polyacrylamides. Nonionic polyacrylamide is composed of acrylamide units only. Anionic polyacrylamides, on the other hand, consist of acrylamide and acrylate units as shown below:

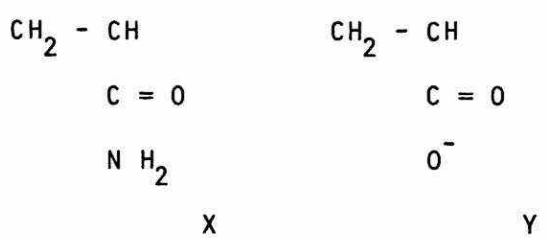

X Y

The counter ion of the acrylate is either sodium, potassium or hydrogen. The percentage of acrylate units is referred to as percent hydrolysis because, under alkaline conditions, acrylamide can be hydrolyzed to acrylate quite easily. Occasionally, organic sulphonates are used as the polymer with acrylamide to make another type of anionic polyelectrolyte.

Cationic polyelectrolytes are very diverse in chemical structure. They are typically quartenary or ternary amines such as poly (diallyldimethyl ammonium chloride) or acrylamide copolymerized with quartenary diethylaminoethylacrylate.

In general, literature reports have shown flocculation effectiveness to be influenced by the nature of charge, charge density or percent hydrolysis (Michaels, 1954), and molecular weight (La Mer and Healy, 1963; Linke and Booth, 1960; Yorke, 1972).

Polyelectrolytes are believed to flocculate particles by adsorption and subsequent bridging of two or more particles (La Mer and Healy, 1963). The electron microscope work of Ries and Meyers (1971) clearly illustrates the existence of long anchored polyelectrolyte threads emanating from particles in the presence of polyelectrolytes. It is probable that these threads from different particles can mesh with each other and, therefore, bridging between the polyelectrolytes anchored to different particles is also a very likely mechanism for flocculation.

8.2 Experimental

8.2.1 Overall procedure

All polyelectrolytes were evaluated with the batch settling apparatus described in Section 2. During the evaluation, the polyelectrolytes were added to alum coagulated samples of Dundas raw domestic wastewater. Samples collected during the tests were analyzed for total phosphorus with the Technicon Auto-Analyzer as described in Section 6.

8.2.2 Polyelectrolyte solutions

Stock solutions were prepared by the gradual dissolution of the required amount of polyelectrolyte in (stirred) distilled water for a final

concentration of 300 mg/l. Identical stirring speeds were used in the preparation of all solutions. The liquid polyelectrolyte stock solutions were prepared on an equal unit cost basis with solid polyelectrolytes, thus allowing convenient equivalent dosing with all polyelectrolytes.

8.2.3 Dosages

The alum dosage of 190 mg/l as $Al_2(SO_4)_3 \cdot 16H_2O$ used in these tests was established in Section 6.

Most evaluations were made with a polyelectrolyte dosage of 0.2 ppm, chosen on the basis of earlier studies that showed this dosage to be very sensitive to differences between polyelectrolytes.

8.3 Results and Discussion

Figure 90 presents a typical set of settling curves generated with a sample of domestic wastewater. Similar curves were obtained with every polyelectrolyte at a dosage of 0.2 mg/l. The ultimate residual concentration and maximum permissible overflow rate for 90% floc removal was calculated from each curve according to the methods described in Section 2. Different wastewater samples were standarized to the initial sample data on the basis of a run with each new sample.

8.3.1 Hydrolyzed acrylamides

8.3.1.1 Molecular weight effects. The summary of the performance of hydrolyzed polyacrylamides, as function of percent hydrolysis and molecular weight, is presented in Figure 91.

The data points are differentiated into two broad categories on the basis of molecular weight. The "very high" group comprises polyelectrolyte molecular weights between 1×10^6 and 8×10^6, while the "ultra high" group polyelectrolytes are greater than 8×10^6 but less than 15×10^6 in average molecular weight. Such molecular weight measurements are generally based on either viscometry or osmometry (Schmidt and Marlies, 1948); as both of these measurements are relatively inaccurate for such large polymers, finer classifications than these two broad ranges were not warranted. As shown in Figure 91, the molecular weight of a polyelectrolyte does not appear to influence ultimate phosphorus removal. On settling velocities, however, the effect of molecular weight was quite pronounced especially in the 10-20% hydrolysis range.

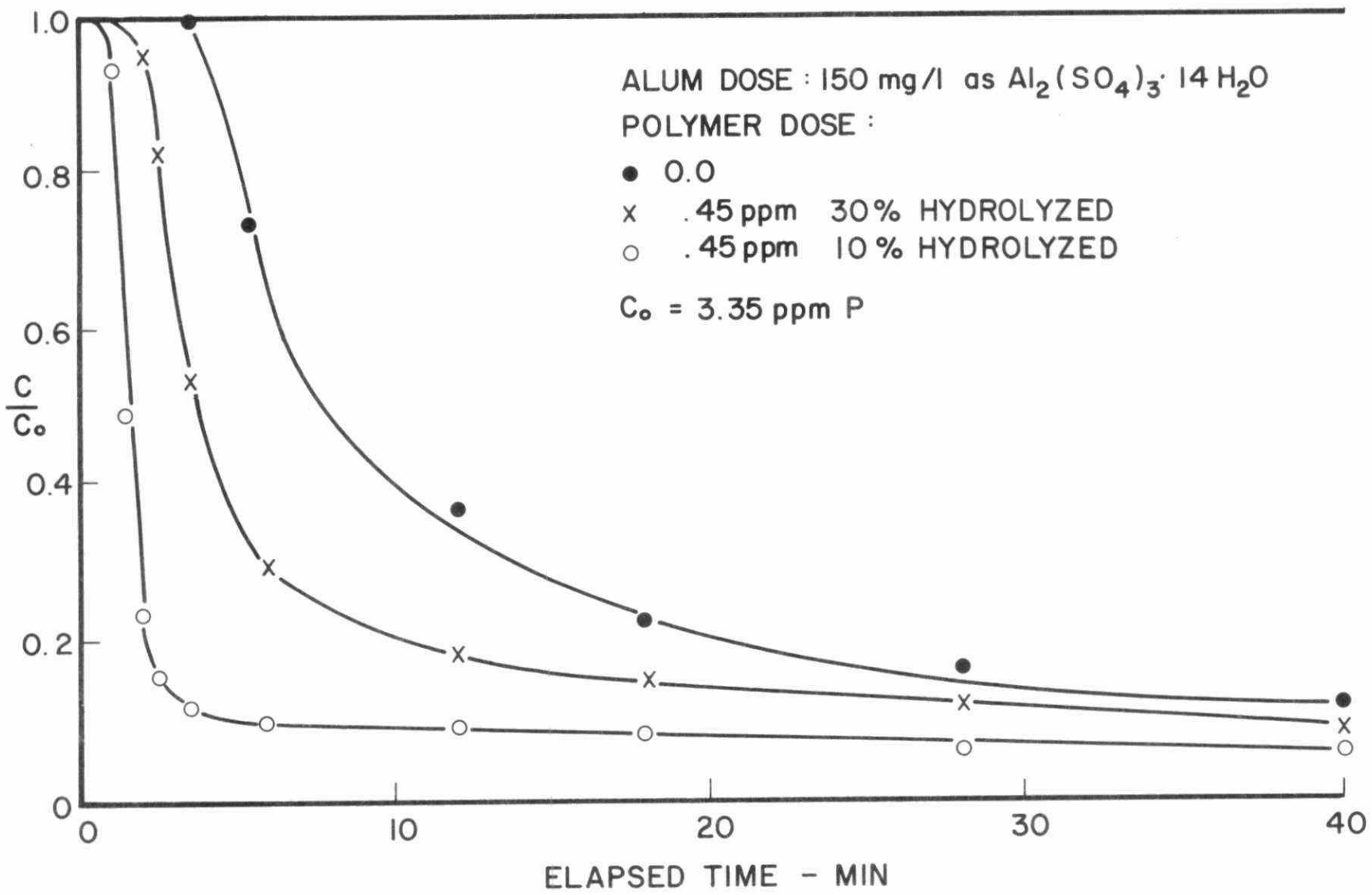

FIGURE 90. SETTLING OF ALUMINUM-PHOSPHATE FLOCS IN NAPANEE RAW SEWAGE

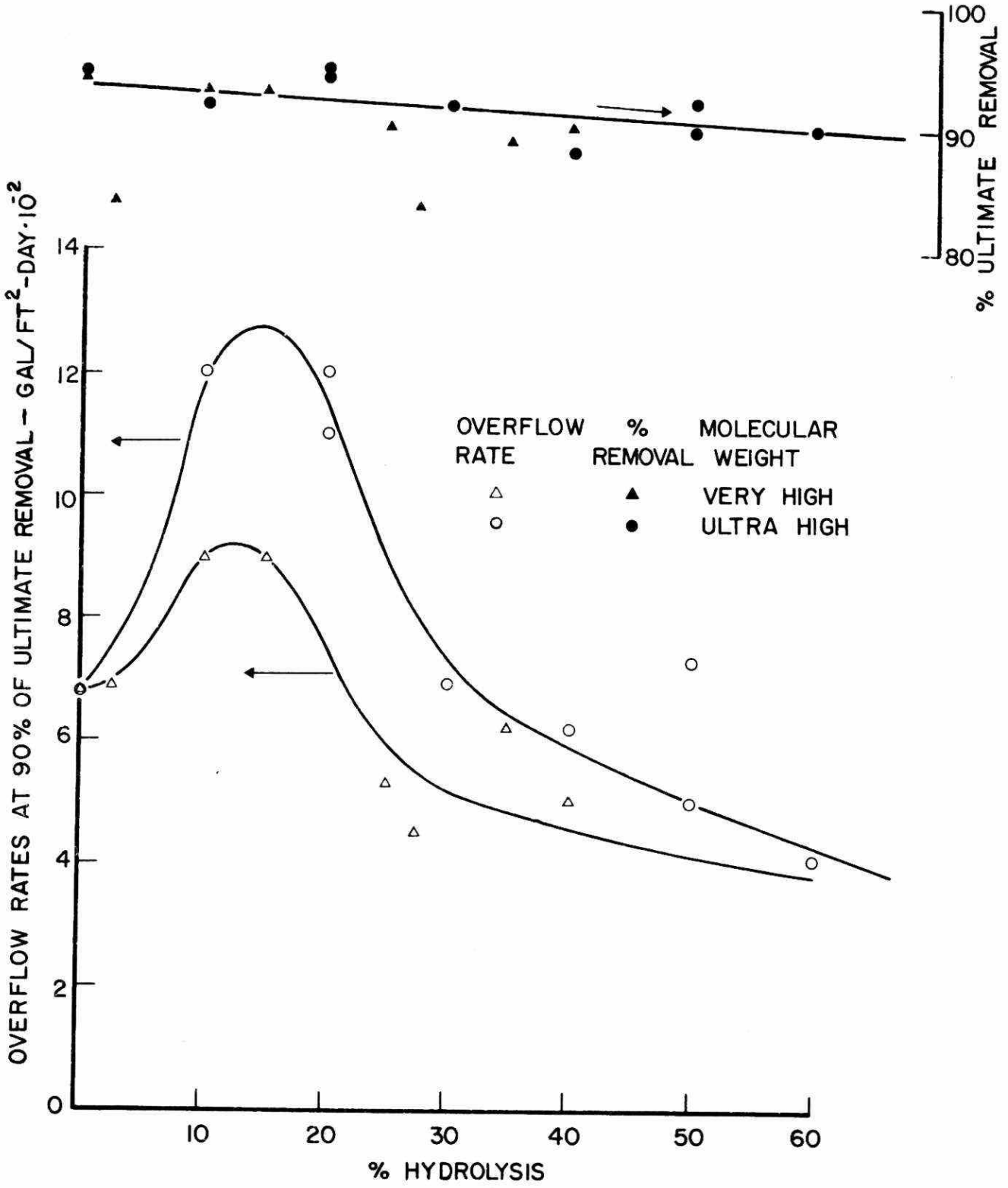

FIGURE 91. POLYELECTROLYTE PERFORMANCE AS FUNCTION OF HYDROLYSIS AND MOLECULAR WEIGHT

The existence of an optimum molecular weight has been proposed by La Mer and Healy (1963). They postulated that increasing molecular weight increases flocculation until molecular diffusivity becomes limiting. For polyacrylamide, La Mer and Healy found this optimum to occur at a molecular weight of 3×10^6 for phosphate slimes. On the other hand, Linke and Booth (1960) observed that increasing polyacrylamide molecular weight improved the flocculation of silica sols, without an apparent optimum. The maximum molecular weight tried by Linke and Booth was 5×10^6.

The current study, in agreement with Linke and Booth, does not indicate the existence of a distinct optimum below a molecular weight of 15×10^6. A maximum molecular weight of alum precipitated wastewater flocs cannot be suggested on the basis of this study. Increasing polyelectrolyte molecular weight, however, beyond the 15×10^6 probably is not warranted as the decrease in diffusivity and the increase in shear degradation (see Section 3) may negate further gains in flocculation.

8.3.1.2 Hydrolysis effects. In light of Figure 91, percent hydrolysis is the most important factor affecting settling rates in alum precipitated domestic wastewater. The optimum percent hydrolysis is apparently between 10 and 20% for both molecular weight groups. This observation is also fully supported by the trials on different sewages discussed in Section 6. In spite of this, most manufacturers recommend their highest hydrolyzed ($\geq$ 30%) polyacrylamide for phosphate floc removal. The disagreement between the data obtained in this study and manufacturers' recommendations is due to the fact that manufacturers use only the ultimate residual concentrations. As can be seen in Figure 91, this test would be essentially insensitive to the type of polyelectrolytes used. As discussed in Section 2, settling rate data is by far the most meaningful data for polyelectrolyte evaluation.

The reason for the optimum occurring in the 10 to 20% hydrolysis range has not been directly established. Nonetheless, one can postulate that 10 to 20% hydrolysis range is the optimum balance between polyelectrolyte stretching and floc density. The stretching of a polyelectrolyte is determined by the repulsion of the charged group (the intensity of which is measured by percent hydrolysis). Stretching increases the reach of

polyelectrolytes for bridging and, therefore, is beneficial to flocculation. On the other hand, high floc density requires short bridges between floc particles.

8.3.1.3 Polyelectrolyte dosage effects. As only a single polyelectrolyte dosage was used to gather the data for Figure 91, a single set of experiments was also run to compare two different but similar molecular weight polyelectrolytes at different dosages. As this set of experiments was self inclusive, the data were not standarized to other runs.

As shown in Figure 92, the addition of increased amounts of polyelectrolyte did not appreciably increase ultimate removals beyond the increase provided by the first 0.2 ppm. The permissible overflow rates rose rapidly below, and relatively slower above, 0.5 ppm for the 10% hydrolyzed polyelectrolyte and 1.0 ppm for the 30% hydrolyzed polyelectrolyte. The difference in overflow rates between the two polyelectrolytes was maximum in the vicinity of 0.2 mg/l (around 68% based on the 10% hydrolysis curve) and decreased gradually to a nearly constant value (approximately 30%) above 1.0 mg/l.

8.3.2 Miscellaneous polyelectrolytes

The polyelectrolytes in Table 8 have been arranged in order of decreasing overflow rates for 90% floc removal on the basis of overflow rates. Molecular weight appears to be the controlling parameter since, regardless of charge, the higher molecular weight polyelectrolytes appear best. When comparing the data in Table 8 to those in Figure 91, it will be noted, however, that the best cationic polyelectrolyte is still not as good as the best anionic polyacrylamide. On the other hand, in the range of percent hydrolysis usually recommended for use (>30%) in phosphorus removal, cationics can outperform anionics. An apparent anomaly in Table 8 contradicts the precept that molecular weight is the governing factor; the worst polyelectrolyte in Table 8 is a "high" molecular weight cationic. This particular polyelectrolyte, while possessing a high molecular weight, also possesses a very high charge density and perhaps its poor performance results from the stretching of the polymer chain as discussed above for highly hydrolyzed polyacrylamides. Phosphate flocs are negatively charged at the

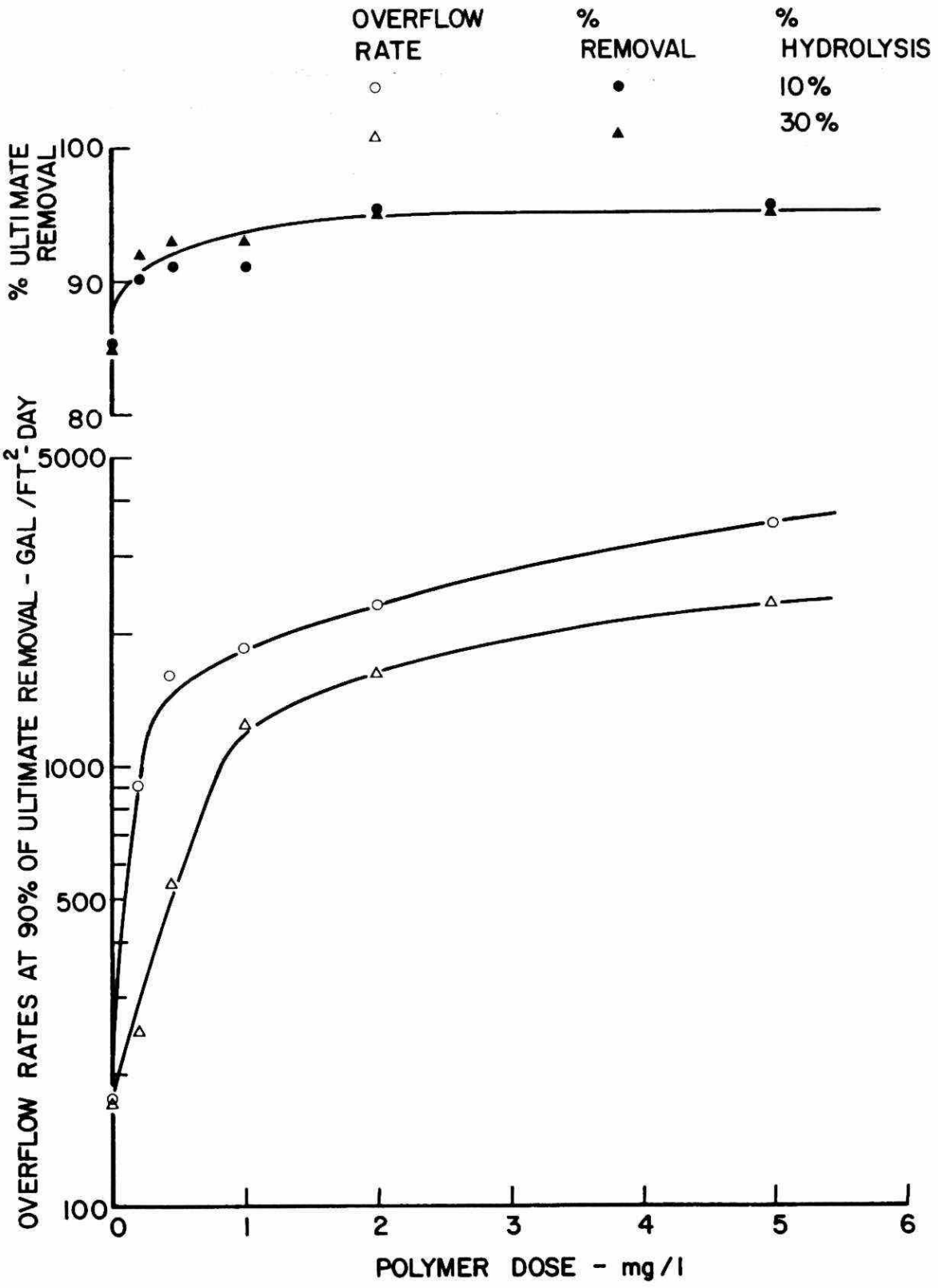

FIGURE 92. POLYELECTROLYTE PERFORMANCE AS FUNCTION OF DOSAGE AND HYDROLYSIS

TABLE 8. PERFORMANCE OF MISCELLANEOUS POLYELECTROLYTES

Ionic Characteristics	State	Molecular Weight*	Chemical Composition	Dosage mg/l	Performance**	
					%R	u
cationic	solid	very high	Acrylamide and diethylaminoethylacrylate	0.2	91.0	640
cationic	solid	very high	Polyacrylamide based	0.2	91.5	600
cationic	solid	very high	Polyacrylamide based	0.2	88.0	520
cationic	solid	ultra high	Acrylamide and MTMMS***	0.2	93.0	500
nonionic	liquid	----------	Polyacrylamide	0.5	92.0	490
anionic	liquid	----------	Polyacrylamide (30% hydrolyzed)	0.5	81.5	480
cationic	liquid	low	Polyalkyl polyamine	0.8	79.5	480
cationic	liquid	low	Polyalkyl polyamine	0.8	86.0	480
anionic	liquid	----------	Polyacrylamide (slightly hydrolyzed)	0.5	93.5	465
cationic	liquid	low	No information	0.8	83.0	400
cationic	solid	high	Polyaminocarbonicacid ester	0.2	90.5	310

* Molecular Weights

ultra high: 8×10^6 - 15×10^6

very high : 3×10^6 - 8×10^6

high : 1×10^6 - 3×10^6

low : 0 - 1×10^6

** % R: % Removal

u: maximum permissible overflow rate for 90% floc removal in $lgpd/ft^2$

*** methocrylaylexyethyltrimethyl-ammonium methyl sulphate

pH of flocculation (see Section 4). Electrostatic attraction to cationic flocculants, however, does not appear to play an important part here.

The 30% hydrolyzed liquid anionic acrylamide appears to perform similarly to the solid polyelectrolytes of Figure 91 on an equal cost basis. On the other hand, the two lower charge density polyacrylamides performed considerably poorer than expected. Thus, low charge density liquid solutions may have a shorter shelf life.

8.4 Conclusions

The following conclusions can be drawn from this study:

1) The ideal properties of polyelectrolytes for use in phosphorus removal from domestic wastewater in conjunction with a metallic coagulant are as follows:

Chemical Composition	:	Anionic (hydrolyzed polyacrylamides)
Percent Hydrolysis	:	10-20%
Molecular Weight	:	$>8 \times 10^6$
State	:	Solid

2) A maximum polyelectrolyte dosage of $\leq$ 1 mg/l is recommended for application at the primary stage.

9. FATE OF THE POLYELECTROLYTE

9.1 Introduction

Laboratory and waste treatment plant investigations of the use of polyelectrolytes for the removal of suspended matter from wastewaters have been mainly concerned with the optimization of polymer dosage to achieve maximum floc settling rate. Recently, there has been some concern that the optimum dosage may result in considerable loss of polymer in the treated effluent with the remainder trapped in the sludge. Polymer remaining in the treated effluent might produce undesirable environmental effects. To date, no technical data have been published on the fate of the polymer during flocculation. This serious lack of information stimulated the initiation of this part of the research investigation, which was intended to provide quantitative data on the fate of the polyelectrolyte during flocculation. In earlier parts of this investigation, it was found that the commercial polyelectrolyte Percol 730 was one of the most effective flocculants in increasing the settling rate of colloidal phosphates. It was, therefore, decided to employ Percol 730 in this experimental investigation of the fate of the polymer during flocculation.

9.2 Experimental

An aqueous solution of ortho, pyro, and tripoly phosphate was coagulated and flocculated with alum and Percol 730 using the jar test procedure described earlier in this report. The total concentration of phosphates was 5 ppm and the ratio of Al:P was 1:1. The dosage of Percol 730 covered the range 0.5-1.5 ppm, which included the optimum dosage. The order of addition of reagents and procedures followed for five jar test runs are summarized in Table 9. The following procedure was used to carry out Run 9-1 in Table 9. This description will serve to explain the contents of this table.

Three litres of distilled water was charged to the jar. 300 mg of $CaCO_3$ and 0.6 ml of concentrated HCl were added to aid the dissolution of the carbonate. 5 ml of each of the following phosphate solutions were added to obtain a total phosphate concentration of 5 ppm: 18.4 g/l sodium phosphate tribasic $Na_3PO_4 \cdot 12\ H_2O$, 2.16 g/l sodium pyrophosphate

TABLE 9. SUMMARY OF FLOCCULATION EXPERIMENTS

Run No.		9-1	9-1a	9-2	9-2a	9-3
Chemical Addition & Procedure.						
	90 rpm					
	Distilled H_2O (ℓ)	3.0	3.0	3.0	3.0	3.0
	$CaCO_3$ (mg)	300	300	300	300	300
	HCl sol'n [a] (ml)	0.6	0.6	0.6	0.6	0.6
	Phosphates [b] sol'n (ml)	15	15	15	15	15
	HCl sol'n [a]	2.4	2.4	2.4	2.4	2.4
	Alum sol'n [c] (ml)	3.0	3.0	3.0	3.0	3.0
Time=0 (min)						
	pH (Measured)	4.9	4.9	4.9	4.9	4.9
t=5	Polymer sol'n [d] (ml)	1.5	1.5	3.0	3.0	4.5
t=6	30 rpm					
	pH (measured)	5.9	5.9	5.8	5.8	5.8
t=20	No stirring					
	Floc Observed (relative size)	small	small	medium	medium	large
	Phosphate removal (%)	70	68	70	70	71
t=320						
	For Supernatant & Flocs Collection, Analysis	See Tables 2 and 3.				

a) concentrated HCl solution
b) 5 ml of ortho sol'n (18.49 gm/ℓ) + 5 ml of pyro sol'n. (2.16 gm/ℓ) + 5 ml of tripoly sol'n (4.62 gm/ℓ).
c) 50.25 gm alum/ ℓ.
d) Percol 730 1.0 gm/ℓ.

$Na_4P_2O_7 \cdot 10\ H_2O$ and 4.62 g/l sodium tripoly-phosphate $Na_5P_3O_{10}$. 2.4 ml of concentrated HCl was added to lower the pH. 3 ml of alum solution (50.25 g/l $Al_2(SO_4)_3 \cdot 16\ H_2O$) were added. The pH should have reached a level of about 5 at this time. Finally 1.5 ml of polymer solution (Percol 730: 0.25 g/250 ml) was added to the jar. The final pH of the supernatant liquid was about 5.9. The stirring speeds and times are noted in Table 9.

The other runs noted in Table 9 were done in a manner similar to that for Run 9-1. The flocs were permitted to settle for about five hours before samples of supernatant liquid were removed for analysis of dissolved polymer. This lengthy period was necessary to ensure essentially complete floc settling. Settled flocs were separated from supernatant liquid by filtration through a 0.45 micron membrane filter. From two to four litres of the supernatant liquid were concentrated to a final volume of about 100 ml of concentrated solution by vacuum evaporation at 40°C. During the concentration by evaporation, new flocs formed and it was, therefore, necessary to add sufficient HCl to lower the pH to about 1.5 to dissolve them. Two ml of the concentrated solution was injected into the gel permeation chromatograph (GPC) to measure the concentration of dissolved polymer. Table 10 summarizes procedures used for the measurement of dissolved polymer in the supernatant liquid. Forty ml of distilled water was added to the filtered flocs and a pH of 1.5 was induced with concentrated HCl. This causes all of the flocs to dissolve. Two ml of this concentrated solution was injected into the GPC to measure the polymer concentration. All of the runs were carried out in a similar manner and Table 11 summarizes procedures used for the measurement of polymer in the flocs. Table 12 summarizes the final results for both supernatant liquid and flocs, showing levels of residual phosphate and the concentrations of polymer in supernatant liquid and flocs.

9.3 Results

Measurements of floc settling rates of Runs 9-1, 9-1a, 9-2, 9-2a and 9-3 indicated that there was an increase with polymer dosage; however, the change in rate in moving from a dosage of 0.5 ppm to 1.5 ppm was quite small. With a concentration of Percol 730 above 0.5 ppm,

TABLE 10. PROCEDURES EMPLOYED TO DETERMINE POLYMER IN SUPERNATANT LIQUID

Run No.	9-1	9-1a	9-2	9-2a	9-3
Supernatant (siphoned out after floc settled)	2 ℓ supernatant	2 ℓ sup.	2 ℓ sup.	2 ℓ sup.	2 ℓ sup.
Volume of concentrated supernatant after vacuum evaporation at 40°C.	106.7 ml (pH=8.4)		95.8 ml (pH=8.3)		87.3 ml (pH=8.
Vol. of Conc. Supernatant after HCl (37%) addition* to make pH=1.5	107.2 ml		96.5 ml		87.9 ml
GPC detected polymer concentration in the above supernatant concentration	8.2 ppm		23.6 ppm		24.0 ppm
Polymer concentration in the original supernatant (calculated)	.22 ppm		.57 ppm		1.05 ppm

* HCl addition necessary to dissolve the flocs formed upon vacuum evaporation.

TABLE 11. PROCEDURE EMPLOYED TO DETERMINE POLYMER IN FLOCS

Run No.	74-1	74-1a	74-2	74-2a	74-3
	↓	↓	↓	↓	↓
	Flocs settled (in remaining ∿1 ℓ of supernatant after siphoning ∿2 ℓ supernatant) were filtered on .45μ membrane filter and collected.				
Distilled H_2O added to collected flocs	↓ 40 ml (pH=7.0)	↓ 40 ml (7.0)	↓ 40 ml (-)	↓ 40 ml (7.0)	↓ 40 ml (6.8)
Vol. of floc concentrates after HCl(37%) addition to make pH=1.5	40.45	40.33	40.5	40.45	40.45
GPC detected Polymer concentration in the above floc concentrates (ppm)	19.0	16.3	23.1	23.5	24.0
Polymer conc. if the above flocs were present in the original 3 ℓ solution (calculated-ppm)	.25	.22	.31	.31	.32

TABLE 12. SUMMARY OF RESULTS ON FATE OF POLYMER

Run No.	9-1	9-1a	9-2	9-2a	9-3
Polymer dosage (ppm)	.5	.5	1.0	1.0	1.5
Polymer left in Supernatant (ppm)	⊢—— .22* —⊣		⊢—— .57* —⊣		1.05
Polymer settled with flocs (ppm)	.25	.22	.31	.31	.32
Phosphate removal (%)	70	68	70	70	71

* No individual figures for 74-1 and 1a, 74-2 and 2a available since the two supernatants were combined to one.

there was an appreciable loss of polymer in the supernatant liquid. In fact, Table 12 clearly shows that, with increase in polymer dosage, the polymer in the flocs remained constant within experimental error, while the polymer in the supernatant liquid increased appreciably from 0.22 ppm to 1.05 ppm.

These results would naturally lead to the following recommendation for the choice of an optimum polymer dosage: when determining optimum dosage one should accept a somewhat lower floc settling rate in order to reduce polymer dissolved in the treated effluent. It will, of course, be impossible to maintain a zero polymer level in the treated effluent, and before an optimum polymer dosage can be determined, acceptable levels of residual polymer in the effluent must be ascertained.

ACKNOWLEDGEMENTS

Mr. J.W.G. Rupke, the project liaison officer, often gave sound advice and, thereby, materially improved the course of this study.

Technical support was provided by many members of the *Wastewater Research Group*, particularly Messrs. M. Pollock, A. Najak and K.W.A. Ho.

REFERENCES

Abdel-Alim, A.H., and A.E. Hamielec, "Shear Degradation of Water-Soluble Polymers - I. Degradation of Polyacrylamide in a High Shear Couette Viscometer", J. Applied Poly. Sci. 17, 3769 (1973).

Abdel-Alim, A.H., and A.E. Hamielec, "GPC Calibration for Water-Soluble Polymers". J. Applied Poly. Sci. 18, 297 (1974).

APHA, AWWA and WPCF, Standard Methods for the Examination of Water and Wastewater, 13th edition, (1971).

Bancsi, J., A. Benedek, and A.E. Hamielec, "Polymers in Waste Water Treatment: The Settleability of Alum Precipitated Phosphorus Flocs", (in press).

Bartow, E., A.P. Black, and W.E. Sansbury, "Formation of Floc by Ferric Coagulants". Trans. ASCE, 100, 263, (1935).

Beeghly, J.H., "Phosphorus Removal using Metallic Salts and Polyelectrolyte in Primary Clarification". Paper presented at the 23rd Annual Meeting of the West Virginia Pollution Control Association, Chalestou, West Virginia, (1969).

Binkner, F.B. and S.J. Margon, "Polymer Flocculation of Dilute Colloidal Suspensions", Journal American Water Wastes Association, 60, p. 175, (1968).

Black, A.P., A.M. Busnell, F.A. Eidoners and A.L. Black, "Review of the Jar Test", Journal American Water Wastes Association, 49, p. 1414, (1957).

Boyko, B.I. and J.W.G. Rupke, "Technical Implementation of Ontario's Phosphorus Removal Programme", Ministry of The Environment, Toronto, (1973).

Camp, T.R., "Lateral Spillway Channels", Trans. ASCE, 105, 606, (1940).

Camp, T.R., "Sedimentation and Design of Settling Tanks", Trans. ASCE, 111, p. 895, (1946).

Canada Water Act Annual Report, 1973-1974.

Cohen, J.M., "Improved Jar Test Procedure", Journal American Water Wastes Association, 49, p. 1425, (1957).

Convery, J.J. "Treatment Techniques for Removing Phosphorus from Municipal Wastewaters". Water and Pollution Control Research Series #17010, 01/70, U.S. Dept. of the Interior, FWQA (1970).

REFERENCES (CONT'D)

Culp, R.L. and G.L. Culp, Advanced Wastewater Treatment. Van Nostrand Reinhold Co. N.Y., (1971).

Domtar Chemicals Ltd., "The Use of Lime in the Treatment of Municipal Wastewaters", Canada-Ontario Agreement on Great Lakes Water Quality, Research Report No. 21, Ottawa, (1974).

Ferguson, J.F., D. Jenkins and J. Eastman, "Calcium Phosphate Precipitation at Slightly Alkaline pH Values", JWPCF, 45 (4), April, (1973).

Ferguson, J.F. and P.L. McCarty, "The Precipitation of Phosphates from Fresh Waters and Wastewaters". Technical Report No. 120, Dept. of Civil Engineering, Stanford University, (1969).

Ford, D.L. and W.W. Eckenfelder, Water Pollution Control, Jenkins Publishing, Austin, (1970).

Gray, I.M., "Phosphorus Removal Study at the Sarnia WPCP", Canada-Ontario Agreement on Great Lakes Water Quality, Research Report No. 15, Ottawa, (1974).

Haas, H.C. and R.L. MacDonald, "Dichotomies in the Viscosity Stability of Polyacrylamide Solutions (I)" Polymer Letters, 10, 461 (1972).

Health Education Services, "Recommended Standards for Sewage Works", Albany, N.Y., (1971).

Ishige, T. and A.E. Hamielec, "Solution Polymerization of Acrylamide To High Conversion", J. Applied Poly. Sci., 17, 1479 (1973).

Jorden, R.M. and L. Vrale, "Rapid Mixing in Water", Journal American Water Wastes Association, 63, p. 52, (1971).

La Mer, V.K. and T.W. Healy, "The Adsorption-Flocculation Reactions of a Polymer with an Aqueous Colloidal Dispersion". Rev. Pure Appl. Chem., 13, 112, (1963).

Lang, D.A., J.B. Nesbitt and R.R. Kountz, "Soluble Phosphate Removal in Activated Sludge Process - a Two Year Plant Scale Study". Dept. of Civil Engineering, the Pennsylvania State University, n.d.

Linke, W.F. and R.B. Booth, "Physical Chemical Aspects of Flocculation by Polymers". AIME Trans., 217, 364, (1960).

L.S. Love and Associates Ltd., "Report on Phosphorus Removal Treatability Studies of the Town of Napanee WPCP for W.O. Chisholm and Associates (Eastern) Ltd.", Brampton, Ont., (1972).

REFERENCES (CONT'D)

Melnyk, P. Unpublished data, McMaster University, Hamilton (1971).

Melnyk, P., "Precipitation of Phosphates in Sewage with Lanthanum: Experimental and Modelling Study", Ph.D. Thesis, Wastewater Research Group, Dept. of Chemical Engineering, McMaster University, (1974).

Michaels, A.S. "Aggregation of Suspensions by Polyelectrolytes", Ind. and Eng. Chem., 1458, July, (1954).

Mukhopadhyay, S., B.C. Mitra and S.R. Palit, "Kinetics of Alkaline Hydrolysis of Polyacrylamide", Indian J. of Chem., 7, 903 (1969).

Najak, A., A. Benedek and J.J. Bancsi, "Effect of Freezing on Suspended Solids", Unpublished Report, Wastewater Research Group, Department of Chemical Engineering, McMaster University, (1974).

Nilsson, R. "Phosphate Separation in Sewage Treatment". Process Biochemistry, May, (1969).

Ontario Ministry of the Environment "Guidelines for Conducting Treatability Studies for Phosphorus Removal at Waste Water Treatment Plants", Toronto, (1972).

Peterson, B. and E. Barlow, "Effects of Salts on the Rate of Coagulation and the Optimum Precipitation of Alum Floc", Industrial and Engineering Chemistry, 20, p. 51, (1928).

Recht, H.L. and M. Ghassemi, "Kinetics and Mechanics of Precipitation and Nature of the Precipitate obtained in Phosphate Removal from Wastewater using Al^{3+} and Fe^{3+} Salts". Water Pollution Control Research Series, #17010 EKI, 04/70, U.S. Dept. of the Interior, FWQA, (1970).

Ries and Meyers "Microdectrophoresis and Electron-Microscope Studies with Polymeric Flocculants". J. Appl. Sci., 15, 2023, (1971).

Rocheleau, A.W., D.G. Parker, D.G. Pessagno and E.M. Gotza, "Phosphorus Removal Feasibility Study", Sarnia Sewage Treatment Plant. Dow Chemical of Canada Report (1970).

Schmidt, A.X. and C.A. Marlies, Principles of High-Polymer Theory and Practice. McGraw-Hill Book Co., Inc., N.Y., (1948).

Smith, G.B. and V.V. Downing Jr., "Objective Method of Data Reduction for Particle Size Analysis by Cumulative Sedimentation Method", Analytical Chemistry, 42: p. 136, (1970).

REFERENCES (CONT'D)

Stumm, W. and J.J. Morgan, Aquatic Chemistry, Wiley-Interscience, N.Y. (1970).

Stumm, W. and C.R. O'Melia, "Stoichiometry of Coagulation", Journal American Water Wastes Association, 60, pp. 414-539, (1968).

Tan, P.G.G., "Generalized, Steady-State Simulation of Wastewater Treatment Plants", M.Eng. Thesis, McMaster University, (1972).

Underwood, McLellan and Associates, Ltd., "Treatability Study for Phosphorus Removal, Dundas, WPCP", Rexdale, Ont., (1972).

Van Fleet, G.L., "Guidelines for Conducting Treatability Studies for Phosphorus Removal at Wastewater Treatment Plants", Ontario Ministry of the Environment, Toronto, (1972).

Ventran Instrument Corp., Cahn Divison, "#2800 Particle Sedimentation Accessory Instructions for the Cahn Electro-balance Model RTL", (1971).

Willcomb, G.E., "Floc Index", Journal American Water Wastes Association, 24, p. 1416, (1916).

Wukasch, R.F. "Phosphate Removal at Grayling, Michigan and Lake Odessa, Michigan". Michigan WPCA Annual Conference (1968).

Yorke, M.A., "Molecular Weight Relationships in Cationic Flocculation", Flocculation by Polyelectrolytes, American Chemical Society, pp. 93-103, (1972).

APPENDIX A

SUPPLEMENTAL FIGURES

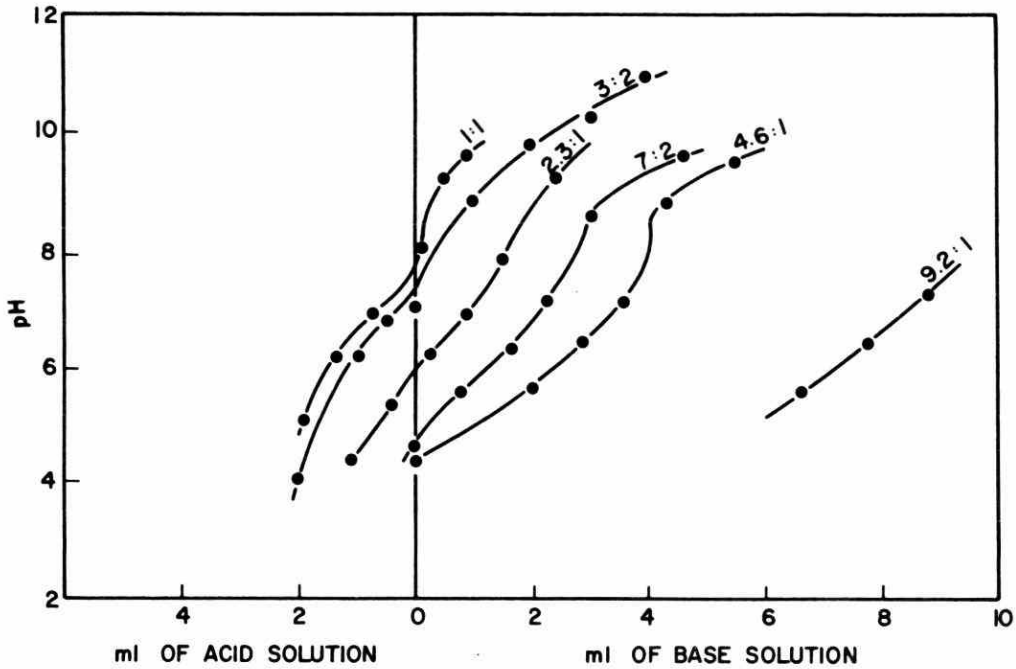

FIGURE 93. pH CONTROL FOR THE ALUMINUM-ORTHOPHOSPHATE SYSTEM

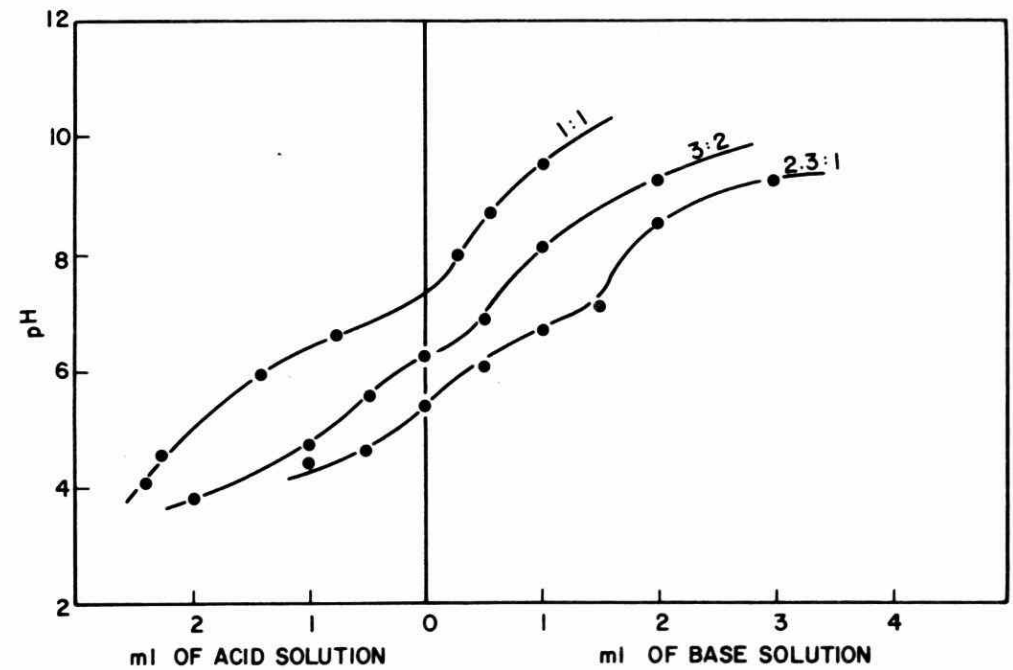

FIGURE 94. pH CONTROL FOR THE ALUMINUM-MIXED PHOSPHATE SYSTEM

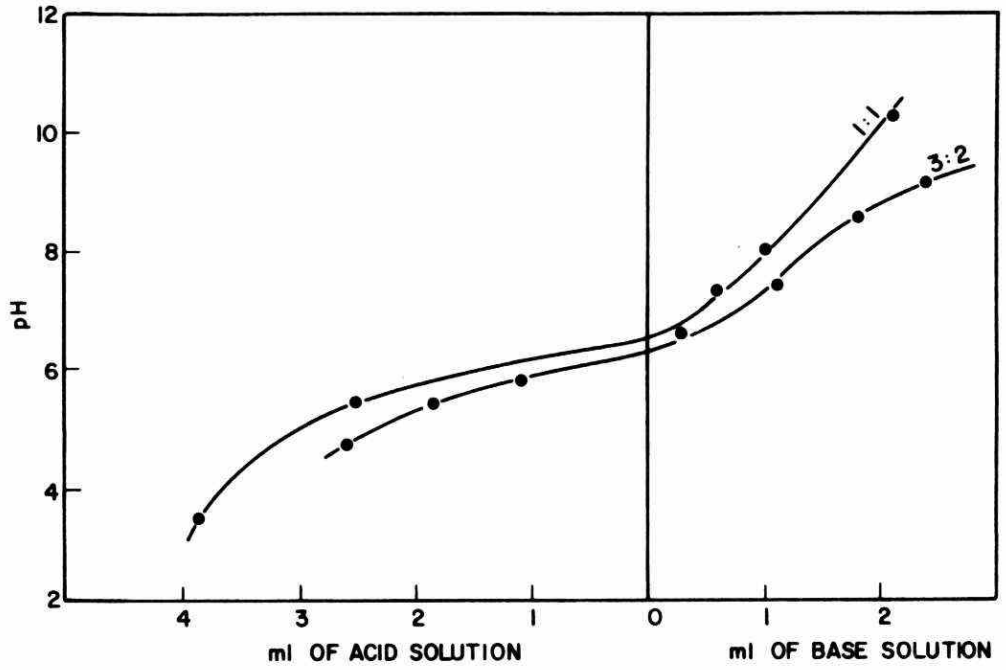

FIGURE 95. pH CONTROL FOR THE ALUMINUM-MIXED PHOSPHATE SYSTEM WITH $CaCO_3$

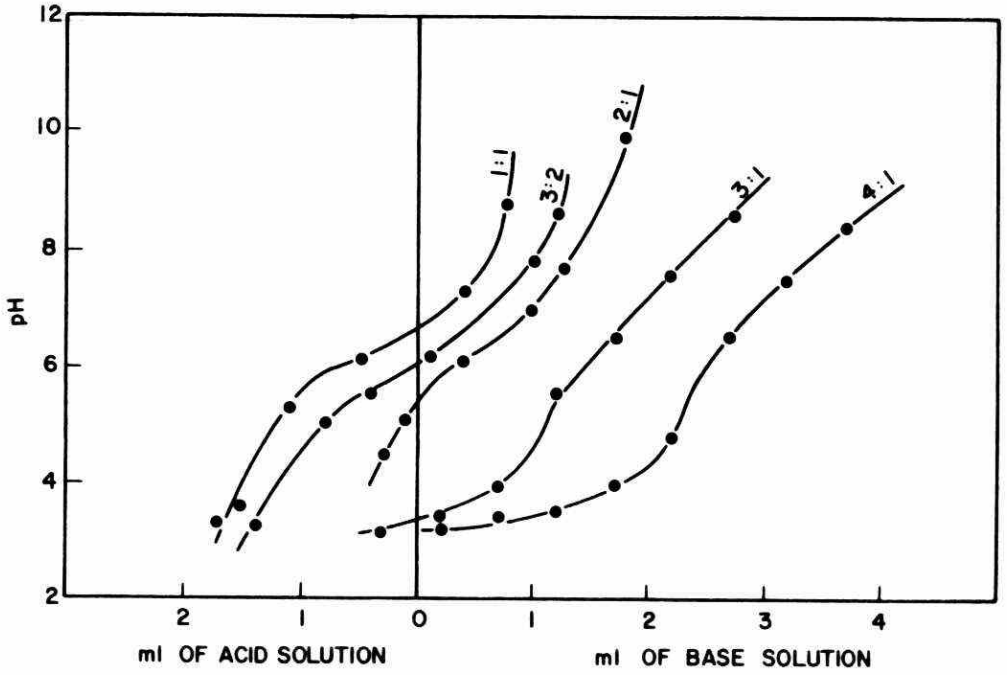

FIGURE 96. pH CONTROL FOR THE IRON-ORTHOPHOSPHATE SYSTEM

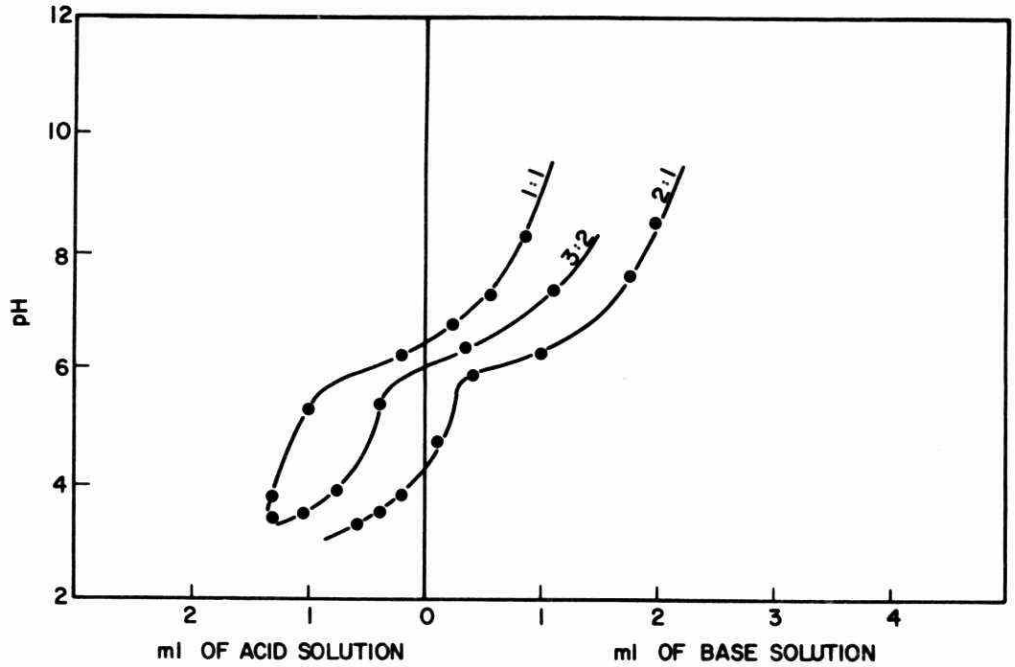

FIGURE 97. pH CONTROL FOR THE IRON-MIXED PHOSPHATE SYSTEM

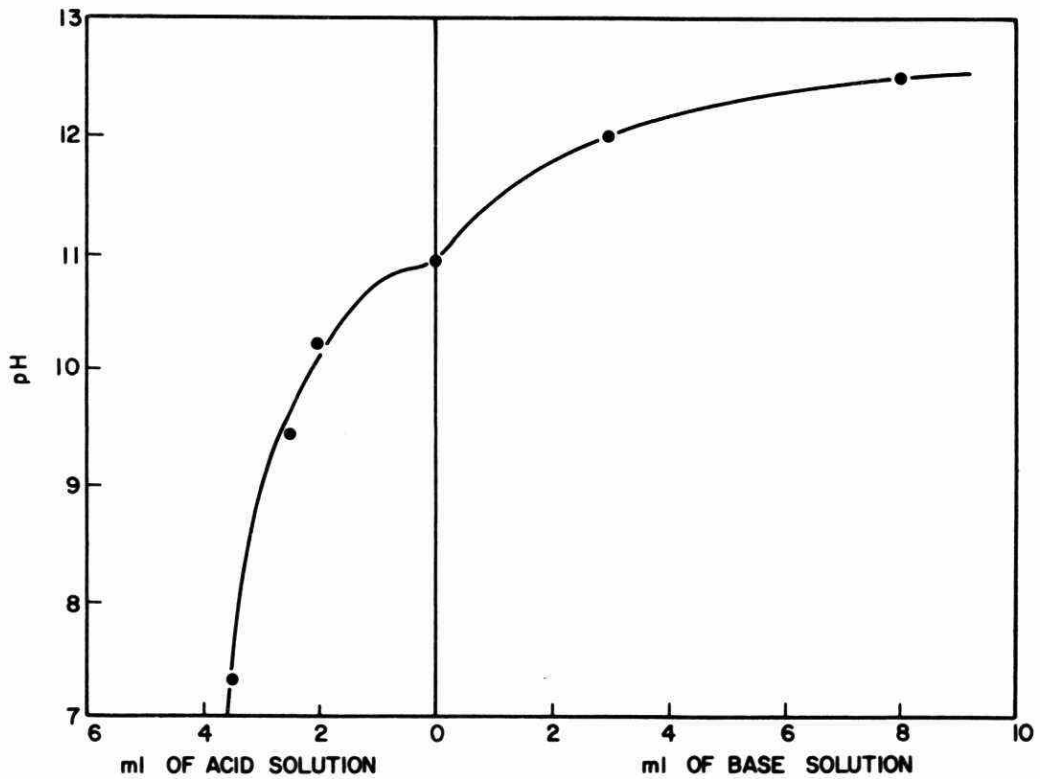

FIGURE 98. pH CONTROL FOR THE CALCIUM-ORTHOPHOSPHATE SYSTEM

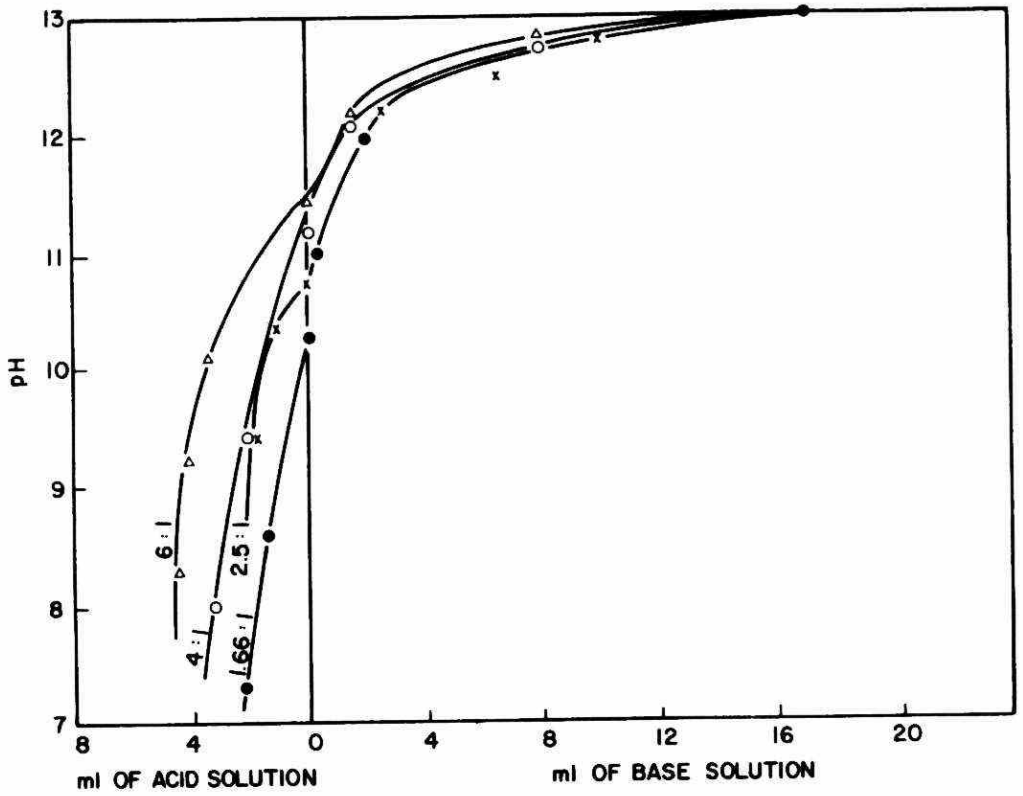

FIGURE 99. pH CONTROL FOR THE CALCIUM-MIXED PHOSPHATE SYSTEM

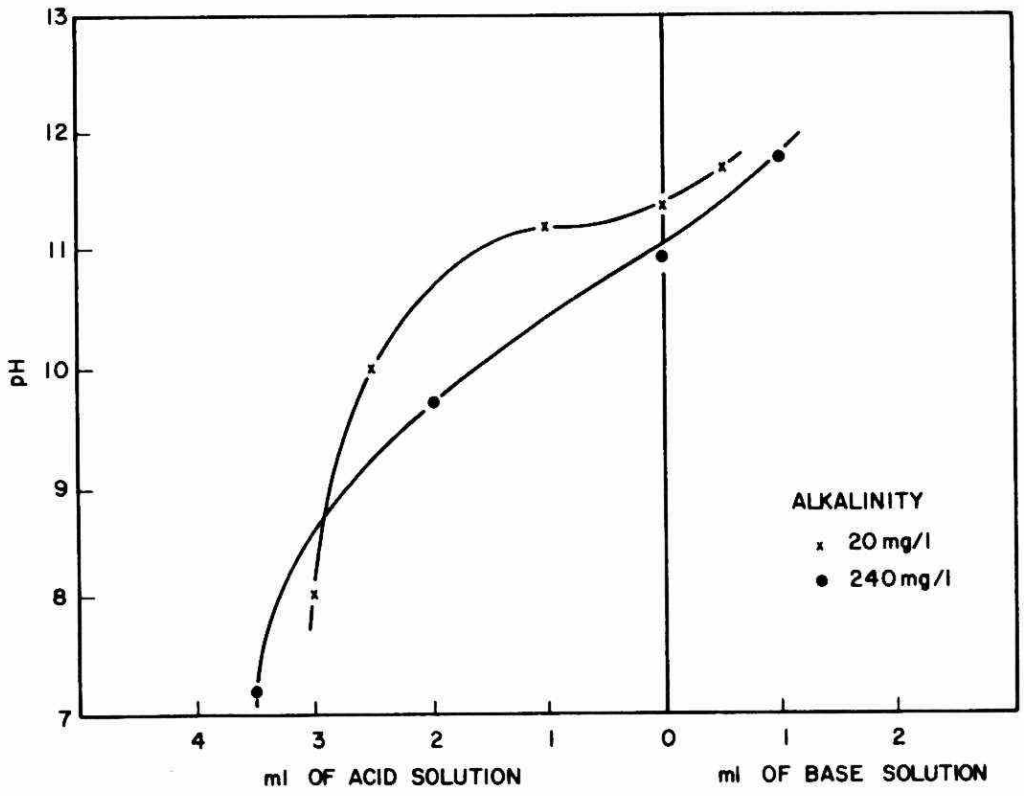

FIGURE 100. pH CONTROL FOR THE CALCIUM-MIXED PHOSPHATE SYSTEM WITH VARYING Mg^{++}

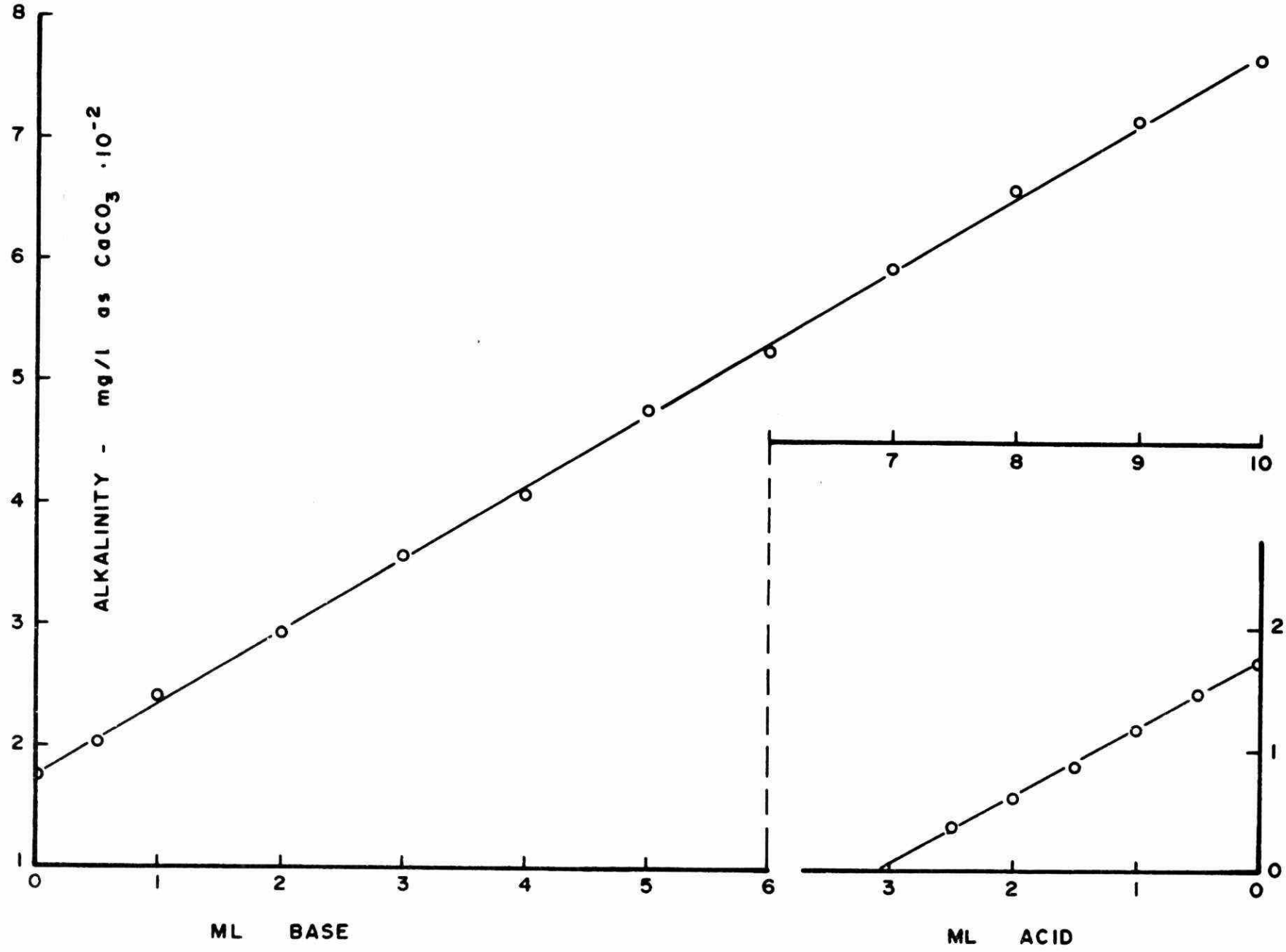

FIGURE 101. INITIAL SOLUTION ALKALINITY AS RESULT OF pH CONTROL FOR THE ALUMINUM-ORTHOPHOSPHATE SYSTEM

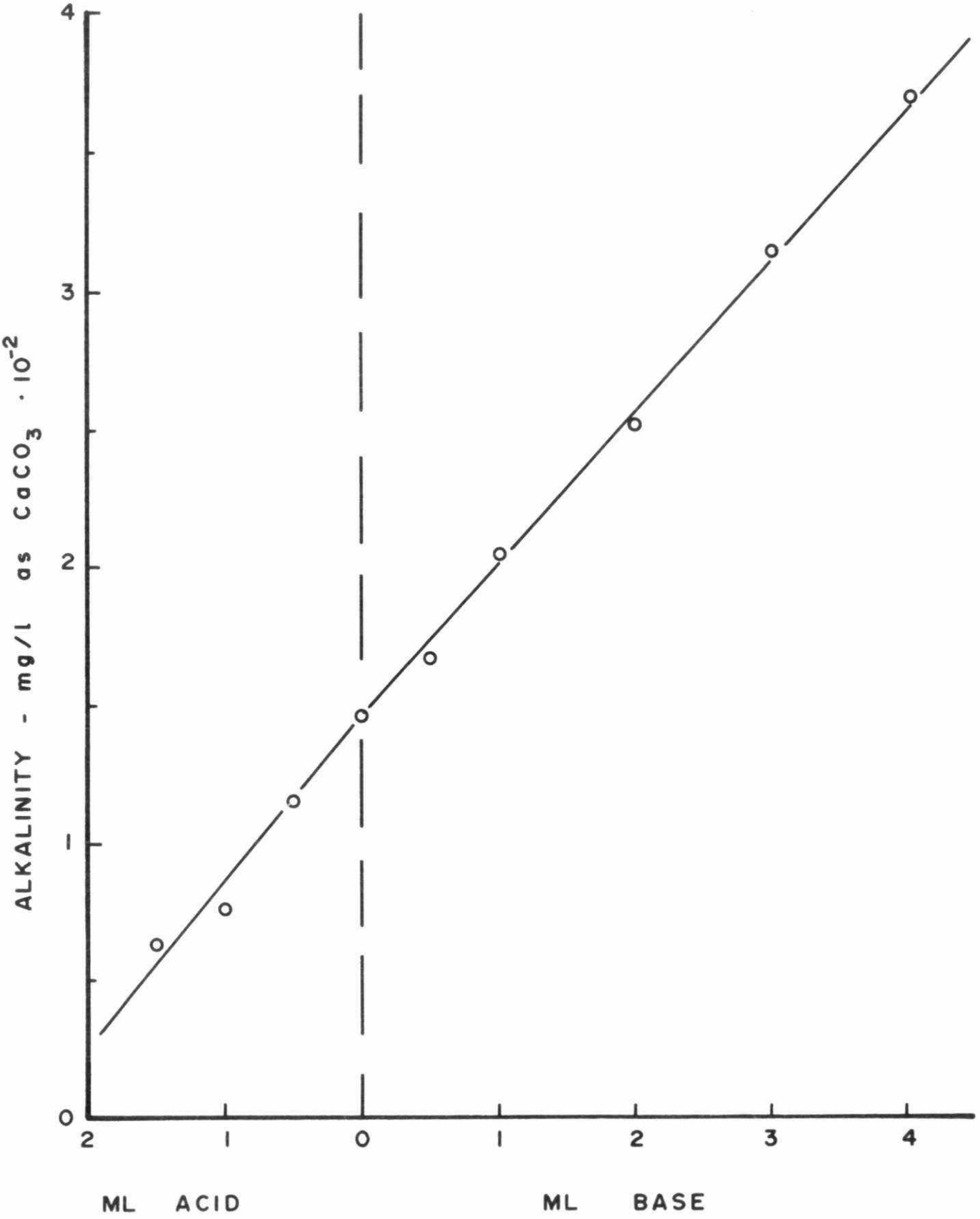

FIGURE 102. INITIAL SOLUTION ALKALINITY AS RESULT OF pH CONTROL FOR THE IRON-ORTHOPHOSPHATE

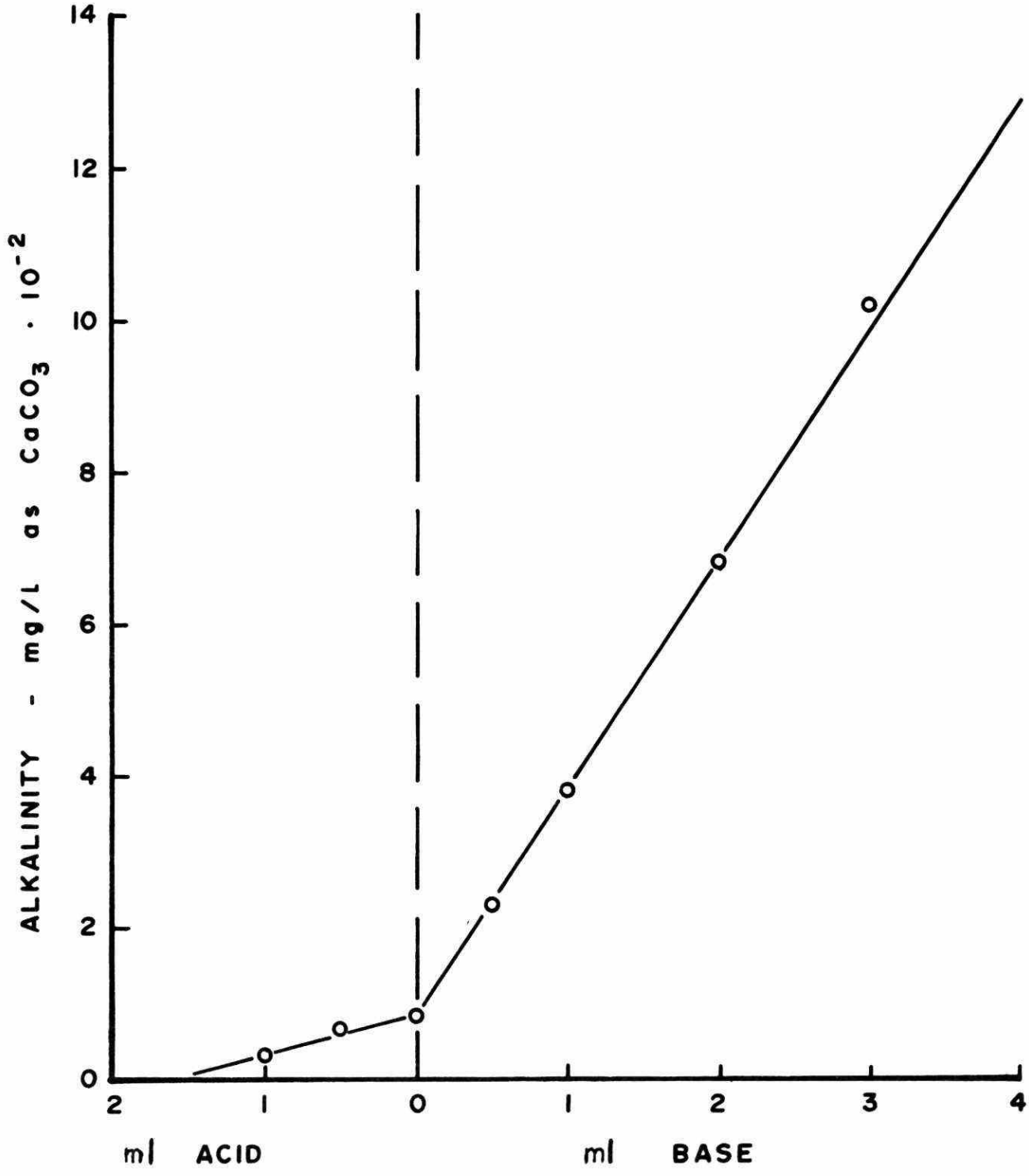

FIGURE 103. INITIAL SOLUTION ALKALINITY AS RESULT OF pH CONTROL FOR LIME-MIXED PHOSPHATE SYSTEM

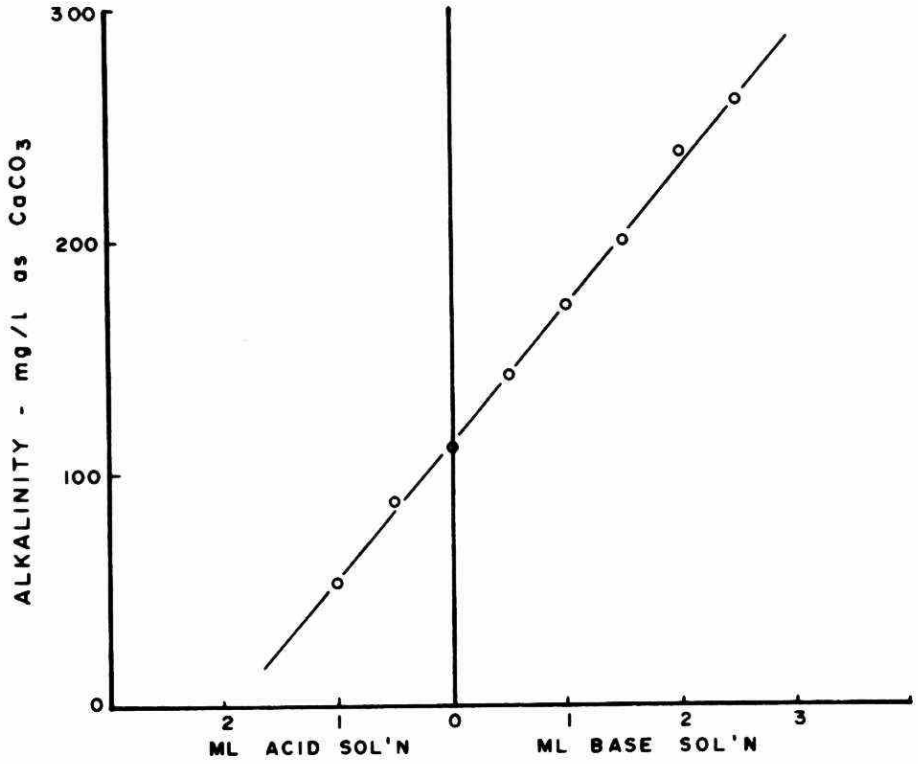

FIGURE 104. ALKALINITY AS RESULT OF pH CONTROL IN THE IRON-MIXED PHOSPHATE SYSTEM

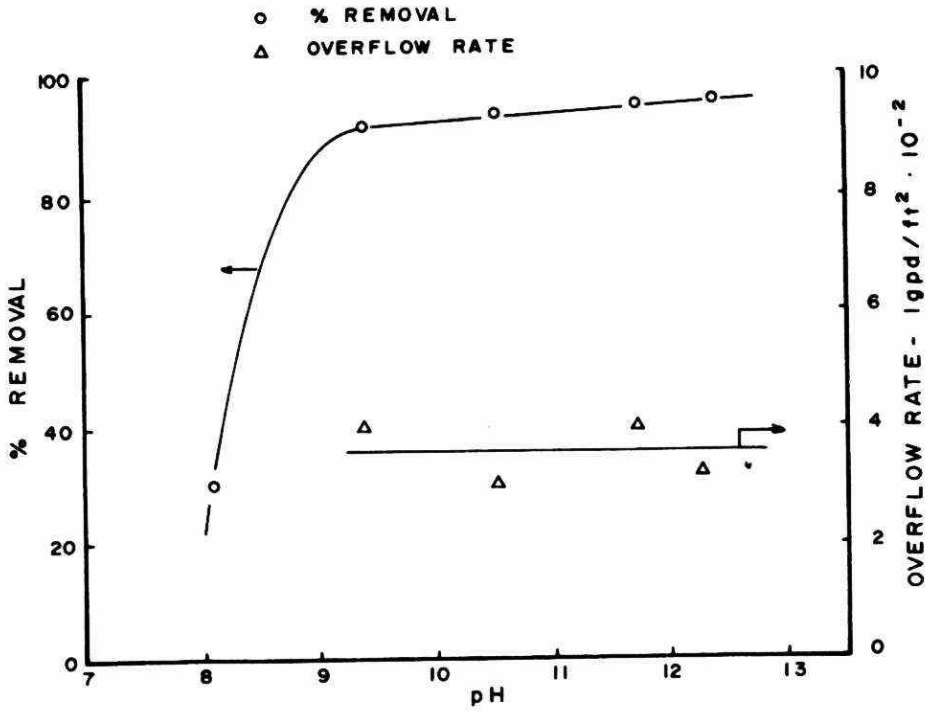

FIGURE 105. ULTIMATE PHOSPHORUS REMOVAL AND MAXIMUM PERMISSIBLE OVERFLOW RATES FOR 90% FLOC REMOVAL IN THE CALCIUM-ORTHOPHOSPHATE SYSTEM

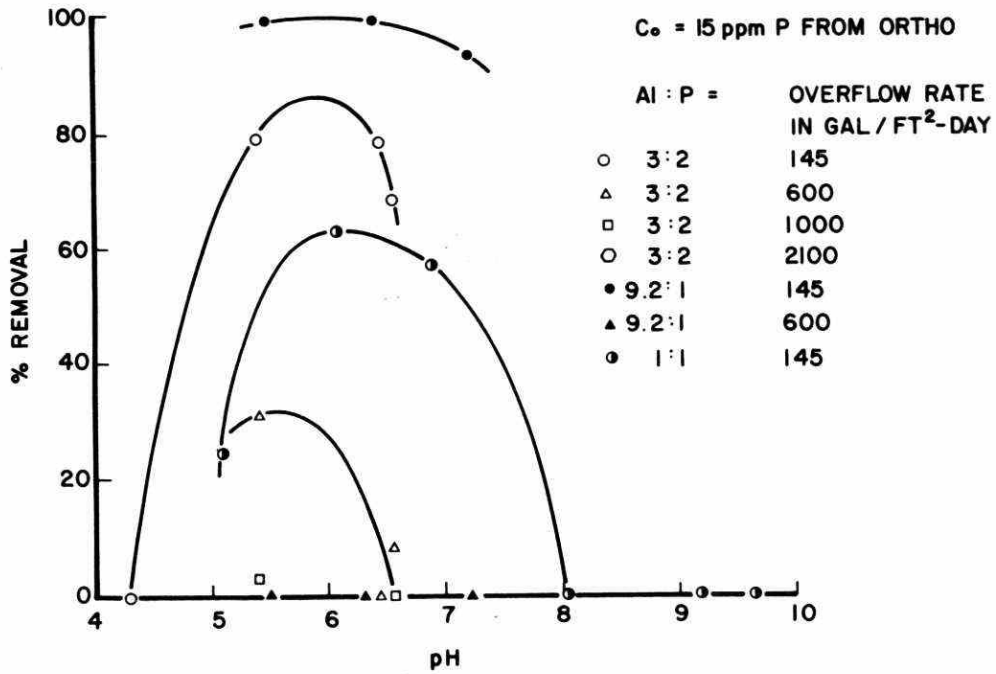

FIGURE 106. PHOSPHORUS REMOVAL IN THE ALUMINUM-ORTHOPHOSPHATE SYSTEM

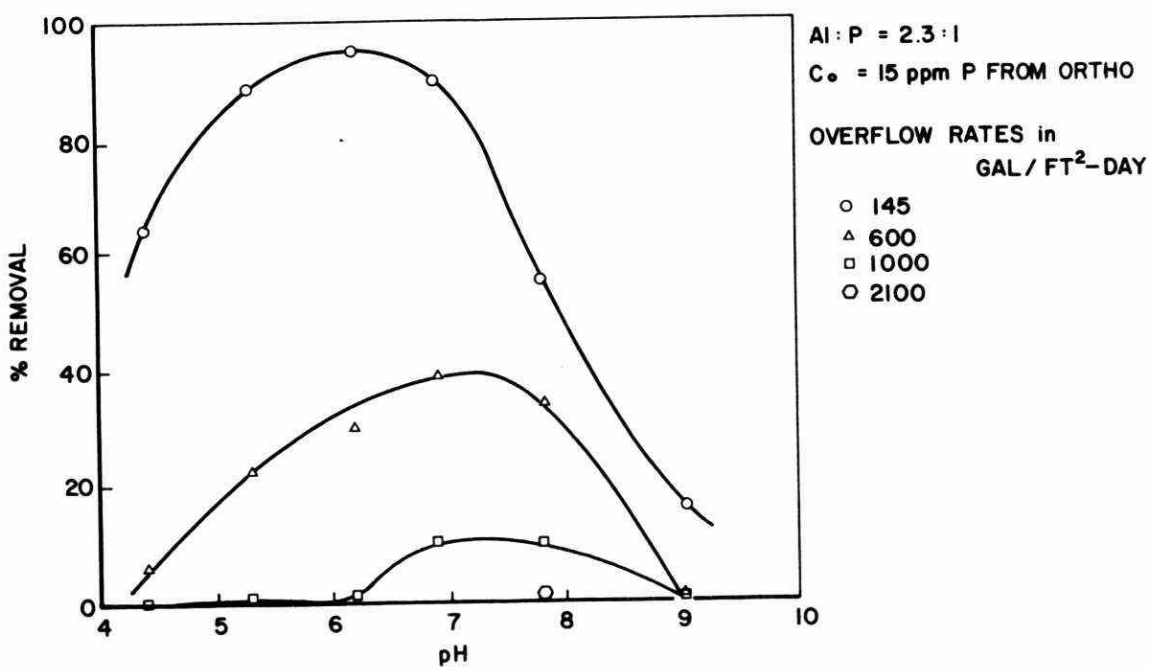

FIGURE 107. PHOSPHORUS REMOVAL IN THE ALUMINUM-ORTHOPHOSPHATE SYSTEM

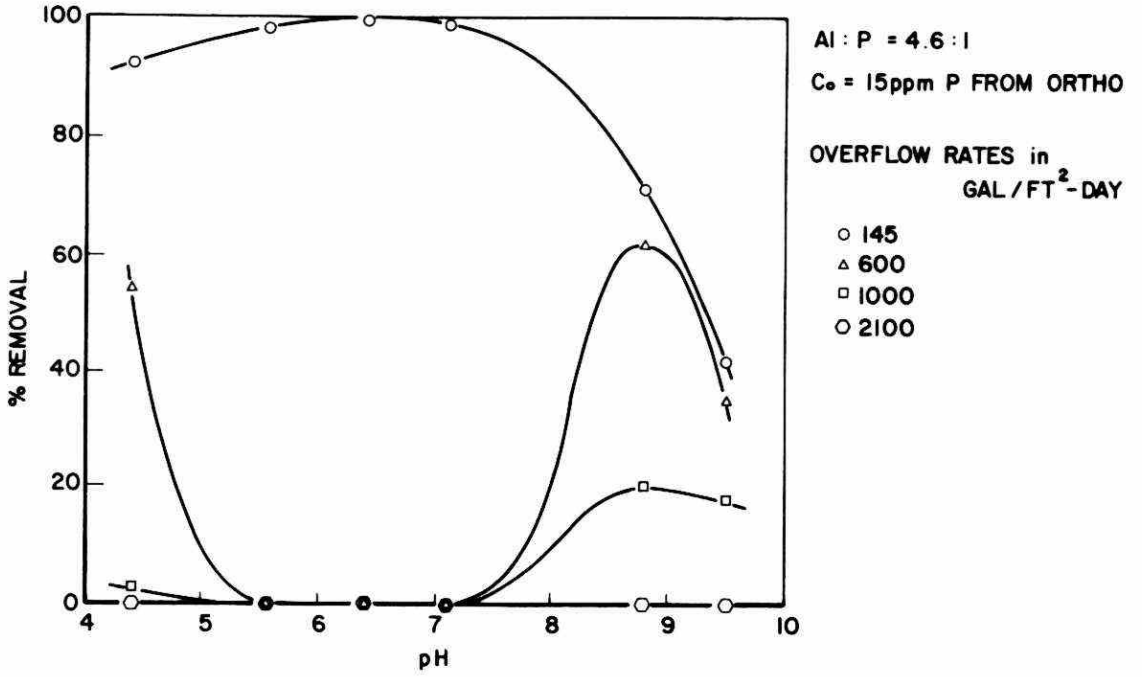

FIGURE 108. PHOSPHORUS REMOVAL IN THE ALUMINUM-ORTHOPHOSPHATE SYSTEM

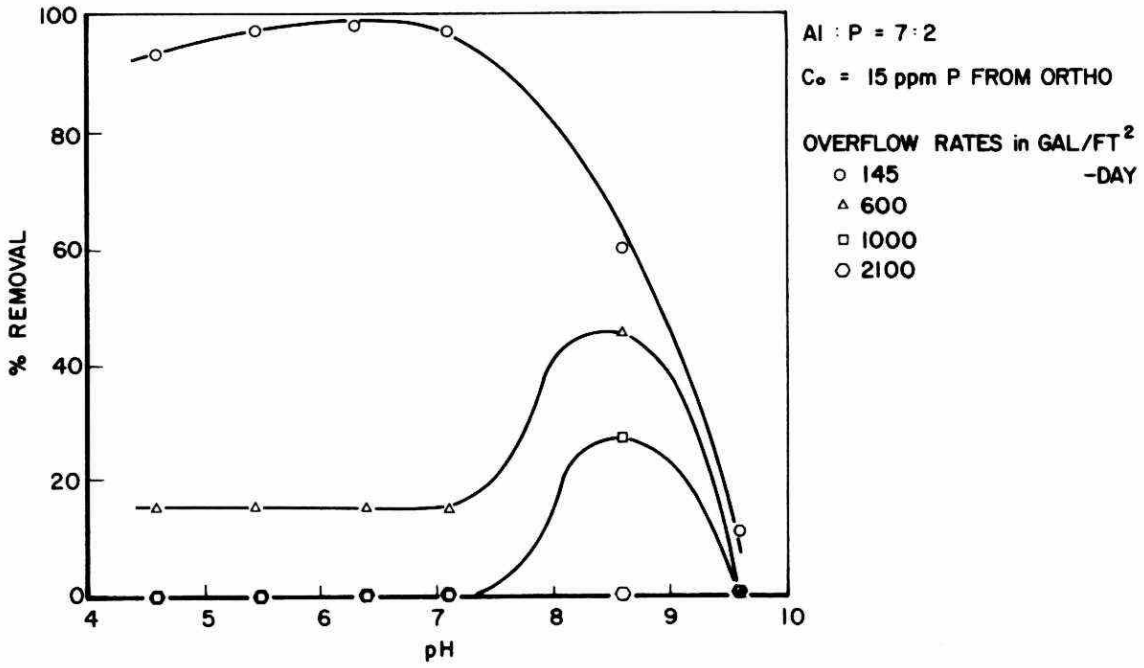

FIGURE 109. PHOSPHORUS REMOVAL IN THE ALUMINUM-ORTHOPHOSPHATE SYSTEM

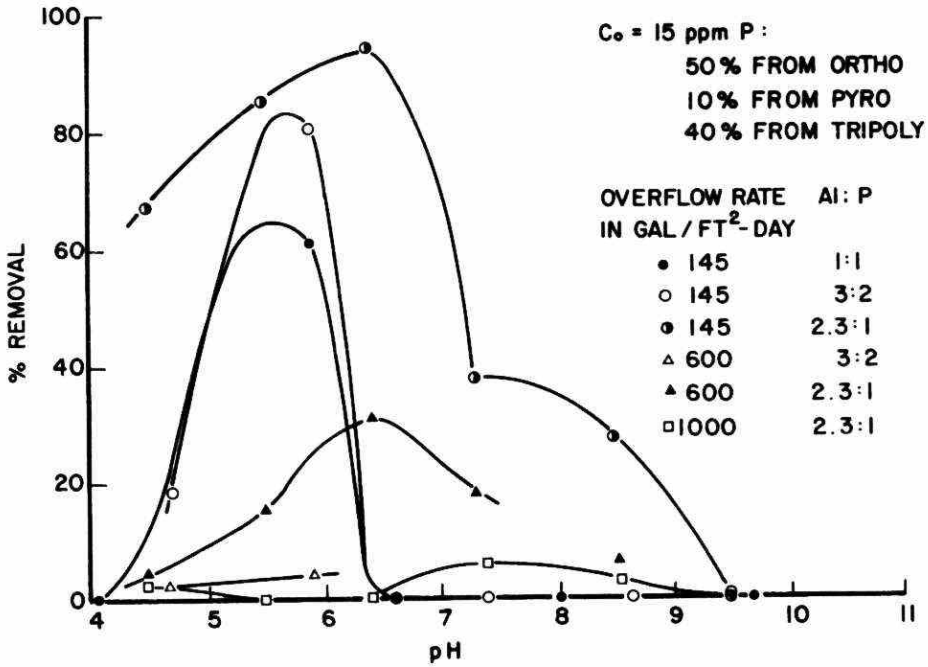

FIGURE 110. PHOSPHORUS REMOVAL IN THE ALUMINUM-MIXED PHOSPHATE SYSTEM

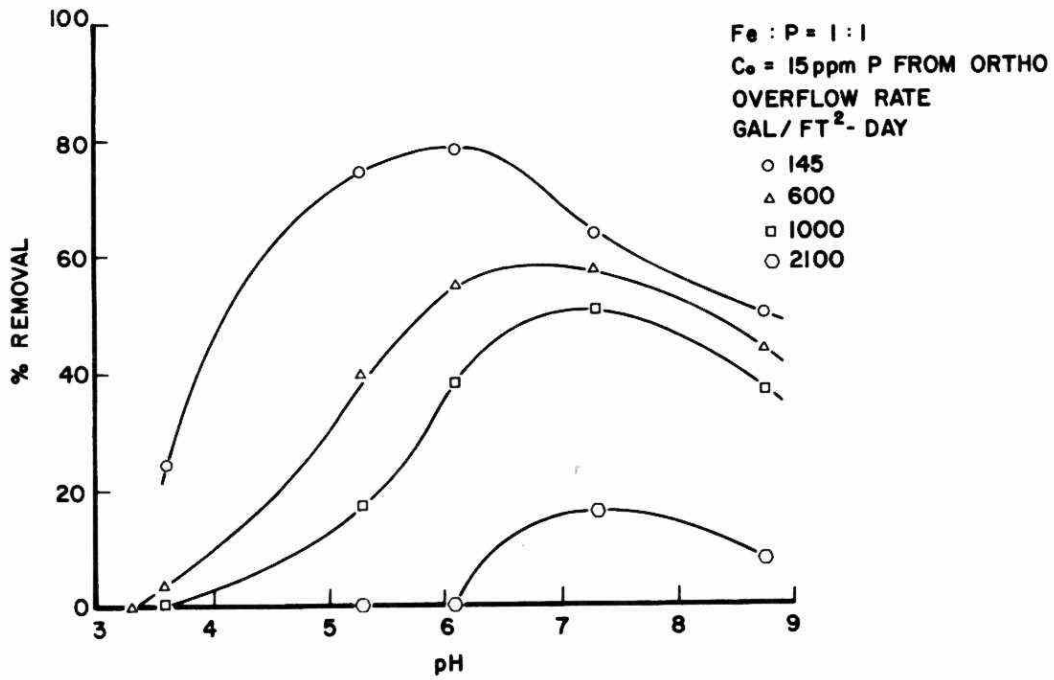

FIGURE 111. PHOSPHORUS REMOVAL IN THE IRON-ORTHOPHOSPHATE SYSTEM

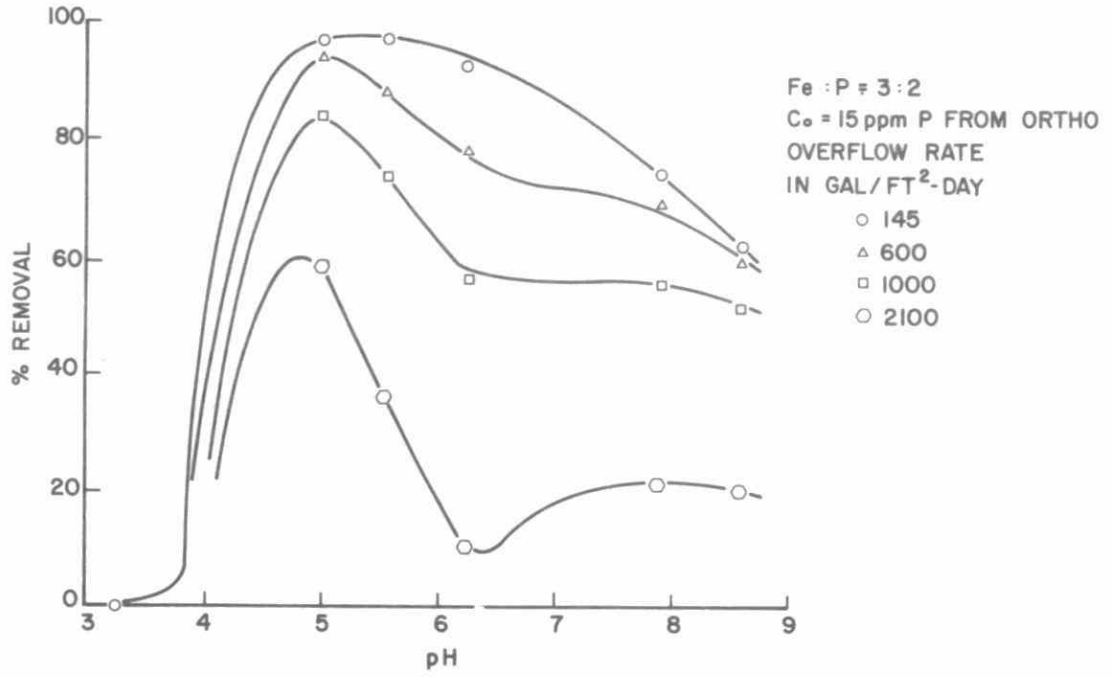

FIGURE 112. PHOSPHORUS REMOVAL IN THE IRON-ORTHOPHOSPHATE SYSTEM

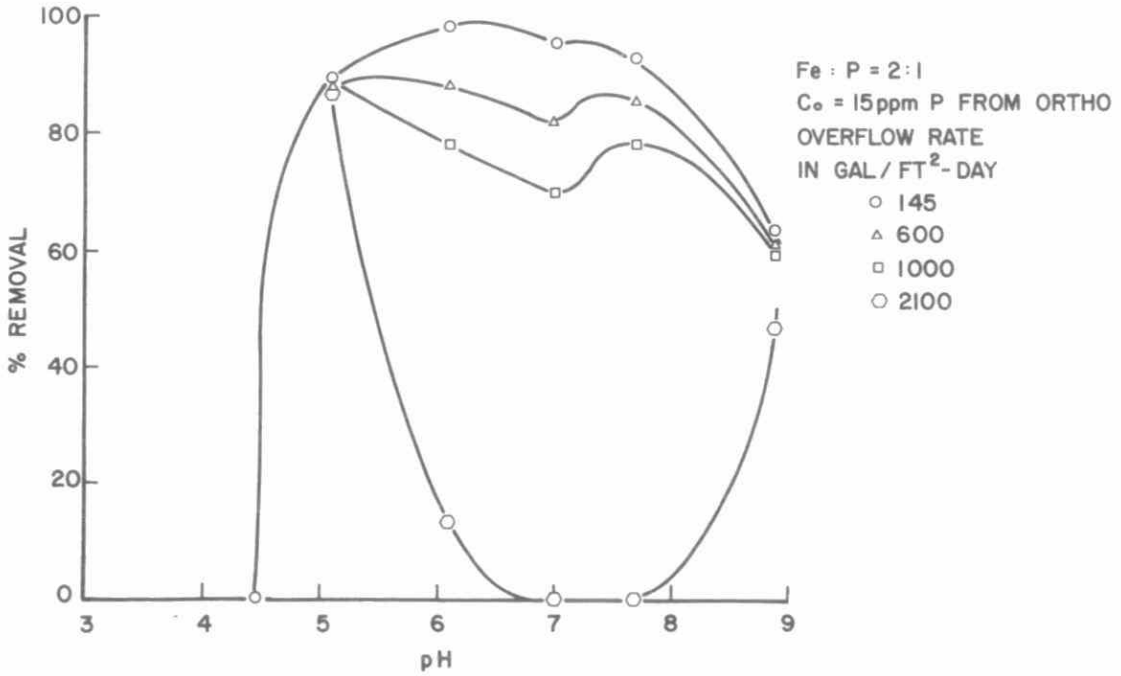

FIGURE 113. PHOSPHORUS REMOVAL IN THE IRON-ORTHOPHOSPHATE SYSTEM

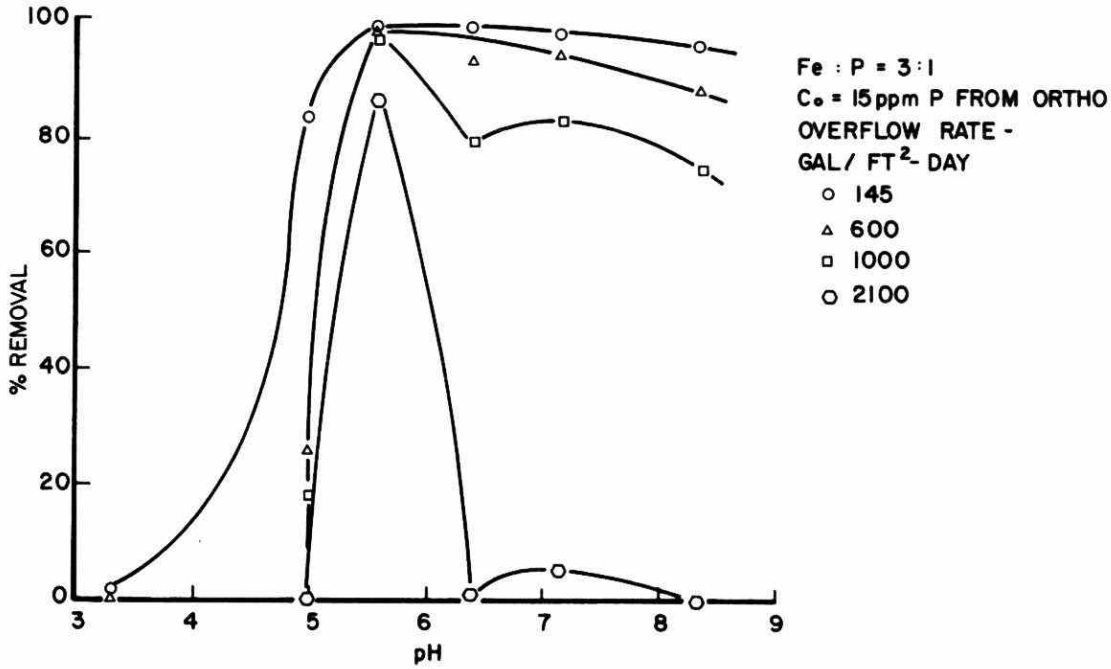

FIGURE 114. PHOSPHORUS REMOVAL IN THE IRON-ORTHOPHOSPHATE SYSTEM

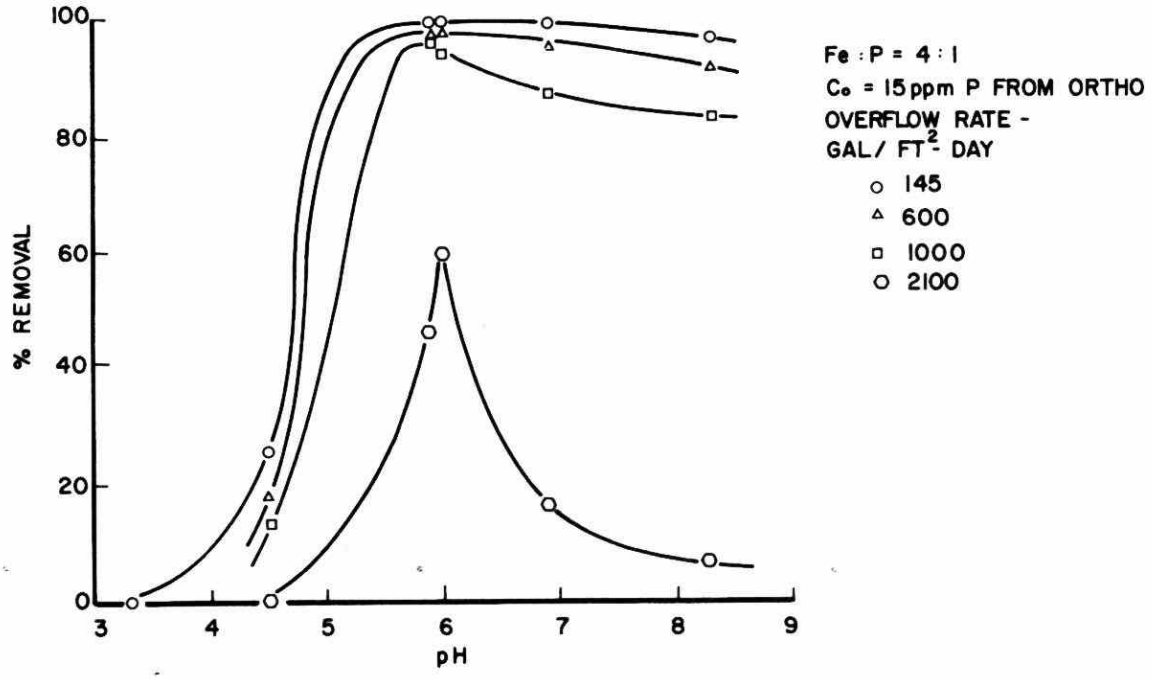

FIGURE 115. PHOSPHORUS REMOVAL IN THE IRON-ORTHOPHOSPHATE SYSTEM

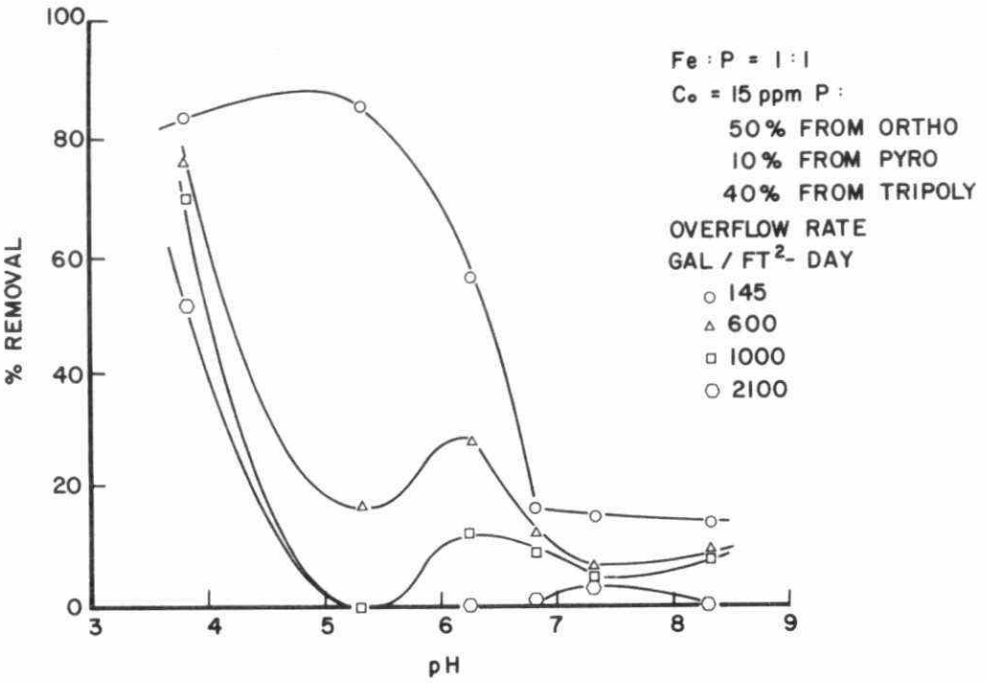

FIGURE 116. PHOSPHORUS REMOVAL IN THE IRON-MIXED PHOSPHATE SYSTEM

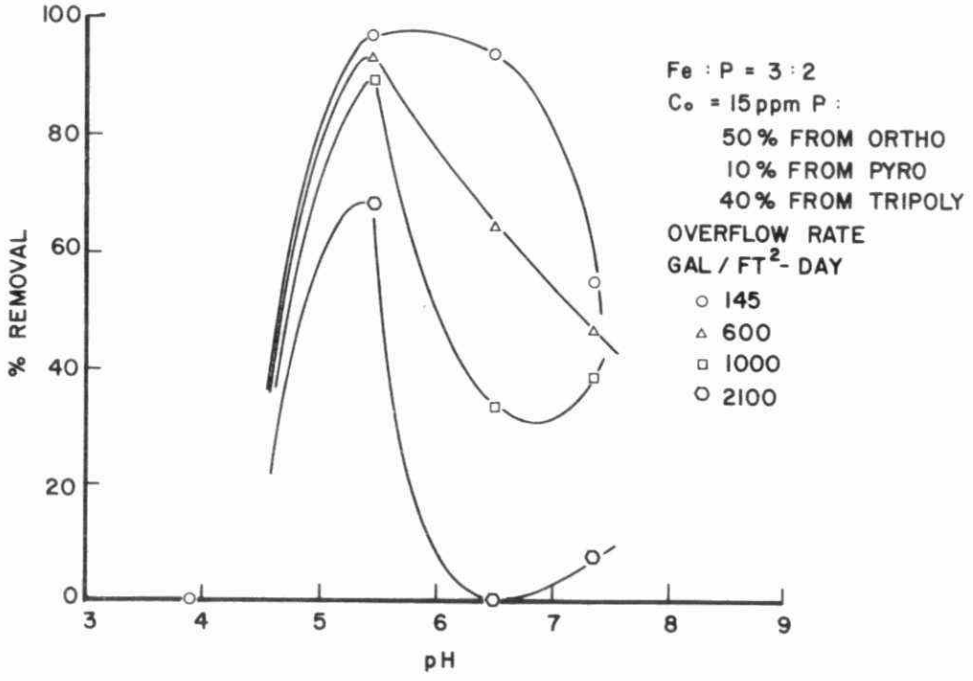

FIGURE 117. PHOSPHORUS REMOVAL IN THE IRON-MIXED PHOSPHATE SYSTEM

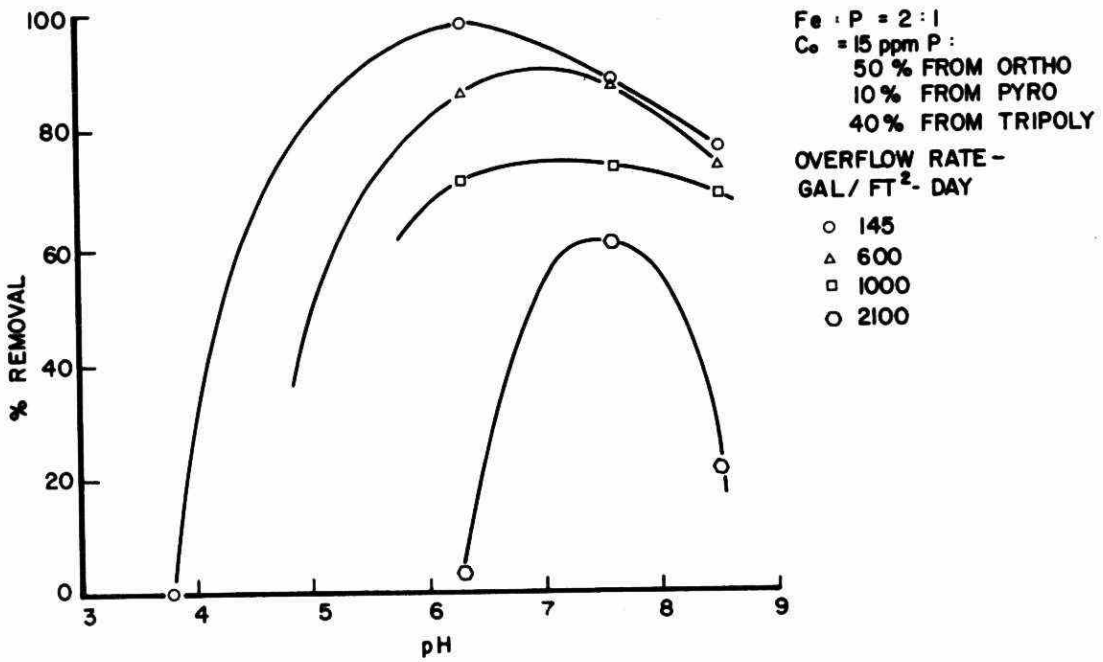

FIGURE 118. PHOSPHORUS REMOVAL IN THE IRON-MIXED PHOSPHATE SYSTEM

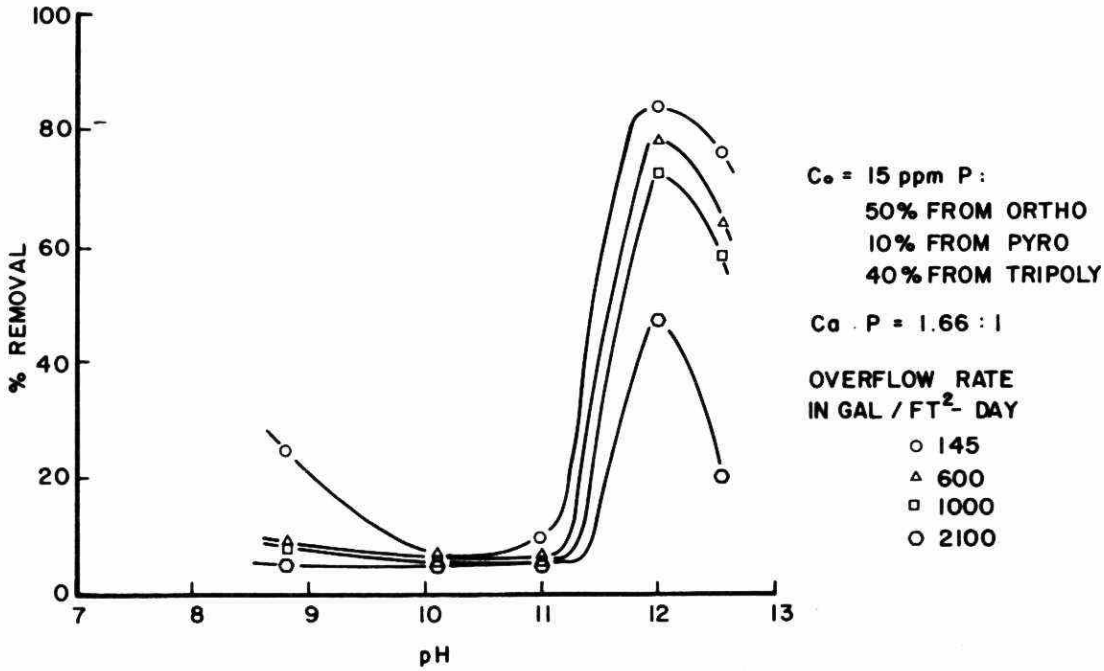

FIGURE 119. PHOSPHORUS REMOVAL IN THE CALCIUM-MIXED PHOSPHATE SYSTEM

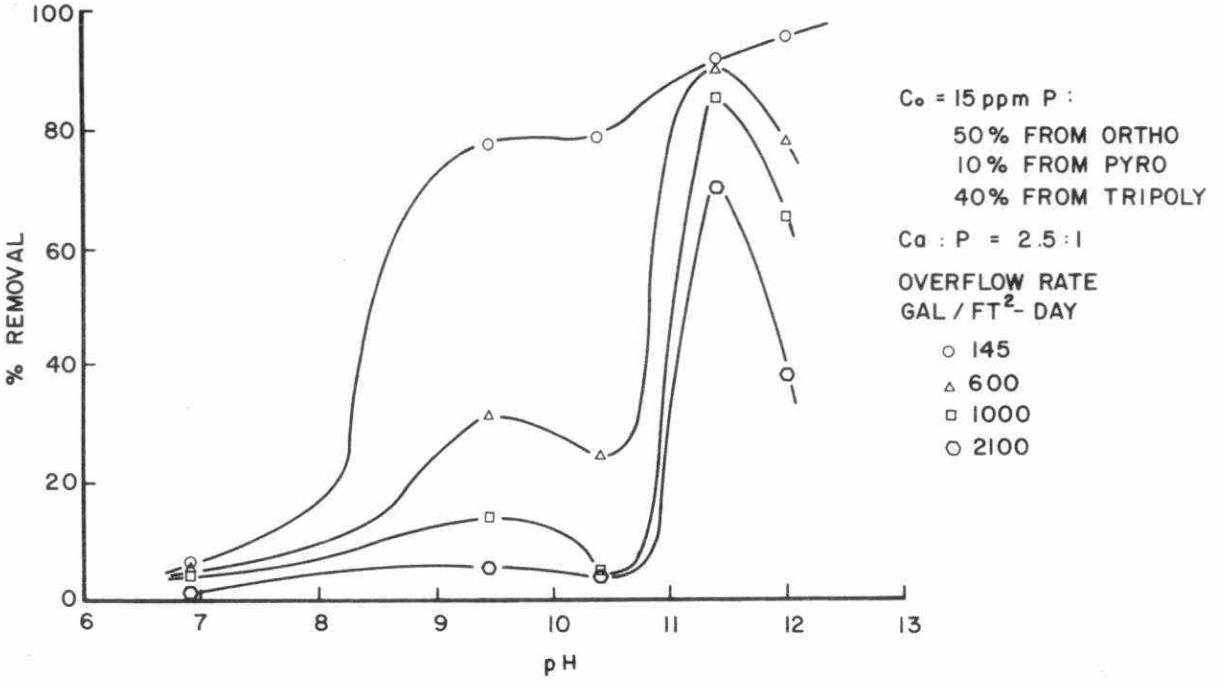

FIGURE 120. PHOSPHORUS REMOVAL IN THE CALCIUM-MIXED PHOSPHATE SYSTEM

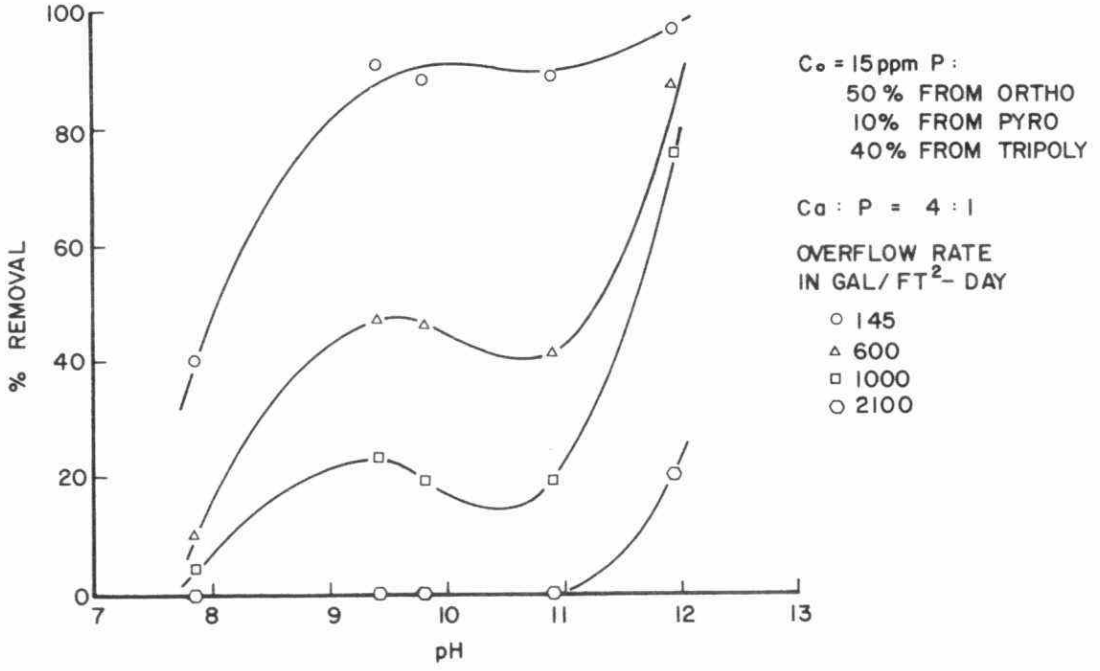

FIGURE 121. PHOSPHORUS REMOVAL IN THE CALCIUM-MIXED PHOSPHATE SYSTEM

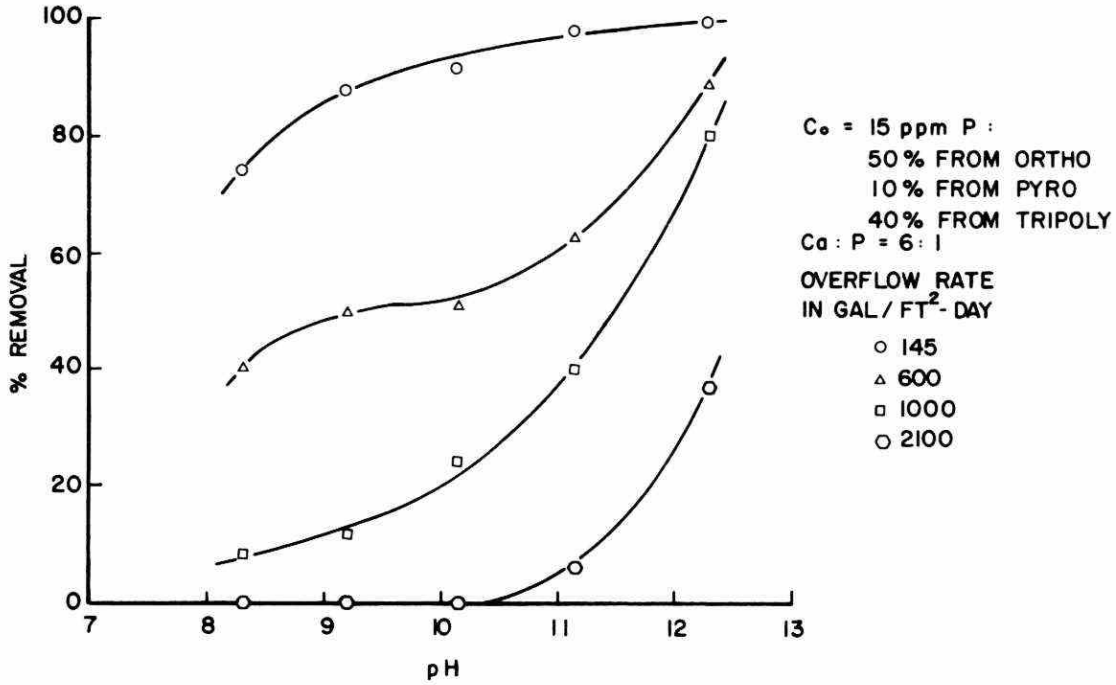

FIGURE 122. PHOSPHORUS REMOVAL IN THE CALCIUM-MIXED PHOSPHATE SYSTEM

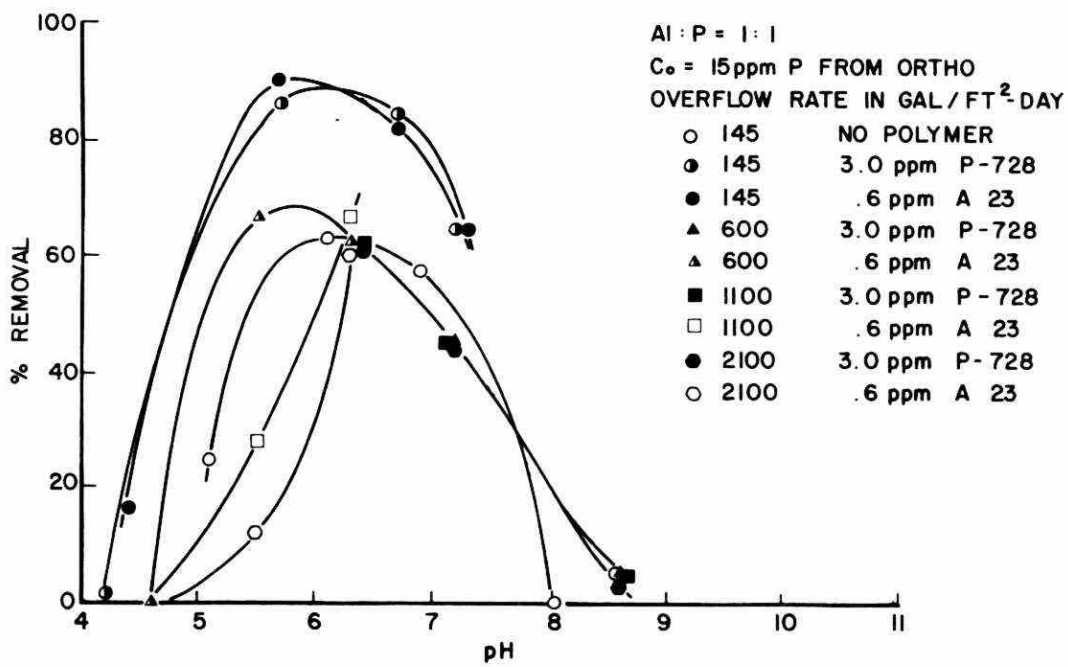

FIGURE 123. PHOSPHORUS REMOVAL IN THE ALUMINUM-ORTHOPHOSPHATE SYSTEM WITH POLYELECTROLYTE ADDITION

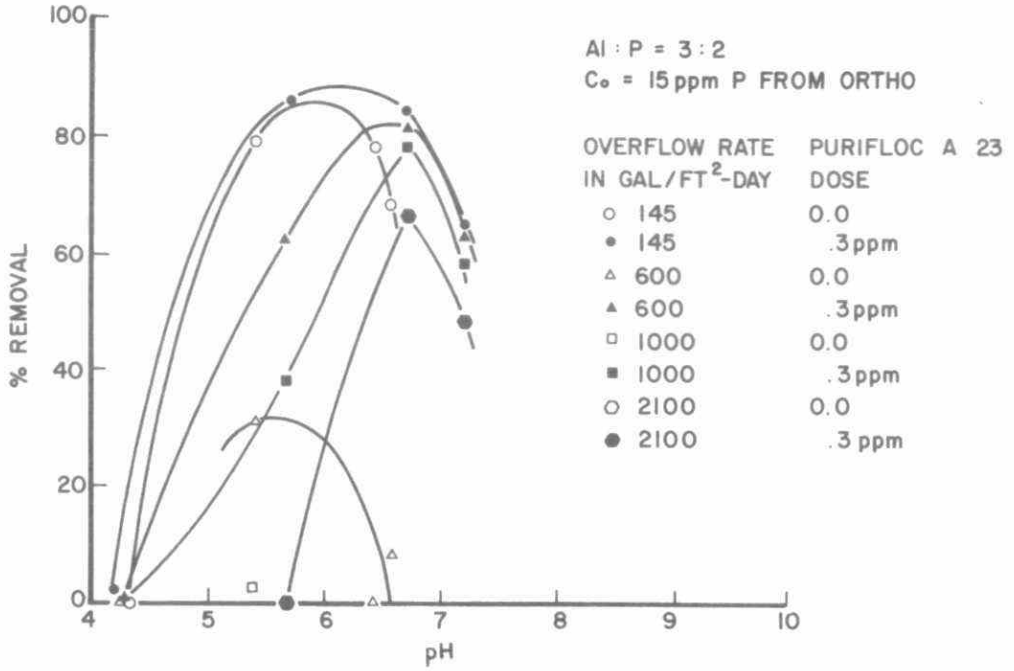

FIGURE 124. PHOSPHORUS REMOVAL IN THE ALUMINUM-ORTHOPHOSPHATE SYSTEM WITH POLYELECTROLYTE ADDITION

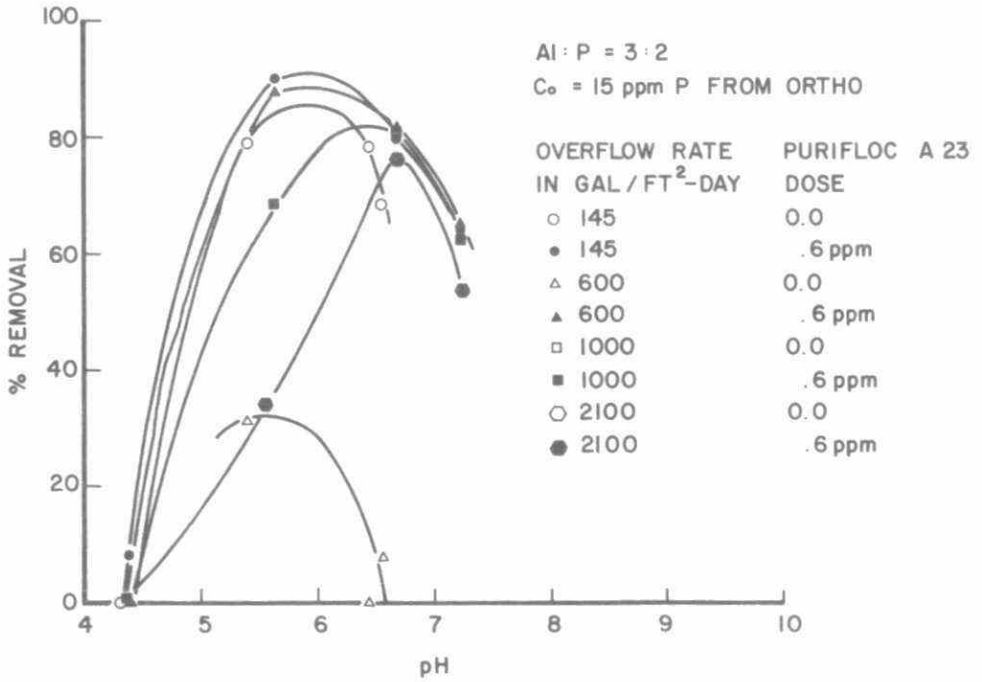

FIGURE 125. PHOSPHORUS REMOVAL IN THE ALUMINUM-ORTHOPHOSPHATE SYSTEM WITH POLYELECTROLYTE ADDITION

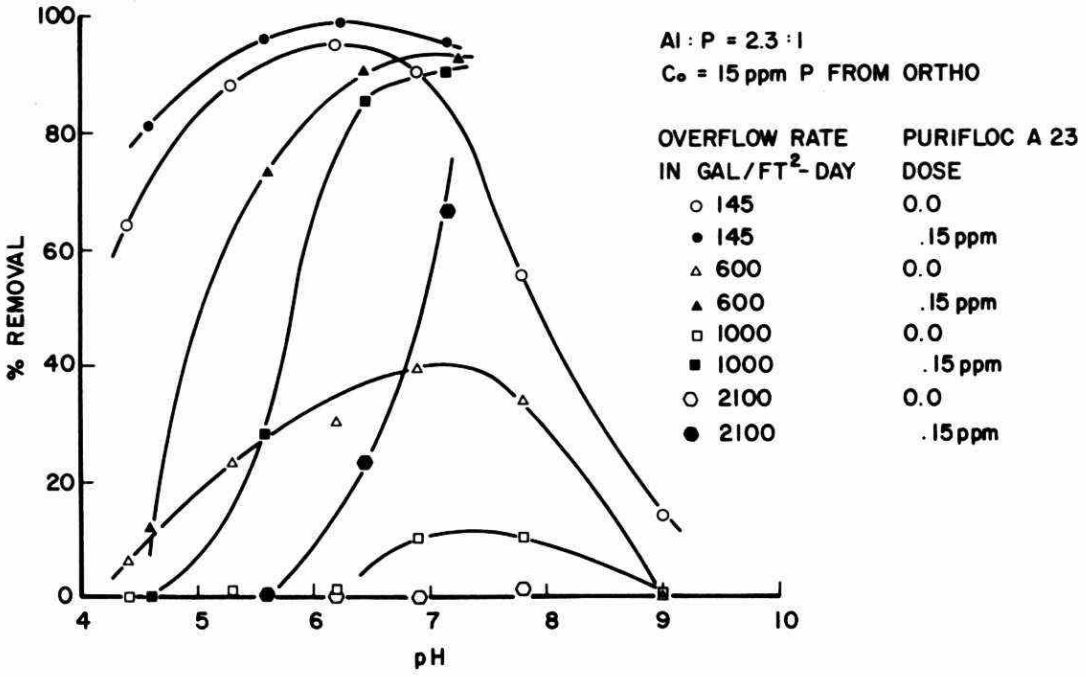

FIGURE 126. PHOSPHORUS REMOVAL IN THE ALUMINUM-ORTHOPHOSPHATE SYSTEM WITH POLYELECTROLYTE ADDITION

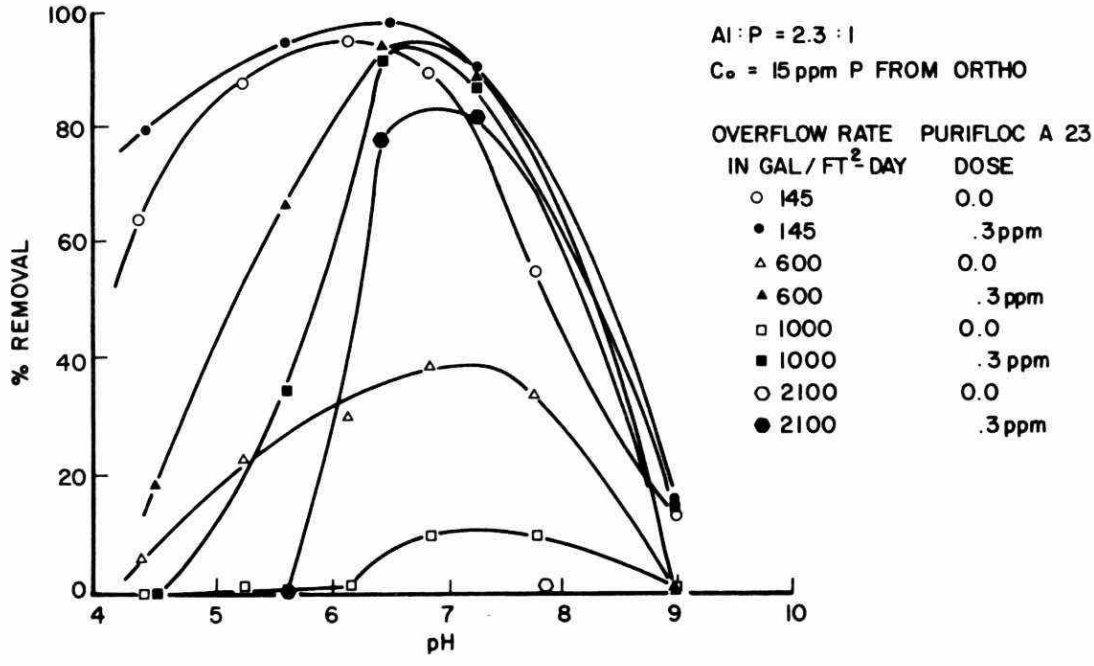

FIGURE 127. PHOSPHORUS REMOVAL IN THE ALUMINUM-ORTHOPHOSPHATE SYSTEM WITH POLYELECTROLYTE ADDITION

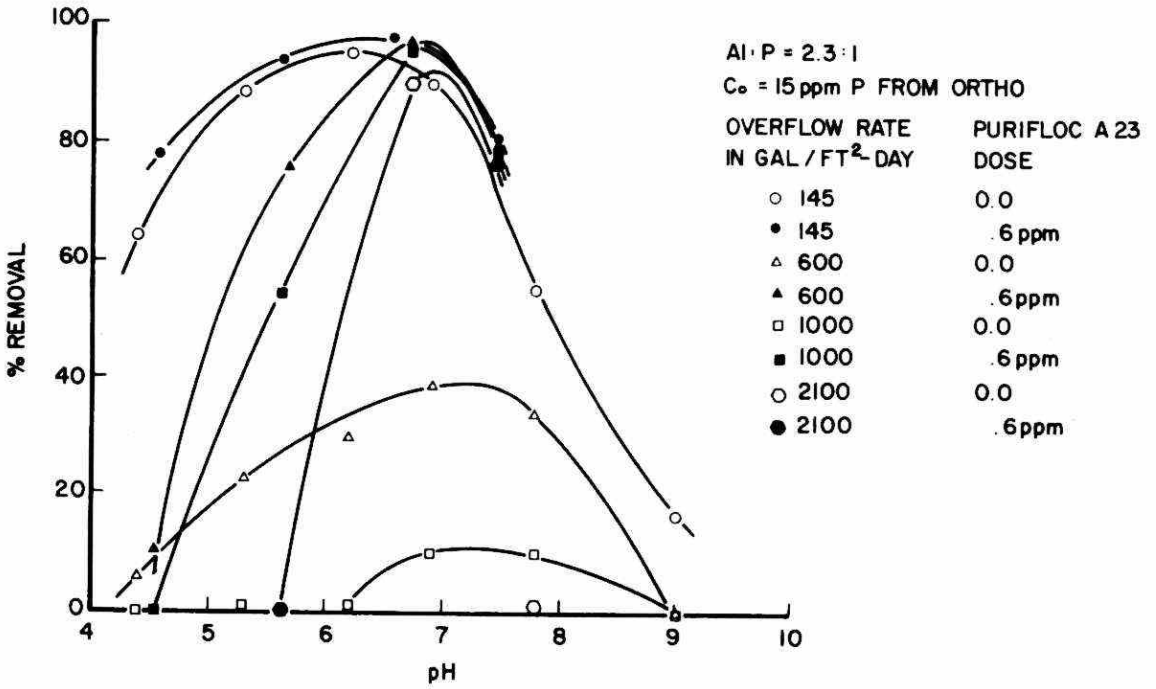

FIGURE 128. PHOSPHORUS REMOVAL IN THE ALUMINUM-ORTHOPHOSPHATE SYSTEM WITH POLYELECTROLYTE ADDITION

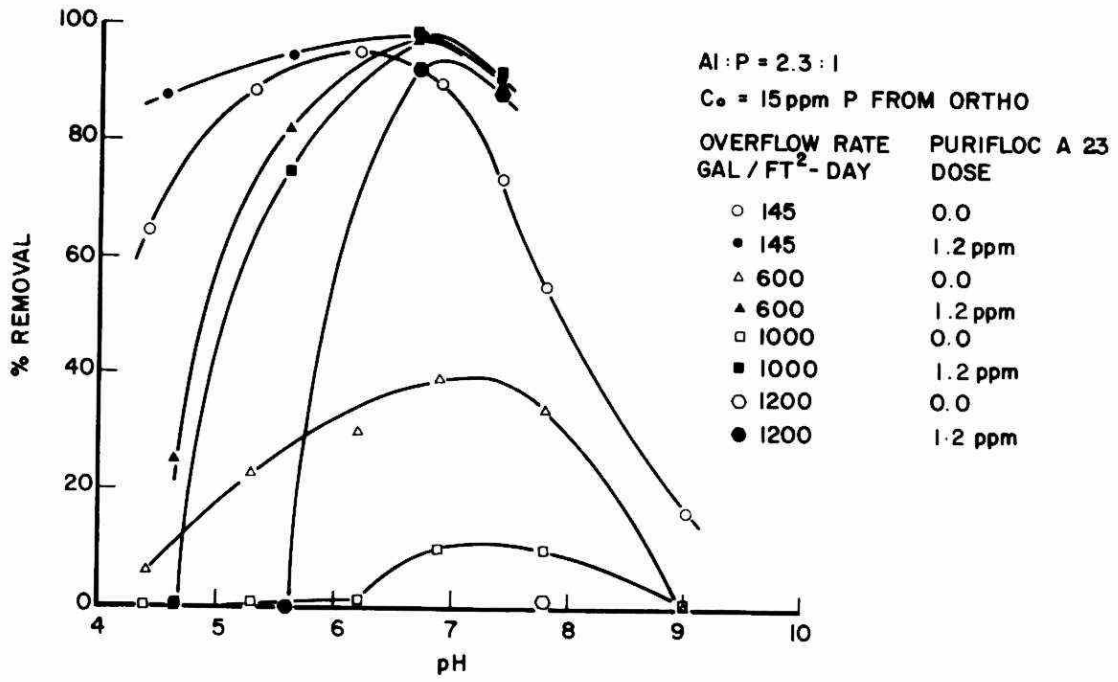

FIGURE 129. PHOSPHORUS REMOVAL IN THE ALUMINUM-ORTHOPHOSPHATE SYSTEM WITH POLYELECTROLYTE ADDITION

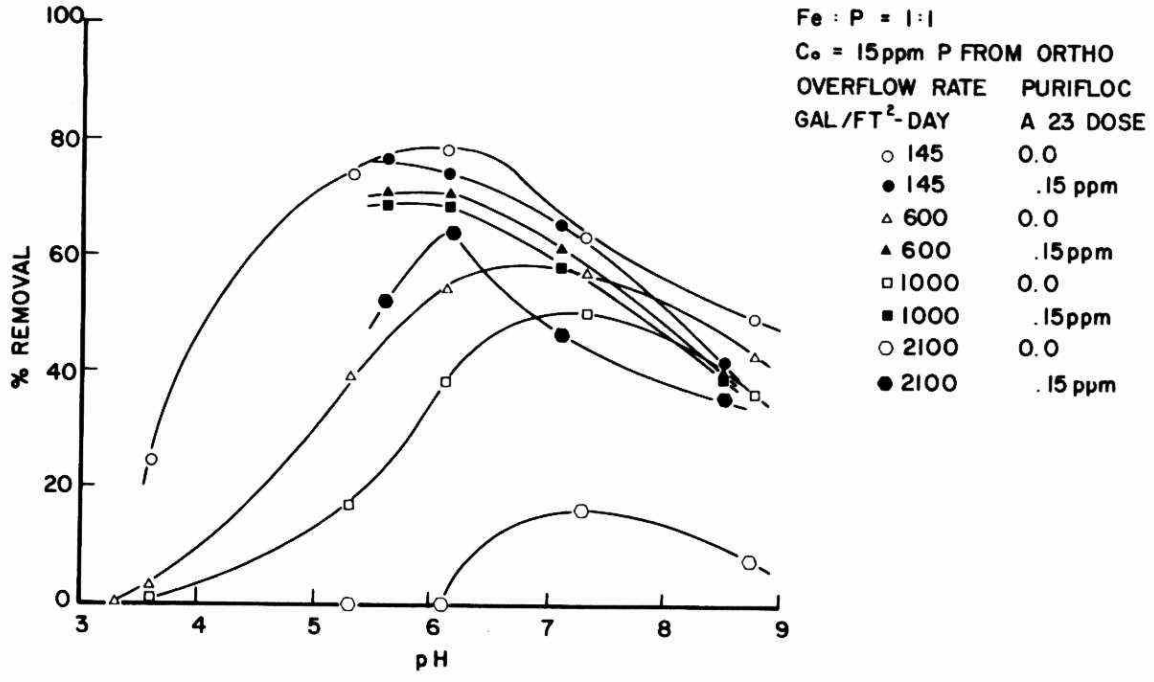

FIGURE 130. PHOSPHORUS REMOVAL IN THE IRON-ORTHOPHOSPHATE SYSTEM WITH POLYELECTROLYTE ADDITION

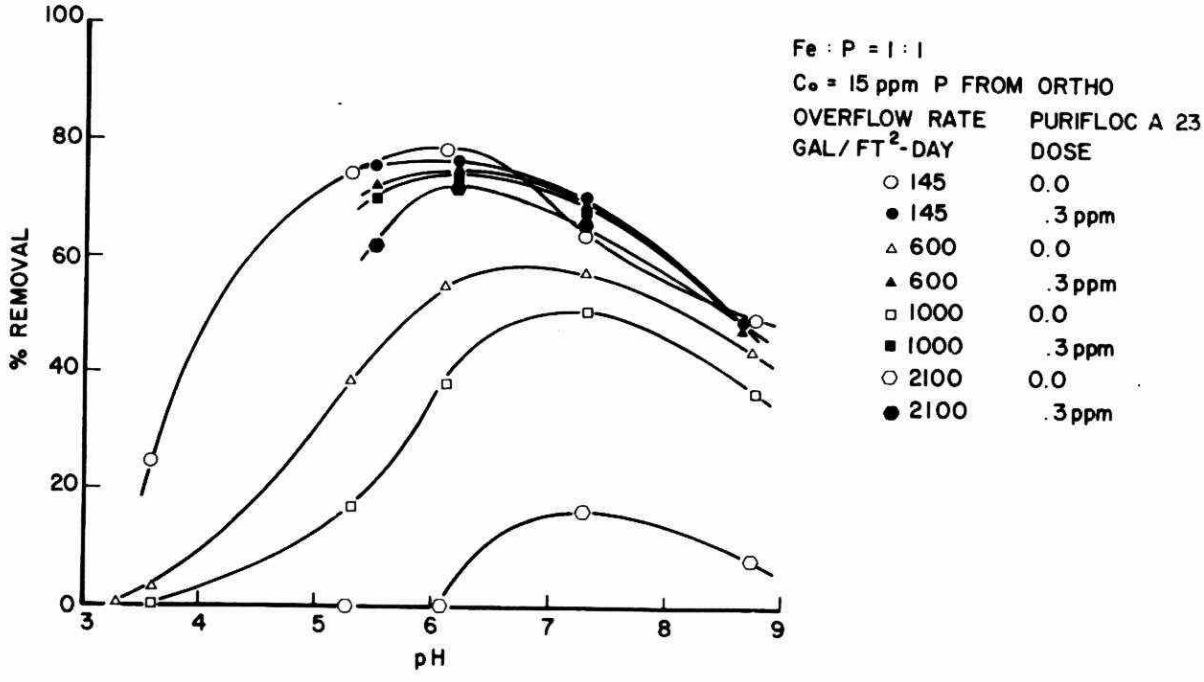

FIGURE 131. PHOSPHORUS REMOVAL IN THE IRON-ORTHOPHOSPHATE SYSTEM WITH POLYELECTROLYTE ADDITION

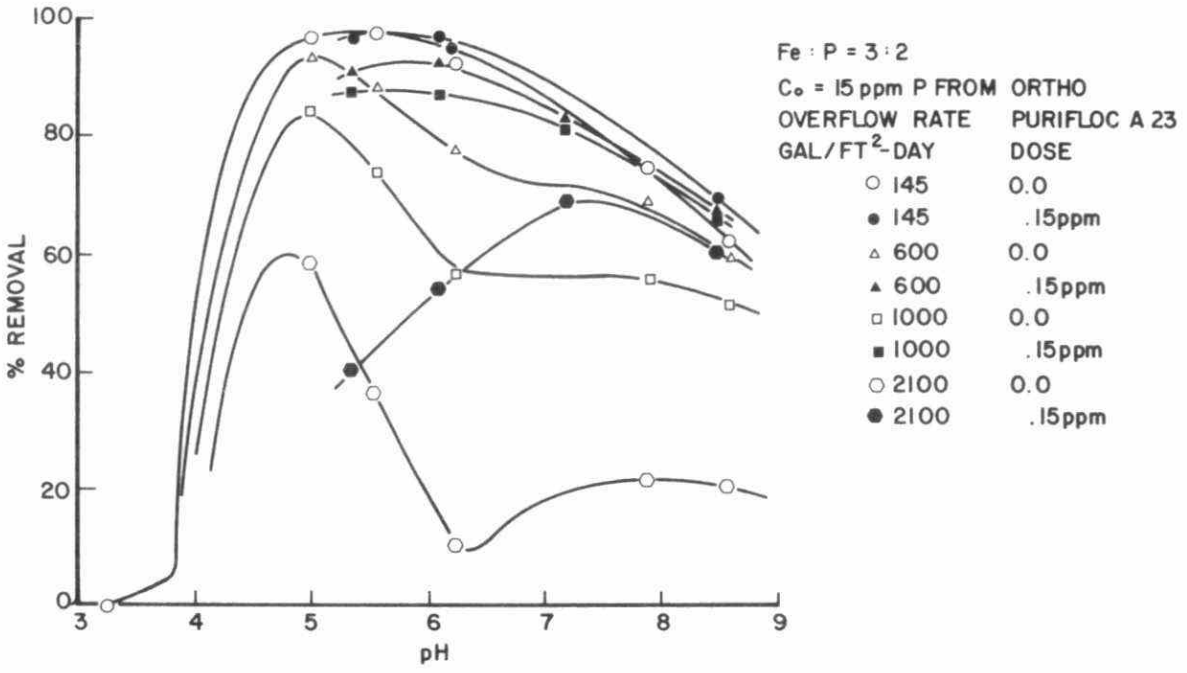

FIGURE 132. PHOSPHORUS REMOVAL IN THE IRON-ORTHOPHOSPHATE SYSTEM WITH POLYELECTROLYTE ADDITION

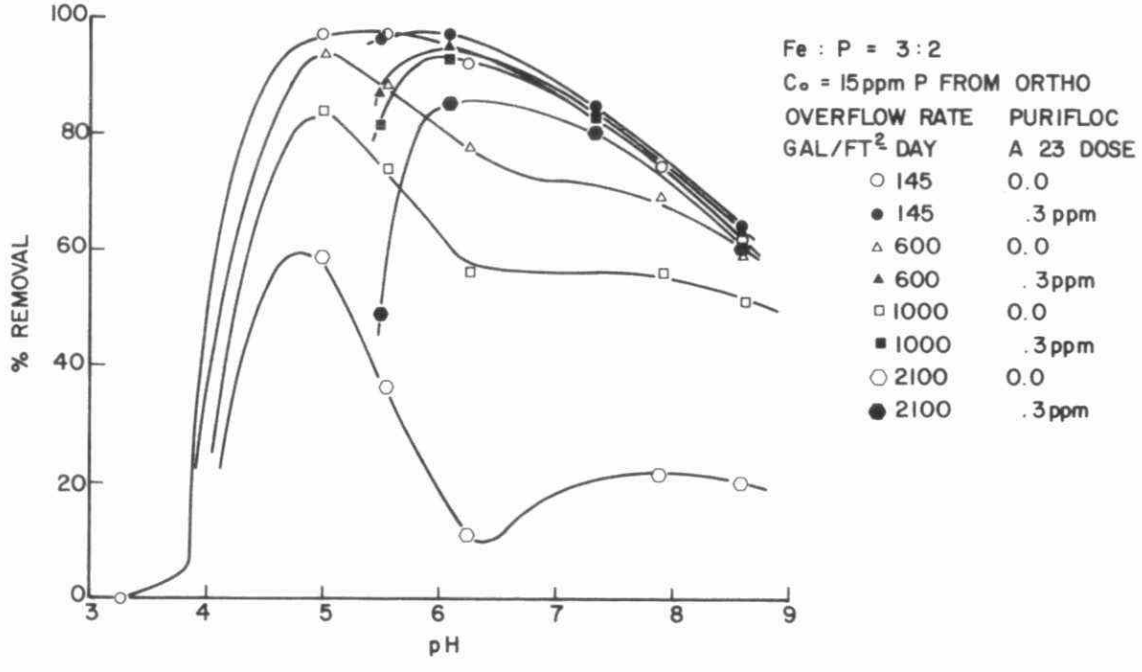

FIGURE 133. PHOSPHORUS REMOVAL IN THE IRON-ORTHOPHOSPHATE SYSTEM WITH POLYELECTROLYTE ADDITION

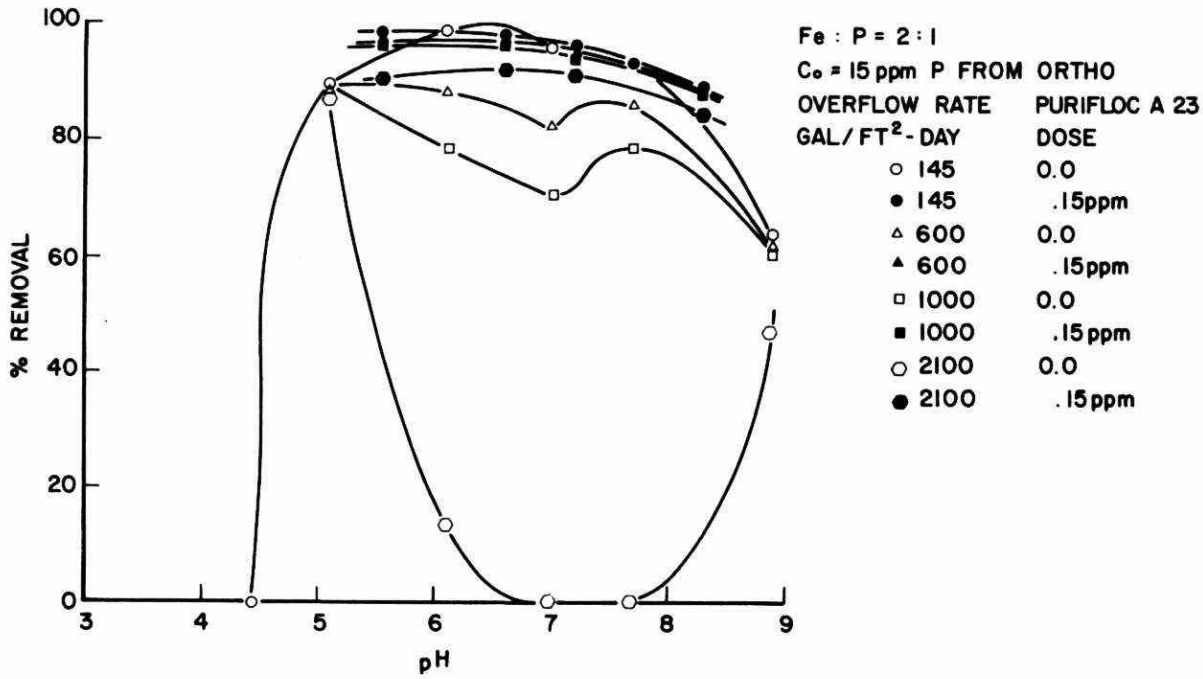

FIGURE 134. PHOSPHORUS REMOVAL IN THE IRON-ORTHOPHOSPHATE SYSTEM WITH POLYELECTROLYTE ADDITION

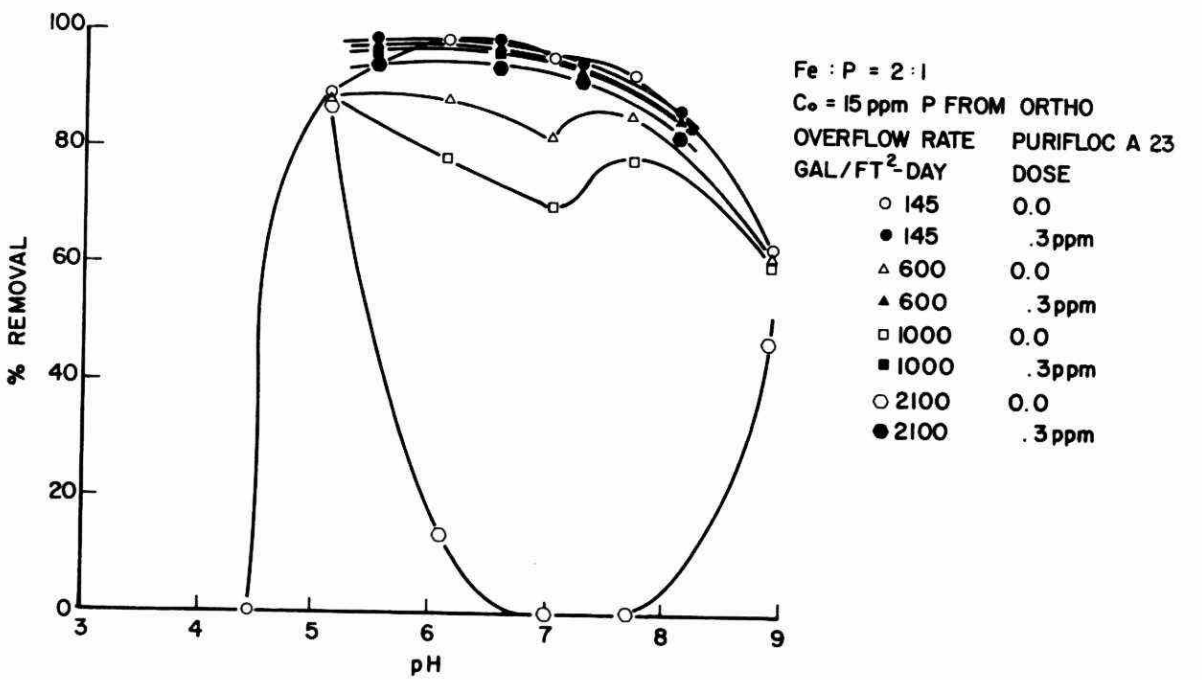

FIGURE 135. PHOSPHORUS REMOVAL IN THE IRON-ORTHOPHOSPHATE SYSTEM WITH POLYELECTROLYTE ADDITION

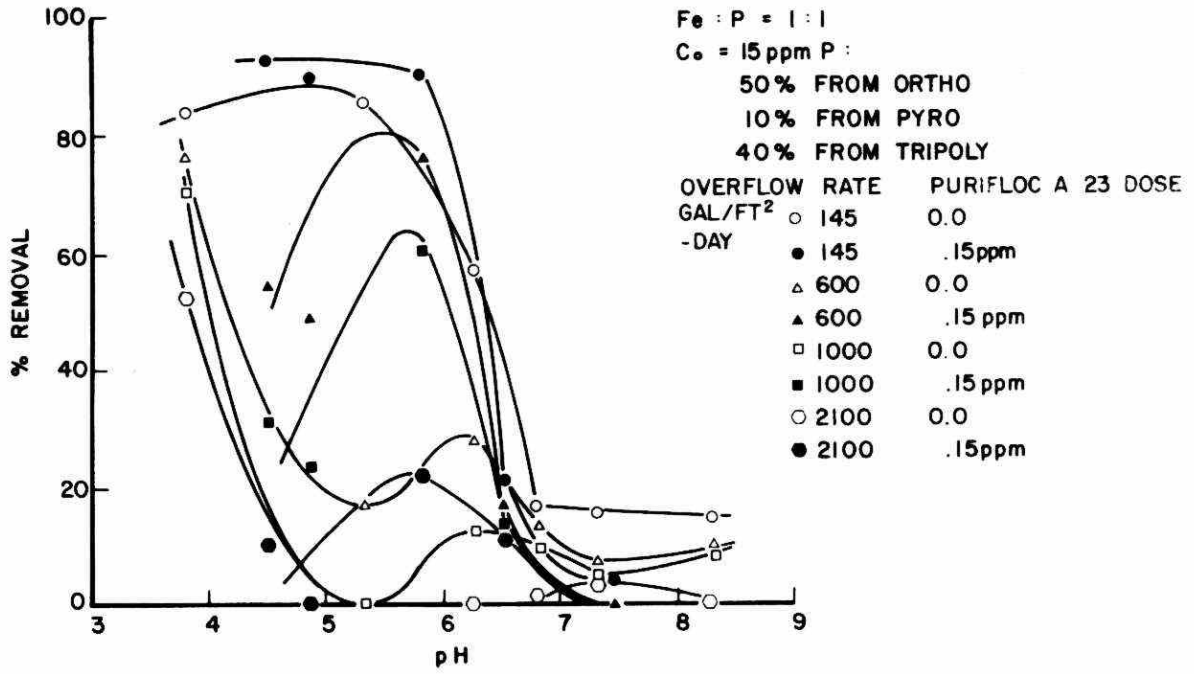

FIGURE 136. PHOSPHORUS REMOVAL IN THE IRON-MIXED PHOSPHATE SYSTEM

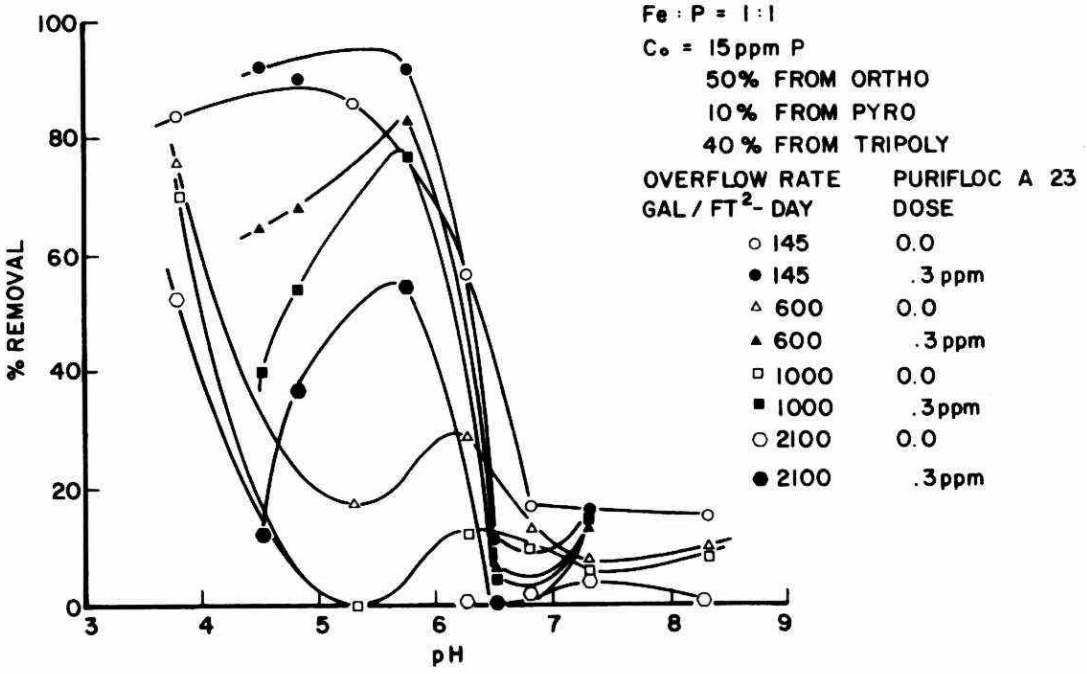

FIGURE 137. PHOSPHORUS REMOVAL IN THE IRON-MIXED PHOSPHATE SYSTEM

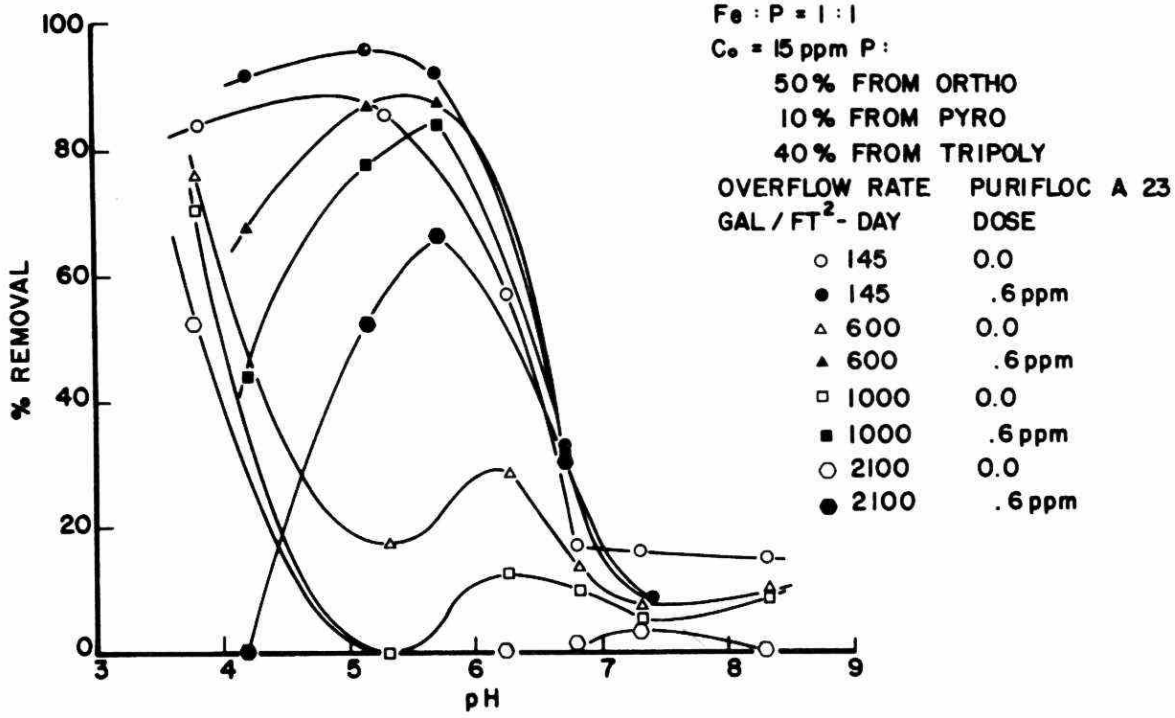

FIGURE 138. PHOSPHORUS REMOVAL IN THE IRON-MIXED PHOSPHATE SYSTEM

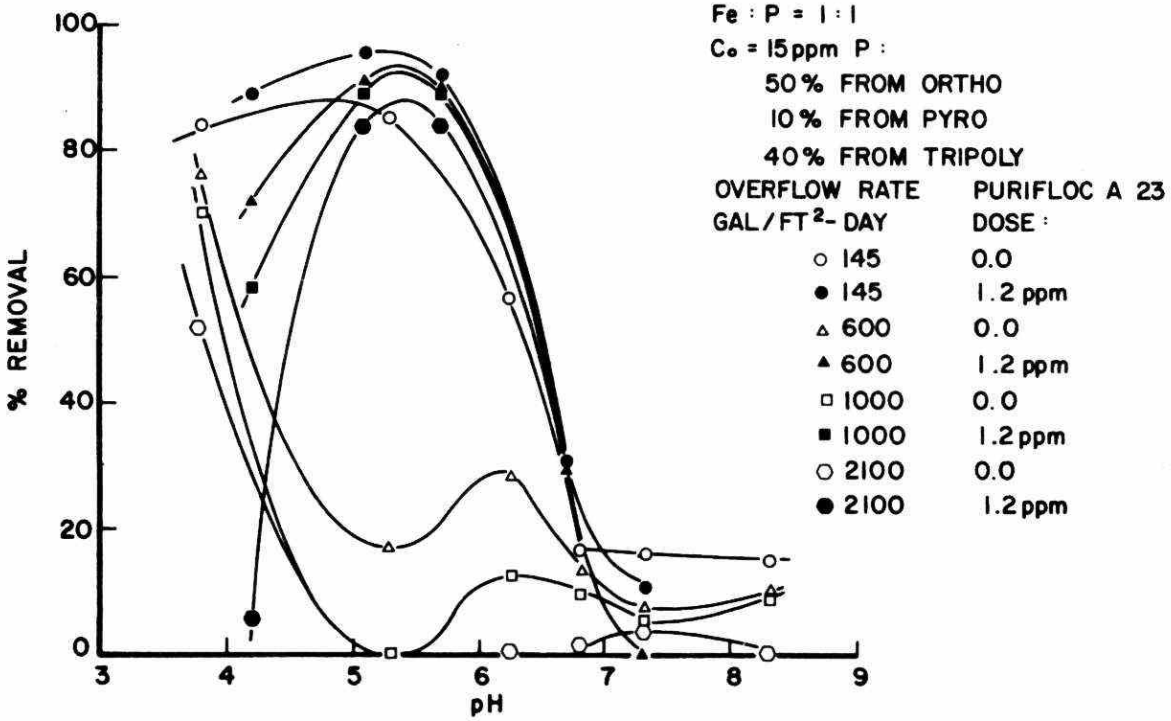

FIGURE 139. PHOSPHORUS REMOVAL IN THE IRON-MIXED PHOSPHATE SYSTEM

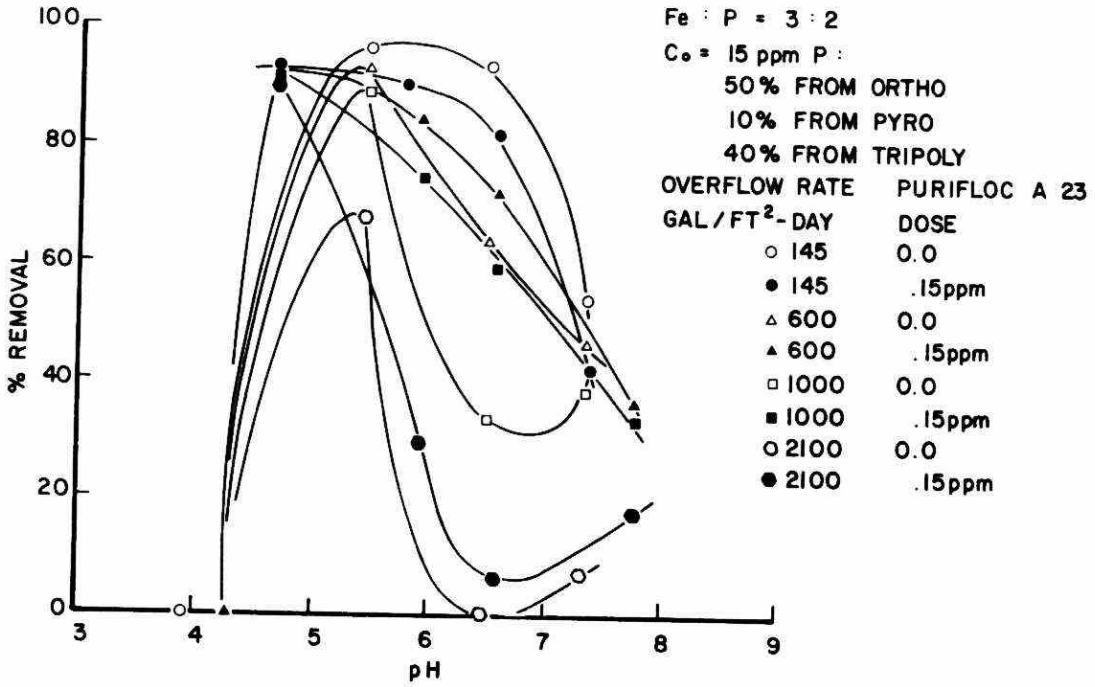

FIGURE 140. PHOSPHORUS REMOVAL IN THE IRON-MIXED PHOSPHATE SYSTEM

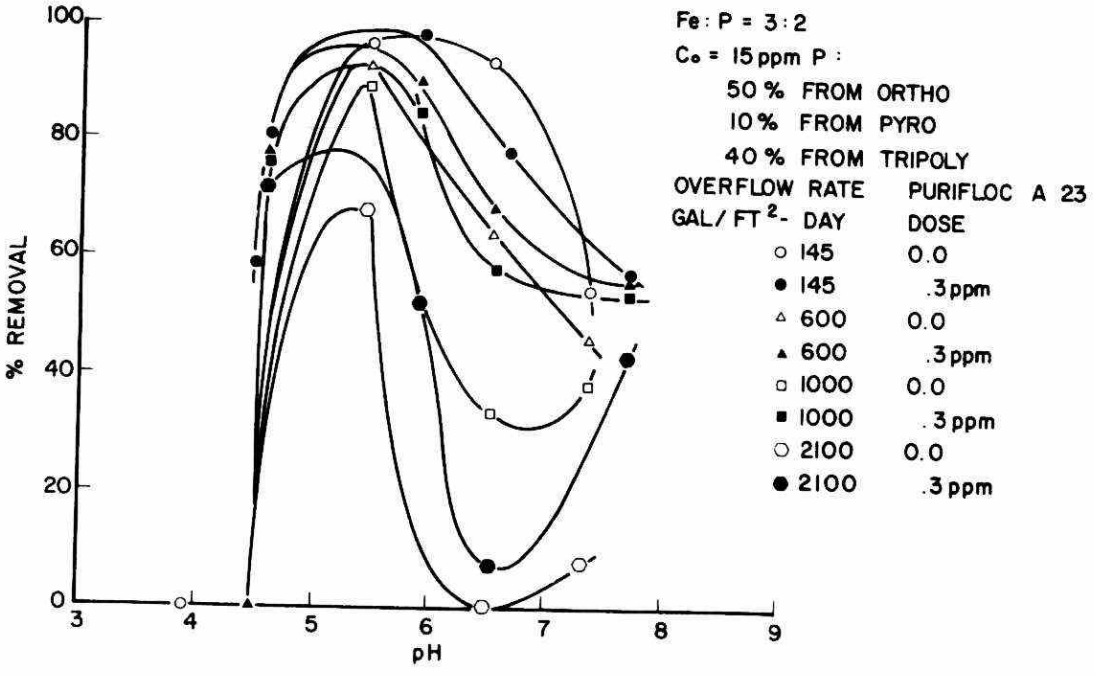

FIGURE 141. PHOSPHORUS REMOVAL IN THE IRON-MIXED PHOSPHATE SYSTEM

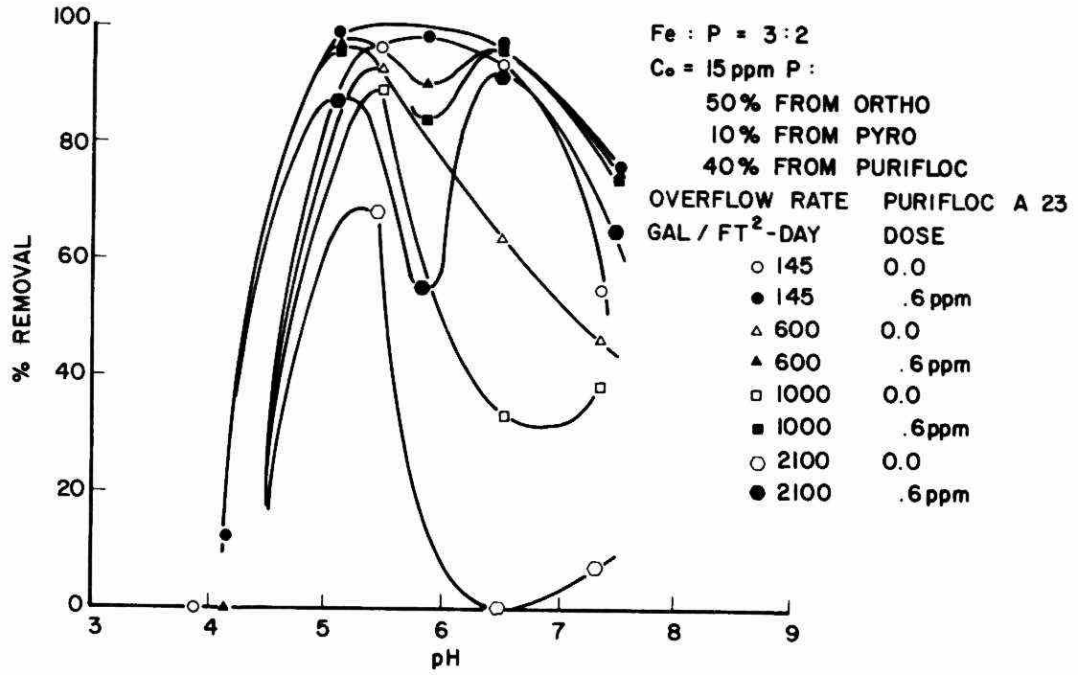

FIGURE 142. PHOSPHORUS REMOVAL IN THE IRON-MIXED PHOSPHATE SYSTEM

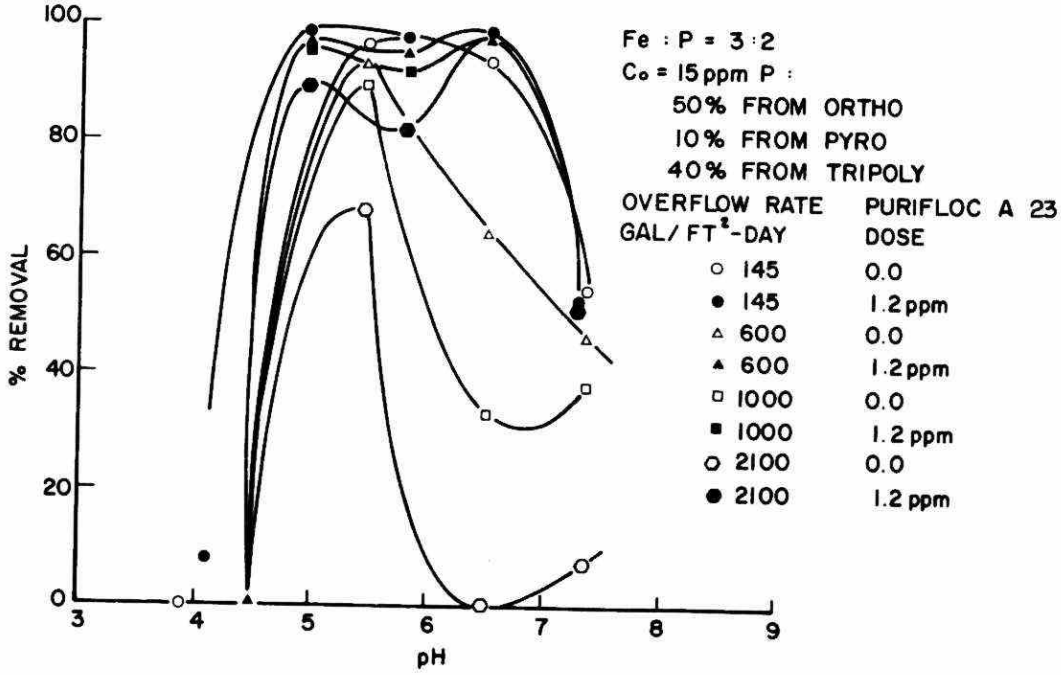

FIGURE 143. PHOSPHORUS REMOVAL IN THE IRON-MIXED PHOSPHATE SYSTEM

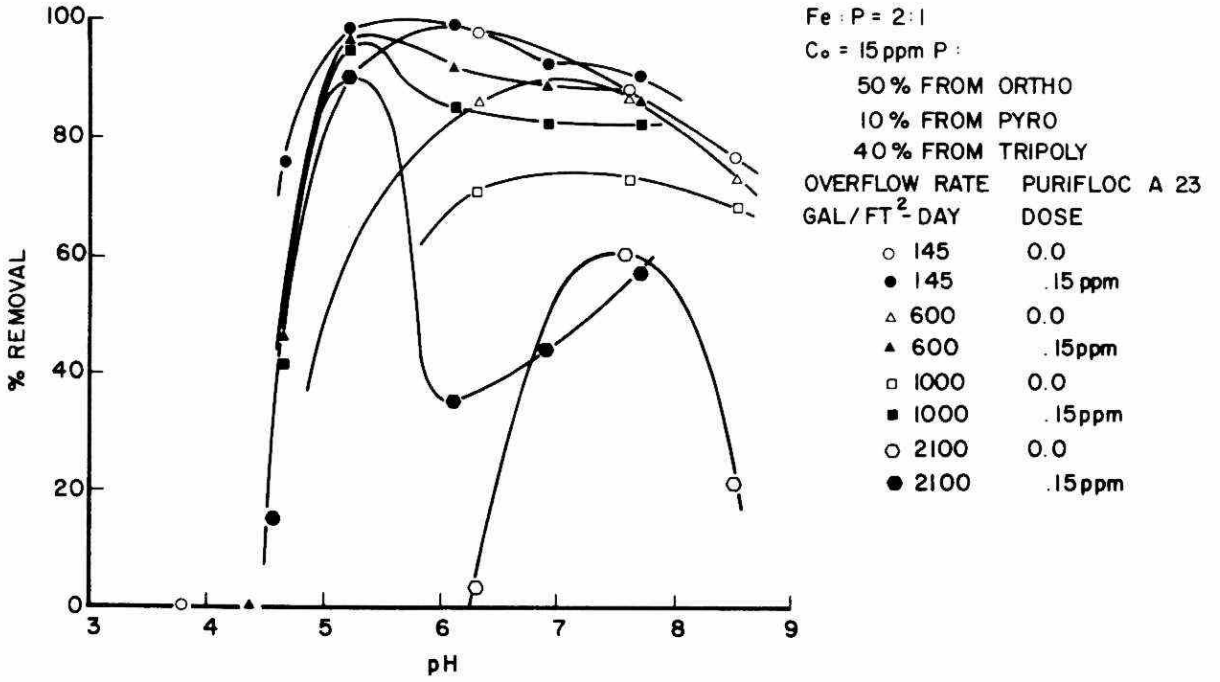

FIGURE 144. PHOSPHORUS REMOVAL IN THE IRON-MIXED PHOSPHATE SYSTEM

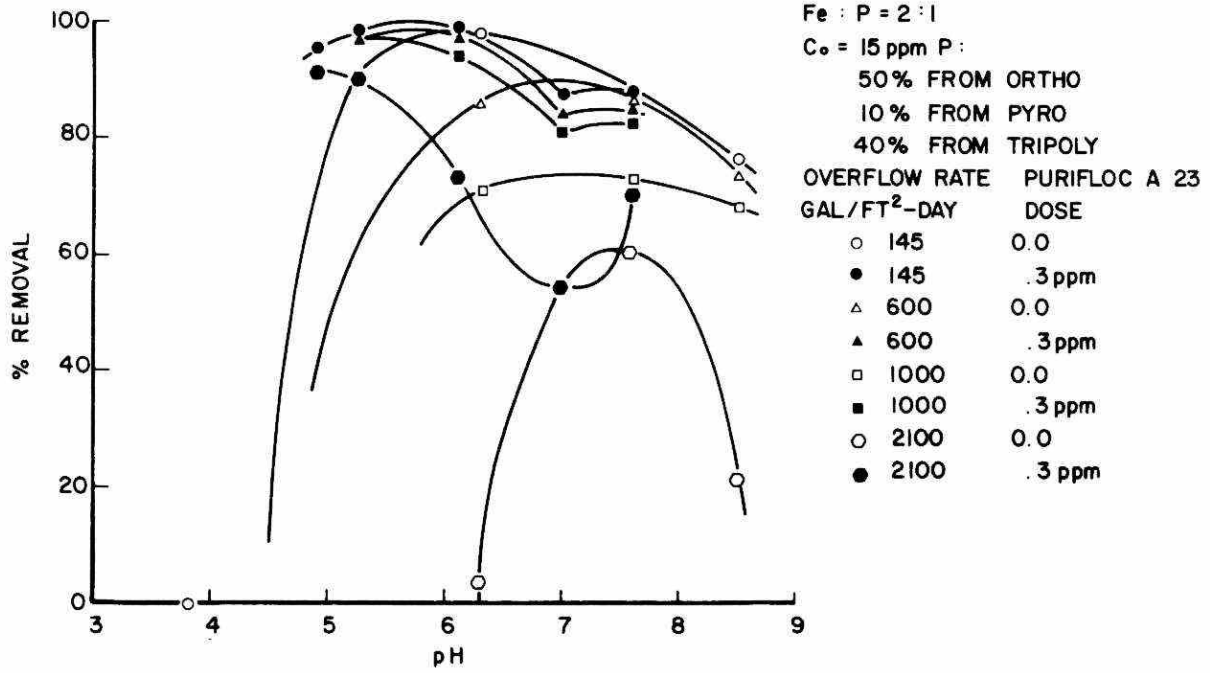

FIGURE 145. PHOSPHORUS REMOVAL IN THE IRON-MIXED PHOSPHATE SYSTEM

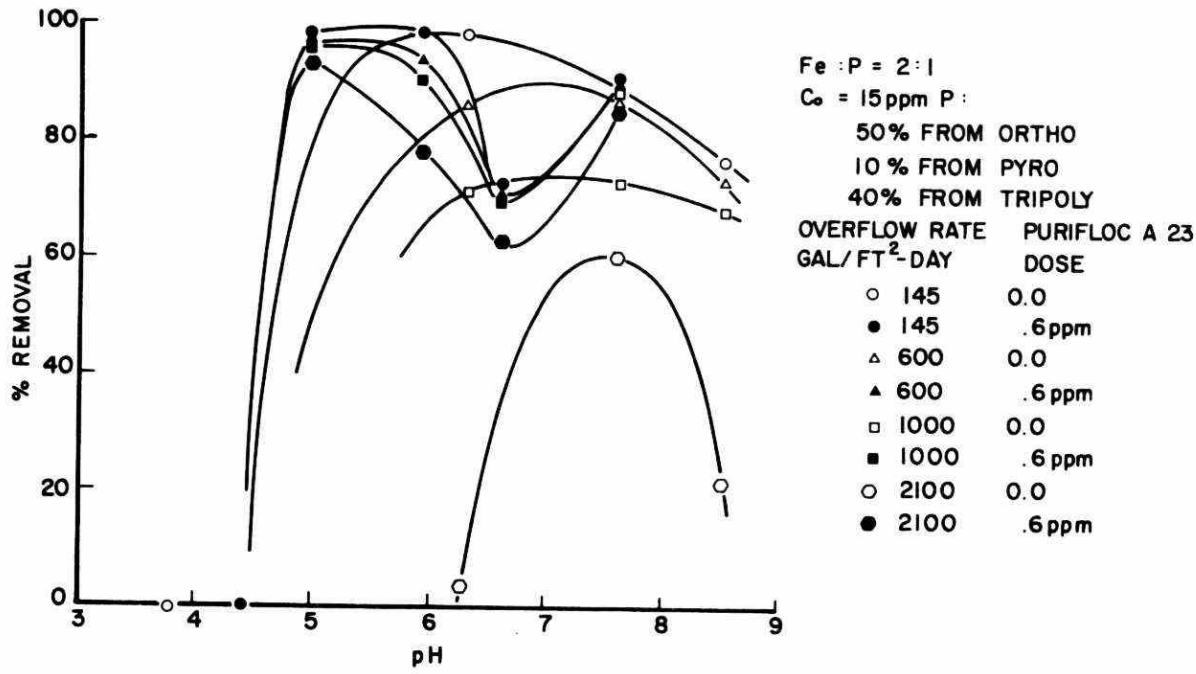

FIGURE 146. PHOSPHORUS REMOVAL IN THE IRON-MIXED PHOSPHATE SYSTEM

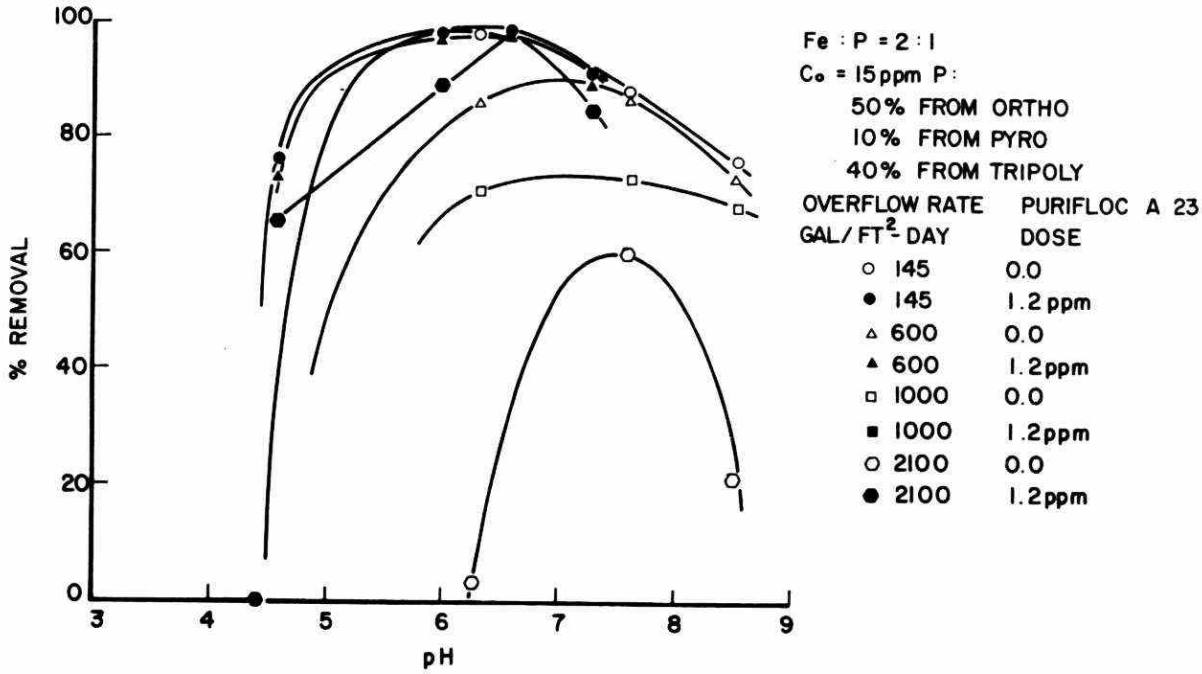

FIGURE 147. PHOSPHORUS REMOVAL IN THE IRON-MIXED PHOSPHATE SYSTEM

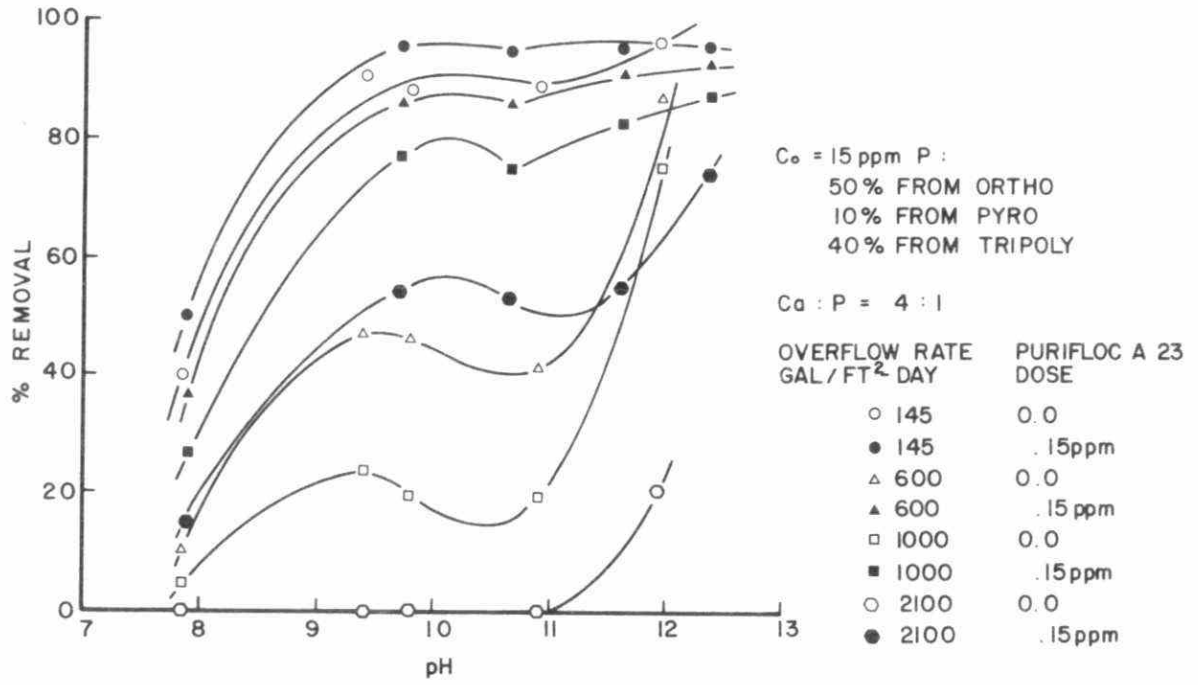

FIGURE 148. PHOSPHORUS REMOVAL IN THE CALCIUM-MIXED PHOSPHATE SYSTEM WITH POLYELECTROLYTE ADDITION

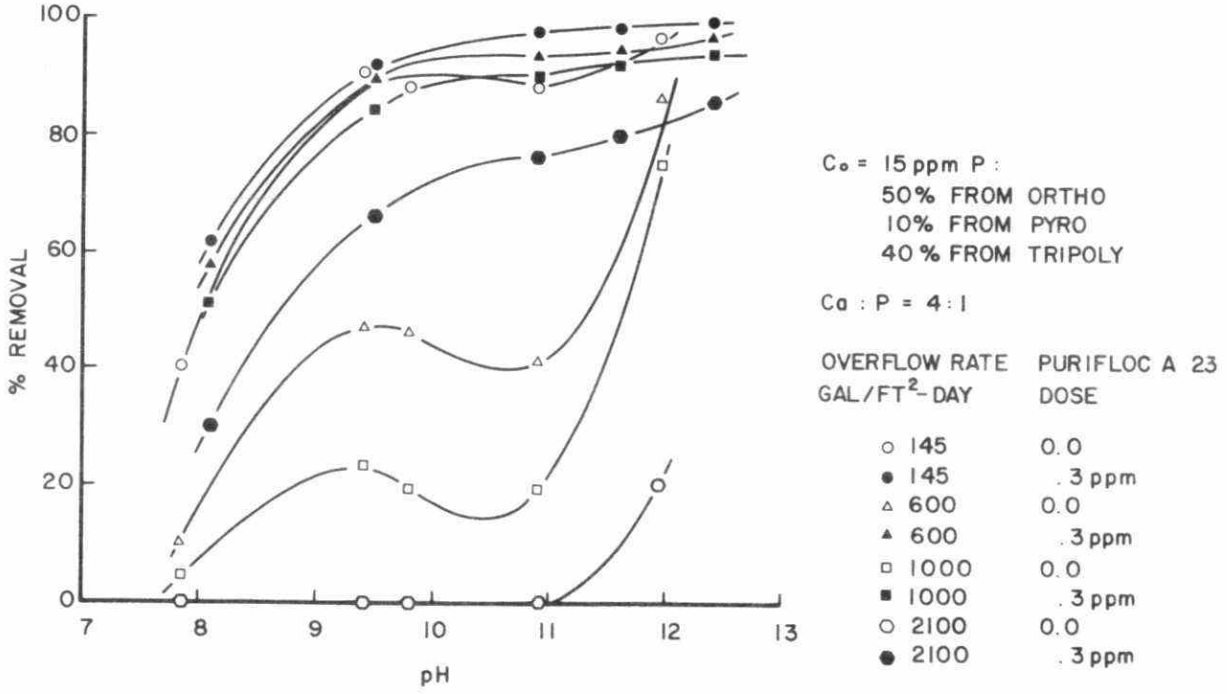

FIGURE 149. PHOSPHORUS REMOVAL IN THE CALCIUM-MIXED PHOSPHATE SYSTEM WITH POLYELECTROLYTE ADDITION

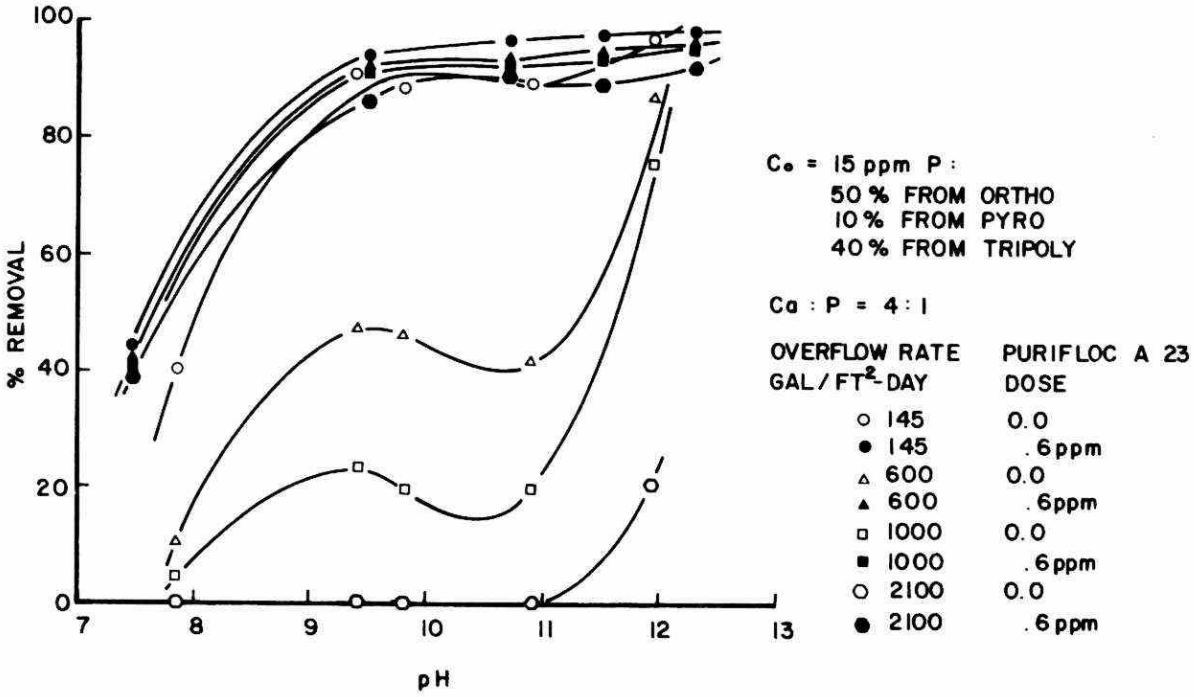

FIGURE 150. PHOSPHORUS REMOVAL IN THE CALCIUM-MIXED PHOSPHATE SYSTEM WITH POLYELECTROLYTE ADDITION

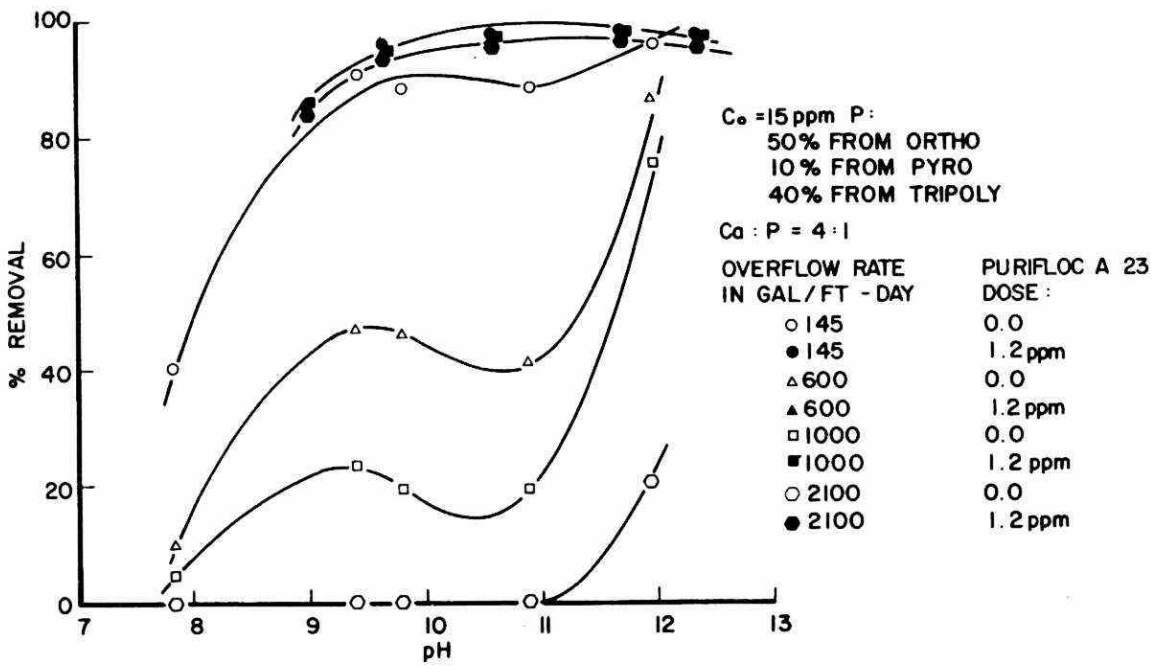

FIGURE 151. PHOSPHORUS REMOVAL IN THE CALCIUM-MIXED PHOSPHATE SYSTEM WITH POLYELECTROLYTE ADDITION

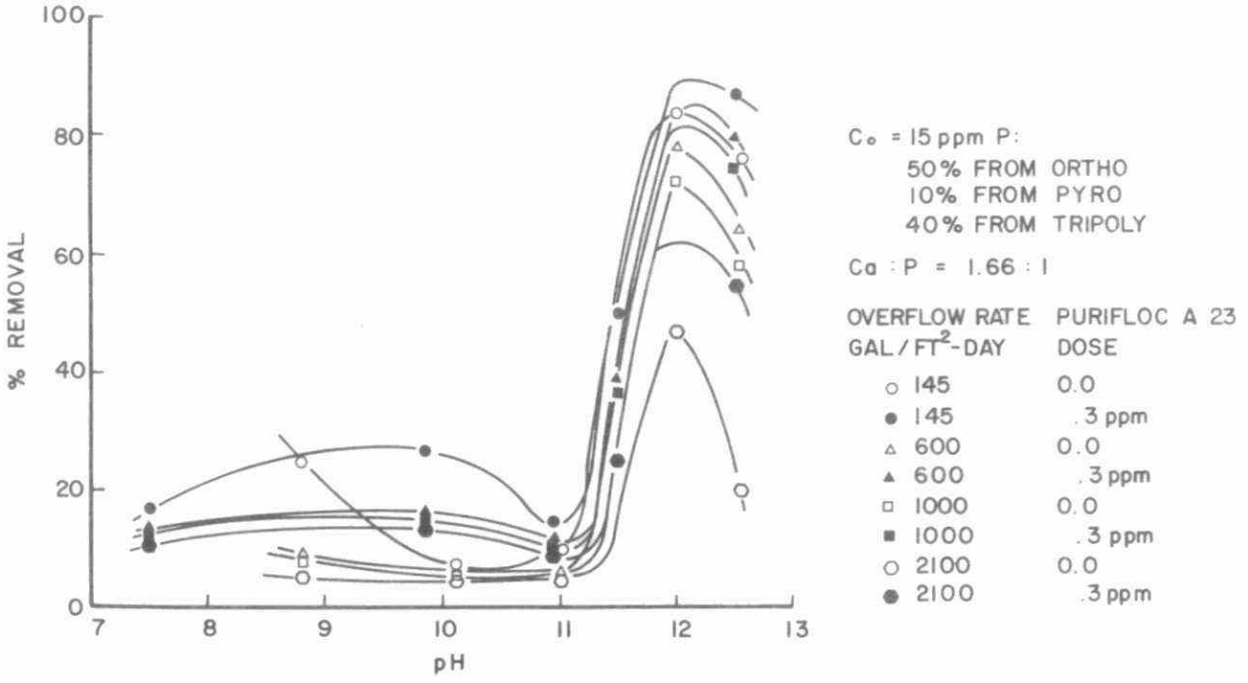

FIGURE 152. PHOSPHORUS REMOVAL IN THE CALCIUM-MIXED PHOSPHATE SYSTEM WITH POLYELECTROLYTE ADDITION

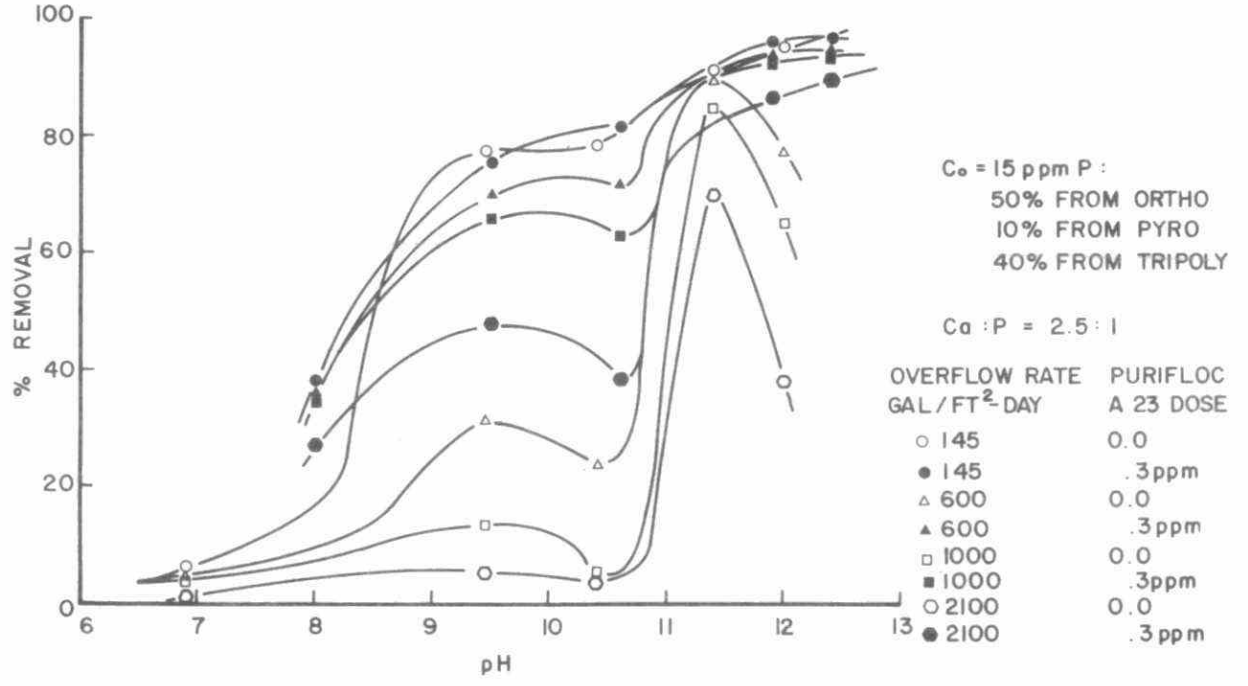

FIGURE 153. PHOSPHORUS REMOVAL IN THE CALCIUM-MIXED PHOSPHATE SYSTEM WITH POLYELECTROLYTE ADDITION

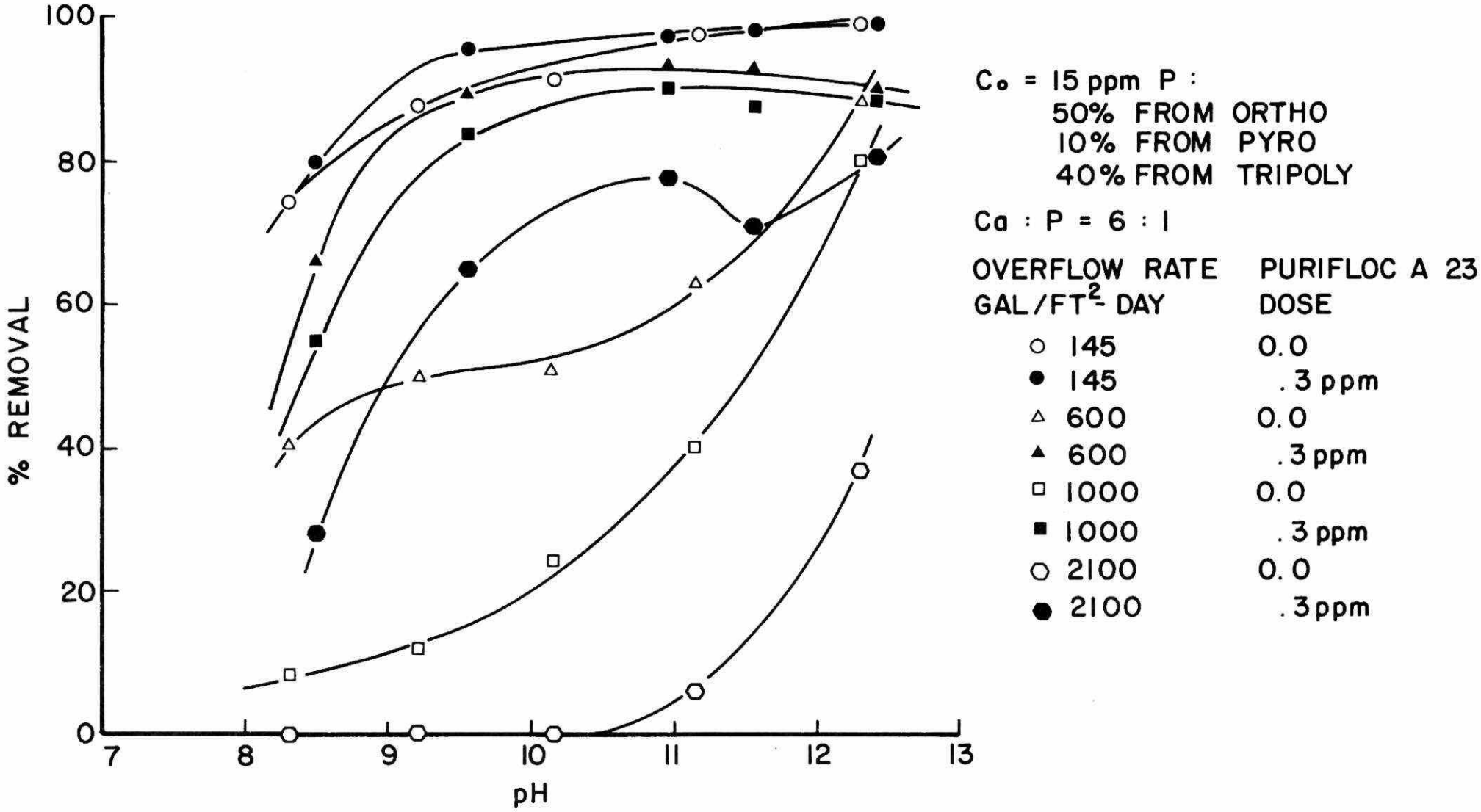

FIGURE 154. PHOSPHORUS REMOVAL IN THE CALCIUM-MIXED PHOSPHATE SYSTEM WITH POLYELECTROLYTE ADDITION

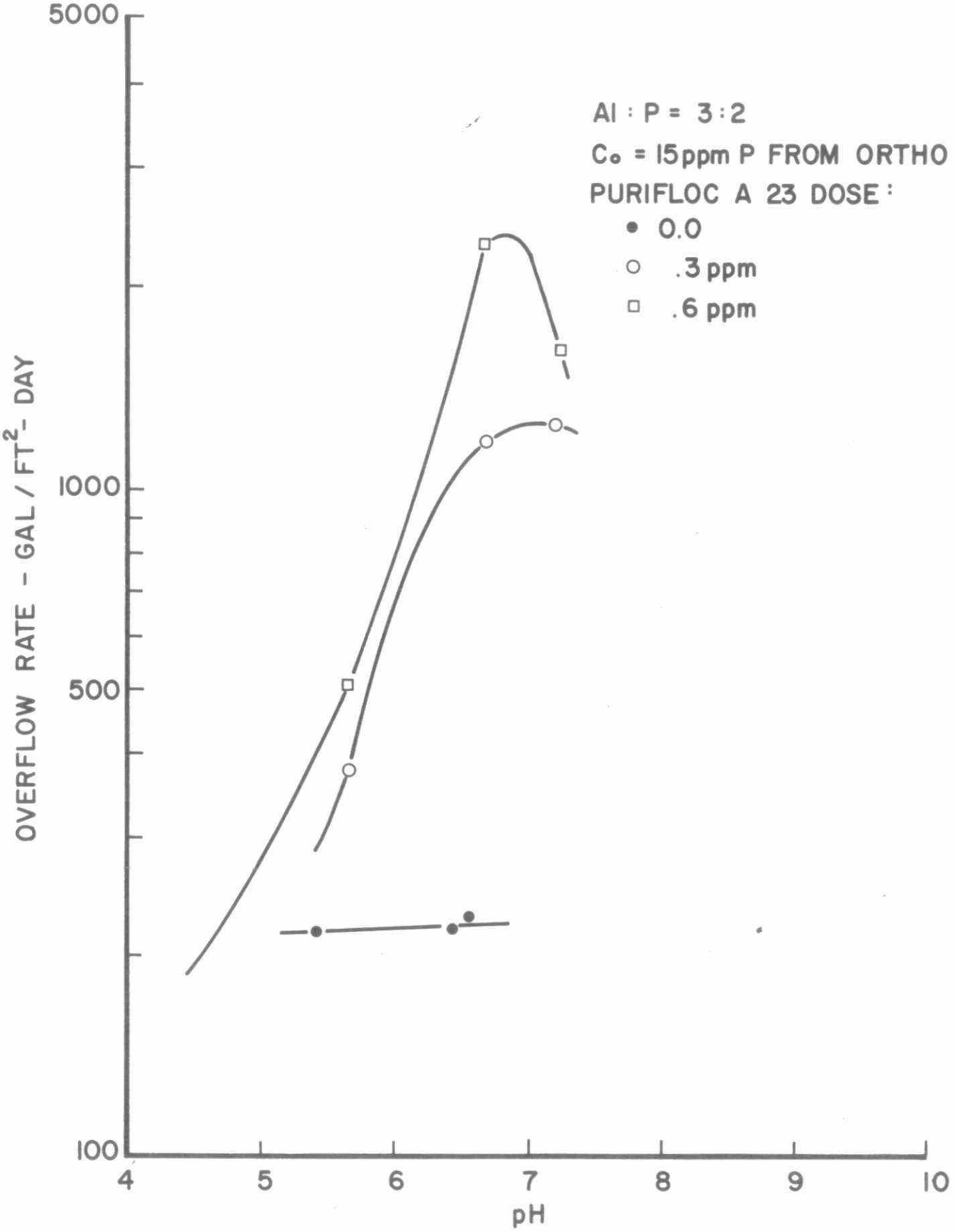

FIGURE 155. MAXIMUM PERMISSIBLE OVERFLOW RATES FOR 90% FLOC REMOVAL IN THE ALUMINUM-ORTHOPHOSPHATE SYSTEM

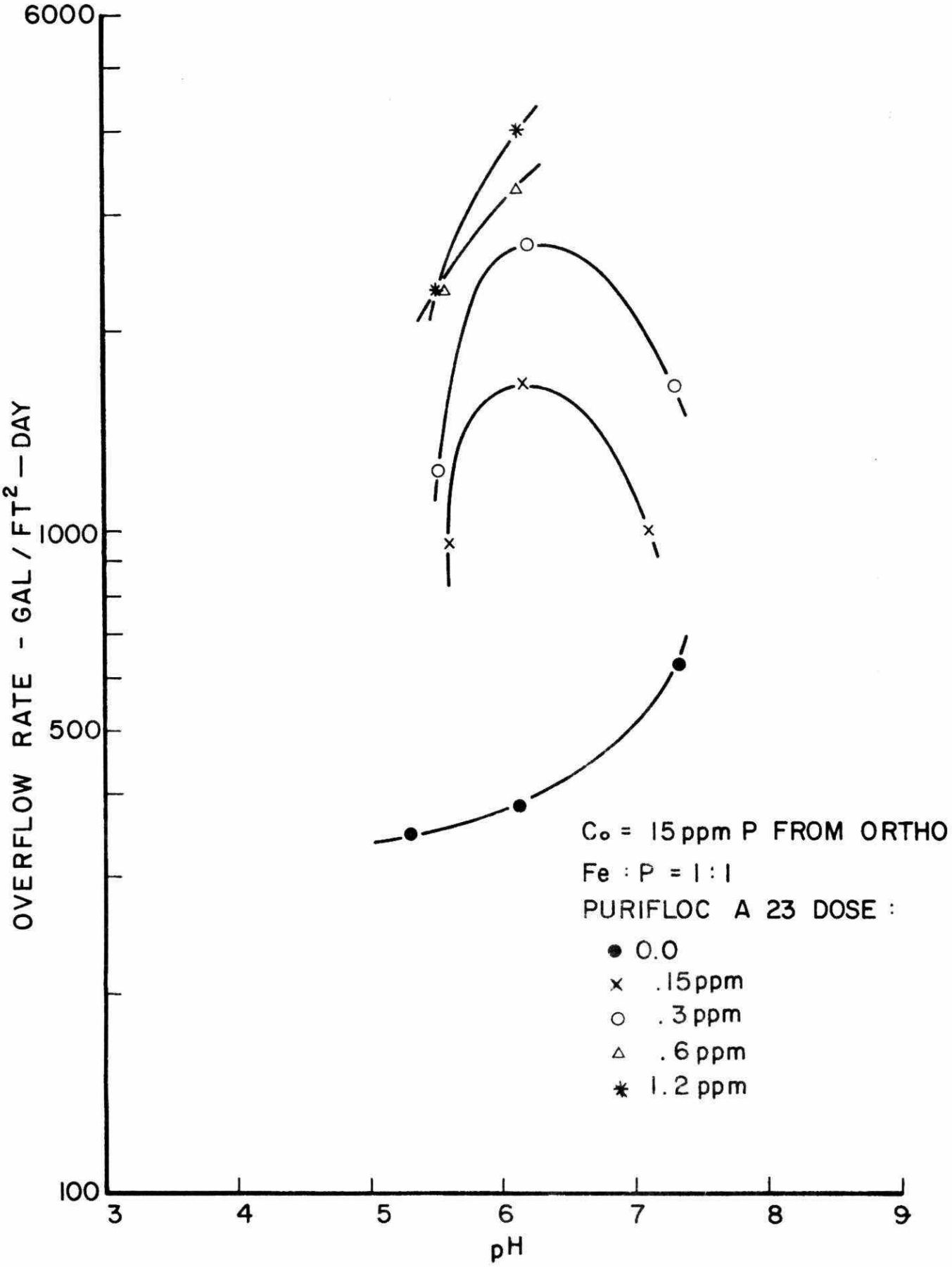

FIGURE 156. MAXIMUM PERMISSIBLE OVERFLOW RATES FOR 90% FLOC REMOVAL IN THE IRON-ORTHOPHOSPHATE SYSTEM

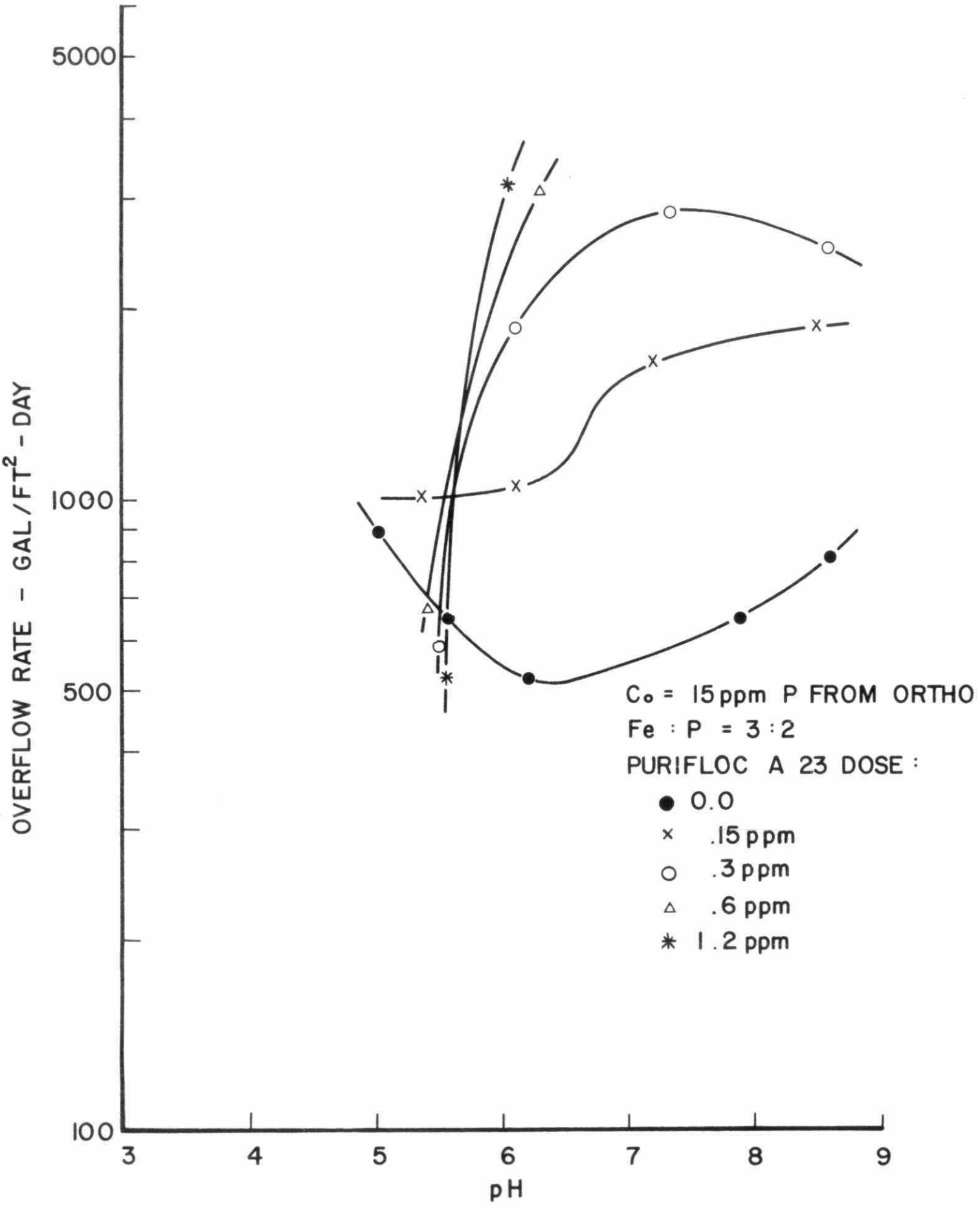

FIGURE 157. MAXIMUM PERMISSIBLE OVERFLOW RATES FOR 90% FLOC REMOVAL IN THE IRON-ORTHOPHOSPHATE SYSTEM

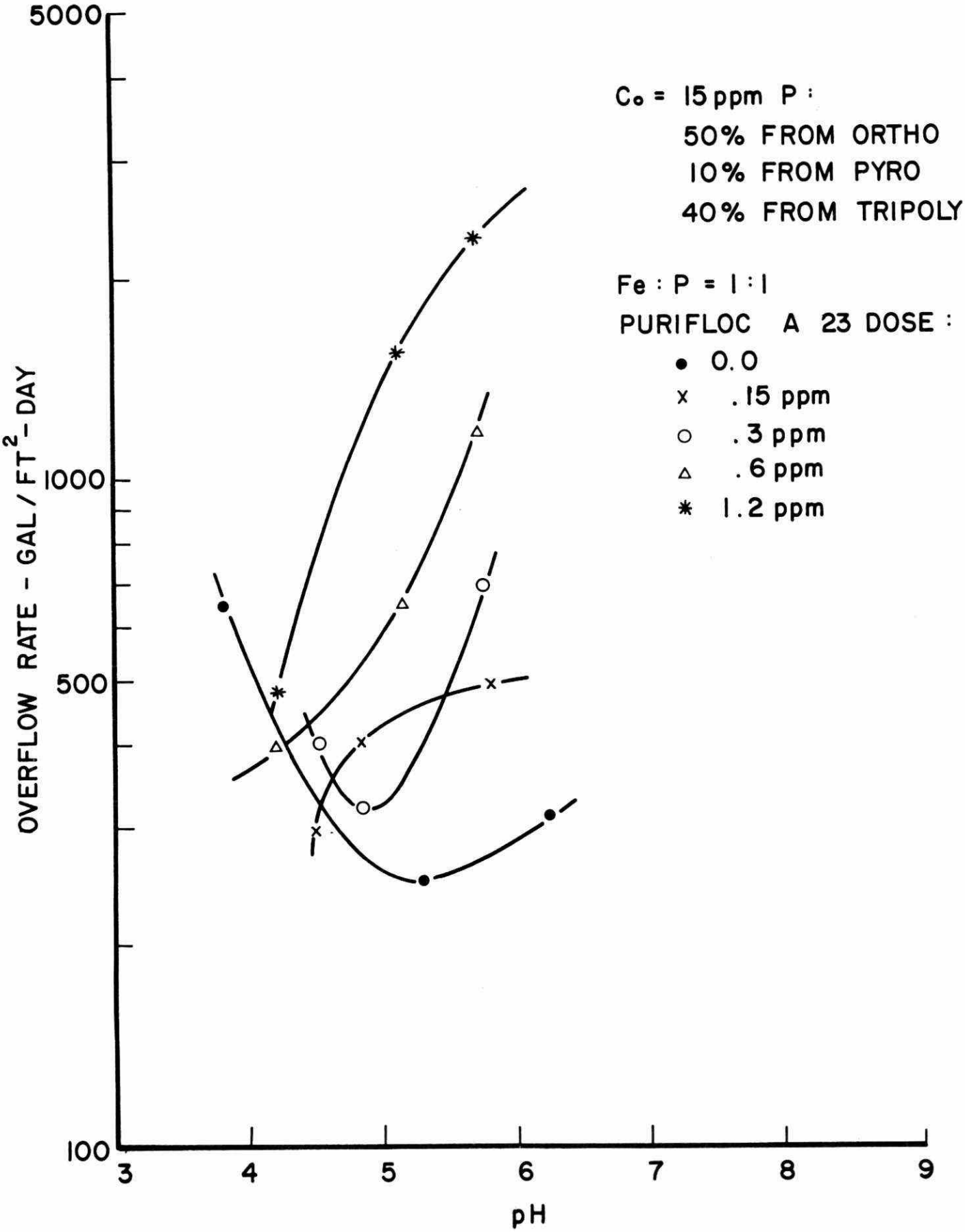

FIGURE 158. MAXIMUM PERMISSIBLE OVERFLOW RATES FOR 90% FLOC REMOVAL IN THE IRON-ORTHOPHOSPHATE SYSTEM

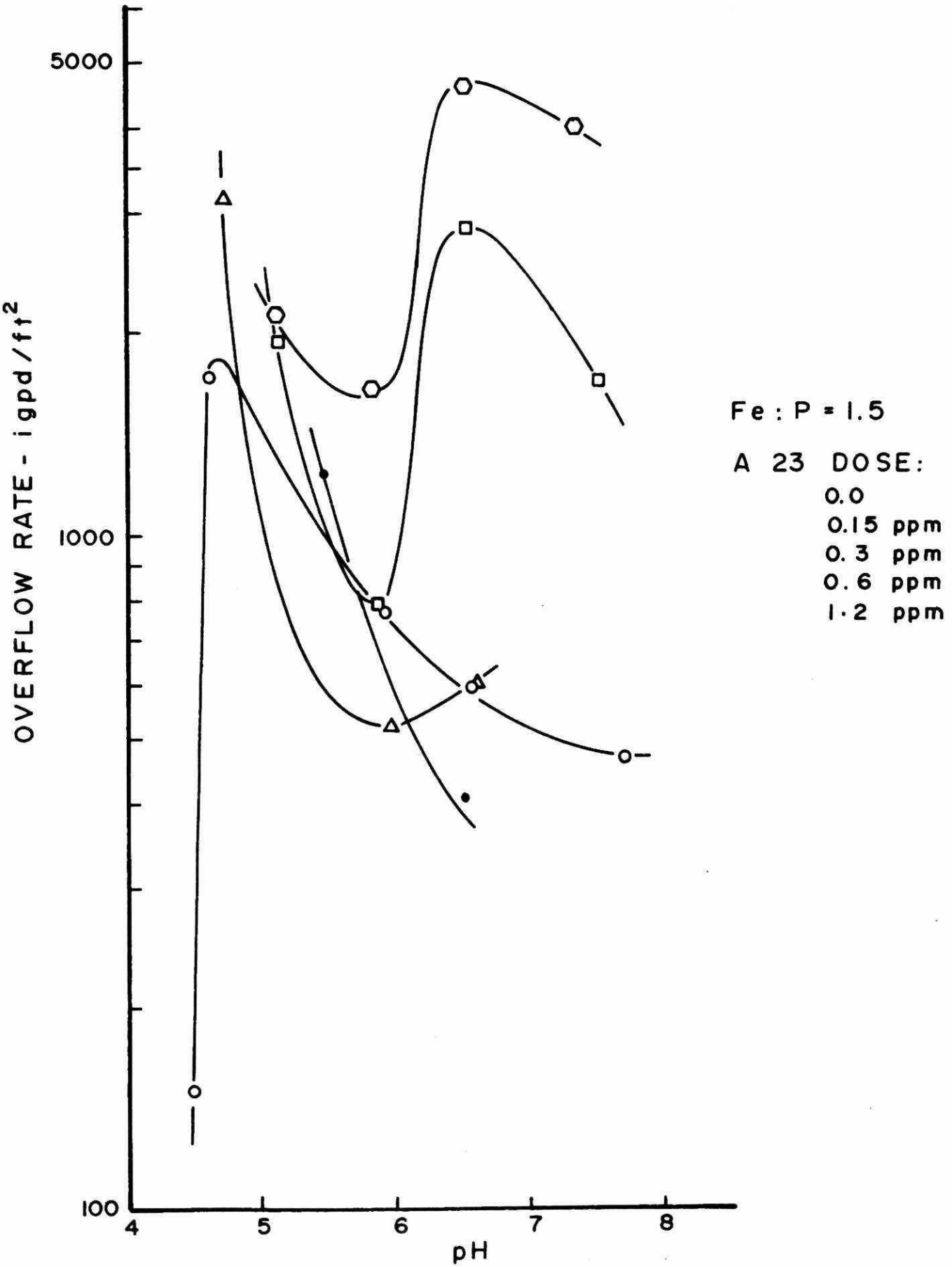

FIGURE 159. MAXIMUM PERMISSIBLE OVERFLOW RATES FOR 90% FLOC REMOVAL IN THE IRON-MIXED PHOSPHATE SYSTEM

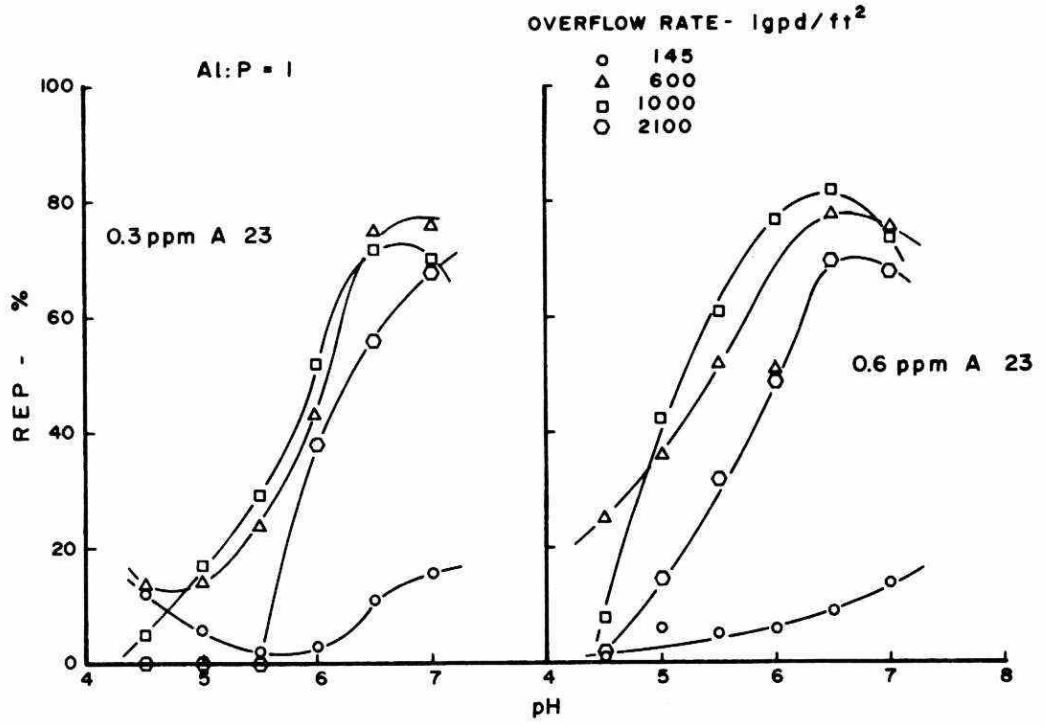

FIGURE 160. REP IN THE ALUMINUM-ORTHOPHOSPHATE SYSTEM

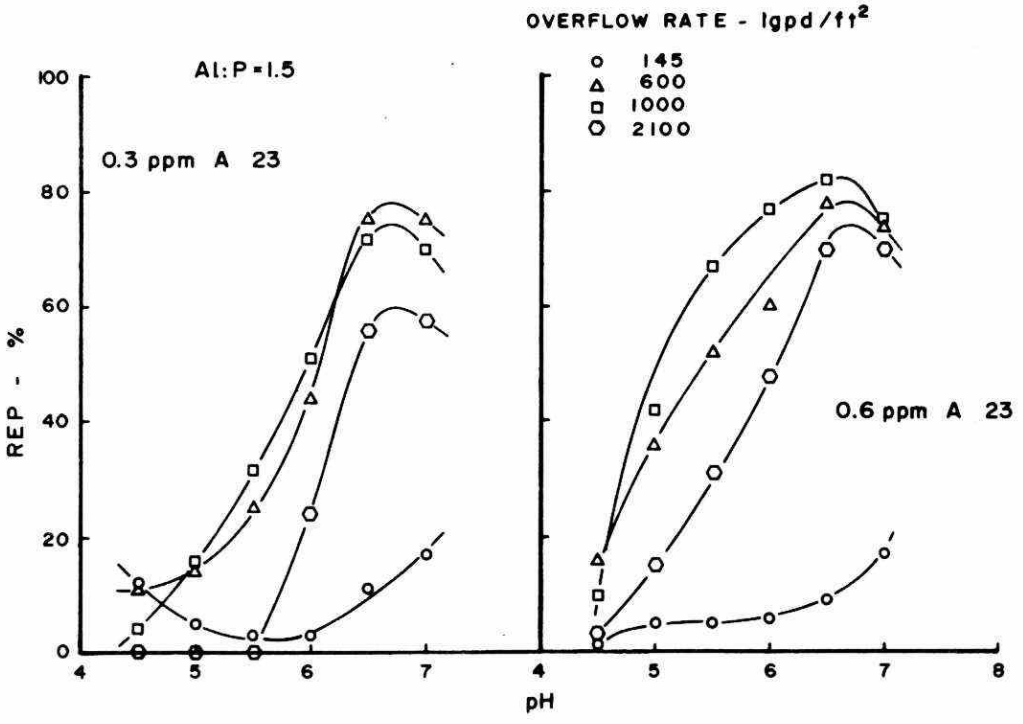

FIGURE 161. REP IN THE ALUMINUM-ORTHOPHOSPHATE SYSTEM

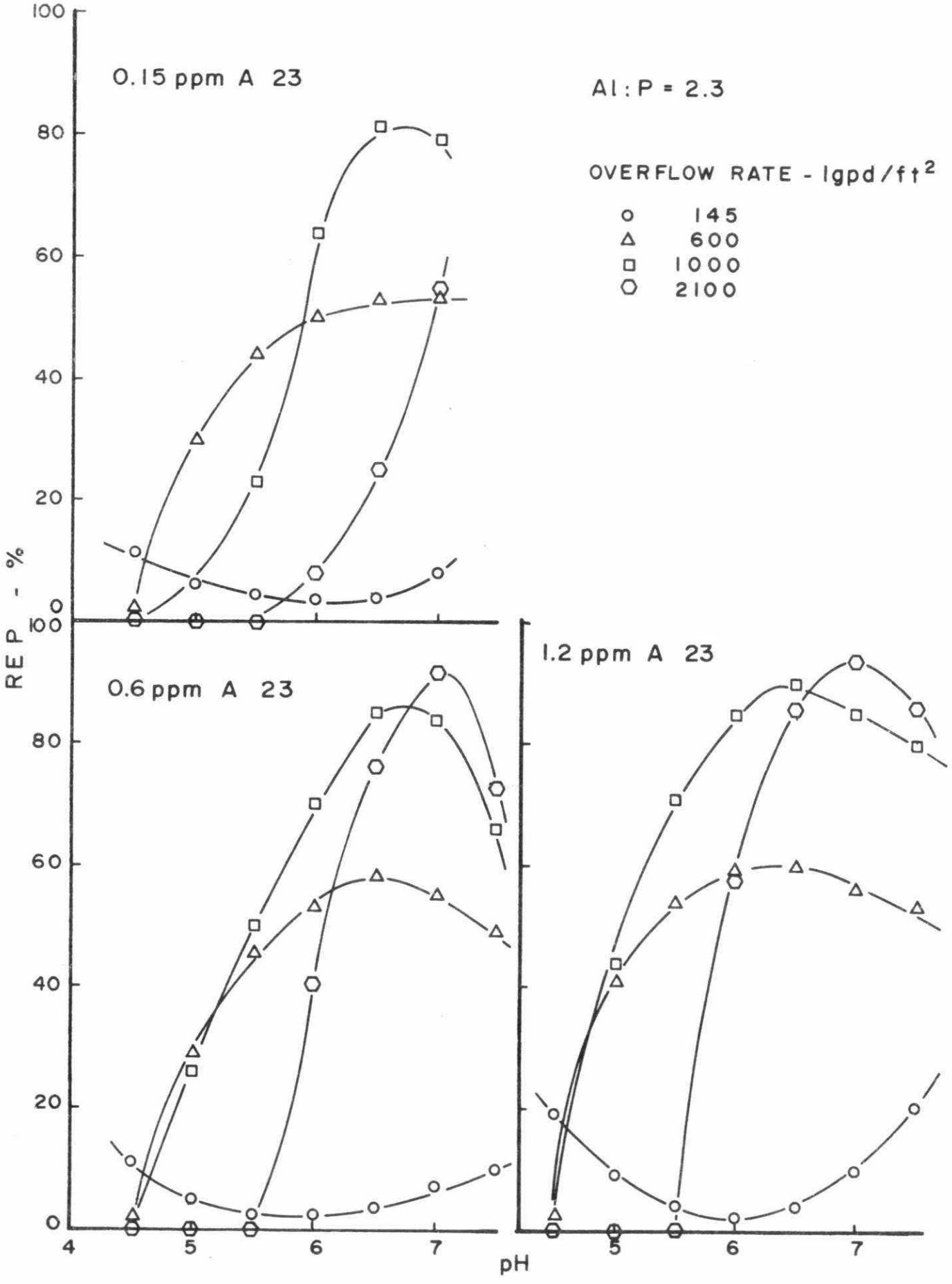

FIGURE 162. REP IN THE ALUMINUM-ORTHOPHOSPHATE SYSTEM

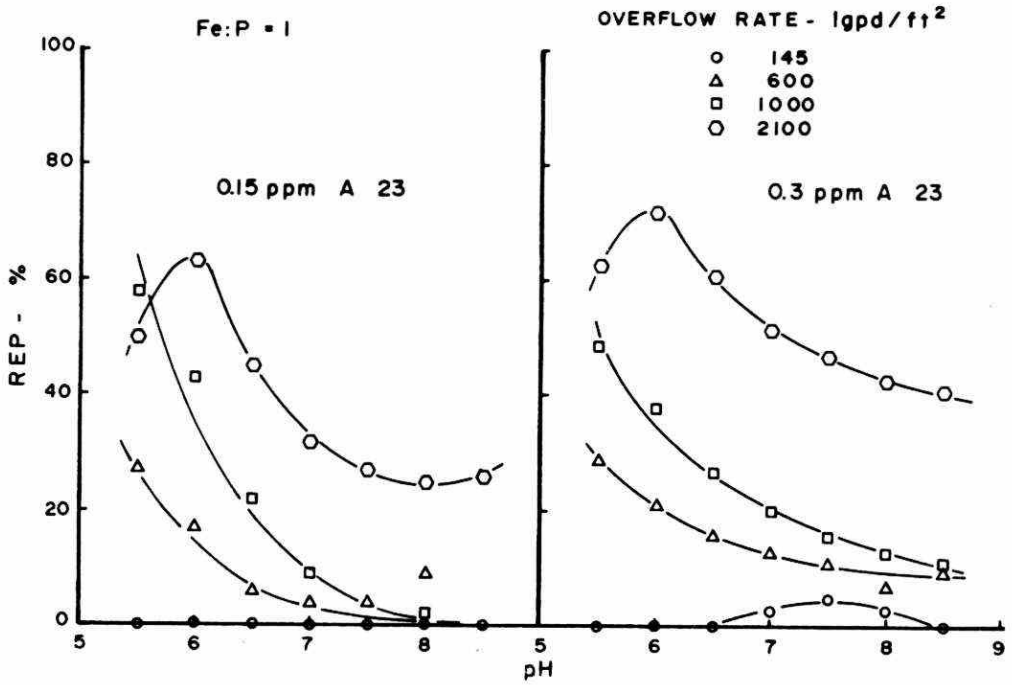

FIGURE 163. REP IN THE IRON-ORTHOPHOSPHATE SYSTEM

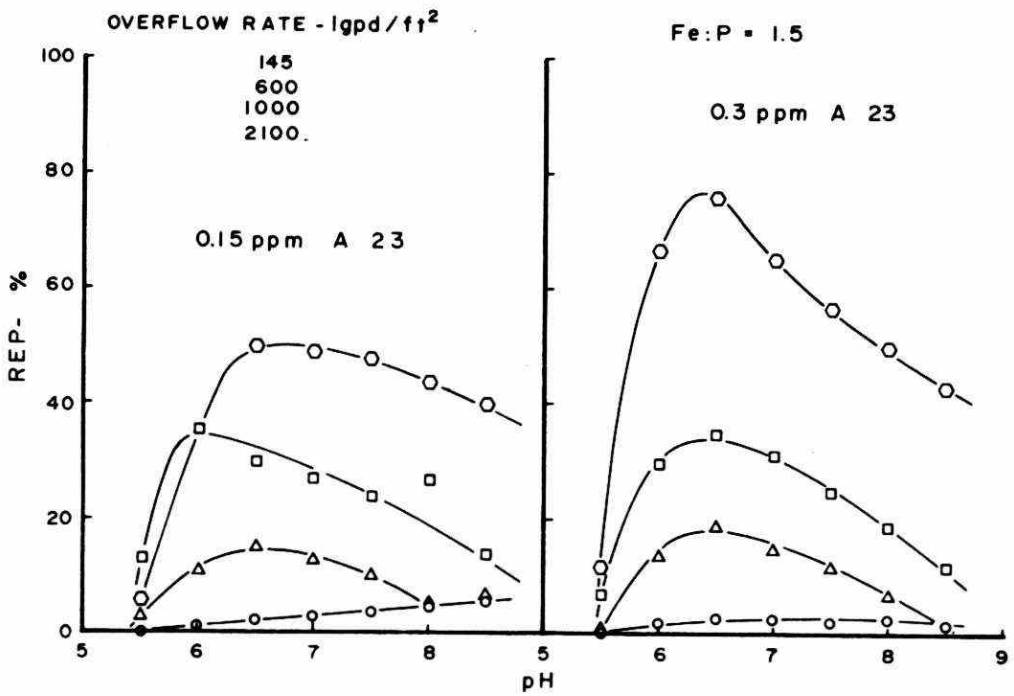

FIGURE 164. REP IN THE IRON-ORTHOPHOSPHATE SYSTEM

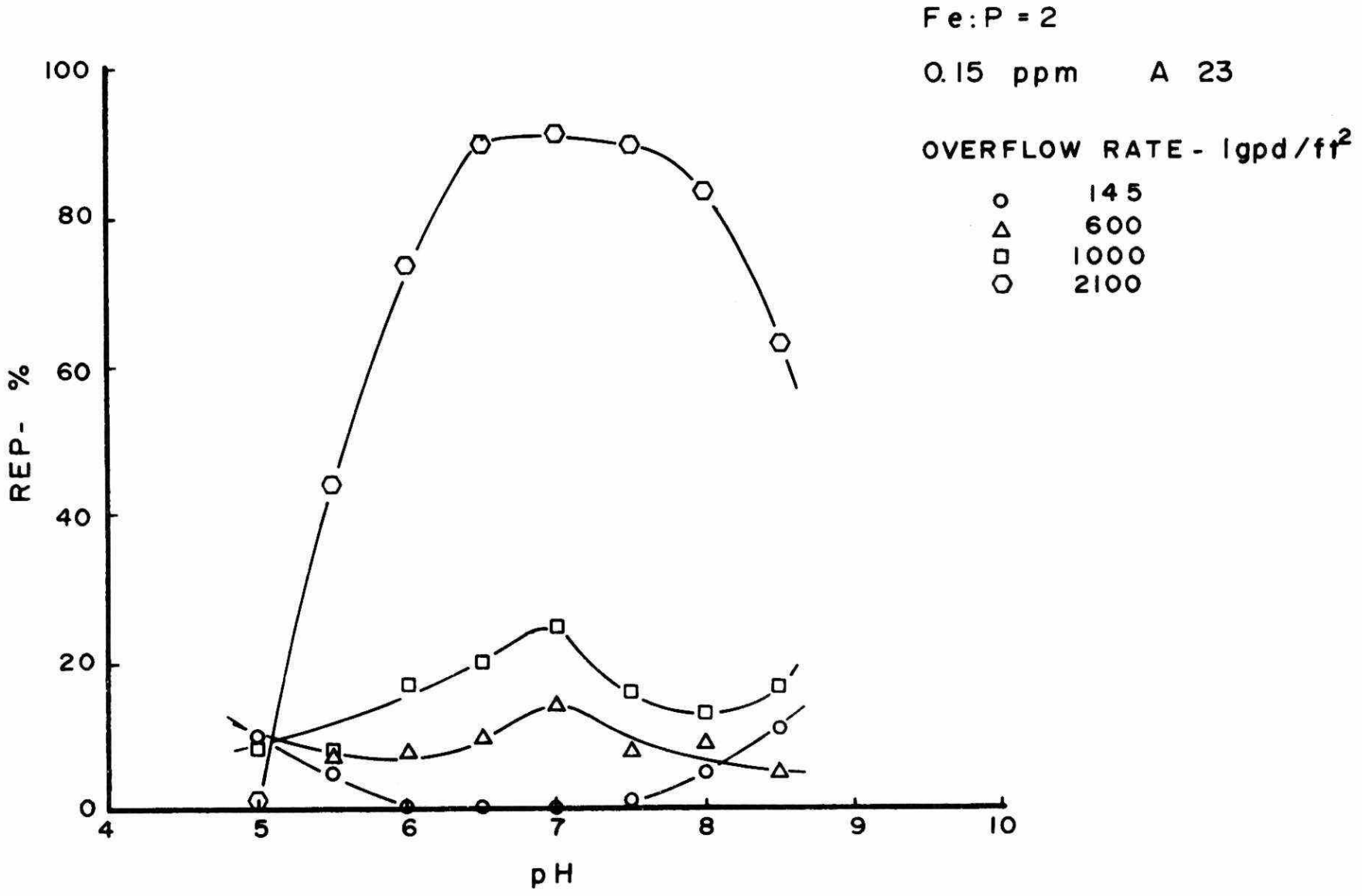

FIGURE 165. REP IN THE IRON-ORTHOPHOSPHATE SYSTEM

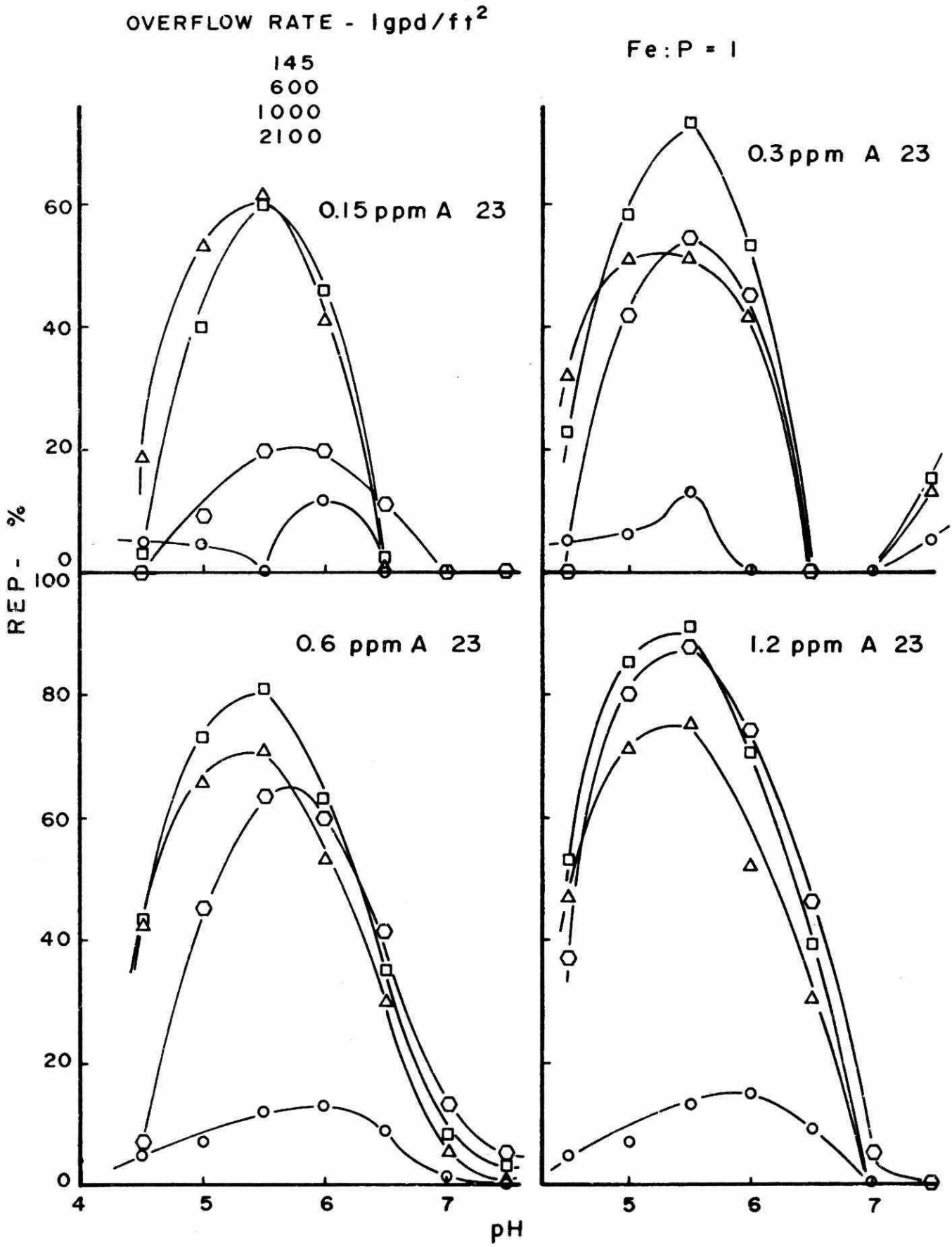

FIGURE 166. REP IN THE IRON-MIXED PHOSPHATE SYSTEM

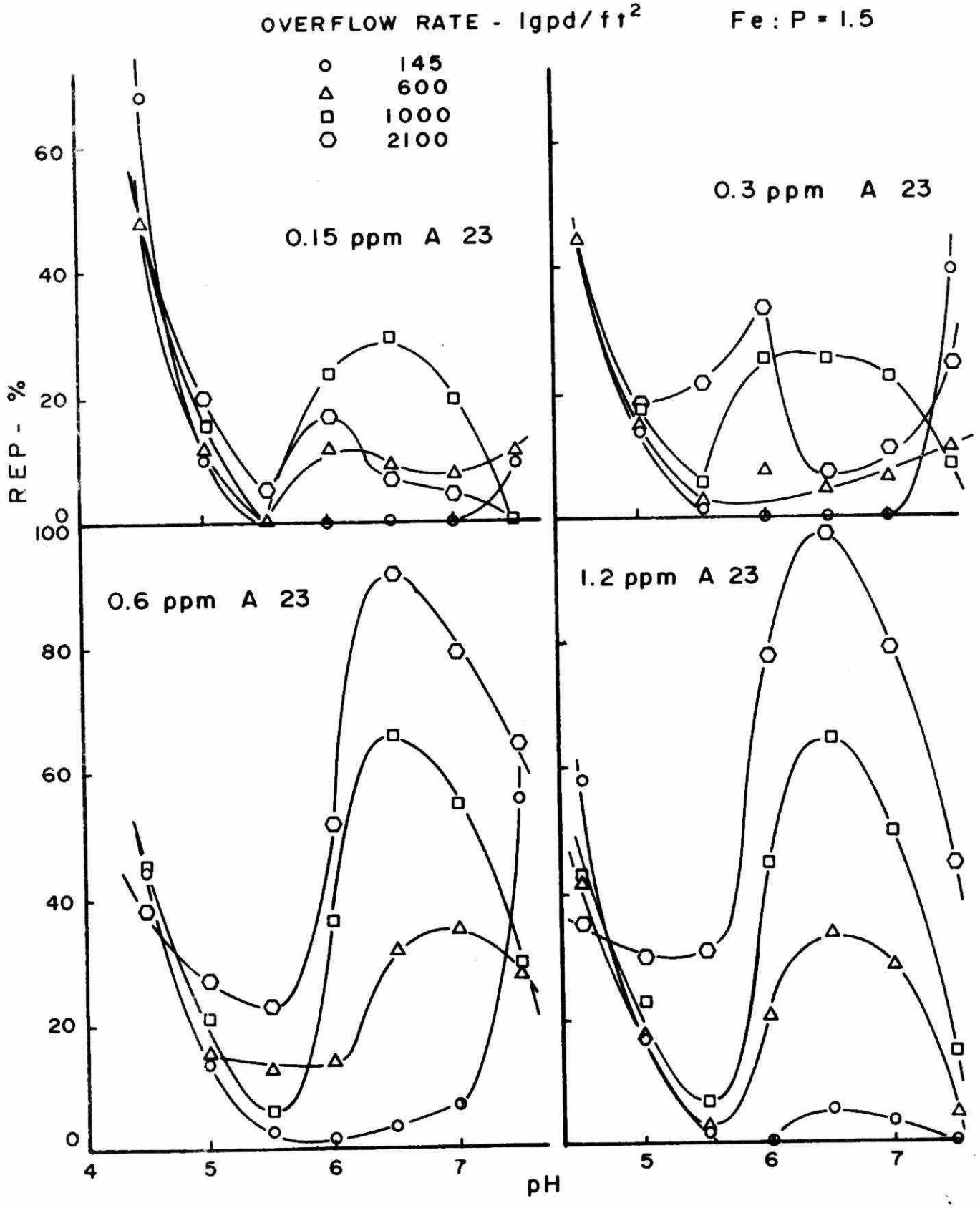

FIGURE 167. REP IN THE IRON-MIXED PHOSPHATE SYSTEM

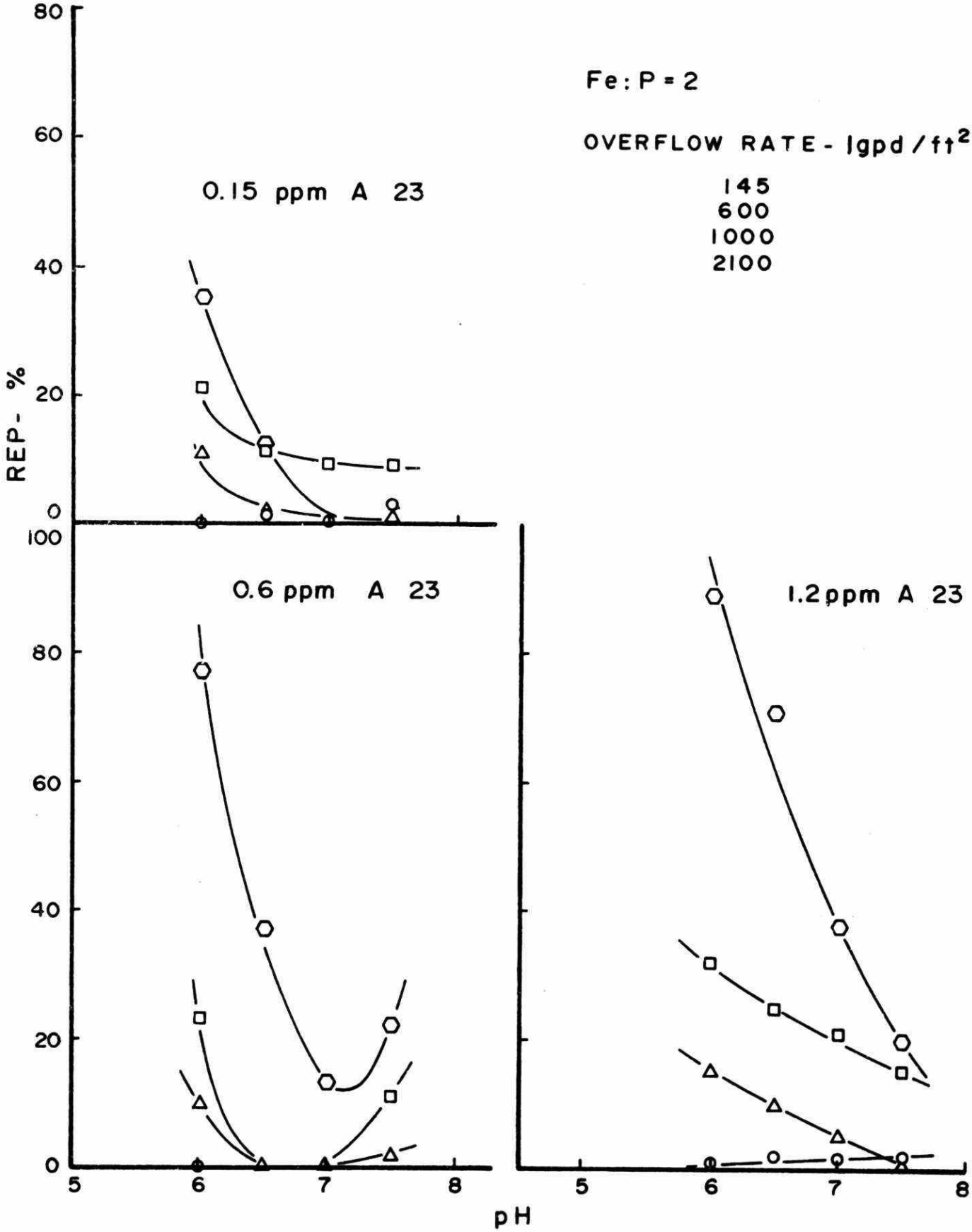

FIGURE 168. REP IN THE IRON-MIXED PHOSPHATE SYSTEM

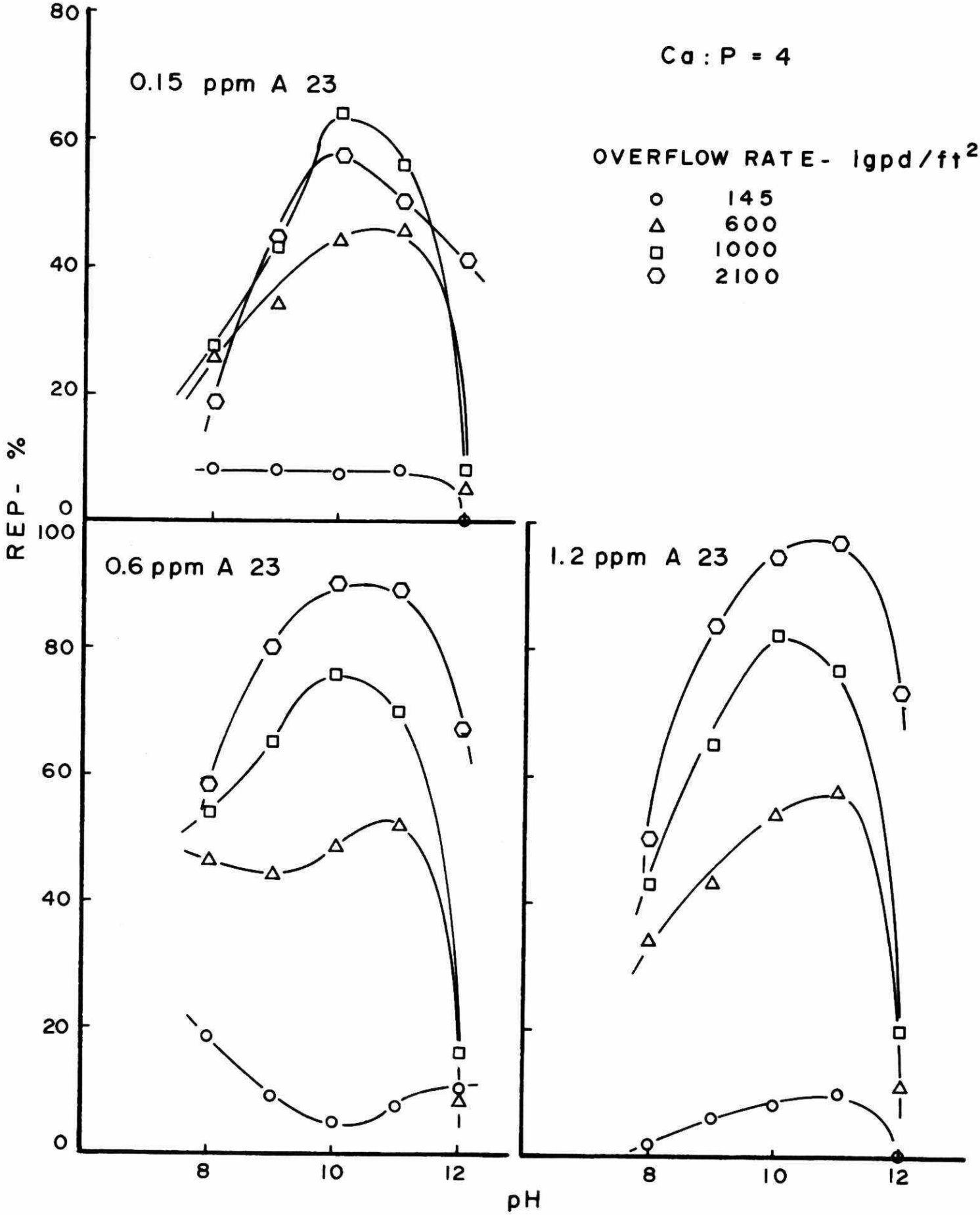

FIGURE 169. REP IN THE CALCIUM-MIXED PHOSPHATE SYSTEM

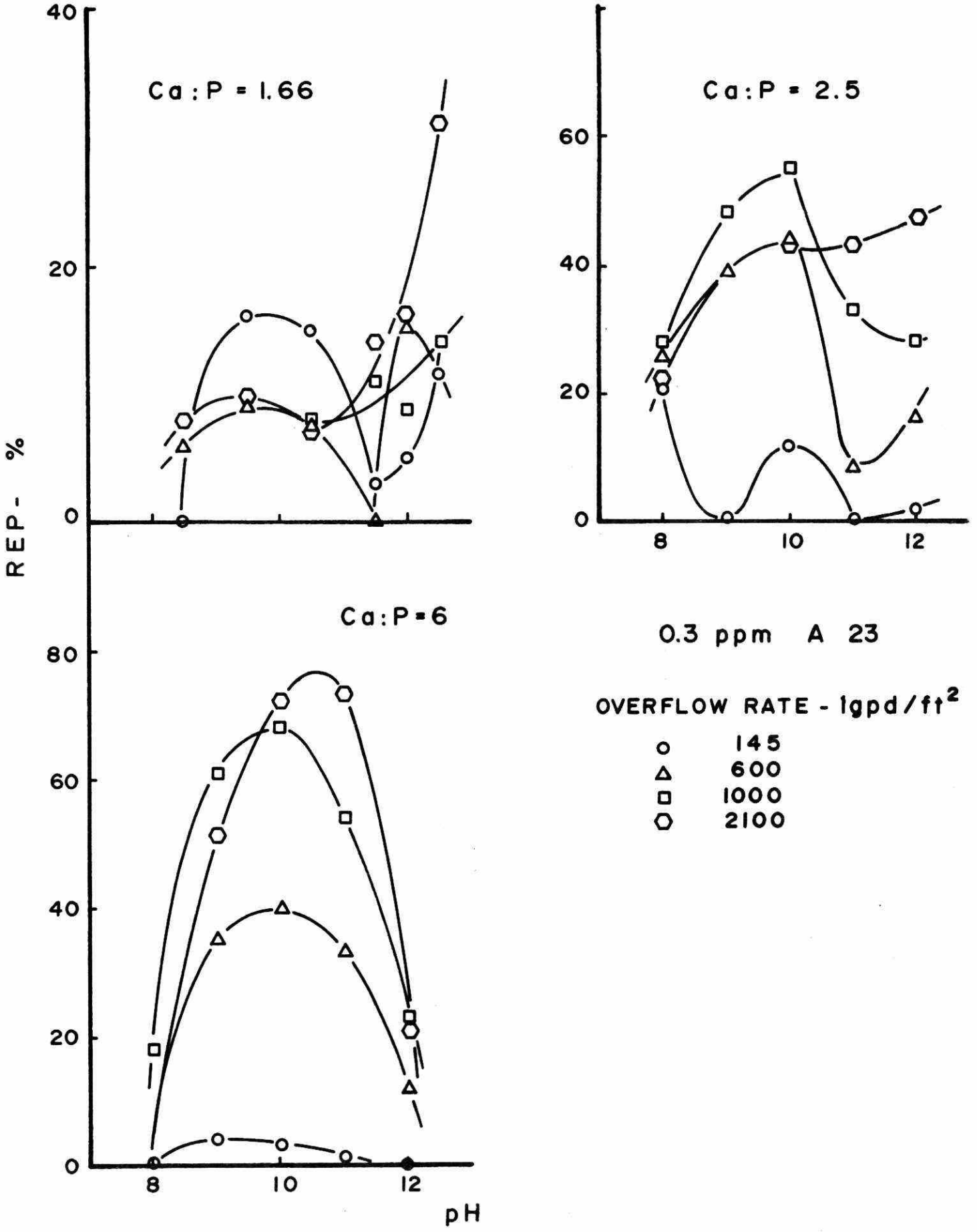

FIGURE 170. REP IN THE CALCIUM-MIXED PHOSPHATE SYSTEM

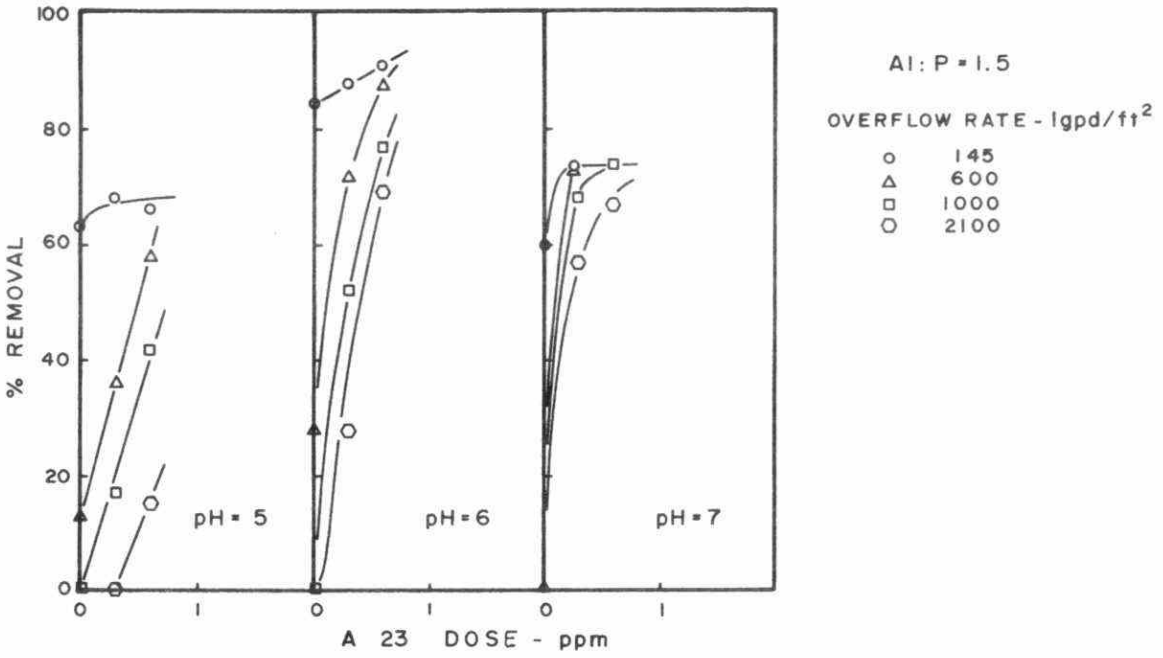

FIGURE 171. PHOSPHORUS REMOVAL AS FUNCTION OF POLYELECTROLYTE DOSAGE IN THE ALUMINUM-ORTHOPHOSPHATE SYSTEM

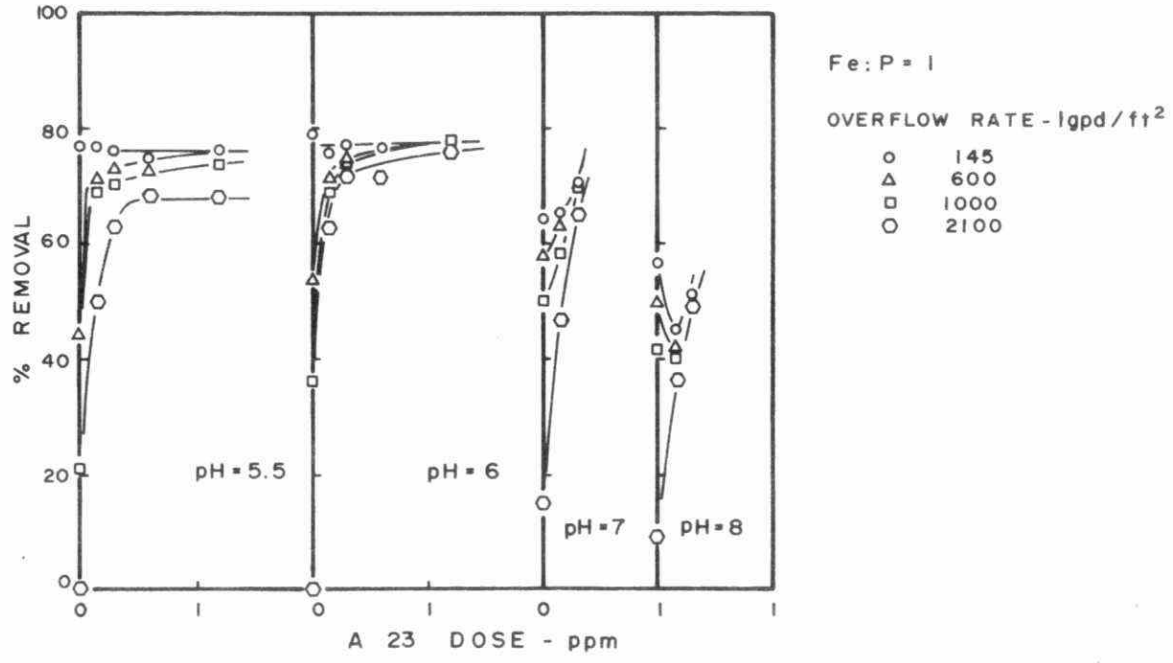

FIGURE 172. PHOSPHORUS REMOVAL AS FUNCTION OF POLYELECTROLYTE DOSAGE IN THE IRON-ORTHOPHOSPHATE SYSTEM

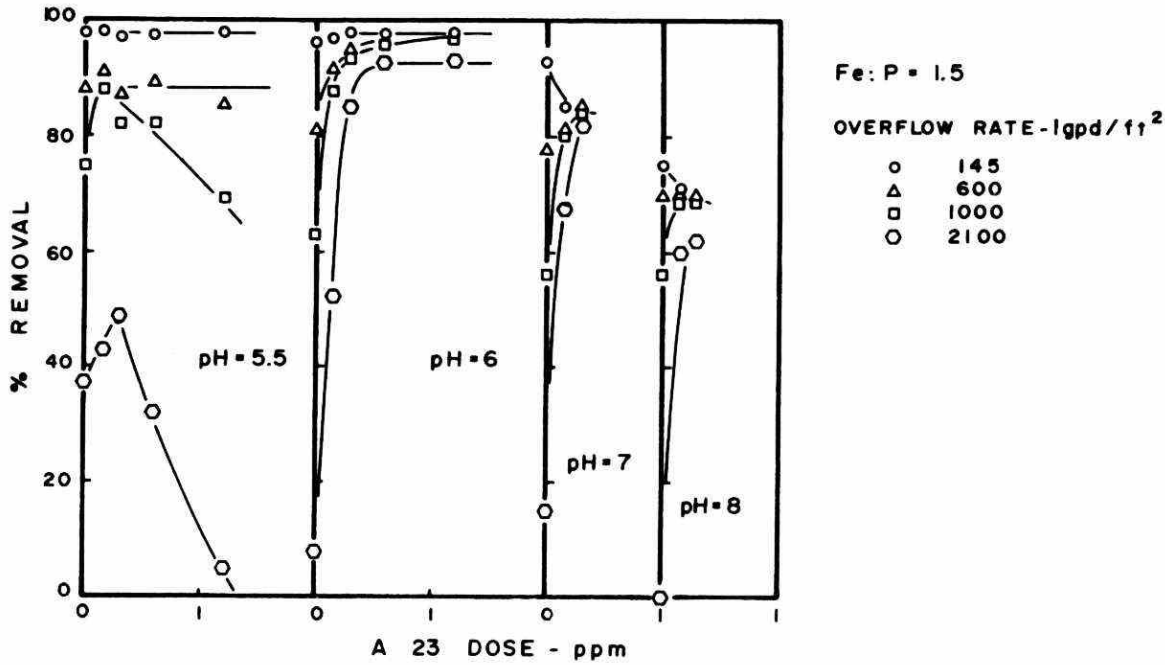

FIGURE 173. PHOSPHORUS REMOVAL AS FUNCTION OF POLYELECTROLYTE DOSAGE IN THE IRON-ORTHOPHOSPHATE SYSTEM

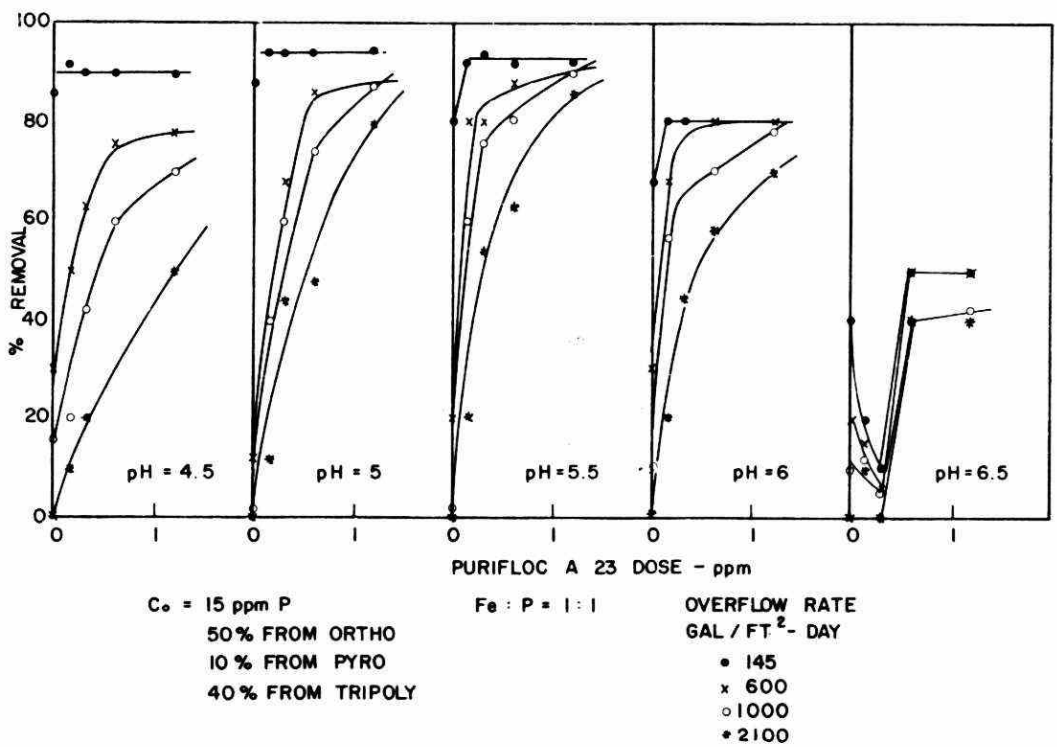

FIGURE 174. PHOSPHORUS REMOVAL AS FUNCTION OF POLYELECTROLYTE DOSAGE IN THE IRON-MIXED PHOSPHATE SYSTEM

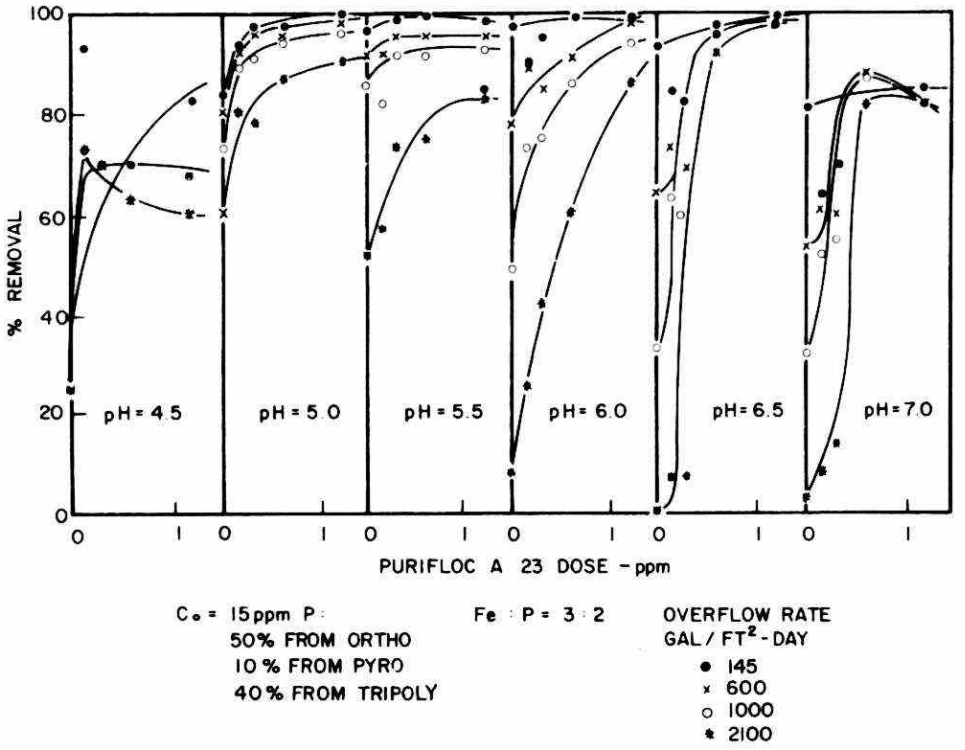

FIGURE 175. PHOSPHORUS REMOVAL AS FUNCTION OF POLYELECTROLYTE DOSAGE IN THE IRON-MIXED PHOSPHATE SYSTEM

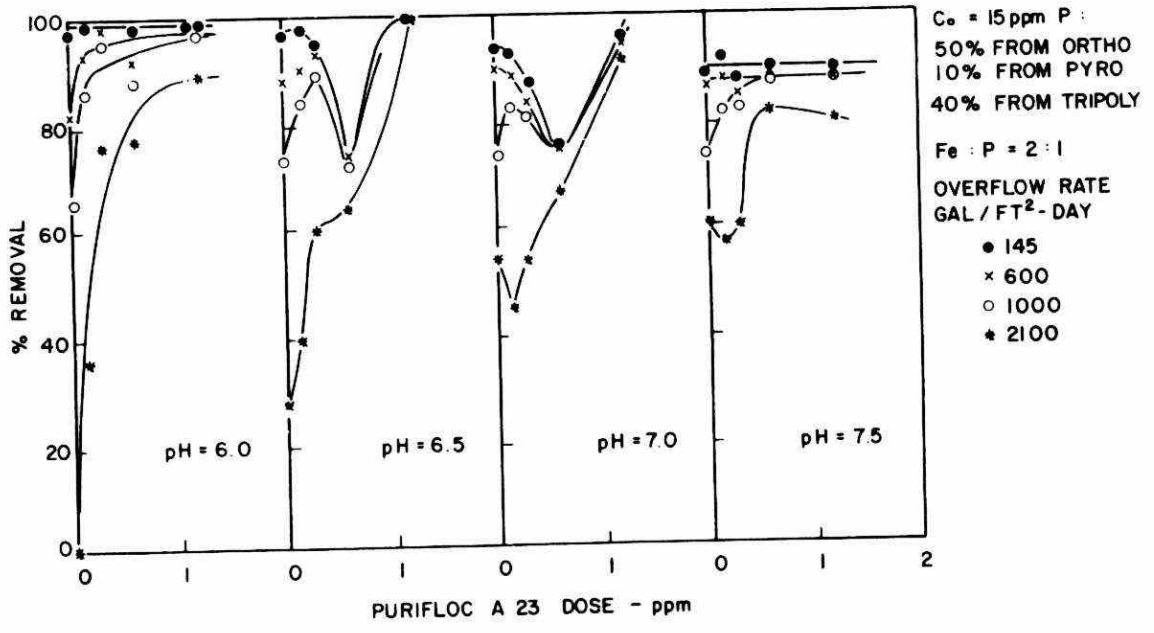

FIGURE 176. PHOSPHORUS REMOVAL AS FUNCTION OF POLYELECTROLYTE DOSAGE IN THE IRON-MIXED PHOSPHATE SYSTEM

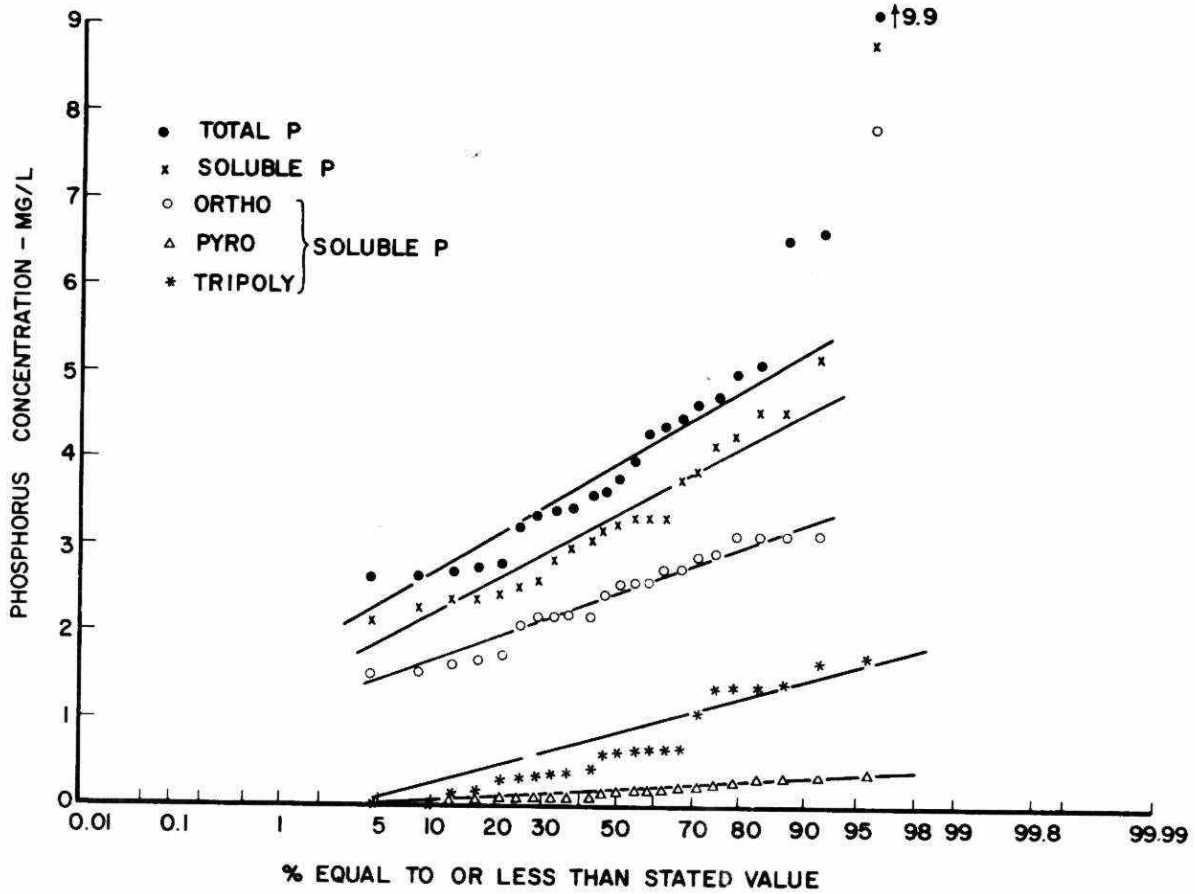

FIGURE 177. DISTRIBUTION OF PHOSPHORUS TYPES IN NAPANEE RAW SEWAGE

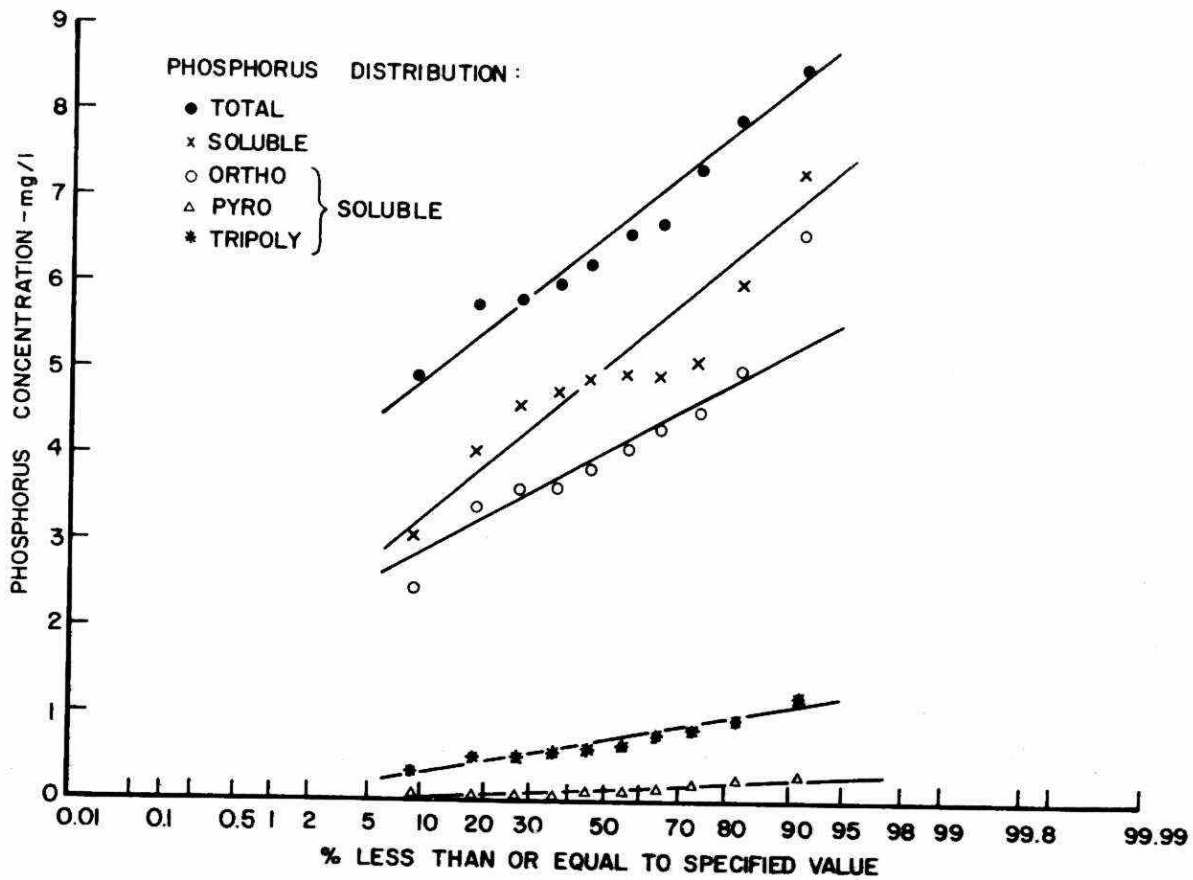

FIGURE 178. DISTRIBUTION OF PHOSPHORUS TYPES IN DUNDAS RAW SEWAGE

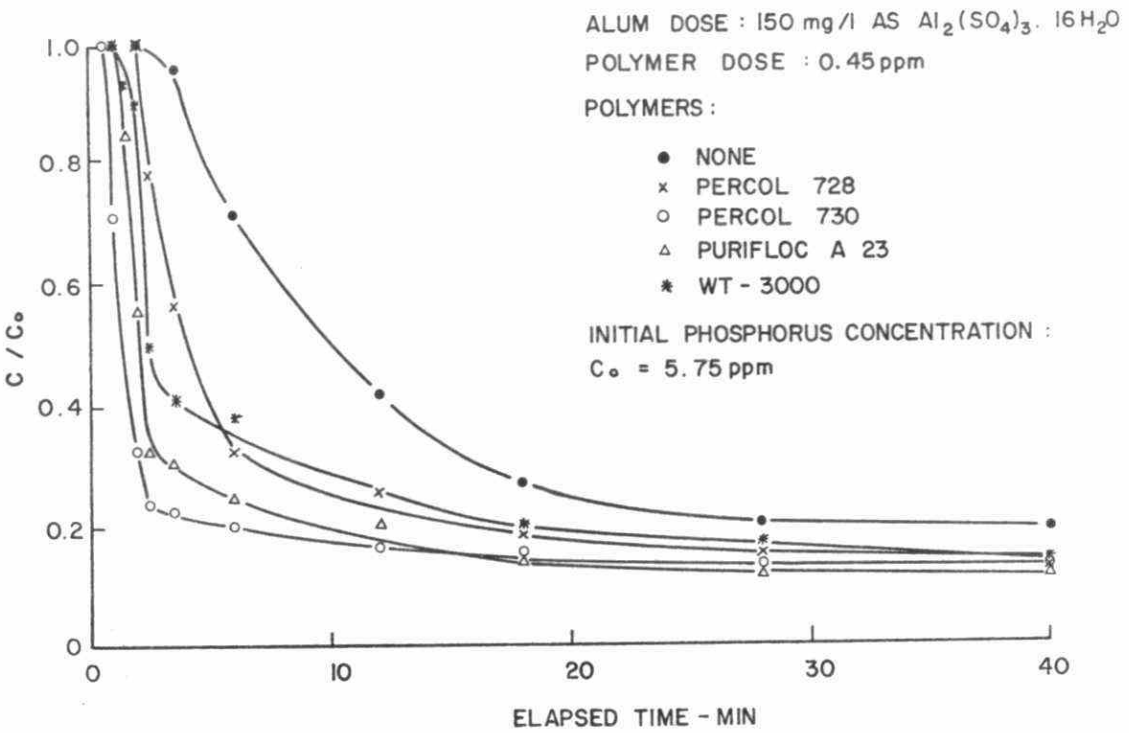

FIGURE 179. INITIAL SOLUTION ALKALINITY AS RESULT OF pH CONTROL FOR THE IRON-ORTHOPHOSPHATE SYSTEM

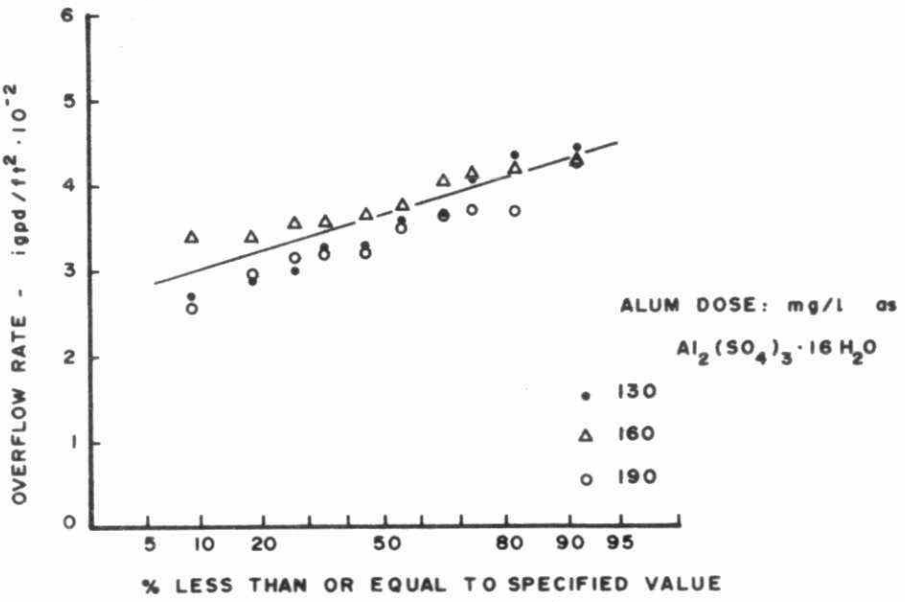

FIGURE 180. PERMISSIBLE OVERFLOW RATES FOR 90% FLOC REMOVAL WITH ALUM ADDITION IN DUNDAS RAW SEWAGE

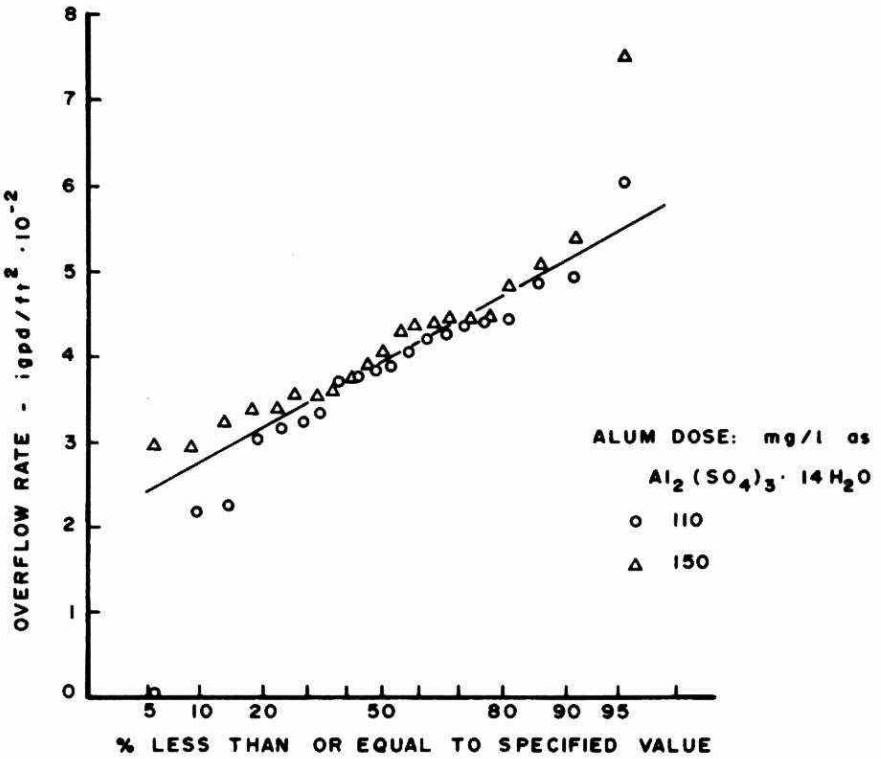

FIGURE 181. PERMISSIBLE OVERFLOW RATES FOR 90% FLOC REMOVAL WITH ALUM ADDITION IN NAPANEE RAW SEWAGE

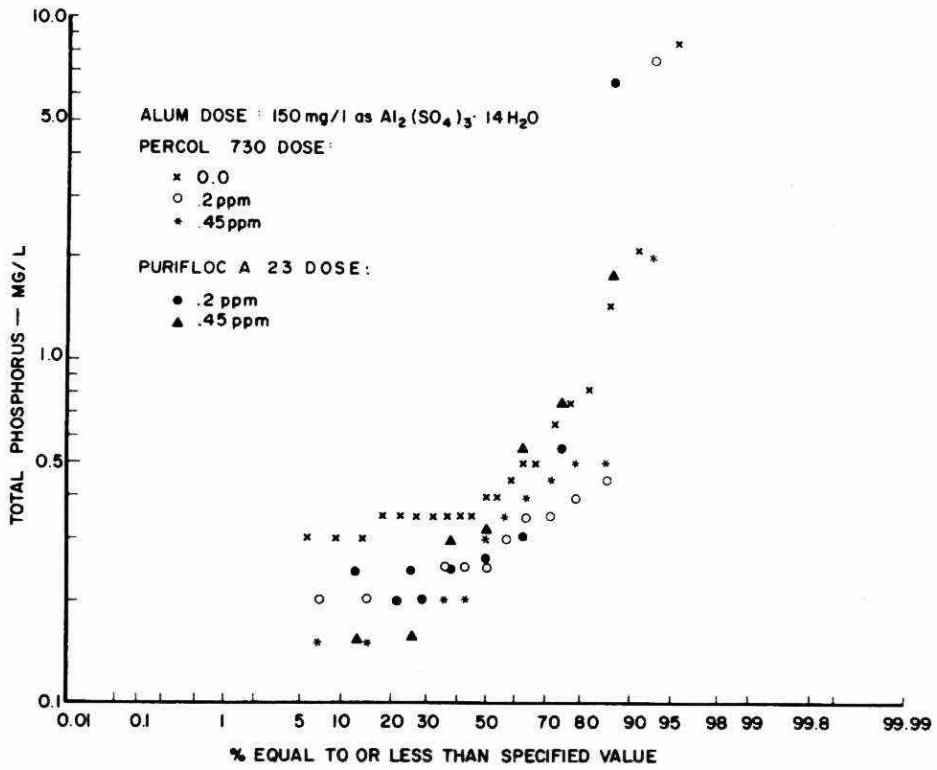

FIGURE 182. ULTIMATE PHOSPHORUS RESIDUALS WITH ALUM (150 MG/1) AND POLYELECTROLYTE ADDITION IN NAPANEE RAW SEWAGE

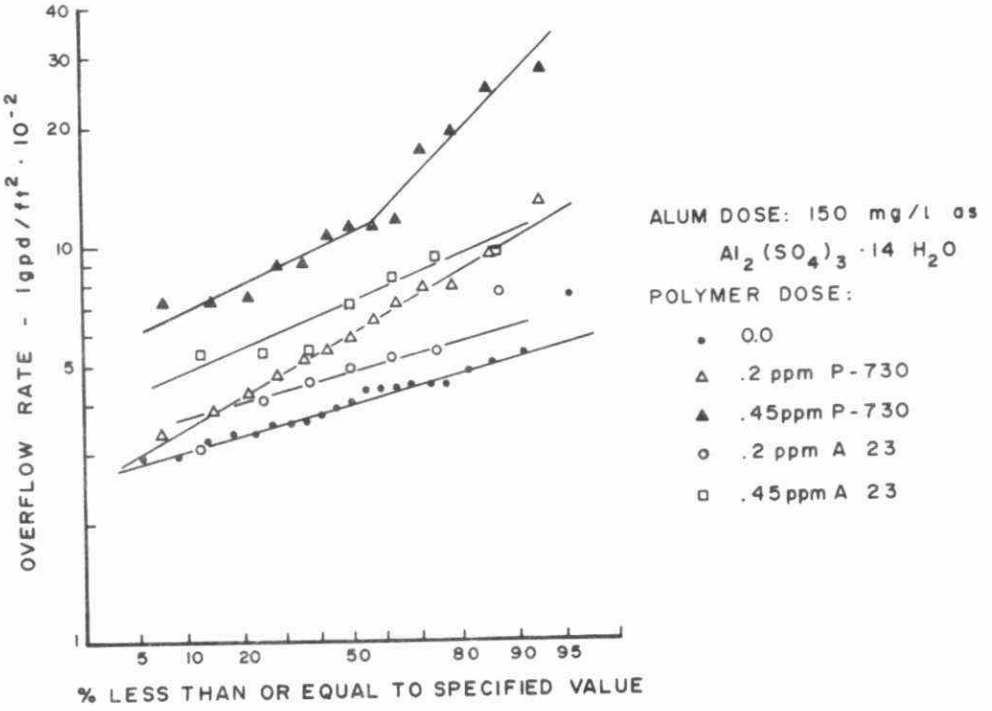

FIGURE 183. PERMISSIBLE OVERFLOW RATES FOR 90% FLOC REMOVAL WITH ALUM (150 MG/1) AND POLYELECTROLYTE ADDITION IN NAPANEE RAW SEWAGE

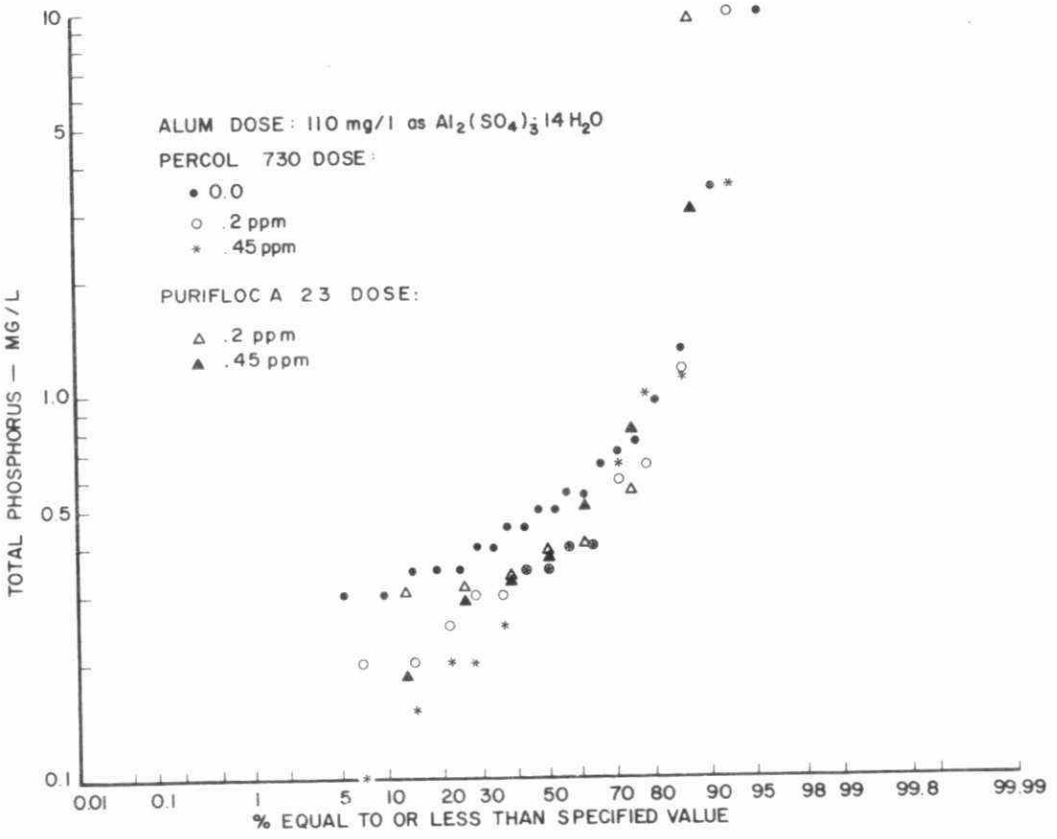

FIGURE 184. ULTIMATE PHOSPHORUS RESIDUALS WITH ALUM (110 MG/1) AND POLYELECTROLYTE ADDITION IN NAPANEE RAW SEWAGE

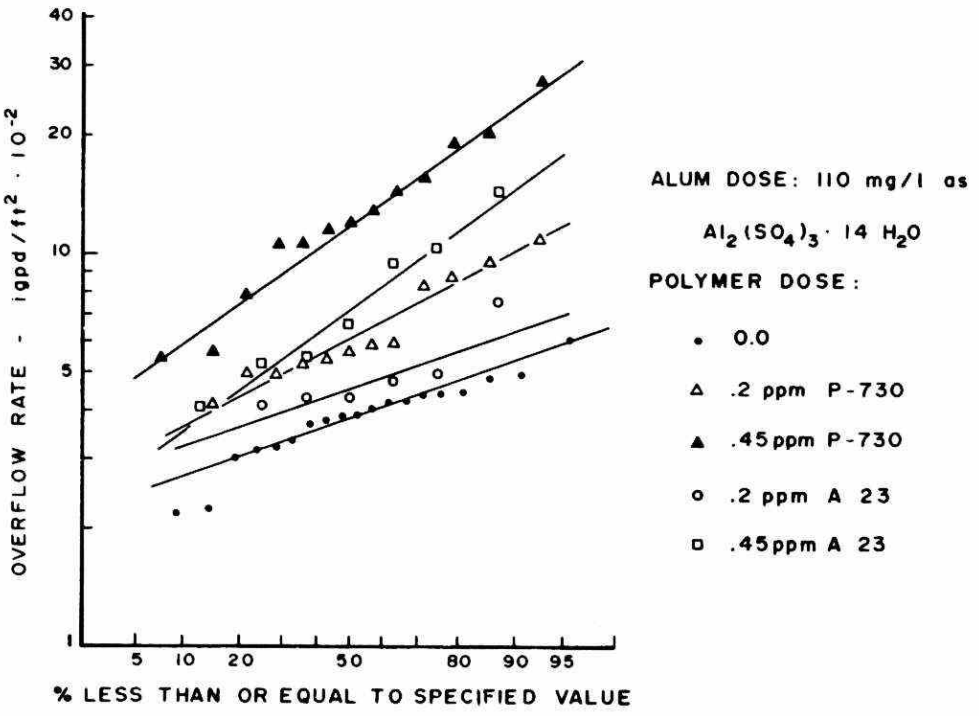

FIGURE 185. PERMISSIBLE OVERFLOW RATES FOR 90% FLOC REMOVAL WITH ALUM (110 MG/1) AND POLYELECTROLYTE ADDITION IN NAPANEE RAW SEWAGE

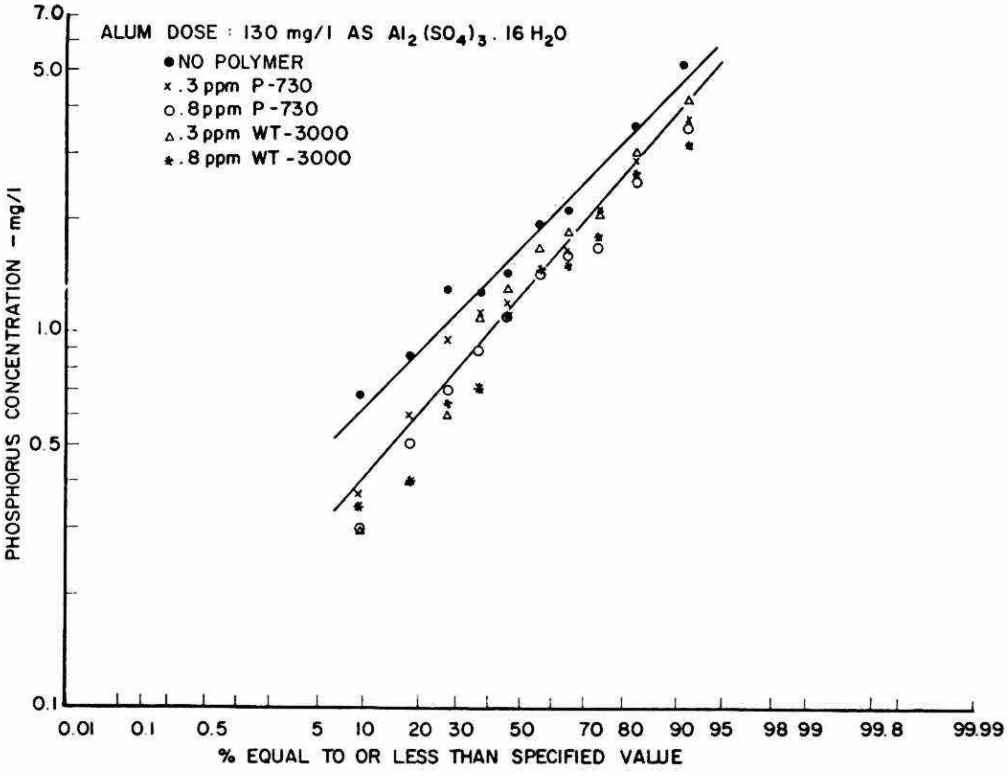

FIGURE 186. ULTIMATE PHOSPHORUS RESIDUALS WITH ALUM (130 MG/1) AND POLYELECTROLYTE ADDITION IN DUNDAS RAW SEWAGE

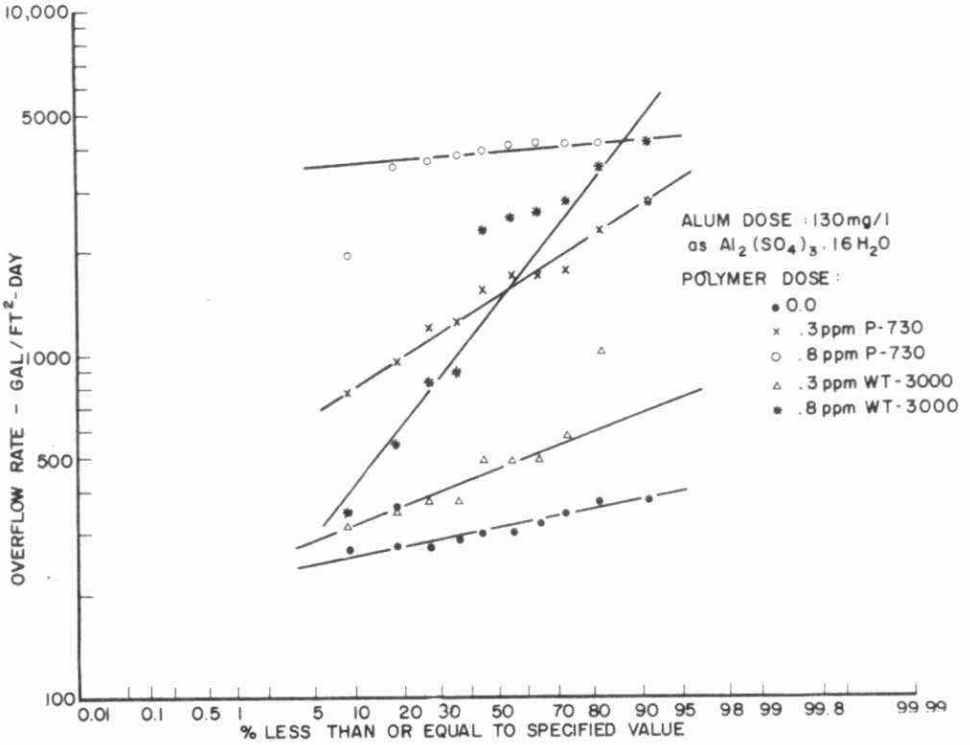

FIGURE 187. PERMISSIBLE OVERFLOW RATES FOR 90% REMOVAL WITH ALUM (130 MG/1) AND POLYELECTROLYTE ADDITION IN DUNDAS RAW SEWAGE

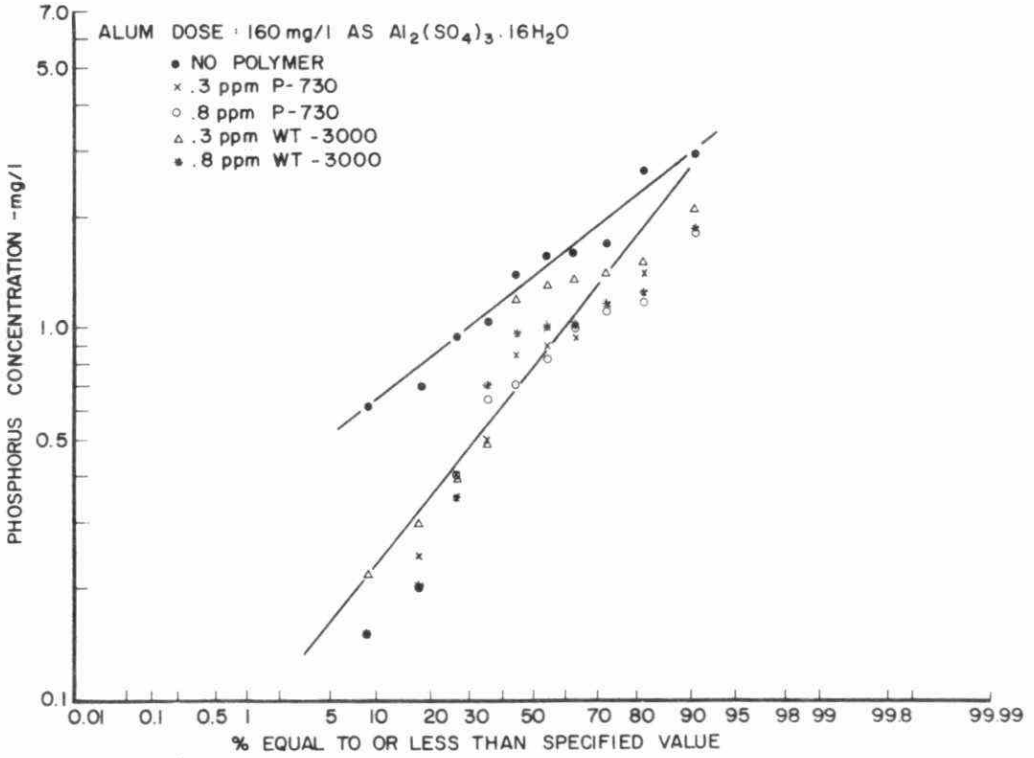

FIGURE 188. ULTIMATE PHOSPHORUS RESIDUALS WITH ALUM (160 MG/1) AND POLYELECTROLYTE ADDITION IN DUNDAS RAW SEWAGE

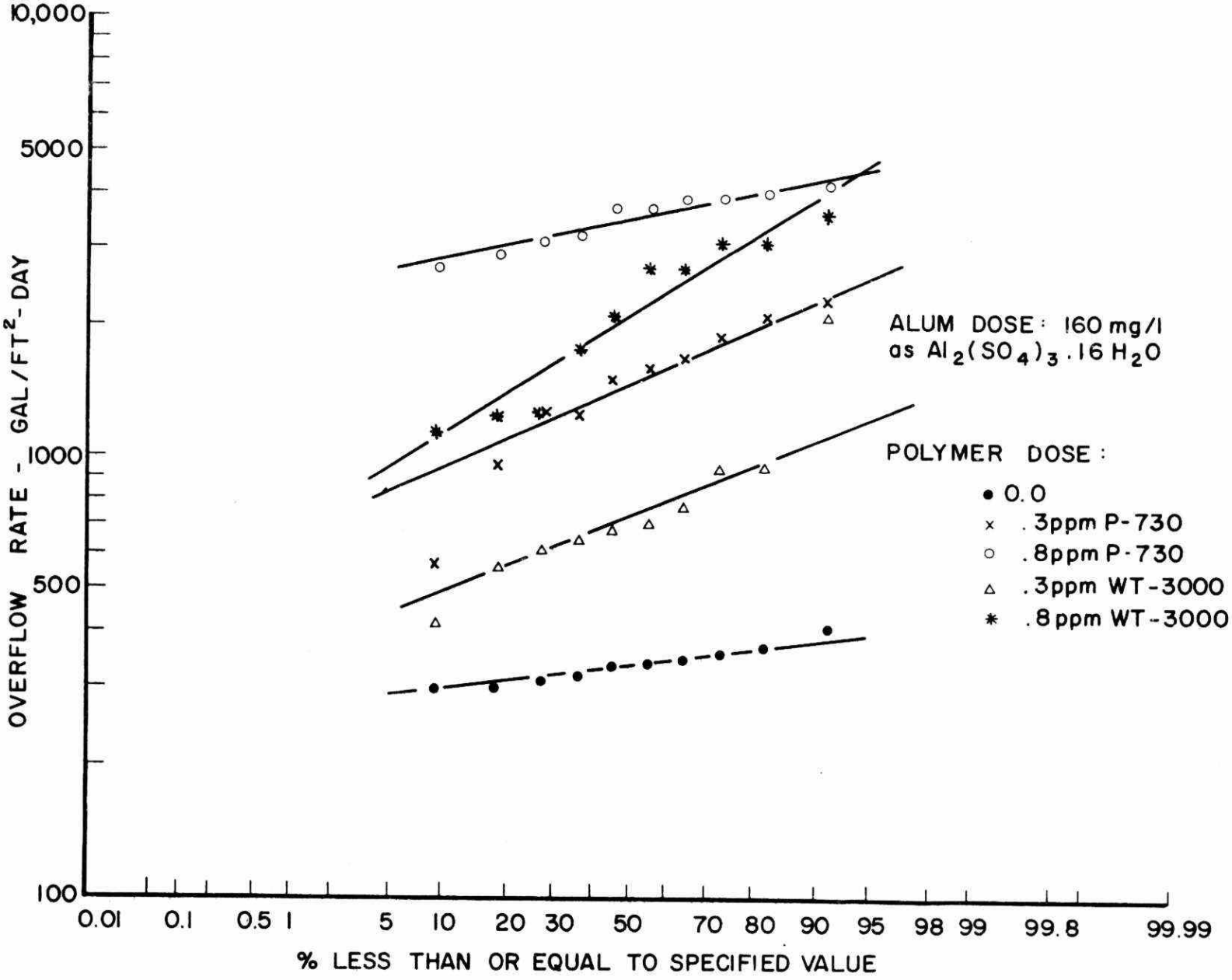

FIGURE 189. PERMISSIBLE OVERFLOW RATES FOR 90% REMOVAL WITH ALUM (160 MG/1) AND POLYELECTROLYTE ADDITION IN DUNDAS RAW SEWAGE

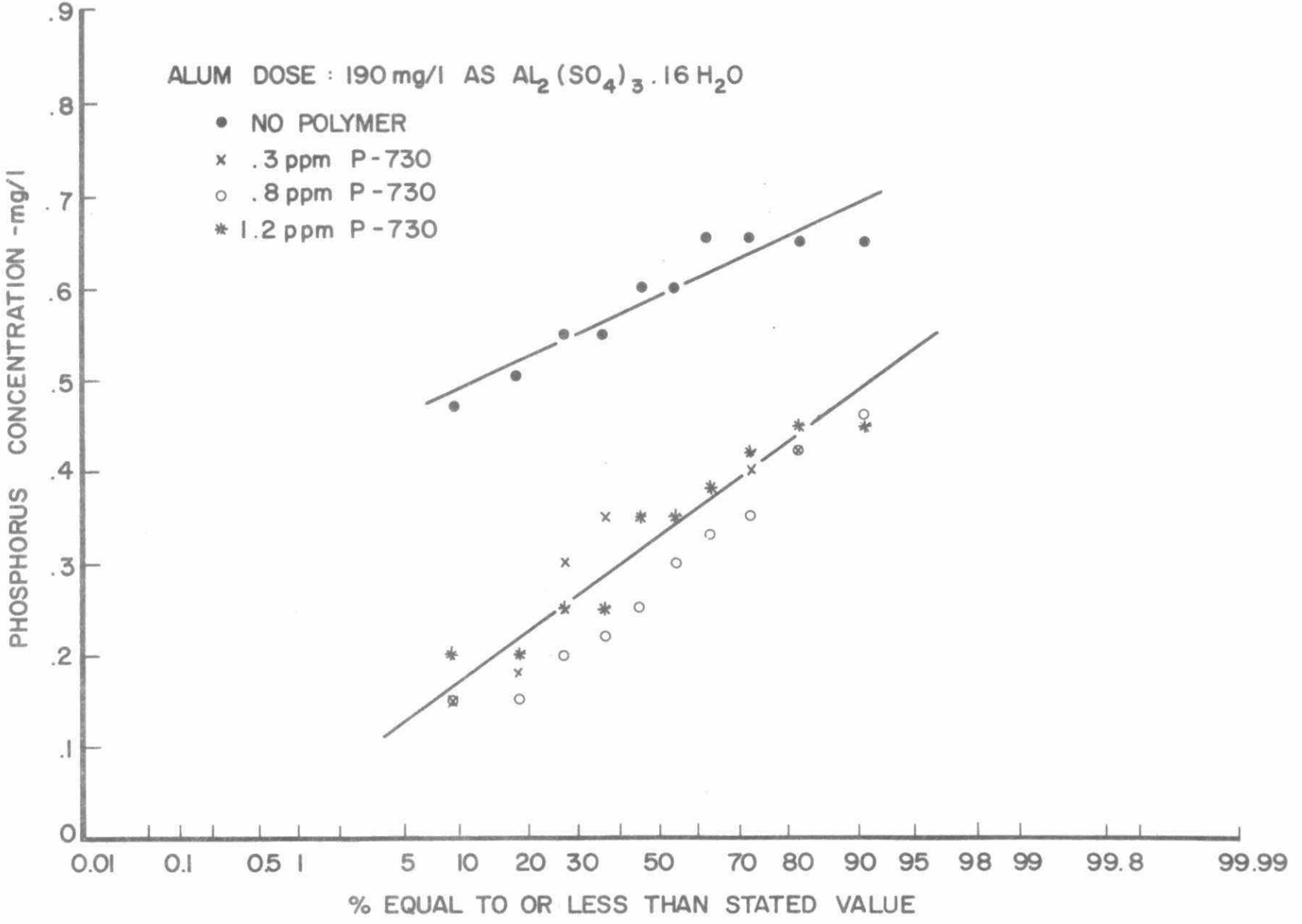

FIGURE 190. ULTIMATE PHOSPHORUS RESIDUALS WITH ALUM (190 MG/1) AND POLYELECTROLYTE ADDITION IN DUNDAS RAW SEWAGE

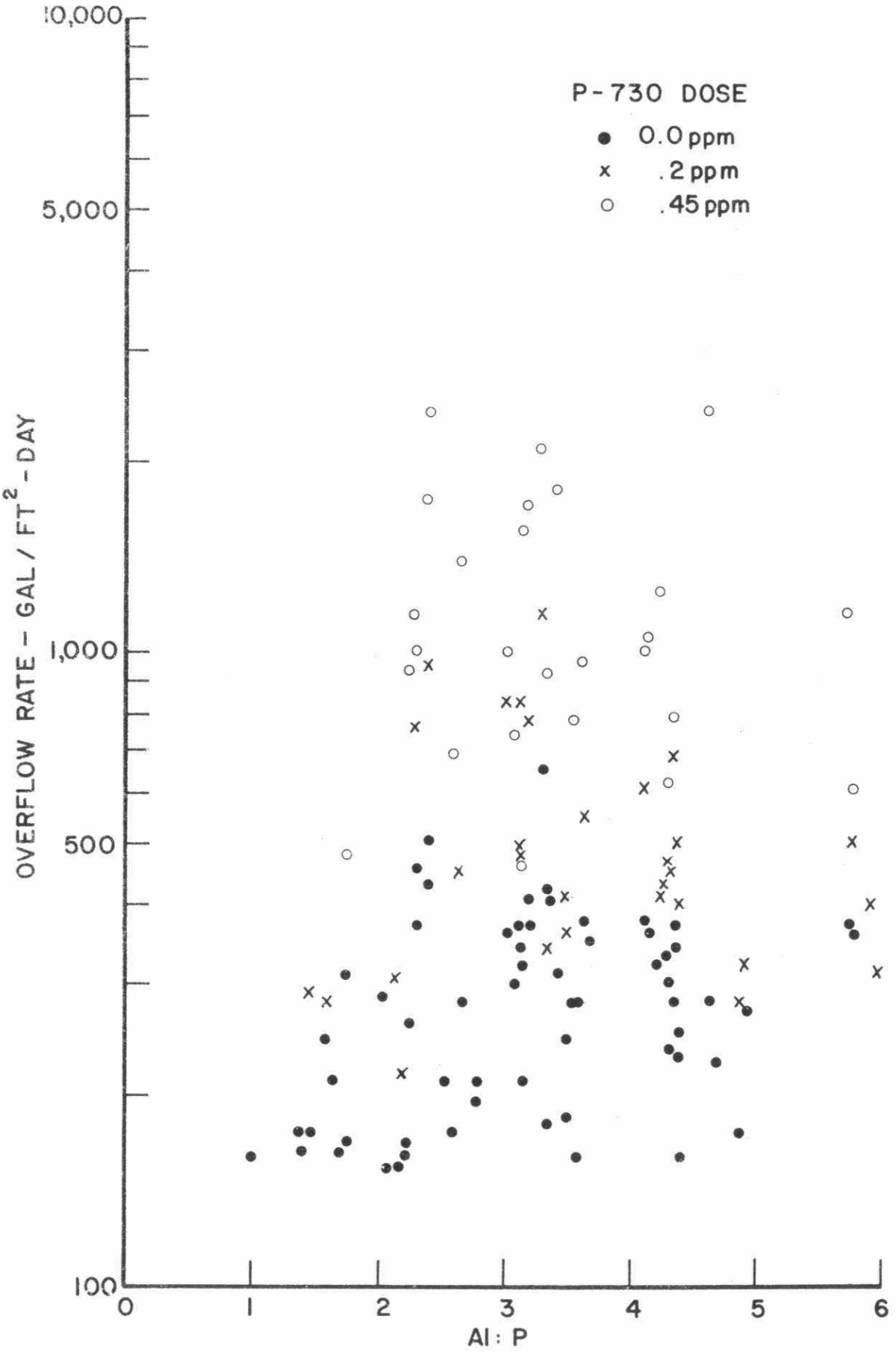

FIGURE 191. PERMISSIBLE OVERFLOW RATES FOR 90% FLOC REMOVAL AS FUNCTION OF Al:P MOLAR RATIO IN NAPANEE RAW SEWAGE

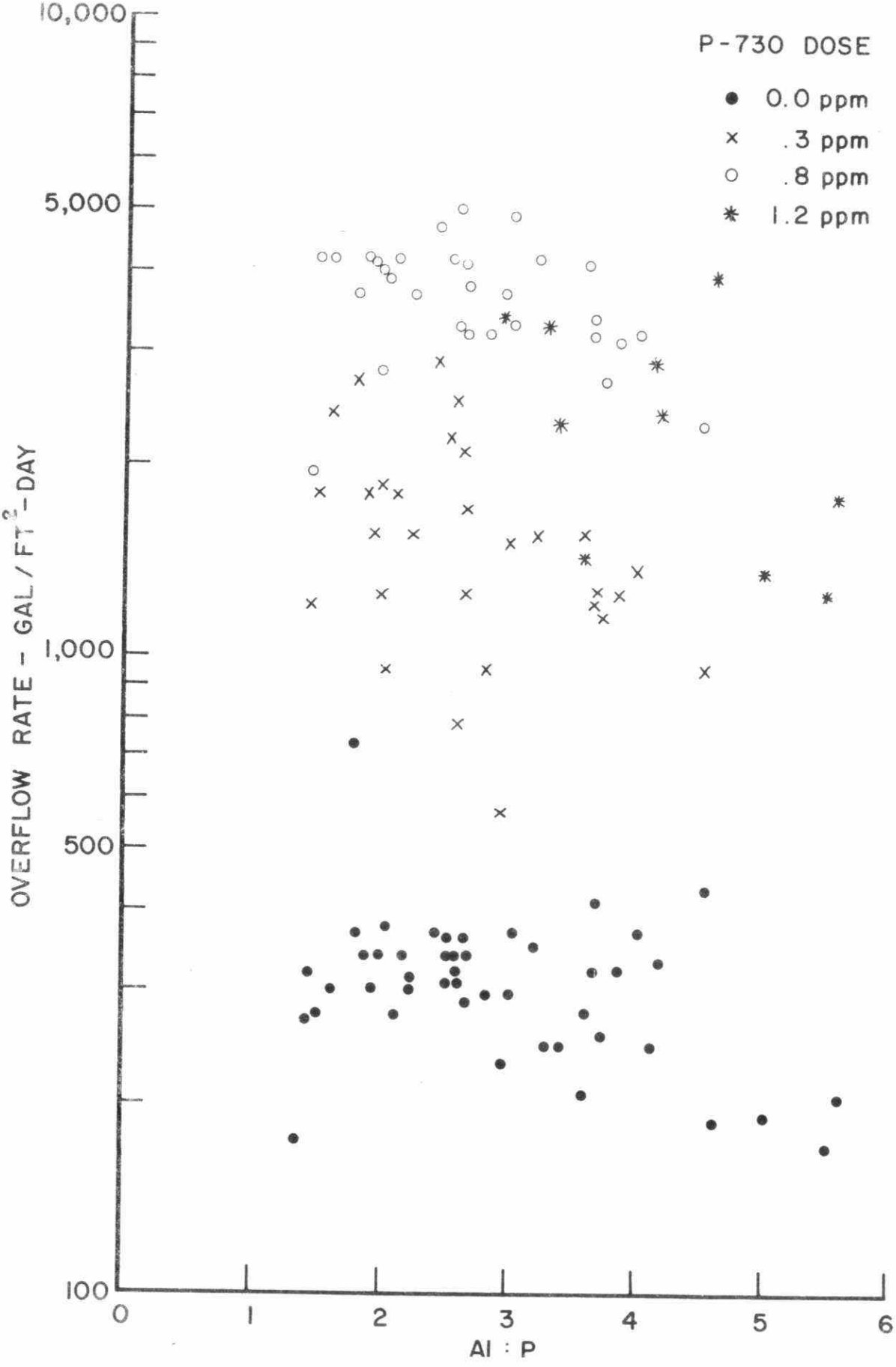

FIGURE 192. PERMISSIBLE OVERFLOW RATES FOR 90% FLOC REMOVAL AS FUNCTION OF Al:P MOLAR RATIO IN DUNDAS RAW SEWAGE

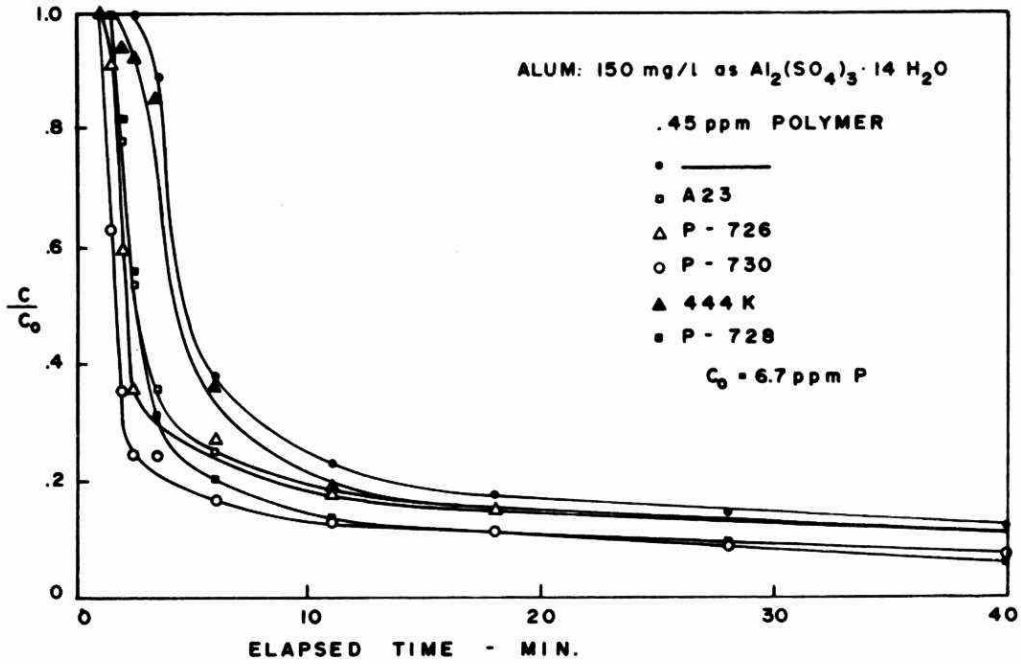

FIGURE 193. TYPICAL SEDIMENTATION CURVES FOR THE WASTEWATER-ALUM-POLYELECTROLYTE SYSTEM

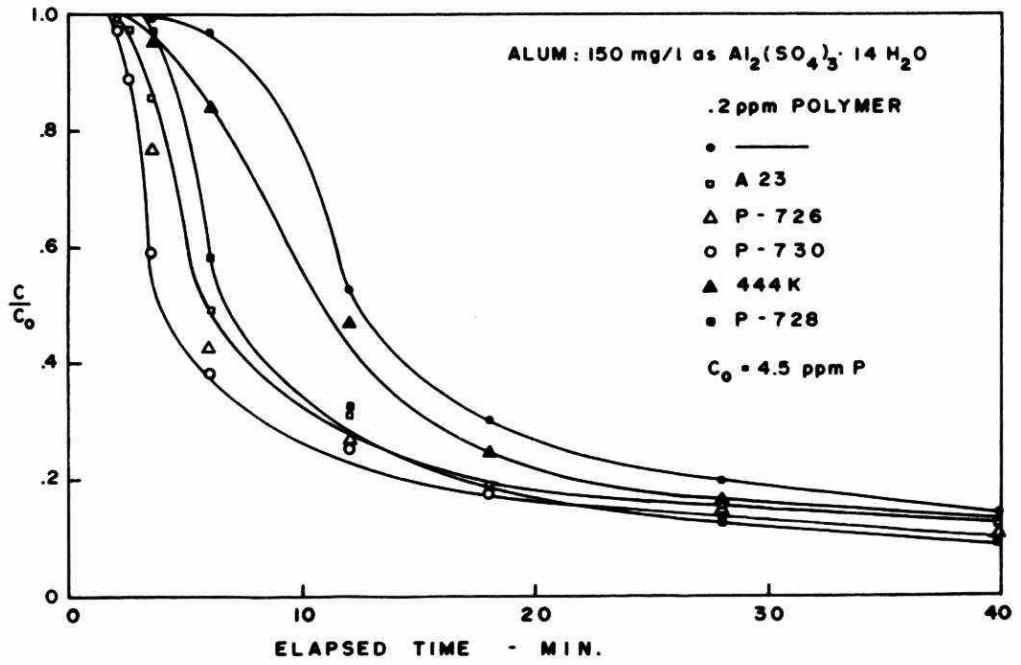

FIGURE 194. TYPICAL SEDIMENTATION CURVES FOR THE WASTEWATER-ALUM-POLYELECTROLYTE SYSTEM

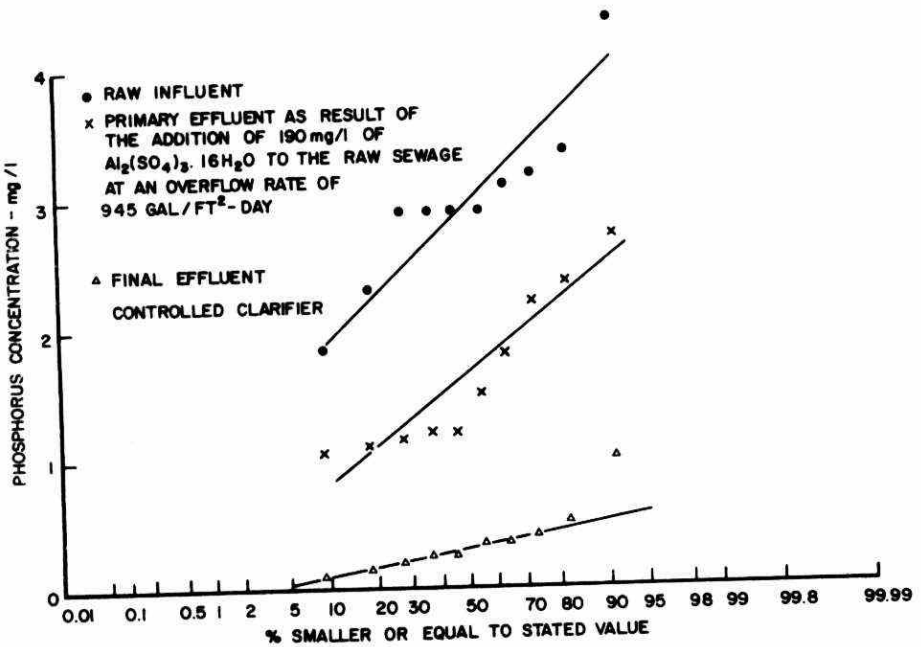

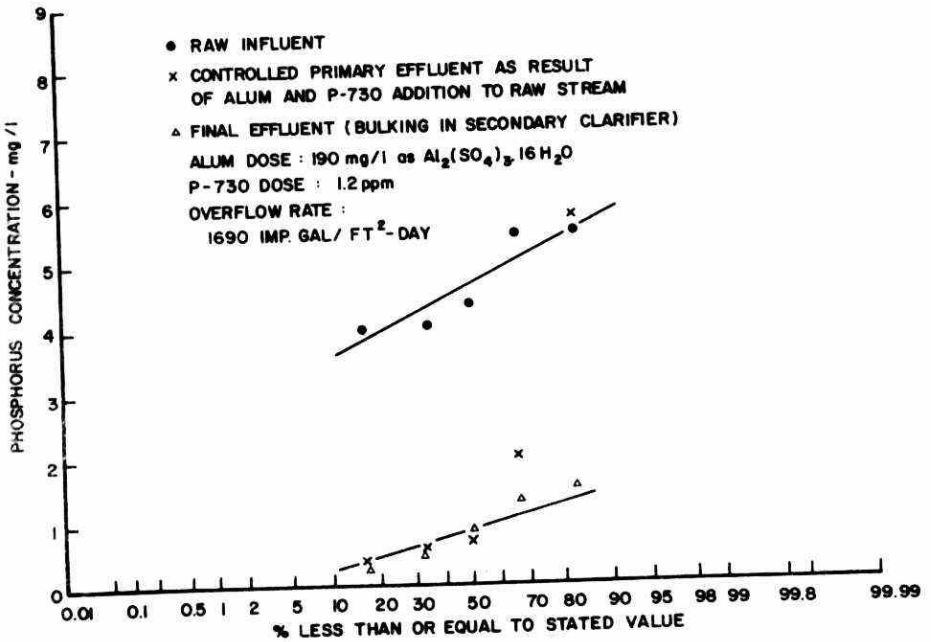

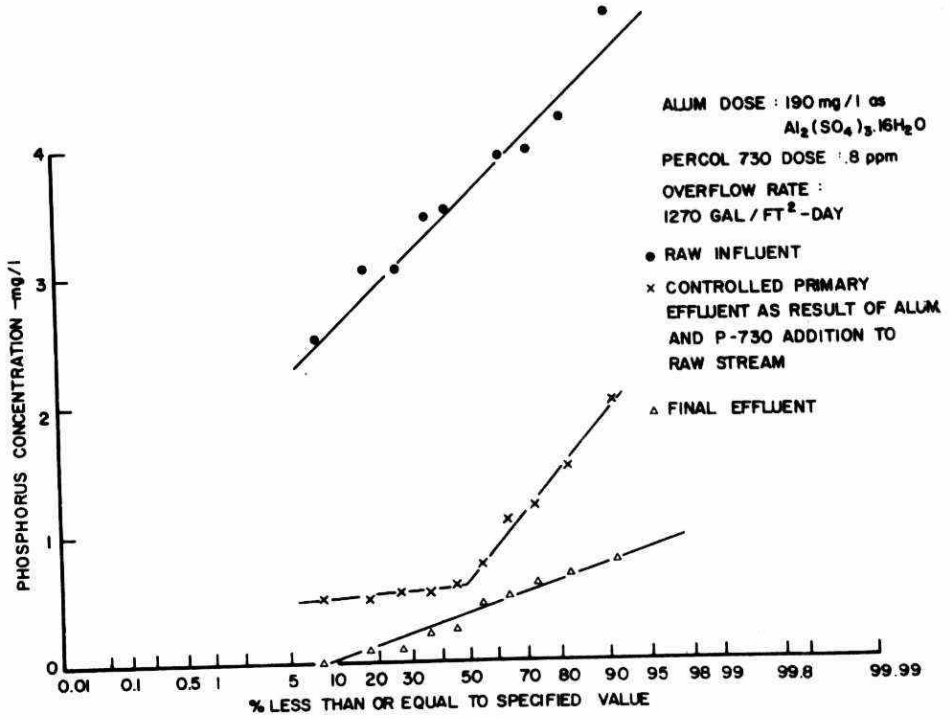

FIGURE 195. PHOSPHORUS CONCENTRATIONS ACROSS THE DUNDAS WPCP

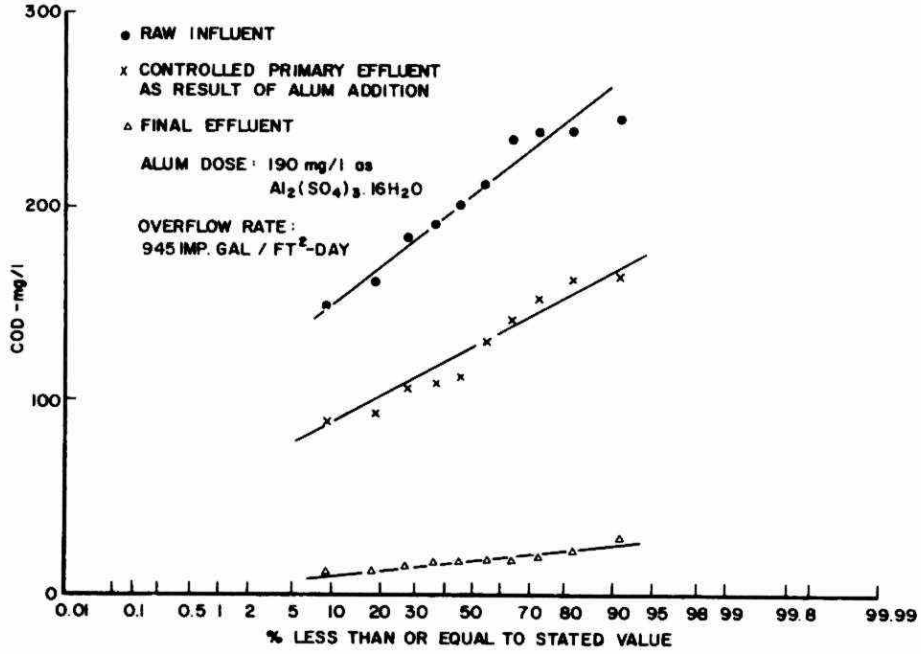

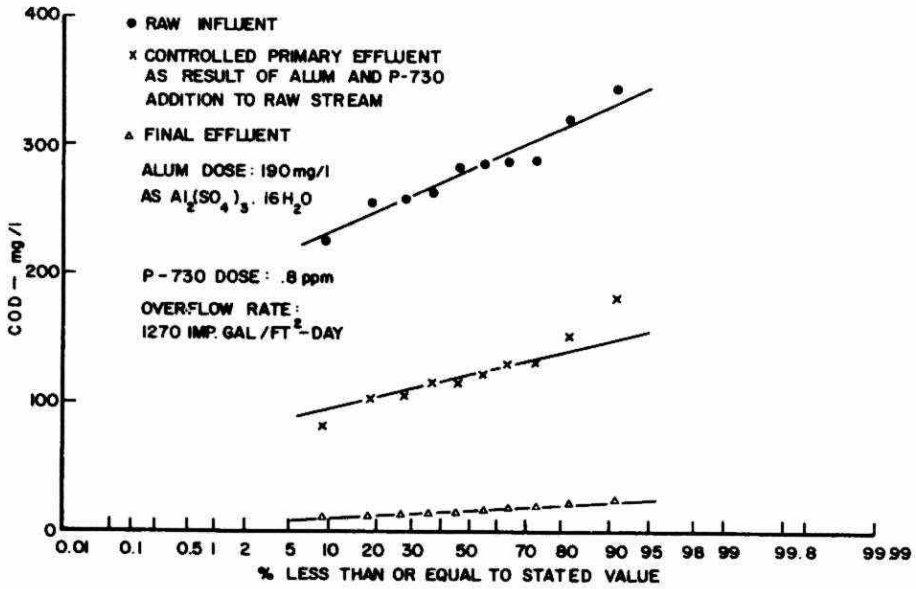

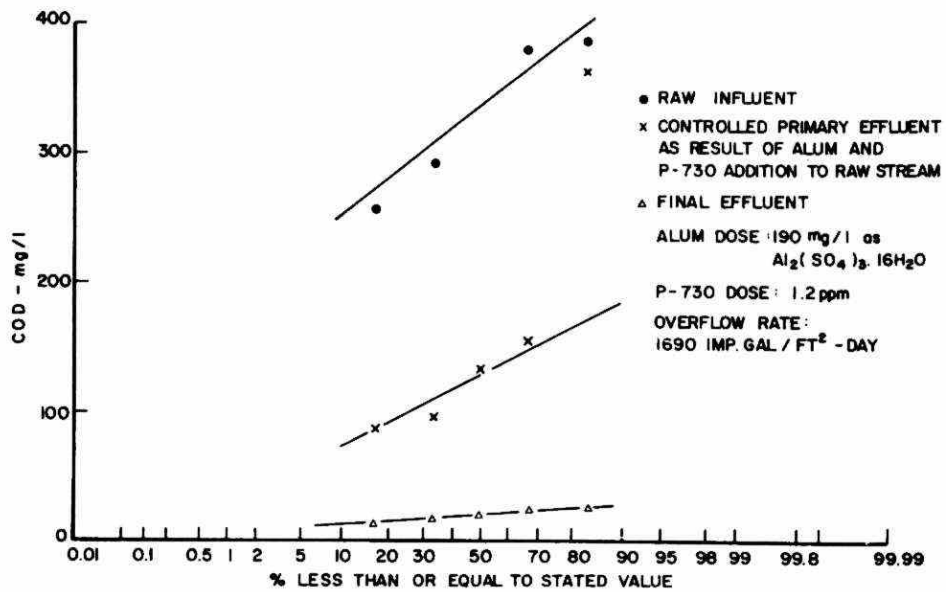

FIGURE 196. COD CONCENTRATIONS ACROSS THE DUNDAS WPCP

APPENDIX B

DETAILS REQUESTED OF MANUFACTURERS OF POLYMERS

APPENDIX B

The Ministry of the Environment and Environment Canada under the terms of the Canada-Ontario Agreement has recently contracted a technical investigation entitled "The Assessment of Polymers as Aids to the Removal of Phosphorous from Waste Water" to be done in the Chemical Engineering Department, McMaster University by Professors A. Benedek and A. E. Hamielec.

The objectives of this investigation are threefold:

(a) to develop meaningful laboratory procedures for the evaluation of benefits derived from polymer addition

(b) to monitor the fate of polymers during flocculation

(c) to apply the developed procedures to a detailed assessment of polyelectrolyte application in a treatment plant designated by Ontario Ministry of Environment Personnel.

We wish to give all manufacturers of polymeric flocculants for waste water treatment an opportunity to participate in this evaluation. Thus we hereby request one pound samples of all polymeric flocculants recommended for waste water clarification. However, in view of time limitations we must restrict the number of samples per company to four.

In order to make our investigation of sufficient generality, we require information on polymer characteristics detailed in Table I. We feel that this information is essential for successful interpretation and extrapolation of data to varying waste types and treatment plant conditions. We have the experience and analytical capability to do our own polymer characterization. Characterization is time-consuming and, therefore, it would be most helpful if companies would supply some or all of the information given in Table I.

We realize that much of this information may be proprietary and, if necessary, all such proprietary information can be kept confidential. Because of time limitations in our program, evaluation of polymers for which too little characterization data is available may not be possible.

The use of polyelectrolytes is new and often misunderstood and, therefore, not yet fully accepted in waste water treatment. Hopefully, our investigation will develop the understanding and procedures necessary for their wide application.

Yours sincerely

AH for
A. Benedek (Dr.)

Archie Hamielec
A. E. Hamielec (Dr.)

Department of Chemical Engineering
McMaster University
Hamilton 16, Ontario

/ms

c.c. Dr. J. W. G. Rupke - Ministry of Environment
Research Branch
4375 Chasswood Drive
Downsview, Ontario

DETAILS REQUESTED OF MANUFACTURERS OF POLYMERS

(1) (a) Chemical Formula of Homopolymer
copolymer compositon
linear polymer
branched polymer

(b) Synthesis route (approximate)
Trace impurities and levels

(2) (a) Physical Characteristics

$\overline{M}n$= ? $\overline{M}w$= ?

Mark-Houwink equation $[\eta] = K \overline{M}n^{a}$

or $K \overline{M}w^{a}$

experimental conditions for K and a

e.g. solvent type
temperature
ph

(b) Degradation characteristics

(3) Recommended procedure when polymers are used as flocculants.

APPENDIX C

SYNTHESIS OF ANIONIC POLYACRYLAMIDES

APPENDIX C

C. SYNTHESIS OF ANIONIC POLYACRYLAMIDES.

C.1 Introduction

The usual method of synthesis of commercial polyelectrolytes is via a free radical mechanism which gives a polymer having a broad molecular weight distribution. The mean of this distribution can be varied widely by changing the polymerization temperature; however, the variance about the mean remains rather large except for very low molecular weight polymers which are of little interest in flocculation. In other words, polyelectrolytes of commercial interest invariably have broad molecular weight distributions. This is unfortunate, as the higher molecular weight species which are most effective as flocculants are present in relatively small concentrations. Manufacturers of polyelectrolytes provide a minimum of information on the molecular weight distribution of their polymers. To elucidate the effect of molecular weight and charge density on flocculant effectiveness independently, it was found necessary to synthesize polymers and to characterize these along with those available commercially. One of the most commonly used polyelectrolytes, and one that is outstanding in the flocculation of colloidal phosphorus, is anionic polyacrylamide. It was, therefore, decided to synthesize nonionic polyacrylamide and then hydrolyze it to different degrees, maintaining its original molecular weight distribution. In this section techniques of synthesis of anionic polyacrylamide are described.

C.2 Experimental

Details of the synthesis of nonionic polyacrylamide may be found elsewhere (Ishige and Hamielec, 1973). In brief, nonionic polyacrylamide was synthesized using aqueous solution polymerization of acrylamide initiated by 4,4 -azobis-4-cyanovaleric acid in the temperature range 25-50^{o}C. In all syntheses, isothermal polymerizations were done to give a polymer having the most probable distribution. A nonionic polyacrylamide labelled Standard B was synthesized at 50^{o}C. Details of its characterization may be found elsewhere (Abdel-Alim and Hamielec, 1973).

It had the most probable distribution given by:

$$W(M) = \frac{M}{\overline{M}_n^2} \exp\left(-\frac{M}{\overline{M}_n}\right)$$

where $W(M)dM$ is the weight fraction of polymer of molecular weight in the range M - M+dM and $\overline{M}_n$ is the number-average molecular weight and is equal to 1.62×10^6 for Standard B. With the most probable distribution, $\overline{M}_w$, the weight-average molecular weight is equal to 3.24×10^6 or exactly twice $\overline{M}_n$.

Standard B was then hydrolyzed to different degrees using a technique which minimizes polymer chain degradation (Makhopadhyay, 1969). In other words, this technique provided a series of anionic polyacrylamides with different charge densities (degrees of hydrolysis) and with all samples having the same molecular weight distribution. This was confirmed by gel permeation chromatography for anionic polyacrylamides having degrees of hydrolysis of 7,10 and 30 wt.%. The degree of hydrolysis is defined as the weight of hydrolyzed monomer units times 100, divided by the weight of all monomer units in the polymer chains.

The hydrolysis procedure is outlined below. The reaction between the amide group on the polymer chain and sodium hydroxide liberates ammonia giving the sodium salt of a carboxy acid as follows:

$$-\overset{\overset{O}{\|}}{C}-NH_2 + NaOH \longrightarrow -\overset{\overset{O}{\|}}{C}-O-Na + NH_3\uparrow$$

The detailed procedure is as follows:

1) Reaction.

0.5 g of Standard B (nonionic polyacrylamide) is dissolved in 70 ml of distilled water in a 250 ml round-bottom flask. The solution is purged with nitrogen for 30 min. at room temperature before 70 ml of 0.1 N NaOH is added. The purge is maintained and the flask is placed immediately into a water bath at 60°C and off-gases are passed through a condenser (using cold water) and finally through a condenser (using cold water) and finally through 40-70 ml of cold 0.1 N HCl kept in an

ice bath. All of the liberated ammonia should be vaporized in the nitrogen stream and absorbed in the 0.1 N HCl solution.

2) Analysis for Degree of Hydrolysis.

The 0.1 HCl solution containing the absorbed NH_3 is titrated with 0.1 N NaOH using methyl red as indicator to determine the amount of NH_3 liberated during polymer hydrolysis.

The polymer solution is titrated with 0.1 N HCl using bromomethyl blue as indicator to determine the amount of unreacted NaOH. Approximately 10-20 ml of the reaction mixture was used for this analysis and the remainder for polymer recovery by precipitation.

3) Polymer Recovery.

Polymer is precipitated from the reaction mixture with the addition of a large excess of methanol (Volume ratio = 10:1). The mixture is filtered and the polymer is dried under vacuum.

C.3 Results

Data on polymer synthesis are tabulated in Table C-1. It was found that direct titration of the reaction mixture to determine degree of hydrolysis was not reliable due to a vague colour change of the indicator and to poor mixing of the rather viscous solution. The measurement of degree of hydrolysis tabulated in Table C-1 was based on the measurement of the NH_3 liberated.

TABLE C-1. POLYMER SYNTHESIS DATA

Run No.	Reaction Time (hr)	Degree of Hydrolysis (%)	Polymer Recovery (%)
C-1	17.5	30.0	44.2
C-2	17.5	25.7	-
C-3	2.0	6.7	49.8
C-4	5.0	10.5	49.9

The low levels of polymer recovery were most probably due to the choice of nonsolvent and the amount employed to precipitate the polymer. No attempt was made here to optimize polymer recovery as the main concern was to provide sufficient polymer for flocculation studies with the modified jar test. Run C-2 in Table C-1 was done with 0.05 NaOH to repeat some literature data in order to evaluate the experimental techniques used in this study. The rate data agreed with literature data to within experimental error, suggesting its reliability. Chromatograms of the three anionic and one nonionic polyacrylamide (0, 7, 10, 30% degree of hydrolysis) measured by gel permeation chromatography indicated that the molecular weight distributions were the same. In other words, degradation of polymer during hydrolysis was negligible. The nonionic and anionic polyacrylamides were evaluated as flocculants for the settling of colloidal phosphorus using the modified jar test. The results are shown graphically in Figure 197. It is clear from observation of the settling curves that there is an optimum degree of hydrolysis where a maximum floc settling rate is observed. The optimum degree of hydrolysis is about 7%. It should be re-emphasized that Figure 197 shows the effect of charge density (degree of hydrolysis) on floc settling rate at constant molecular weight. In other words, the molecular weight distribution for the four polymers investigated (0, 7%, 10% and 30% hydrolysis) was the same.

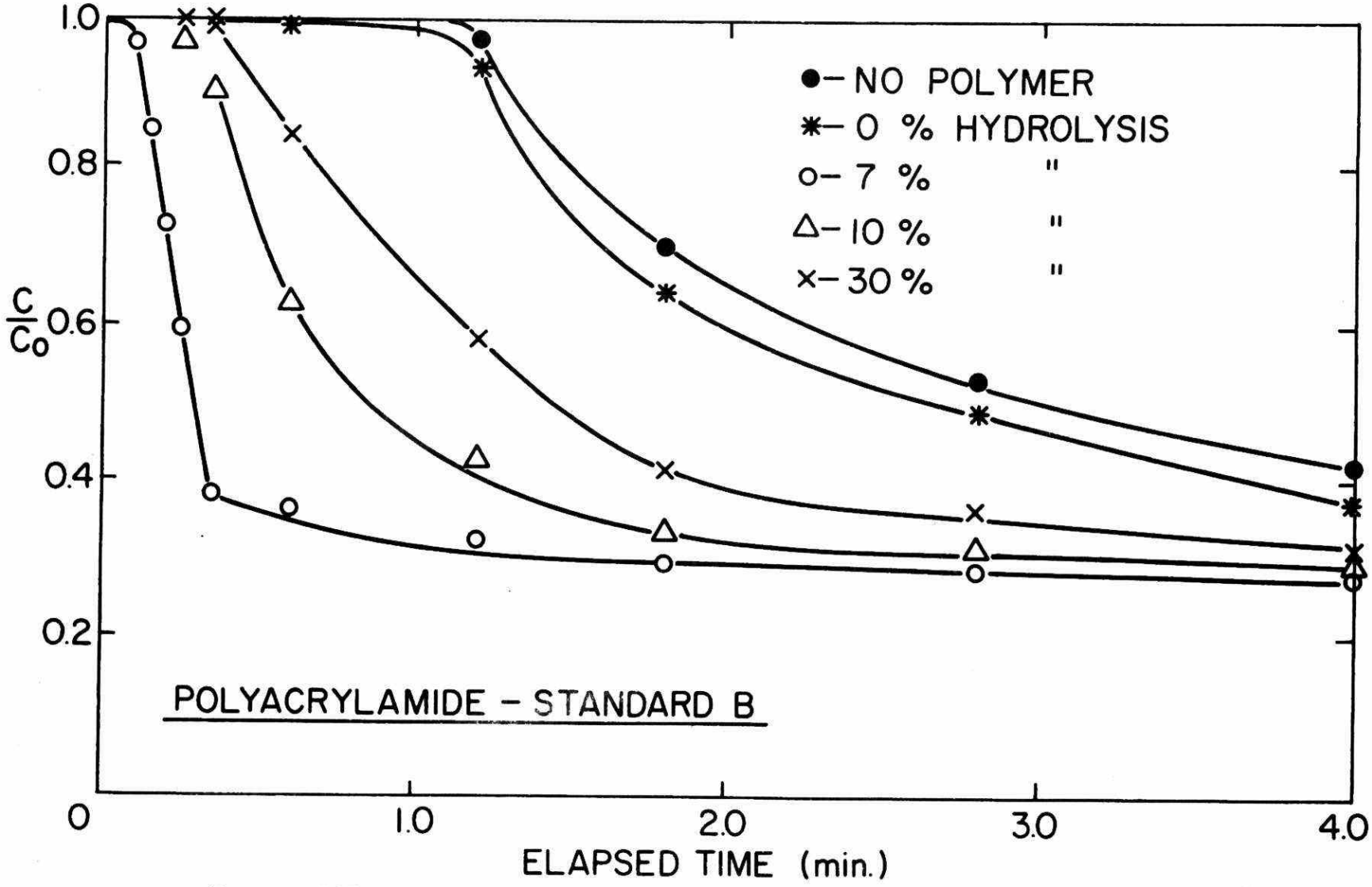

FIGURE 197. SETTLING CURVES FOR THE REMOVAL OF COLLOIDAL PHOSPHORUS COMPOUNDS BY POLYMER FLOCCULANTS - POLYACRYLAMIDE STANDARD B WITH DIFFERENT DEGREES OF HYDROLYSIS (ALUMINUM TO PHOSPHORUS RATIO = 1, INITIAL PHOSPHORUS CONCENTRATION: 5 PPM AS P-50% ORTHO, 10% PYRO, 40% TRIPOLY)